# FUNCTIONALISED MACROPOROUS AFFINITY MATRICES

A THESIS SUBMITTED TO THE

UNIVERSITY OF PUNE

FOR THE DEGREE OF

DOCTOR OF PHILOSOPHY

(IN CHEMISTRY)

BY

SUPRIYA DESHPANDE

POLYMER SCIENCE AND ENGINEERING DIVISION

NATIONAL CHEMICAL LABORATORY

PUNE-411008 (INDIA)

JULY 2007

# Certificate

Certified that the work incorporated in this thesis entitled "**Functionalised Macroporous Affinity Matrices"** submitted by Supriya Deshpande was carried out under my supervision. Such material as obtained from other source has been duly acknowledged in this thesis.

**July 2007,**

**Pune** **Dr. C. R. Rajan**

**(Research guide)**

## Declaration

I hereby declare that thesis entitled "**Functionalised macroporous affinity matrices**", submitted to the University of Pune for Ph. D degree in chemistry, has been carried out under the supervision of Dr. C. R. Rajan at the Polymer Science and Engineering, Chemical Engineering and Process Development Division, National Chemical Laboratory, Pune, India. The work is original and has not been submitted in part or full by me for any degree or diploma to this or any other University.

July 2007 (Supriya Deshpande)
Pune

**Dedicated to,**

**my daughter,**
***Rujuta*…..**

**Acknowledgement**

The first person to whom I express my sincere gratitude is my guide and mentor, Dr. C. R. Rajan, for giving me permission to work under his guidance. His support helped me throughout during all these years. I have no words to thank Dr. S. Ponrathnam. He showed me the way through the dark like a guiding star. He introduced me to the fascinating area of polymer chemistry. His scientific guidance, stimulating suggestions, and encouragement related to this work helped me at every stage of this work. Besides this, I am indebted to both of them for their kind care and concern in the laboratory.

My thanks are also due to Dr. Smita Mule for patiently doing HPLC and DSC samples. I am grateful to her for teaching me HPLC technique and all the help she offered during the work.

I am taking this opportunity to thank Mr. Gaikwad for SEM and Mrs. Deepa Dhoble for IR analysis. I am thankful to all the colleagues past (Dr. Aarika Kotha, Dr. Anjali Lodha, Dr. Ramesh Ghadage, Dr. Rajkumar, Dr. Pathak, Avinash, Lijo, Rahul, Pallavi, Trupti, Senthil) and present (Pujari, Hari, Ganesh, Praveen, Timothy, Sunny, Wasif, Abhijeet, Eldho) for their co-operation and helping hand. Special thanks are due to my best friends Shubhangi, Rupali and Padmaja who were always there when I needed them, with whom I share a beautiful relationship, which will last forever.

I whole heartedly thank Mr. Sathe and Mr. Giri for their technical help.

The co-operation and support rendered by my family, especially by my husband Shrirang is beyond words. This thesis would not have been possible without the help and blessings of my parent-in-laws and parents. The patience shown by them and by my daughter Rujuta encouraged me to complete this work. The inspiration given by my grandmother-in-law always boosted my morale. My thanks are also due to my sister, brother-in-law, to my uncles and aunties, to my cousins, who loaded me with their love and wished the best for me.

I am also grateful to all of those who were involved directly or indirectly in this work.

Finally, I thank Dr. S. Sivaram, Director, National Chemical Laboratory, Pune for permitting me to submit this work in the form of thesis. I would also like to thank Council of Scientific and Industrial Research for awarding the fellowship.

Supriya Deshpande

# Table of Contents

## List of figures

## List of Tables

## List of schemes

**Abstract**

Optically active chiral compounds are of immense importance on account of their widespread occurrence in nature. Thus, proteins, nucleic acids and polysaccharides, which are key building blocks of life, are all examples of chiral materials. Chirality was introduced in 1815 and it was Louis Pasteur who separated the first pair of enantiomers in 1848. Based on his observations he made the proposal: Optical activity of organic solutions is determined by molecular asymmetry, which produces non-superimposable mirror-image structures. The proposal unraveled the relationship between the molecular asymmetry and optical activity.

Live organisms consist of left amino acids and right sugars. Their interaction with other chiral molecules such as drugs, pesticides etc. leads to specific biological response. This may lead to differences in biological activities such as pharmacology, pharmacokinetics, metabolism, toxicity, immune response etc. Indeed, biological systems can recognise the two enantiomers as two different substances, and their interaction each other will therefore elicit different responses. As the demand for pure enantiomeric forms of the drugs is increasing, newer methods for their separation have been exploited. The interest in this area was largely academic for a long period. However, in the early 1980s, the commercial interest in chiral substances suddenly increased, particularly in chiral drugs, and this interest proliferated very rapidly. The world market for enantiomeric drugs exceeded $ 96 billion in 1995 and chiral drug sales surged toward $100 billion per year.

With the constantly increasing stringent regulatory conditions and need for chiral drugs, careful comparative evaluations of the activities, toxicities and pharmacokinetics of the two enantiomers are required. During the preclinical and clinical drug development it is important to have analytical methods suitable for conducting pertinent studies. High-performance liquid chromatography is a pre-eminent tool for analytical and preparative enantioselective separations.

The chromatographic methods are fast and easy and provide separation as well as quantitation. The chromatographic methods are based on two approaches:

1. Indirect, which utilises chiral derivatising agents and

2. Direct, which uses chiral stationary phases (CSPs) or chiral mobile phase additives

Direct separations on CSPs are the method of choice for fast and easy separations. Many CSPs have been developed to satisfy the needs to separate a variety of racemates. Depending upon the type of CSP, many racemic compounds can be resolved. The polymer based CSPs have also been developed as against the conventional silica based CSPs. There are three broad classes of the synthetic polymers used for chiral separations namely; optically active polymers (natural and synthetic), molecularly imprinted polymers (MIPs), and polymers bearing pendant chiral ligands.

The matrix or the support, which forms the major part of the stationary phases, must possess specific physical and chemical properties to be suitable as a stationary phase in HPLC. Such materials must have sufficient mechanical strength to withstand the high column pressure without breakage or deformation. Furthermore, the physical properties, e.g. pore size, porosity and particle diameter, must be controlled within narrow tolerances to enable the manufacture of reproducible packing materials. Especially the porosity is of great importance, since this determines the surface area and, together with other parameters, also retention and selectivity.

Among the various techniques for the preparation of macroporous polymers, one can distinguish, three different routes: The first involves the use of gases as the void-forming medium. The second approach is based on the intermediate of emulsions, formed by tailor-made block-copolymers and the subsequent removal of the dispersed phase (Synthetic strategies for porous polymers). The third category is classified by the use of a phase separation process to generate a two-phase morphology, finally resulting in a porous morphology.

The present study was aimed at investigating the effectiveness of polymer supports of differing characteristics for use as chiral stationary phases. Different methods of generating spherical, porous particles useful for attachment chiral ligand/ immobilisation of enzyme were studied. The methods involved synthetic methods like suspension and concentrated emulsion polymerisation and physicochemical method like Thermally Induced Phase Separations (TIPS). Porosity generation in the above methods by changing the parameters like crosslinker, pore generating solvent in case of synthetic

methods was studied. The role of nucleating agent in generation of porosity in case of TIPS was also studied.

The use of moderately polar monomers like glycidyl methacrylate, hydroxyethyl methacrylate in concentrated emulsion polymerisation is restricted because of their inability to form stable emulsions. However, the use of these monomers bearing epoxy and hydroxy groups is beneficial for further modifications. The possibility of generating porous polymers with well defined pore structures by varying parameters like crosslink density; internal phase water, initiator and suspending agent is investigated.

The modifications of the polymers are carried out with simple, cheaply available chiral ligands such as L(+)tartaric acid (TA) and it derivatives as well as β-cyclodextrin (CD). The dependence of ligand loading onto the polymers is investigated with reference to several factors such as crosslink density (CLD), surface area (SA), pore volume (PV) etc. Evaluation of these materials in terms of their usability as chiral supports is studied. The binding of tartaric acid and/or its derivatives to the polymers is through one of the two carboxylic acid groups. The drug molecules known to be resolved by the chiral ligands such as amlodipine (antihypertensive) and citalopram (antidepressant) were selected for this study. The stereoselective binding was studied by carrying out batch adsorption experiments. The study revealed that the synthesised polymeric ligands could be considered as potential candidates for use in chromatographic chiral resolution of certain drugs.

Porous poly(ethylene-co-propylene) particles were prepared using TIPS. The role of sorbitol based nucleating agents in the formation of porous structures was studied. The porous particles were used for immobilisation of *Candida rugosa* Lipase, which was evaluated for stereospecific esterification of NSAID (non-steroidal antiinflammatory) drug naproxen. This thesis is presented as 7 chapters as described below.

**Chapter 1. Introduction.**

The chapter includes a brief introduction to chiral chemistry, resolution of racemic mixtures and importance of chiral discrimination, especially of drug enantiomers. Chromatographic methods are discussed in detail. Various types of chiral stationary phases with special emphasis on polymeric phases are reviewed. The chapter also includes physical and chemical synthetic methods of matrix/support preparation. The

chemical methods such as suspension polymerisation, High Internal Phase Emulsion (HIPE) polymerisation and physical methods like Thermally Induced Phase Separations (TIPS) leading to porous polymers are elaborated. Lipase immobilisation on the olefinic polymers like polypropylene and immobilised enzyme (lipase) mediated chiral resolution has also been addressed.

**Chapter 2. Aims and objectives.**

The broad objective behind taking up this study with specific aims is explained.

**Chapter 3. Synthesis and characterisation of polymers by suspension and medium/high internal phase emulsion polymerisation.**

The chapter deals with the synthesis of beaded, porous polymers bearing functional groups for further modifications. The polymers were synthesised using glycidyl methacrylate, hydroxyethyl methacrylate as monomers and ethylene dimethacrylate and divinylbenzene as crosslinkers. The synthesis was carried out by two different polymerisation methods; suspension and medium/high internal phase emulsion polymerisation (MIPE/HIPE). The effect of variable internal phase volume, initiator type (oil/water soluble), crosslink densities, porogens etc., on the morphology, surface area, porosity, and accessible epoxy groups of the polymers is discussed. The effect of amount of crosslinker, type of crosslinker, nature of porogen in suspension polymerisation has been studied. The porous characteristics of the polymers were analysed by SEM, mercury intrusion porosimetry and nitrogen adsorption.

**Chapter 4. Modification of the polymers with ß cyclodextrin and evaluation of the modified polymers for chiral resolution of citalopram.**

Attachment of β cyclodextrin to the GMA-DVB polymers, which showed highest pore volumes, synthesised using hexanol as pore-generating agents through hexamethylene diisocyanate and sebacoyl chloride spacers is discussed. The characterisation of the polymers after modification has been carried out using IR, titrimetric methods. The amount of bound CD was determined using phenol-sulphuric acid method. The polymer bound CD was successfully used for the inclusion of substituted phenol (p-cresol). The polymeric ligand was shown to be selective for S-citalopram, an antidepressant drug. The therapeutic activity of this drug lies only in the S form.

**Chapter 5. Modifications with tartaric acid / derivatised tartaric acid and evaluation for chiral resolution of amlodipine.**

The GMA-EGDM polymers (MIPE/HIPE) were subjected to functionalisation with different chiral ligands. Synthesis of L (+) and D (-) diacetyl and dibenzoyl tartaric anhydride as well as dibenzoyl tartaric acid as chiral resolving agents and anchoring the ligands to the functionalised polymers by simple organic reactions is described. The tartaric acid bound polymers were tested for the stereospecific binding of antihypertensive drug amlodipine. The study was carried out in batch adsorption mode and with different molar ratios of bound TA:amlodipine. The homopolymer of glycidyl methacrylate was synthesised and modified using L (+) TA. The modifications lead to crosslinked products, where both the –COOH groups of TA were used in the crosslinking process. The materials were also evaluated for adsorption of enantiomers of amlodipine.

**Chapter 6. Porous poly(ethylene-co-propylene) for lipase immobilisation.**

Various sorbitol based nucleating agents were synthesised as nucleators for poly(ethylene-co-propylene). The ability of these nucleators to enhance porous properties of the polymer has been studied. The effect of concentration of nucleating agent on the morphology and porosity of the polymer has been studied. The polymers are evaluated as supports for lipase immobilisation. The immobilised lipases have been used for stereoselective esterification of NSAID drug naproxen.

**Chapter 7 Conclusions and future work.**

Conclusions on the work carried out and directions for future research in this area are indicated in this chapter.

# Chapter 1

## Introduction

# 1 Introduction

## 1.1 The origin of chirality

'Chirality', a Greek term implying handedness, was first introduced in 1815, by Jean-Baptiste Biot[1]. He introduced the concept of optical activity, property by which a substance can rotate the plane of polarised light. In 1832 he observed that tartaric acid obtained from tartar (potassium salt of tartaric acid) was optically active, rotating the plane of polarised light clockwise (dextro-rotatory). An optically inactive, higher melting form of tartaric acid, called racemic acid was also known. Nearly a decade later, Louis Pasteur conducted a careful study of the crystalline forms assumed by various salts of these acids[2]. He noticed that under certain conditions, the sodium ammonium mixed salt of the racemic acid formed a mixture of enantiomorphic hemihedral crystals, as shown in the Figure 1.1. After picking the different crystals apart with a tweezer, he found that one group yielded the known dextrorotatory tartaric acid measured by Biot; the second led to a previously unknown laevorotatory tartaric acid, having the same melting point as the dextro-rotatory acid. Today, we recognise that Pasteur had achieved the first resolution of a racemic mixture, and laid the foundation stereochemistry[2]. Based on his observations, he postulated that: Optical activity of organic solutions is determined by molecular asymmetry, which produces non-superimposable mirror-image structures. The proposal unraveled the relationship between the molecular asymmetry and optical activity.

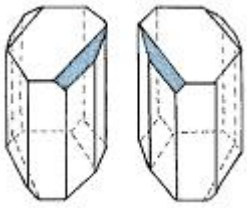

**Figure 1.1. Enantiomorphic hemihedral crystals of tartaric acid.**

Following Kekule's recognition in 1858 that carbon has a valence of four[3], Vant' Hoff and Le Bel independently recognised that when four different groups are attached to a carbon atom, arrayed at the corners of a tetrahedron, then the arrangements can be in two different forms[4]as shown schematically below in Figure 1.2 A.

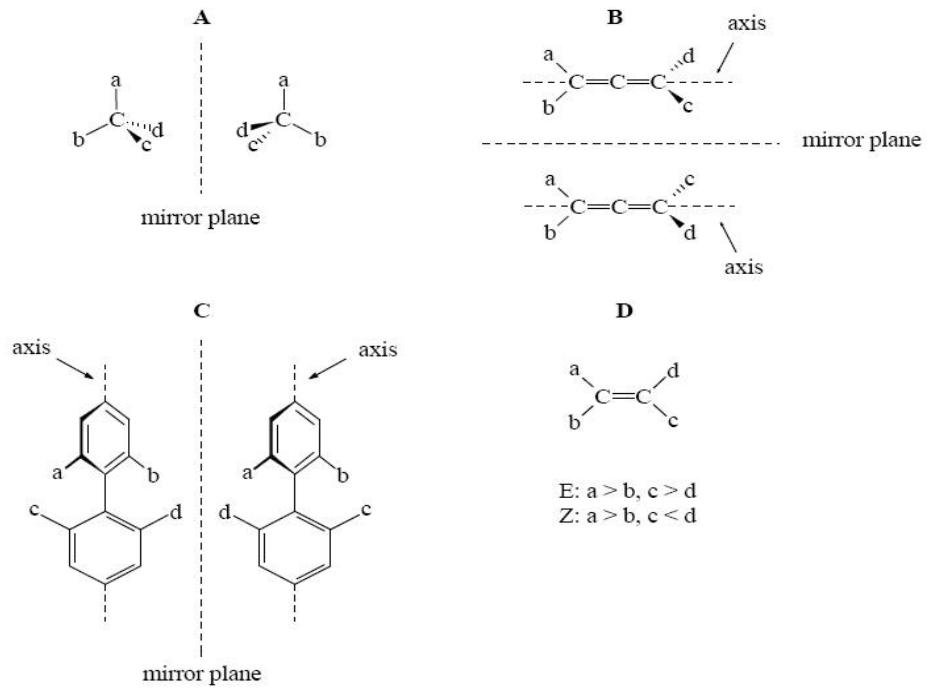


**Figure 1.2. Mirror images of pairs of enantiomers: (A) Central chirality (B) Axial chirality (C) Atropisomerism (D) E/Z isomerism= geometric isomerism.**

When the four atoms or groups attached to the carbon are not identical, they become non-superimposable on their mirror images thus causing optical activity. The enantiomers are thus defined as the stereoisomers, which possess different spatial arrangements and are non-superimposable mirror images of each other (Figure 1.2). The carbon atom in the two molecules on either side of the mirror plane is surrounded in a tetrahedral spatial arrangement by four different substituents, which make it an asymmetrically substituted carbon atom. In such an arrangement, the carbon atom is called a stereogenic centre or a centre of chirality. A molecule can have multiple chiral centres without being chiral overall if there is a symmetry element (a mirror plane or inversion centre), which relates the two (or more) chiral centres. Such molecules are called meso compounds (Figure 1.3). It is also possible for a molecule to be chiral without having actual point chirality. Commonly encountered examples include allenes and cumulenes, which have axial chirality. In the former class, the substituents have not necessarily to be different since the second double bond causes the loss of the C3 rotational symmetry element. In the latter class, only the members with an odd number of cumulated carbon atoms are potentially chiral, whereas an even number of carbon atoms

results in E-/Z-isomerism (D) (geometric isomerism). Another type of axial chirality is represented by atropisomers, which possess conformational chirality (C): As long as the *ortho*-substituents in tetrasubstituted biaryls are large enough, the rotation around a C-C single bond will be hindered and prevent the two forms from interconverting. Helicity is a special form of chirality and often occurs in macromolecules such as biopolymers, proteins and polysaccharides[5, 6]. A helix is always chiral due to its right-handed (clockwise) or left-handed (counter-clockwise) arrangement. When a stereoisomer has more than one stereogenic centre, *e.g. n* chirality centres, the number of theoretically possible diastereoisomers can be derived from 2*n*.

It was Emil Fisher, who made the first serious attempts to relate the absolute stereochemistry of optical isomers and determined configuration of (+) glucose, for which he received the Nobel Prize[7]. Together with A. M. Rosanoff, Fischer introduced his projection representation of molecular configuration, and arbitrarily assigned a D configuration to (+)-glyceraldehyde. This assignment immediately pertained to a group of structurally related compounds, including tartaric acid. In 1951, Johannes Martin Bijvoet, a Dutch crystallographer, established the true or absolute configuration of (+)-tartaric acid by means of an anomalous X-ray dispersion study of its sodium rubidium double salt. In this way, he showed that Emil Fischer had guessed right when he drew the Fischer projection of tartaric acid some 58 years earlier[8]. Thus, the foundations of chiral chemistry were established.

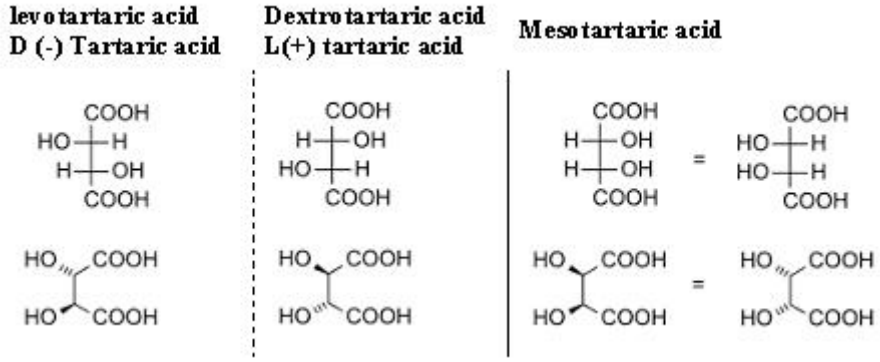


**Figure 1.3. Enantiomers of tartaric acid.**

### *1.1.1 Racemates and their resolution*

The enantiomers possess similar chemical and physical properties except that they rotate the plane of polarised light in opposite directions. The isomer, which rotates the plane to the left, is known as laevorotatory (-) while the one that rotates the plane to the right is dextrorotatory (+). Although the individual molecules are optically active, the substance in the bulk may not be optically active. This is because of the presence of equal numbers of dextro and laevorotatory molecules that the average rotation is zero. Such an assembly of molecules is known as racemic modification. Crystalline racemates belong to one of three different classes that are conglomerates (mechanical mixture of crystals of the two pure enantiomers), racemic compound (equal quantities of enantiomers present on a well defined arrangement within the crystal lattice) and solid solution (enantiomers coexisting in an unordered manner in the crystal); the most common being racemic mixture. The separation the two enantiomers that constitute a racemate is called a resolution or optical resolution[9].

There are two broad categories of optical activation methods that include resolutions and stereoselective synthesis. The most commonly used resolution methods include:

a. Separation of enantiomers by crystallisation (spontaneous resolution, preferential crystallisation, etc.) and
b. Chemical separation of enantiomers via diastereomer.

#### *1.1.1.1 Separation of enantiomers by crystallisation*

**Spontaneous resolution:** During crystallisation if both enantiomers of the racemate deposit in equal quantities as enantiomorphous crystals, the substance is said to be spontaneously resolved. The mixture of equal quantities of the enantiomorphous crystals is called as conglomerate. This type of resolution is rare and can be applied to only a few compounds. There are certain racemic compounds, which do not crystallise as conglomerate, however can be converted to derivatives that exist as conglomerates, without using chiral reagent. Amino acids such as alanine, leucine and tryptophan crystallise as racemic compounds but their benzenesulphonate salts are conglomerates[10].

The manual separation of individual crystals leads to pure enantiomers. The process being quite tedious and time taking is seldom used.

**Preferential crystallisation:** When a saturated or supersaturated solution of racemate is seeded with crystals of one of the isomers, the crystallisation occurs in such a manner that only the seeded isomer crystallises preferentially. This is known as preferential crystallisation. The process works only for substances that are conglomerates. In this process the seed crystals of one of the enantiomers are dissolved by heating in a solution of a racemate. The seeded enantiomer then crystallises upon cooling due to supersturation[11].

*1.1.1.2. Chemical separation via diastereoisomers*

Diastereoisomers are those stereoisomers, which do not have mirror image relationship with each other. Diastereoisomers are characterised by differences in physical properties, and by some differences in chemical behaviour towards achiral as well as chiral reagents.

Although an enantiomeric pair cannot be separated by ordinary chromatographic means or fractional recrystallisation, the diastereomeric pair can often be separated easily by these means as they differ in their physical and chemical properties. After separation, the pure enantiomers can then be regenerated by chemical means. There are two types of diastereomers namely, covalent compounds and dissociable complexes. The covalent diastereomers are generally separated by chromatography while the separations of diastereomeric complexes depend on crystallization techniques that are based on solubility differences[9]. Although the most popular method remains the formation and separation of crystalline diastereomeric salts, there are many other approaches for the resolution of racemates. They include separation via Lewis acid-base complexes, metal complexes and inclusion compounds. The compounds lacking functionalities e.g. chiral alkenes, aryls etc. can be resolved by incorporation into diastereoisomeric metal complexes or by reaction with chiral π-acids. Preferential inclusion of one of the enantiomers within chiral cavities (crown ethers, cyclodextrins etc.) or clathrates (cage like structures) is widely used. The inclusion is a result of hydrogen bonding and van der Waals attraction between the host and guest molecules[11]. The methods are very easy and

regeneration of the constituents is almost immediate. The formation of diastereomeric complexes can be illustrated schematically as shown below:

$$dlAH \xrightarrow{dB} \{dA^-, dBH^+\} + \{lA^-, dBH^+\} \qquad 1.1$$

For separation of diastereomeric salts to occur they should not co crystallise, their solubilities must differ, they should not form double salts and either one or both of them should be crystalline. The most widely used acidic chiral resolving agents include L (+) tartaric acid, dibenzoyl tartaric acid, camphor-10-sulphonic acid, camphoric acid, mandelic acid, malic acid etc. The basic reagents include brucine, cinchonidine, cinchonine, ephedrine, phenylethylamine, 2-amino-1-butanol, etc.

When the interactions of the enantiomers with chiral selector transforms the enantiomers at a different rate into new chemical entities, the resolution is said to be kinetically controlled; whereas the selector when forms labile adducts differing in stability, it is known as thermodynamic resolution[12].

*1.1.2 Enantiomeric purity determination*

The importance of optical purity in the context of biological activity has created a growing need for accurate unequivocal methods for the determination of the optical purities.

*(i) Optical rotation:* This classical method involves measurement of specific optical rotation.

**Optical puriy** = $\alpha / \alpha_0$ **x 100** 1.2

where, [α] = specific optical rotation of the mixture and $[\alpha]_o$ = specific optical rotation of the pure enantiomer.

**Enantiomeric excess (% ee)** = $\mathbf{R_{isomer} - S_{isomer} / R_{isomer} + S_{isomer}}$ **x 100** 1.3

where, R and S are the relative proportions (ratio) of the two enantiomers. In practice, this may often lead to some confusion since the optical rotation is dependent upon various conditions of measurements such as solvents, temperature, purity etc. and ambiguity may exist if the compound is new or not well documented in literature.

*(ii) HPLC (high performance liquid chromatography) Methods*: As enantiomers have the same adsorption properties, they are not amenable to direct chromatographic separation on achiral adsorbents. However, this can be accomplished *via* the formation of

diastereomers either by derivatisation of sample with suitable chiral reagent or formation of transient diastereomers via the interaction of enantiomers with chiral stationary phase/mobile phase additive.

*(iii) GLC (gas-liquid chromatography) Methods*: For compounds that are readily vapourised without decomposition, gas chromatography on chiral stationary phase constitutes an accurate and reliable method for enantiomeric purity determination. The technique has inherent advantages of simplicity, speed, reproducibility and sensitivity.

*(iv) NMR (nuclear magnetic resonance) Methods*: NMR is a widely used technique for enantiopurity determination and one well-tested method involves conversion of mixture of enantiomers to a mixture of diastereomers by optically pure reagents eg. Mosher's reagent. A closely related method employs the use of chiral Lanthanide shift reagents (LSRs), having the property of shifting the NMR signals of substrates *via* diastereomeric complex formation[11].

## 1.2 Importance of chiral resolution

The relationship between chirality and biological activity was discovered when Pasteur showed the selective fungal metabolism of chiral tartaric acid in 1857. He showed that only the dextro isomer of racemic ammonium tartrate was totally consumed by a fungus *Penicillium glaucum* while the laevo form remained intact[13]. The history of using chiral drugs dates back to 2735 BC when the Chinese plant, *Ma Huang*, was used for its content of enantiomeric ephedrine. Opium was known in 300 BC, its active agent being isolated in 1805 and named morphium after the God of Dreams. Bayer was the first company to manufacture a semi-synthetic chiral drug in 1898: this was heroin and it was marketed as a non-addictive cough medication! By the end of the 20th century, 25% of all drugs were racemic and 25% single isomers – nearly all being natural products. Now, a large proportion of all drug containing a chiral centre are marketed as single enantiomers[14].

The separation of chiral compounds has become an interesting area over the past few years. It is now well established that majority of biomolecules like proteins, amino acids, sugars are chiral and exist in only one of the two possible enantiomeric forms in nature[15]. Due to this property they show specific biological responses to certain drugs and other chemicals like pesticides etc. This may lead to differences in biological activities

such as pharmacology, pharmacokinetics, metabolism, toxicity, immune response etc. Indeed, biological systems can recognise the two enantiomers as two different substances, and their interaction with each other will therefore elicit different responses. The reason for chiral recognition by drug receptors can be explained by "three-point interaction" of the drug with the receptor site, as proposed by Easson and Stedman in 1933[16] and by Ogston in 1948[17]. The difference between two enantiomers of a drug with its receptor site is illustrated in Figure 1.4 using a hypothetical interaction between a chiral drug and its chiral binding site. In this case, one enantiomer is biologically active while the other enantiomer is not. The substituents of the active enantiomer drug labeled A, B, and C must interact with the corresponding regions of the binding site labeled a, b, and c of the receptor in order to have an alignment Aa, Bb, Cc. The fitting interaction can produce an active biological effect, whereas the inactive enantiomer cannot bind in the same way with its receptor when it rotates in space; consequently there is no active response. This phenomenon is similar to a hand fitting into a glove or to a key into a lock. A right hand can only fit into a right hand glove, so a particular enantiomer can only fit into a receptor site having the complimentary shape. The other enantiomer will not fit, like a right hand in a left glove, but may fit into a receptor site elsewhere in the body and cause an eventual unwanted or toxic effect. On the other hand, enantiomers can show different chemical behaviour due to different chiral discrimination by diastereomeric formations with a chiral environment[18].

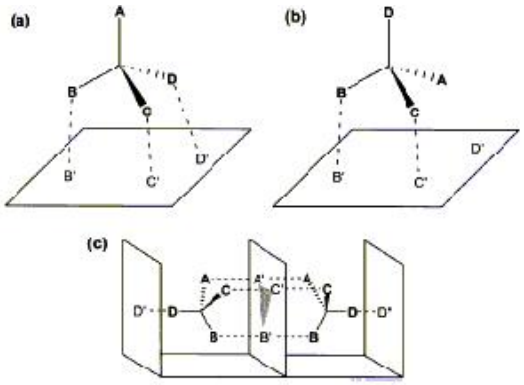


**Figure 1.4. Schematic diagram of an interaction of drug and its binding site.**

As the demand for pure enantiomeric forms of the drugs is increasing, newer methods for their separation have been exploited. The interest in this area was largely academic for a long period. However, in the early 1980s, the commercial interest in chiral

substances suddenly increased, particularly in chiral drugs, and this interest proliferated very rapidly. The major concern arose from the unfortunate birth defects initiated by one of the enantiomers of a drug known as Thalidomide. In 1960's a racemic drug was marketed as sedative Thalidomide. The administration of this drug to pregnant women resulted in birth of several malformed babies. This happened because of S (-) enantiomer of the drug was teratogenic and caused serious fetal malformations. The desired physiological activity was found to reside solely in the R (+) isomer, which, unfortunately, was discovered rather late[19].

The thalidomide disaster evoked the interest of all pharmaceutical manufacturers and also the drug regulatory committees. In 1992, the Food and Drug Administration (FDA) issued new guidelines governing stereoisomerism in new-drug development[20]. The guidelines strongly encourage the development of single isomers and discourage stereoisomeric mixtures. Since then, the stereoisomeric composition of drugs has become a key issue in their development, regulatory approval and marketing. The demand for enantiomerically pure drugs rose rapidly and in 1993, the world market in enantiomerically pure drugs exceeded $35 billion, the majority of which were cardiovascular and antibiotic drugs. As a result, most new chiral drugs are being developed as single enantiomers. The world market for enantiomeric drugs exceeded $ 96 billion in 1995 and chiral drug sales surged toward $100 billion per year[21]. However, there are many older agents that are still available in racemic form. As these drugs reach the end of their patent life, manufacturers become interested in marketing single enantiomer equivalents. This is called 'chiral switching' (CS) and it has been claimed that it will bring clinical benefits in terms of improved efficacy, more predictable pharmacokinetics or reduced toxicity. Many new CS drugs are in development e.g., (S)-oxybutynin for urinary incontinence and escitalopram for depression. Along with CS two more approaches for the chiral drug development have been explored. These are, chiral metashifts (CM), and new single-isomer chemical entities (NSICEs). In a CM, a chiral metabolite of a drug is developed in single-isomer form, as an agent with advantages over the parent. Among the current CM drugs in development are (+)-norcisapride (safer gastrointestinal prokinetic agent than the racemic parent cisapride) and (S)-desmethylzopiclone (antianxiety agent, metabolite of the sedative-hypnotic zopiclone).

Many NSICEs are in development, e.g., rosuvastatin as an antihypercholesterolemic, posaconazole as an antifungal, sitafloxacin as a fluoroquinolone antibacterial, pregabalin as an anticonvulsant, abarelix as an antineoplastic, etc.[22]

The racemic drugs can be classified into three categories based on the biological activities. The majority of the racemic drugs contain one major bioactive component called eutomer and other inactive or less effective or harmful component called distomer. Most of the cardiovascular drugs such as β blockers (atenolol, acebutolol, propranolol, carvedilol, etc.), calcium channel antagonists (verapamil, amlodipine, nicardipine, nimodipine, nisoldipine, felodipine, mandipine) etc. constitute this class of drugs[23]. Besides these many anticonvulsant, antihistaminic, antihyperlipidemic, local anesthetics, anticoagulants, antibiotics, psychostimulants as well as proton pump inhibitors fall into this category[24, 25].

The drugs containing both bioactive enantiomers are very few and these are antineoplastics, antiarrhythmic and antidepressants[26]. The third category consists of drugs, which can undergo chiral inversion e.g. nonsteroidal anti-inflammatory drugs (NSAID), namely ibuprofen, ketoprofen, fenprofen, benoxaprophen, etc. For this group, only S-enantiomer is active i.e. has an analgesic and anti-inflammatory effect. For example, S-ibuprofen is over 100-fold more potent as an inhibitor of cyclo-oxygenase I than (R)-ibuprofen. In the body, only inactive R enantiomer can undergo chiral inversion by hepatic enzymes into the active S-enantiomer and not vice-versa[24, 27].

With the constantly increasing stringent regulatory conditions and need for chiral drugs, careful comparative evaluations of the activities, toxicities and pharmacokinetics of the two enantiomers are required. During the preclinical and clinical drug development it is important to have analytical methods suitable for conducting pertinent studies[28]. High-performance liquid chromatography is a pre-eminent tool for analytical and preparative enantioselective separations.

### 1.3 Chromatographic methods

The chromatographic methods are fast and easy and provide separation as well as quantitation. The chromatographic methods are based on two approaches: (1). Indirect, which utilises chiral derivatising agents and (2). Direct, which uses chiral stationary phases or chiral mobile phase additives[11].

*1.3.1 Indirect chromatographic methods*

In the indirect method the racemic mixture, which has to be separated, is allowed to react with a chiral reagent to form a pair of diastereomers and then they are separated using an achiral column. The diastereomers, being physiochemically different, can be separated on achiral columns. This method does not require expensive chiral columns. It, however requires prior derivatisation of the analyte leading to side reactions such as racemisation.

*1.3.2 Direct chromatographic methods*

A chiral chromatographic separation of enantiomers can be obtained either direct with help of a chiral stationary phase (CSP) or indirect via addition of a chiral mobile phase additive (CMPA).

*1.3.2.1 Chiral mobile phase additives (CMPA)*

Separation of enantiomers on an achiral HPLC column can be acieved by use of chiral mobile phase additives. The chiral additive forms a diastereomeric complex with the racemic analyte, which is then separated on the achiral column. The separation takes place as a result of differences in the stabilities of diastereomeric complexes, solvation effects of the mobile phase as well as interaction with the solid support. α, β and γ cyclodextrins have been successfully used as chiral mobile phase additives [29- 31].

*1.3.2.2 Chiral stationary phases (CSP)*

In this technique the stationary phases are made with a chiral molecule that forms an integral part of the support. The analyte can be separated based on its ability to form complex by interaction with the CSP[15].

## 1.4 Principles of chiral recognition by CSPs

Chiral liquid chromatography is dependent of the consecutive formation of diastereomeric complexes between a chiral selector (S) and the two enantiomer analytes (A1 and A2):

$$S + A_1 \underset{}{\overset{K_1}{\rightleftharpoons}} SA_1$$
$$S + A_2 \underset{}{\overset{K_2}{\rightleftharpoons}} SA_2 \qquad 1.4$$

The relative binding strengths of these diastereomeric complexes determines enantioselectivity. In order to obtain a chiral separation one of the enantiomers must form

a weaker complex with the selector than the other i.e. K2 ≥K1. Different types of interactions can appear between the analyte and the stationary phase; for example ionic, hydrophobic, hydrogen bonding and π-π interactions. The mobile phase can be chosen in a way that a specific type of interaction is favoured e.g. high or low pH, polar or nonpolar solvents and so on. Dalgliesh proposed his three points interaction theory in 1952 to explain the origin of a chiral discrimination, as visualised in scheme below Figure 1.5[32].

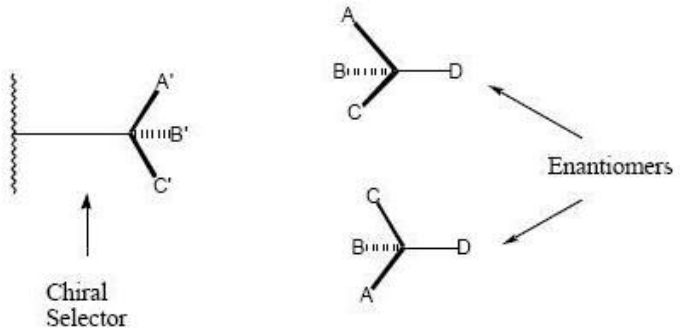


**Figure 1.5. Schematic diagram of the "Three Point Rule" of chiral discrimination.**

The three point rule can be stated as "Chiral recognition requires a minimum of three simultaneous interactions between the CSP and at least one of the enantiomers, with at least one of these interactions being stereochemically dependent. That is, at least one of the interactions will be absent or significantly altered by replacing one enantiomer with the other, without conformational change in any component. The three-point rule differs from Ogsten's theory in that it does not require all three interactions to be attractive (i.e., "bonding"). In many cases, repulsive steric interactions are invoked, usually in combination with one or more bonding interactions, to explain chiral recognition[33].

## 1.5 Types of CSPs

First developed by Gil-Av et al. in 1966, chiral stationary phase for gas chromatography have now been used extensively[34]. The stationary phases based on chiral crown ethers were introduced in 1976 and cyclodextrins were first used as chiral resolving agents in 1978[35, 36]. Cyclodextrins were successfully used as mobile phase additives for chiral separations by thin-layer chromatography for the separation of enantiomers by Armstrong in 1980[37].

The chiral stationary phases can be divided into 6 major classes as follows:(1) Pirkle Type CSPs (π donor and π acceptor)/ brush type CSPs, (2) Polysaccharide and derivatized polysaccharide based, (3) Chiral cavity (cyclodextrins and crown ethers etc.), (4) Ligand exchange, (5) Protein based columns and (6) Macrocyclic antibiotic based columns [15].

*1.5.1 Pirkle type CSPs*

Pirkle and House in 1979 developed the chiral stationary phases with π-donors and π-acceptors[38]. They explained that there must be at least three simultaneous interactions between the chiral stationary phase and the analyte and one of these must be stereochemically dependent for the chiral resolution to take place. This is known as "Three Point Rule". The chiral resolution is dependent on the intermolecular interactions such as hydrogen bonding, π-π, dipole-dipole, steric and hydrophobic interactions[39].

The CSPs can separate a variety of racemic compounds like alkyl, aryl carbinols, hydantoins, lactams, succinamides, phthalides, sulphoxides, sulphides etc.[40]. The most commonly used commercial chiral stationary phase of this type is Whelk-O1 manufactured by Regis Technologies Inc., USA. The structure of (S, S) Whelk-O1 CSP is shown in the Figure 1.6 below.

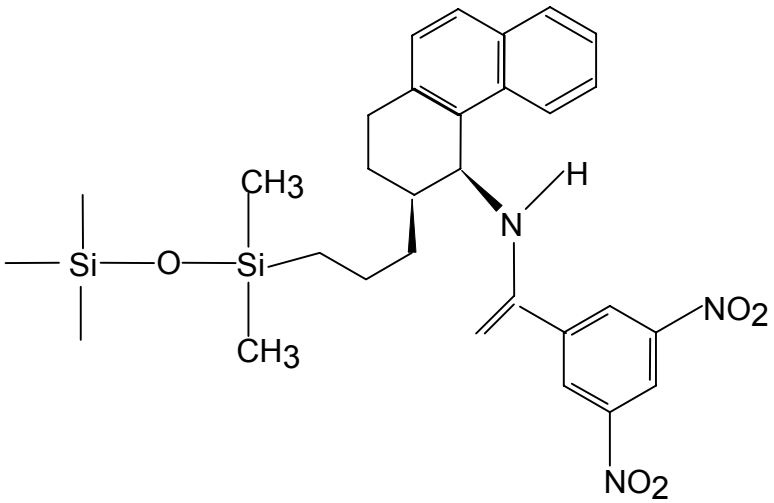


**Figure 1.6. Structure of (S, S) Whelk-O1 CSP.**

*1.5.2 Polysccharide CSPs*

Dalgliesh in 1952 first resolved the amino acids on cellulose by TLC[32]. This work initiated the use of cellulose, cellulose derivatives as well as other polysaccharides for chiral separations in liquid chromatography.

Cellulose, a polymer of D-glucose linked together by β-1,4-glycosidic linkages, is a high molecular weight, crystalline polymer. It contains polymer chains held together by intermolecular and intramolecular hydrogen bonds. The chains are stacked leading to formation of sheets. The monomer unit i.e. D-glucose contains five chiral centres, by virtue of which the polymer becomes chiral. Native cellulose, however, cannot be used as such as chromatographic supports because of the highly polar hydroxyl groups that are responsible for non-specific binding of the analyte. It was, however, observed that after derivatisation cellulose could be effectively used to resolve racemates in chromatography. A number of cellulose-based columns are now commercially available and can separate a wide variety of compounds (Figure 1.7).

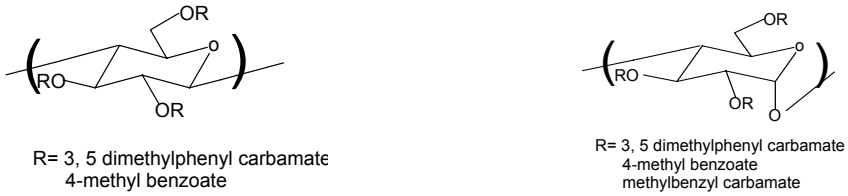


**Figure 1.7. Derivatives of cellulose and amylose used as CSPs.**

Along with cellulose, derivatised amyloses are also used for chiral separations. Although both the polymers are made up of D-glucose units, they differ in their glycosidic linkages (β- in cellulose and α- in starch), which results in different enantioselectivity[41]. Besides cellulose and amylose, other polysaccharides such as chitosan, chitin and amylopectin are also used for the preparation of CSPs[42-44].

*1.5.3 Inclusion type CSPs*

The CSPs are based on the mechanism by which the guest molecule is included into the cavity of the host molecule. Cyclodextrins (CD), which are cyclic oligosaccharides, are most commonly used hosts. They are made up of D-glucose units linked together by α- 1,4-glycosidic linkages. There are 3 types of CDs α-,β- and γ-. They consist of 6-, 7- and 8-glucopyranose units respectively. They possess a peculiar toroidal shape, the surface of which is hydrophilic and the cavity, which is hydrophobic.

Furthermore, each sugar molecule contains five asymmetric atoms, which will cause the chiral discrimination of an analyte by both its size and stereochemistry[45]. Out of these β-CD is the most easily available and economical. Also its cavity dimensions are such that most of the solute molecules can closely fit in (Figure 1.8). For these reasons it has been most often used in chromatographic applications.

Van der Waal's forces, hydrophobic interactions and hydrogen bonds govern the inclusion phenomenon. These are principally responsible to hold the cyclodextrin and its guest together. The extent to which these forces contribute depends on the nature of the enclosed guest molecule. The inherent ring structure is decisive, as inclusion complexes are formed only if there is a tight spatial fit between the host and guest components[46, 47].

Today, derivatised analogues of β-CD, such as heptakis(2,3,6-tri-O-methyl) or hydroxyalkyl-β-cyclodextrin, are also utilised to achieve enantioseparations in either liquid chromatography or electrophoresis, as they are usually more water-soluble than native cyclodextrins. Some commercially available cyclodextrin bonded phases are cyclobond (Astec), nucleodex (Machery-Nagel) etc. Other types of inclusion CSPs include crown ethers, which are heteroatomic macrocycles. Crown ether CSPs are made up of crown ethers covalently bonded to a silica gel support or polystyrene matrix[48].

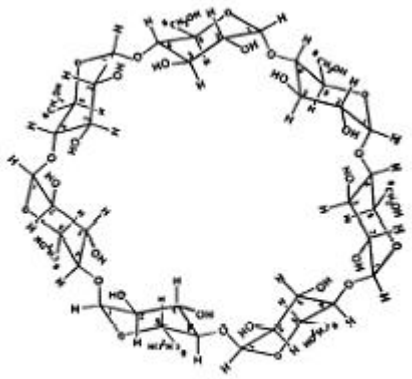

**a**.

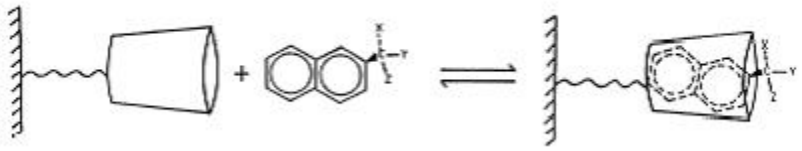

**b.**

**Figure 1.8. Structure of β-cyclodextrin ) (a), Mechanism of inclusion (b).**

*1.5.4 Ligand exchange CSPs*

Davankov et al. first introduced this type of chromatography in 1971[49]. The chromatography involves the formation of reversible coordination complexes between a bidentate analyte, a divalent metal ion and a chiral ligand immobilised on a stationary phase.

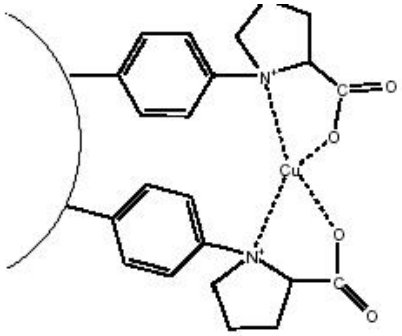

**Figure 1.9. Structure of ligand exchange CSP.**

Generally, the metal ion is from transition metal series, usually, $Cu^{2+}$ and chiral ligand is an amino acid. The factors affecting selectivity and efficiency of enantioseparations include the pH, ionic strength and column temperature (Figure 1.9).

*1.5.5 Protein CSPs*

Proteins, which are made up of chiral amino acids, have been successfully used in chiral chromatography. Proteins like bovine serum albumin (BSA)[50], human serum albumin (HSA)[51], ovomucoid (OVM)[52], avidin[53] etc. bonded to either agarose or silica supports are known. The stationary phases based on α1-acid glycoprotein and human serum albumins bonded to silica matrix are commercially available under the names Chiral-AGP and Chiral-HSA. These are generally used for the separation of enantiomers carrying secondary and tertiary amines and for substances containing nitrogen in a ring [54].

*1.5.6 Macrocyclic antibiotics as CSPs*

Macrocyclic antibiotics were shown to be very effective chiral selectors for HPLC and CE. The glycopeptides such as vancomycin (Figure 1.10a), teicoplanin (Figure 1.10b), ristocetin A, avoparcin as well as the polypeptide thiostrepton and rifamycin B have been used for the preparation of chiral HPLC phases[55-58].

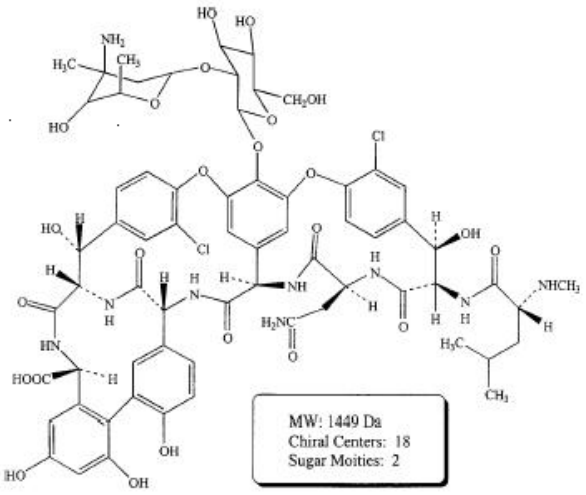


**a.**

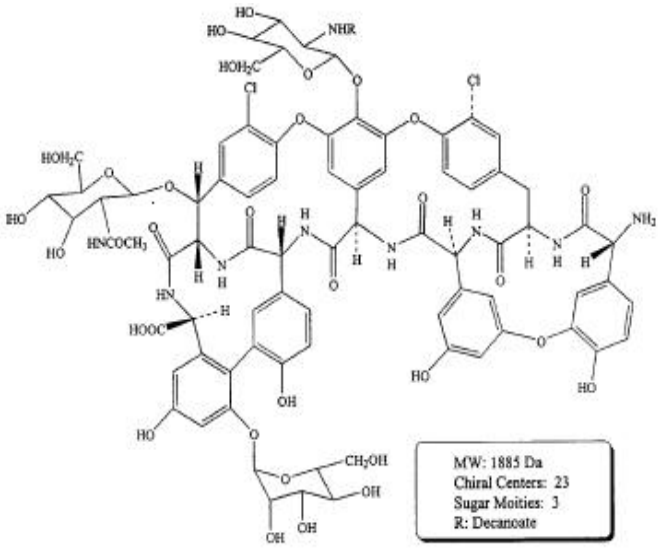


**b.**

**Figure 1.10. Structure of macrocyclic antibiotics; (a) vancomycin, (b) teicoplannin.**

These possess several characteristics that allow their interaction with the analyte. A large number of stereogenic centres and functional groups enhance the possibilities of multiple interactions with the analyte and hence much better chiral resolutions of many classes of compounds. Structurally they contain aglycone portion of fused macrocyclic rings, which forms a characteristic basket shape and carbohydrate moieties attached to the aglycone basket. The aglycone basket consists of three or four fused macrocyclic rings composed of linked amino acids and substituted phenols. The carbohydrate moieties consist of carbohydrate or saccharide groups. The glycopeptide antibiotics differ in the number and type of pendant carbohydrate groups[59]. The sugar groups attached to the aglycon basket are free to rotate and can assume a variety of orientations.

Vancomycin based CSPs were introduced first followed by teicoplannin based CSPs. They are commercially available under the name Chirobiotic V and Chirobiotic T (Astec). Derivatised vancomycin and teicoplannin based phases are also available now (Chirobiotic V2 and T2). The vancomycin CSP has been used to resolve a number of substituted racemic pyridones[60]; pyrimidine carboxylates (DHPMs) which are analogs of nifedipine-type dihydropyridine calcium channel, enantiomers of citalopram and its desmethylated metabolites in human plasma[61]; alpha and dansyl-amino acids[62]; cyclic imides, barbiturates, piperdine-2, 6-diones, and mephenytoin semisynthetic ergot alkaloids[63].

## 1.6 Synthetic polymers for chiral chromatography

Inherently chiral, naturally occurring polymers such as cellulose, amylose, chitin, chitosan etc. have been successfully used for the chiral separations. The efforts to mimic the properties of these materials in order to overcome the drawbacks of these materials as chiral resolving agents have opened up an enormous area of synthetic polymers. There are three broad classes of the synthetic polymers used for chiral separations namely; optically active polymers, molecularly imprinted polymers (MIPs), and polymers bearing pendant chiral ligands.

### *1.6.1 Optically active polymers*

The polymers of this class are generally synthesised using achiral monomers and chiral catalysts. It has been shown that by using lithium salts of non-racemic amines as anionic initiators, monomers such as triphenylmethyl methacrylate polymerise to give

stereoregular polymers of helical chirality[64, 65]. Copolymerisation of chiral acrylamides with ethylene diacrylate as cross-linking agent gave polymeric beads as CSPs[66–68]. These CSPs were not stable to high pressure and were only used for preparative purposes. This problem was circumvented through copolymerisation of chiral acrylamide with methacryloyl silica gel[69]. CSPs in the form of beads were also synthesised by polymerising monomers bearing amino acids and (-) menthone and (+) menthol[70]. A synthetic polymeric chiral stationary phase for liquid chromatography based on N,N'-[(1R, 2R)-1,2-diphenyl-1,2-ethanediyl] bis-2-propenamide monomer was prepared via a simple solution initiated radical polymerisation. This stable chiral stationary phase showed enantioselectivities for a large number of racemates in polar organic and normal phase modes and high sample loading ability[71]. A review by T. Nakano gives an account of chiral polymers being developed as stationary phases[72].

*1.6.2 Molecularly imprinted polymers (MIPs)*

Molecular imprinting is a technique for creating three-dimensional networks that have a "memory" of the shape and functional group positions of the template molecule. The resulting molecular imprint polymers (MIPs) can selectively recognize the template molecule used in the imprinting process, even in the presence of compounds with structure and functionality similar to those of the template[73, 74]. Wulff used the technique for the chiral separation in 1976 for the first time[75]. In this technique a template molecule is either attached covalently to the monomer and cleaved off upon polymerization leaving a cavity, or the template molecule is bound by electrostatic interactions to the monomer and can be removed by washing with suitable solvents[76]. Several imprinted polymers have been developed using monomers such as methacrylic acid and crosslinker ethylene dimethacrylate[77]. Other monomers used are 4-vinyl pyridine, 2-vinyl pyridine[78], etc. There are certain other polymers which have been developed for specific applications, for example, polymers such as polyphenols[79] poly(aminophenyl boronate)[80], poly(phenylene diamine)[81], poly(phenylene diamine-co-aniline)[82], polyurethanes[83], and overoxidised polypyrrole[84] have been used. Compared to polymers based on acrylic and vinyl monomers, the use of other polymers seems to be somewhat restricted due to their limited choice of available functional groups[85].

During the last few years, work with MIPs in chromatography was focused on two key aspects. The first of these is the synthesis of uniformly shaped and sized particles with narrow pore-size distributions and improved mass transfer properties. The second is the development of MIPs with better quality binding sites, ideally using stoichiometric ratios of the template and functional monomer.

Although, the MIPs are potential candidates for liquid chromatography there are certain lacunae in their commercialisation. They need enantiomerically pure templates for the entrapment; sometimes they could be so selective to specific substrate similar to imprint that it would become necessary to make imprinted polymer for each analyte to be tested, which is certainly not economical[86].

*1.6.3 Polymers bearing pendant chiral ligands*

Rogozhin and Davankov made first attempts to anchor L-proline onto crosslinked polystyrene[50]. The $Cu^{2+}$ chelate of this polymeric ligand was then used to resolve amino acids via ligand exchange mechanism[87-91]. A labile metal complex, (N-carboxymethyl-L-valine)copper (II)**,** which had been previously shown to coordinate L-amino acids more strongly than their D enantiomers, has been chemically bound to a styrene-divinyl benzene (S-DVB) copolymer. The resulting ligand-exchange resin has been used chromatographically to partially resolve several optically active amino acids. In all cases, the D enantiomers eluted first, and the degree of resolution increased with an increase in the bulkiness of the side chain on the α-carbon of the amino acid[92]. The lightly crosslinked resins showed high enantioselectivity and high exchange capacity. These however suffered from low pressure resistance and slow mass transfer. In order to overcome this problem Davankov et al. prepared chiral ligand exchange packings by bonding polystyrene chains bearing chiral ligands onto the suface of microparticulate silicas. The presence of silica surface in close proximity to the copper (II) ion chiral co-ordination site resulted in changes in the magnitude and the sign of enantioselectivity[93]. Adam et al. did a *in situ* modification of a commercial column from Waters for the resolution of amino acid racemates in order to avoid technical difficulties associated with the preparation of chiral column by the conventional method[94]. The mechanism of ligand exchange for resolution of DL- amino acids using S-DVB copolymers bearing different substituents and chiral ligand L-proline, was studied by Jin et al.[95] The S-DVB

copolymers were functionalised with N-phthloyl L-Leucine by Friedel-Craft acylation by reacting with N-phthloyl L-Leucine acid chloride[96]. Other than styrene polymers crosslinked poly(vinyl alcohol)[97], polyacrylamide[98], poly(vinyl pyridine) grafted with chiral ligands[99] were also used successfully as supports.

## 1.7 The matrix

The matrix or the support, which forms the major part of the stationary phases, must possess specific physical and chemical properties to be suitable as a stationary phase in HPLC. Such materials must have sufficient mechanical strength to withstand the high column pressure without breakage or deformation. Furthermore, the physical properties, e.g. pore size, porosity and particle diameter, must be controlled within narrow tolerances to enable the manufacture of reproducible packing materials. Especially the porosity is of great importance, since this determines the surface area and, together with other parameters, also retention and selectivity[100-104]. Besides these hydrophilicity, chemical stability, resistant to microbial and enzymatic degradation are also necessary. The matrix also should be easily modifiable. The most commonly used matrix is silica. The limited chemical stability of silica, however, is a major disadvantage and is one of the driving forces behind improved synthesis strategies[105]. This is also stimulating the ongoing research for alternative, more stable substrates. Many supports based on synthetic, cross-linked, macroporous polymers are available nowadays. Besides biopolymers like agarose, cellulose, dextran, pullulan, etc, synthetic polymers have been used extensively as support materials for affinity chromatography. They offer some advantages over biopolymers. They typically have superior chemical and physical stability. Most polymeric matrices can withstand changes in ionic strength or buffer composition. Many are stable in organic solvents and can tolerate extremes in pH without decomposition[106]. An additional advantage is that reactive groups can be easily incorporated onto polymer during the polymerisation process itself. Incorporation of monomers with suitable functional groups can provide activation sites on these supports for ligand immobilisation. Usually monomers containing primary and secondary hydroxyl groups are used to prepare synthetic supports. Presence of hydroxyl groups offers both suitable coupling chemistries as well as hydrophilicity to the matrix. Desired

properties can be obtained by proper choice of monomers and polymerisation conditions. The most widely used synthetic polymers are vinyl (acrylic) polymers.

### *1.7.1 Methodologies to obtain porous beaded polymers*

Among the various techniques for the preparation of macroporous polymers, one can distinguish, three different routes: The first involves the use of gases as the void-forming medium. The second approach is based on the intermediate of emulsions, formed by tailor-made block-copolymers and the subsequent removal of the dispersed phase (synthetic strategies for porous polymers). The third category is classified by the use of a phase separation process to generate a two-phase morphology, finally resulting in a porous morphology. The latter processes are described below in detail.

### *1.7.2 Synthetic strategies for porous polymers*

Chemically the porous, beaded polymers can be obtained by suspension, emulsion and dispersion polymerisation; suspension being the most frequently used. Emulsion and dispersion polymerisation products are useful for coatings and adhesives while the particles prepared by suspension polymerisation are often used in molding plastics, as matrices for ion exchange resins and as flocculating agents[107].

#### *1.7.2.1 Suspension polymerisation*

The suspension polymerisation technique has generally been used for the preparation of macroporous copolymer networks in the form of beads of diameter ranging from 0.1 and 1 mm, with the majority in the range 200-600 μm. Hoffman and Delbruck first developed suspension polymerisation in 1909[108]. In suspension polymerisation the initiator is soluble in the monomer phase, which is dispersed by commuting into the dispersion medium (usually water) to form droplets. The solubility of the dispersed monomer (droplet) phase and also the resultant polymer in the dispersion medium are usually low. The volume fraction of the monomer phase is usually within the range 0. 1-0. 5. Controlled agitation and the presence of drop stabilisers are necessary to maintain the suspension. When water insoluble monomers are dispersed in water as continuous phase it is termed as oil-in-water (o/w) suspension. For water-soluble monomers like acrylamide, hydroxyethyl methacrylate etc. the dispersant phase can be oil, which makes them water-in-oil suspensions (w/o). This process is also known as inverse suspension polymerisation.

Suspension polymerisation usually requires the addition of small amounts of a stabiliser to hinder coalescence and break-up of droplets during polymerisation. The size distribution of the initial emulsion droplets and, hence, also of the polymer beads that are formed, is dependent upon the balance between droplet break-up and droplet coalescence. This is in turn controlled by the type and speed of agitator used, the volume fraction of the monomer phase, and the type and concentration of stabiliser used. If the polymer is soluble in the monomer, a gel is formed within the droplets at low conversion leading to harder spheres at high conversion. If the polymer is insoluble in the monomer solution, precipitation will occur within the droplets, which will result in the formation of opaque, often irregularly shaped particles. The most important issue in the practical operation of suspension polymerisation is the control of the particle size distribution. The size of the particles will depend on the monomer type, the viscosity change of the dispersed phase with time, the type and concentration of stabiliser and the agitation conditions in the reactor. In the case of large monomer droplet in the continuous phase, nucleation predominantly occurs in the droplets and each polymerising droplet behaves as an isolated batch polymerisation reactor. The notation suspension polymerisation is reserved for systems where nucleation occurs in the monomer droplet and the average number of radicals per particle is very high ($10^2$ to $10^6$). This is usually obtained if the droplets are larger than 1 μm. In principle, in the suspension polymerisation process, large particles are obtained. But the suspension polymerisation of vinyl monomers generally also results in a small fraction of polymer particles below 1 μm as well as large beads[109]. The small particles were thought to be the result of nucleation in the aqueous phase and subsequent latex polymerisation. Smaller droplets are thermodynamically less stable than larger ones and undergo Ostwald ripening. The addition of hydrophobe lowers the chemical potential and prevents the diffusion of the monomer to large droplets. This leads to bimodal particle distribution with one fraction below 1 μm and the other one can be adjusted between 20 and 500 μm[110].

The type and concentration of the suspending agent plays an important role in the tendency of droplets to coalesce. As the suspension polymerisation proceeds, the viscosity of a monomer–polymer droplet increases with conversion. Hence, the physical behaviour of the droplets is not the same during the process. When dispersible material is

added to the existing stabilised drops, the new material and existing drops can remain segregated for significant amounts of time[111]. The increasing viscosity of the suspended droplets, as polymerisation proceeds, makes the quantitative analysis of suspension polymerisation a complex problem[112]. It is possible to establish a number of special factors, apart from the free-radical polymerisations that exert an important influence on particle size and particle size distribution[113-115]:

1. Geometric factors of the reactor such as profile, type of stirrer, stirrer diameter D relative to the reactor dimensions, bottom clearance of the stirrer, and internal fittings.
2. Operating parameters: Stirrer velocity N, stirring and polymerisation time, phase volume ratio φ, fill level of reactor and temperature T.
3. Substance parameters: Dynamic viscosities $\eta_c$ and $\eta_d$, and densities $p_c$ and $p_d$, of the continuous and discontinuous phases, and the interfacial tension σ.

The weight ratio of the discontinuous monomer phase to the continuous water phase varies from 1:1 to 1:4 in most commercial processes. Lower ratios are not limited but are seldom practical for economical production. Use of higher ratios is excluded, by the proportion of water being insufficient to fill the volume between the monomer droplets[106]. In most cases bulk viscosity of the slurry is near that of water, which allows good mixing of the reactor contents, thereby improving the heat transfer in polymerisation reactor. The generation of pores during suspension polymerisation is disussed in the next section.

*1.7.2.2 Porosity and surface area*

It is now well understood that a phase separation during the formation of the network is mainly responsible for the formation of porous structures in a dried state. In order to obtain macroporous structures, a phase separation must occur during the course of the crosslinking process so that the two-phase structure is fixed by the formation of additional crosslinks[116]. The free-radical crosslinking copolymerisation system for the production of macroporous copolymers includes a monovinyl monomer, a divinyl monomer (crosslinker), an initiator and inert diluent. The decomposition of the initiator produces free radicals, which initiate the polymerisation and crosslinking reactions. After a certain reaction time, a three-dimensional network of infinitely large size may start to

form. The term ‘infinitely large size', according to Flory[117], refers to a molecule having dimensions of an order of magnitude approaching that of the containing vessel. At this point (the gel point) the system (monomer–diluent mixture) changes from liquid to solid-like state. Continuing polymerisation and crosslinking reactions decreases the amount of soluble reaction components by increasing both the amount and the crosslinking density of the network. After complete conversion of monomers to polymer, only the network and the diluent remain in the reaction system.

The internal structure of the resin beads can be controlled by different parameters in the polymerisation process, such as amount of crosslinking monomer used, type and volume of diluent/ porogen/ pore generating solvent added to the monomer phase. Three main classes of porogens are known: (i) solvents for the polymer structure (e.g. toluene in case of S-DVB copolymer resins); (ii) non-solvents for the polymer (e.g. aliphatic hydrocarbons, organic alcohols in case of S-DVB copolymer resins) and (iii) polymer soluble in monomer. The last option gives only large pores. The molar mass of the porogen is then an important parameter. The pore volume is large (up to 1 mL/g) when the molar mass is high[118]. When solvating diluent is used, large amounts of diluent and crosslinking agent are necessary to get permanent porosity. In such conditions high surface areas, in excess of 500 $m^2/g$ and a narrow distribution of very small pores (10 nm), are obtained together with a limited pore volume (around 0.3 mL/g) of large-size pores[119]. The most complex and often studied case is where a non-solvating diluent is used as porogen. Then, as initially proposed by Kun and Kunin[120] and later on experimentally observed by Jacobelli and coworkers[121], the bead contains large agglomerates of microspheres (100-200 nm), which look like cauliflowers, and each microsphere shows smaller nuclei (10-30 nm) more or less fused together. In between the nuclei, there is a first family of very small pores (5-15 nm), which are mainly responsible for the high surface area of these materials. In between the microspheres, a second family of intermediate pores (mesopores) is observed (20-50 nm) which may account for moderate surface areas (up to 100 $m^2/g$). A third family of large pores (50-1000 nm) is located between the agglomerates. This family is responsible for the high pore volumes (up to 3 mL/g), which can be achieved, mainly when the amount of diluent is high. This structure of macroporous resin is illustrated in Figure 1.11 [119].

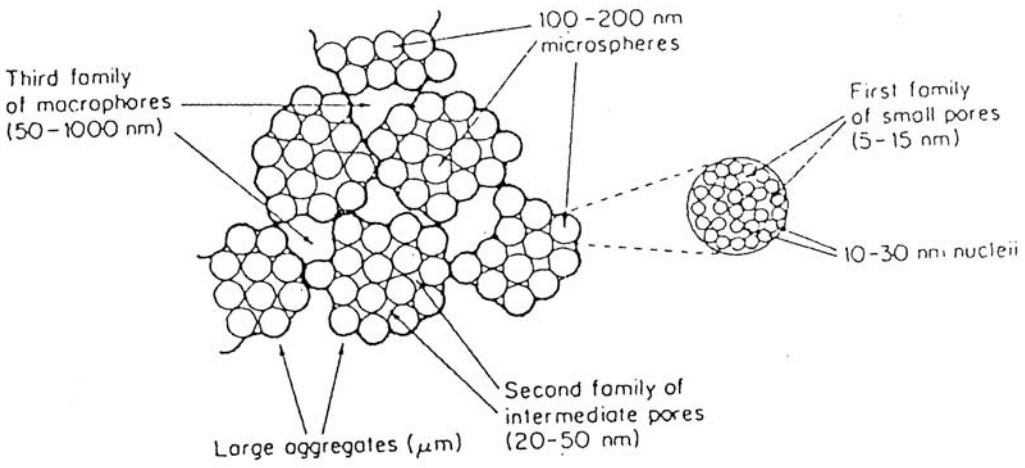


**Figure 1.11. Schematic representation of the structure of macroporous domain.**

*1.7.2.3 Particle size*

In chromatographic processes, flow properties of column are governed by the particle size, particle size distribution and rigidity of the column material. There is no exact theory that can be used to predict and control the size and size distribution of the particles for the suspension polymerisation process. This is mainly because of two reasons. First, the design of reactor and stirrer plays a very important role in determining the shear distribution at various locations inside the reactor. Secondly, the characteristics of the system change during the polymerisation because of the very large increase in the viscosity inside the discontinuous phase.

There are a number of factors that determine particle size. For example, small particles are obtained by increasing the water /monomer ratio or diluting the organic phase with a solvent for the polymer to be produced. Increasing amount of crosslinker has the opposite effect. However, the two most important factors that control this are the choice of the suspending agent and the stirring process. A typical water-insoluble organic monomer has a lower surface tension than water. When such a monomer is mixed continuously as a dispersed phase in a continuous phase of water with no surfactants present, an unstable dispersion forms due to the continuous breakup and coalescence of monomer droplets. If the agitation stops, the monomer - water system will separate into two phases.

Two types of suspending agent (stabiliser) known are: (i) Water soluble suspending agent and (ii) Water insoluble suspending agent. Water-soluble stabilisers include organic polymers, both natural and synthetic polymers. Organic polymers, which are insoluble in monomer droplets and have relatively low solubility in the suspension medium, are highly effective as droplet stabilisers. Among the most commonly used organic stabilisers for o/w suspension system are poly(vinyl pyrrolidone) and poly(vinyl alcohol). A wide range of other water -soluble polymers such as methyl cellulose, gelatin and natural gums are also used[122]. As the polymeric stabiliser dissolves in the aqueous phase, it acts in two ways. First, it decreases the interfacial tension between the monomer droplet and water to promote the dispersion of droplets. Second, the stabiliser molecules are adsorbed on the surface of the monomer droplets to produce a thin layer, which prevents coalescence when a collision occurs. Insoluble suspending agents are mostly inorganic powders, which include talc, bentonite, calcium sulphate etc. In general a small concentration of surfactant is sufficient. Large addition of surface-active agents prevents formation of polymer beads by leading to emulsion polymerisation and latex formation. Another important processing factor, the stirring process is very effective, especially during the sticky period of polymerisation. Agitation must be sufficient to redisperse droplet pairs and clusters. It must also be sufficient to prevent separation of the dispersion because of differences in specific gravity between two phases. Generally, particle size decreases with increasing rate of agitation, in a given system.

Advantages of suspension polymerisation process, compared to other polymerisation processes (bulk, solution and emulsion), are: (i) easy heat removal and temperature control; (ii) low dispersion viscosity; (iii) low levels of impurities in the polymer product; (iv) particle size can be controlled to a fairly narrow range; (v) the ratio of surface area to volume for small drops or particles is relatively high and local heat transfer is good and (vi) low cost of conversion with flexibility to vary the particle properties. The disadvantages of suspension polymerisation are: (a) polymer build up on the reactor wall, baffles, agitators and surfaces; (b) waste water problems; (c) difficulty in producing homogeneous copolymer composition; (d) lower productivity for the same reactor capacity (compared to bulk) and (e) application only to free radical processes. Agitation is critical because as the viscosity within the bead rises, the reaction rate

increases suddenly (Trommsdorff effect). This leads to a surge in heat generation, which does not usually occur in solution or emulsion polymerisation. Problems associated with continuous suspension polymerisation process are deposition of polymer on the wall of the reactor during polymerisation (which affects the heat transfer through the reactor jacket) and difficulty in achieving high conversion.

The development of organic polymer-based sorbents for HPLC is much more limited because of the microparticulate size. The polymers to be used as HPLC sorbents need to possess uniform particles in the range of 1-10 μm[123-125]. Suspension polymerisation can be used to produce large particles but with broad size distribution. Dispersion polymerisation was found to be an alternative method of preparing monodisperse particles, however is limited to noncrosslinked or very slightly crosslinked polymer particles. The processes were studied in detail and the characteristics of the products were found to be related to their unique particle formation mechanism[108, 126-133].

*1.7.2.4 High internal phase emulsion polymerisation*

When water is added slowly to a stirred solution of a surfactant of low hydrophilic–lipophilic balance dissolved in the oil phase, an internal phase volume of water up to 99 % is achievable, and, in this state, the water droplets in the oil phase strongly interact[134]. When the continuous oil phase is composed of a monovinyl–divinyl monomer mixture, the crosslinking polymerisation in the continuous phase results in a solid crosslinked polymer, which contains the water droplets[135]. Removal of the water droplets by washing with ethanol, and vacuum drying, yields a highly porous monolith of extremely low density (about 0.2 g/mL compared to 1.1 g/mL) polymer[135, 136]. This porous material has an open pore structure indicating that there are holes in the walls separating the water droplets. Such porous materials are called PolyHIPE (HIPE; water-in-oil high internal phase emulsion).

The high internal phase emulsions are known for many years. These highly concentrated emulsions were also known as High Internal Phase Ratio Emulsions (HIPRE), aphrons, biliquid foams, hydrocarbon gels and gel emulsions[137]. They can be defined as emulsions in which the dispersed phase occupies more than 74% of the volume, which is the maximum packing fraction of monodispersed spheres. The

continuous phase constituted of monomers and crosslinkers occupying less than 26% of the final volume. The polymerisation of the monomers in the continuous phase leads to porous material known as PolyHIPE. They can be produced easily using a simple procedure. The discontinuous phase (water) is added slowly to the continuous phase i.e. mixture of monomer and the crosslinker along with the surfactant and initiator. The mixture is agitated during addition at very high speed in order to break up large droplets to smaller ones. After the addition of internal phase is complete, the emulsions are subjected to curing. The total porosity achievable using this technique is upto 99 % as opposed to conventional polymerisation techniques. Their defining characteristic is an internal (droplet) phase volume ratio of greater than 96%, this number representing the maximum volume that can be occupied by uniform spheres when packed into a given space in the most efficient packing arrangement as shown in Figure 1.12. In HIPEs, therefore, the droplets are either spherical and polydisperse, or are deformed into polyhedrons as shown in the Figure 1.12. The materials are themselves are highly porous and, usually, extremely permeable, due to a very high degree of interconnection between cavities throughout the matrix[138].

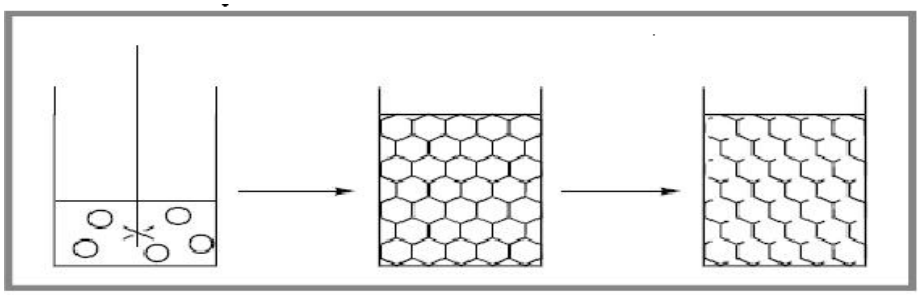

**Figure 1.12. Schematic diagram of formation of HIPE.**

These emulsions tend to be unstable because of higher ratio of water to oil. However, selection of appropriate monomer/crosslinker concentration, temperature and agitation conditions controls the formation of stable emulsions. Slight changes in any of the parameters can cause emulsions to separate into distinct oil and water phases.

Recognising the practical significance of concentrated emulsions, Lissant, Nixon and Beerbower and many others studied their potential utility in a range of applications [139]. Efficient methods to prepare highly stable emulsions were developed. Numerous patents dealing with high internal phase ratio emulsions have been awarded to Lissant

from 1967 onwards. An early application of the HIPEs is for a suspension medium for solids[140]. The high static viscosity of HIPEs prevents particles from settling and hence can be used as transport fluids for particulates through pipelines[141]. The emulsions were then used to prepare isotopic, open cell, polymeric foams by polymerisation and the process was patented by Unilever in 1982[135]. The materials have found a variety of applications such as membranes[142], an alternative to hollow fiber membrane modules [143], absorbents[144] and demulsifiers for highly stable dispersions[145]. Refinement of the manufacturing process resulted in a technique whereby either very small pore sizes (<1 μm) or very large pore sizes (>60 μm to ~ 1 mm) of porous polymers could be obtained[146].

.

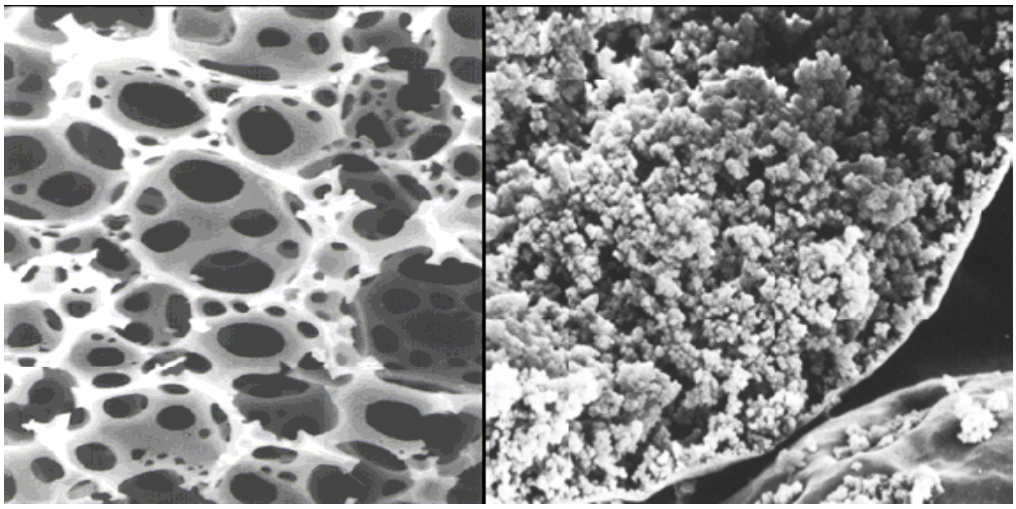

**a.** **b.**

**Figure 1.13. a. SEM photomicrograph of typical macroporous resin formed by polymerising HIPE. Larger, regular cavities interconnected by smaller pores are seen. b. Internal structure of the macroporous resin formed by conventional polymerisation techniques, as revealed by SEM. The pores are irregular and a skin can be seen at the periphery of the bead, which limits their use in certain application like chromatography.**

The major application of porous polymeric foams is absorbent materials for diaper type articles for absorbing body fluids. A number of patents have been filed in this area by various companies like Procter and Gamble, Dow, Pharmacia, Biopore etc. An attractive feature of these materials to be useful as absorbent material is their high void volume and low density. For example a 98 weight percent internal phase HIPE can

produce foam with 49 g capacity for water per gram of foam assuming foam density 1g/cm$^{3}$, [147]. The g/g capacity of the foam can be increased by increasing the void volume, which in turn can be achieved by increasing the internal phase ratio of the emulsion or by including inert oil in the external phase. The typical porous foam formed by polymerising HIPE is shown in the Figure 1.13

The HIPE structures are characterised by the presence of very large pores of micrometer dimensions ("cavities") as opposed to pores associated with microporous or macroporous polymers having only Angstrom dimensions. Furthermore, these large cavities are interconnected by a series of smaller pores, thereby enabling each to communicate with those adjacent. The void size is determined by emulsion droplet size immediately before gelation. More stable emulsions have higher interfacial area, therefore smaller droplets. Foam structure is templated from the emulsion structure.

Los Alamos National laboratory started work with HIPE polymerised foams in the mid 1980s and has developed an extensive knowledge base on HIPE technology. These efforts primarily have been focused on the variation of S-DVB HIPE systems to produce structural foams having glass transition temperature of ~ 100 °C. Such materials are useful as heat resistant in the aerospace industry during processing and use[148]. Another attractive feature of these materials, which makes them useful in a variety of applications including supports for chromatography, is their production in different forms like blocks, films, sheets, etc. Since PolyHIPEs are produced by a simple moulding process, in which the liquid precursor emulsion is placed in some polymerisation vessel or mould, a wide range of sample shapes and sizes is available.

The morphology of the resulting foams at the interface between the mould surface and emulsion was shown to be dependent on the type of the material used as mould. PTFE was found to be suitable material since it produces foams with open cellular morphology at the mould surface[149]. Glass, polypropylene and PVC were less useful as they produced foams with the skin on the surface, thus hampering their porous properties. The use of these foams as solid supports in catalysis and chromatography was however limited because of their low surface areas. Their surface areas were in the range of 3-20 $m^2$ /g. The chromatographic supports however require large surface areas (200-300 $m^2$ /g). The high surface areas provide increased solute retention and selectivity together

with a superior loading capacity and, consequently, a wide dynamic range of analysis. Incorporation of a water immiscible, non-polymerisable organic solvent along with a high crosslinker content produced porous materials with surface areas as high as 350 $m^2/g$.

Choosing the appropriate solvent depending upon the solubility parameter could control the mechanical properties of these polymers. Another problem associated with large-scale production of HIPE polymers is removing the surfactants and residual monomers from these low-density highly absorbent materials. In order to overcome these difficulties the HIPE emulsions are polymerised using suspension polymerisation. The resulting microbeads thus formed possess the cellular structure similar to typical PolyHIPE. Also the beads formed are skinless and can be easily washed to remove the unpolymerised emulsion components[150].

The most investigated base material is polystyrene crosslinked with divinylbenzene. The other hydrophobic water immiscible monomers include ethylhexyl acrylate, ethylhexyl methacrylate, butyl acrylate and isobornyl acrylate. The w/o emulsions of relatively low hydrophobic monomers are usually not stable because of the partitioning of the organic phase. However, o/w emulsions of these monomers can be polymerised. Use of supercritical carbon dioxide was found to be useful for making polyHIPEs with hydrophilic monomers[149]. The porous polymers can be functionalised using appropriate reaction conditions by polymer analogous reactions. Many simple organic reactions can be used to activate support for the desired application.

### *1.7.3 Use of phase separation techniques to obtain porous polymers*

This concept of porogenesis relies on polymer-solvent phase separation processes. The phase separation can be induced throughout polymerisation and cross-linking in different ways: (a) by addition of a non-solvent to a polymer/solvent mixture (e.g. immersion techniques), chemically induced (e.g. the polymerisation is performed in a monomer/non-solvent mixture, the polymerisation itself depletes the monomer, and insolubility is induced), and (b) thermally induced phase separation (TIPS).

#### *1.7.3.1 TIPS (Thermally induced phase separation)*

TIPS is one of the techniques, which has been extensively used for making porous membranes and foams for various applications. The method was first introduced by Castro in the late 1970s and early 1980s[151, 152]. The basic idea behind this technique is to

utilise heat as a latent solvent; in contrast, in the phase-inversion method, a non-solvent is added to the system. By lowering the temperature of an appropriate polymer solvent system, phase separation can be induced, i.e., a transition from a one-phase homogeneous solution to a two-phase heterogeneous system[153]. This technique has been applied to produce low-density microcellular foams, thermally reversible porous gels, uniform porous membranes, and asymmetric membranes[154-161]. Industrially important membranes of particular interest are the membranes that can withstand high temperatures and harsh chemical environments, and membranes that have narrow pore size distribution. Specific targets are improved membranes for biological separations (such as hemodialysis and virus removal from blood), more robust membranes for industrial process streams, and more efficient separators for lithium ion batteries and NiCd batteries. There are some distinct advantages of using TIPS for membrane formation like: (1) application to a wide range of polymers, including those that can not be easily cast due to the lack of suitable solvents; (2) generation of a variety of microstructures, including relatively thick isotropic structures suitable for controlled release; and (3) relative ease of process control[162]. Several studies about the membrane formation by the TIPS process have been devoted to the mechanisms of phase separation, including the effects of diluents and polymer molecular weight, as well as the concentration and temperatures profiles[163]. Besides these TIPS also can be used for making porous particles. By changing the reaction parameters like solvents e.g. hydrocarbons, alkyl esters, phenyl ethers etc., total solids content, aging time, temperature and also the cooling time, the particles with narrow particle size distribution and different pore volumes could be obtained[164, 165]. Microporous polymers in different forms like films, sheets, blocks can be obtained from a number of polymers using the TIPS process[166].

Compared with numerous works on the membrane preparation by the TIPS process, there have been reported a few studies on the particle formation. Schaaf et al. prepared polymer particles from crystallization of semidilute solutions of polyethylene in poor solvents by the TIPS process[167]. The morphologies reflected the interplay of a liquid–liquid phase separation process and nucleation of the polymer crystals. Liquid–liquid phase separation phenomena that take place prior to crystallisation could induce characteristic polymer morphologies. They also observed that the homogenous and

heterogenous nucleation results in smooth and rough globules respectively. Hou and Lloyd reported the preparation of fairly uniform particles of nylon[168]. The phase separation was done by taking a 1~wt% solution in a θ solvent above the θ temperature and cooling it rapidly. The surface roughness of the particles was dependent on the kind of nylons.

*1.7.3.2 Morphology and generation of pores during TIPS*

Liquid-liquid demixing processes play an important role in most of the TIPS processes. In addition, crystallisation of the polymer from solution, gelation (and vitrification) of the polymer solution, and associations between the components in solution can occur. Some of these processes can also induce the formation of structures in solution. The combinations of liquid-liquid demixing with crystallisation of the polymer, vitrification, association, and also crystallisation of the solvent are of special importance for the generation of porous structures[169].

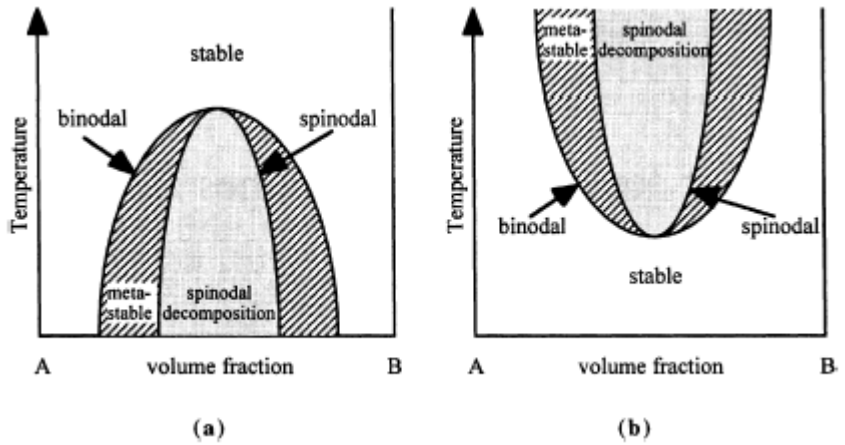


**Figure 1.14. Schematic phase diagrams displaying: (a.) upper critical solution temperature (USCT) behavior; (b.) lower critical solution temperature (LCST) behaviour.**

The schematic phase diagrams shown in Figure 1.14 contain two lines and several regions: The inner line is called the *spinodal line* and the outer line the *binodal line*. The binodal line results from the free energy curve by interconnecting all the points having a common tangent as a function of the temperature. Hence, this represents the equilibrium or coexistence curve. Entering the *metastable region*, which is limited by the spinodal and binodal line, will initiate phase separation, which will proceed via a *nucleation and*

*growth mechanism*. Similar to the construction of the bimodal line, the spinodal line results from the summation of inflection points of free energy curves as a function of temperature. If the area enclosed by the spinodal line is entered, the phase separation will take place via *spinodal decomposition.*

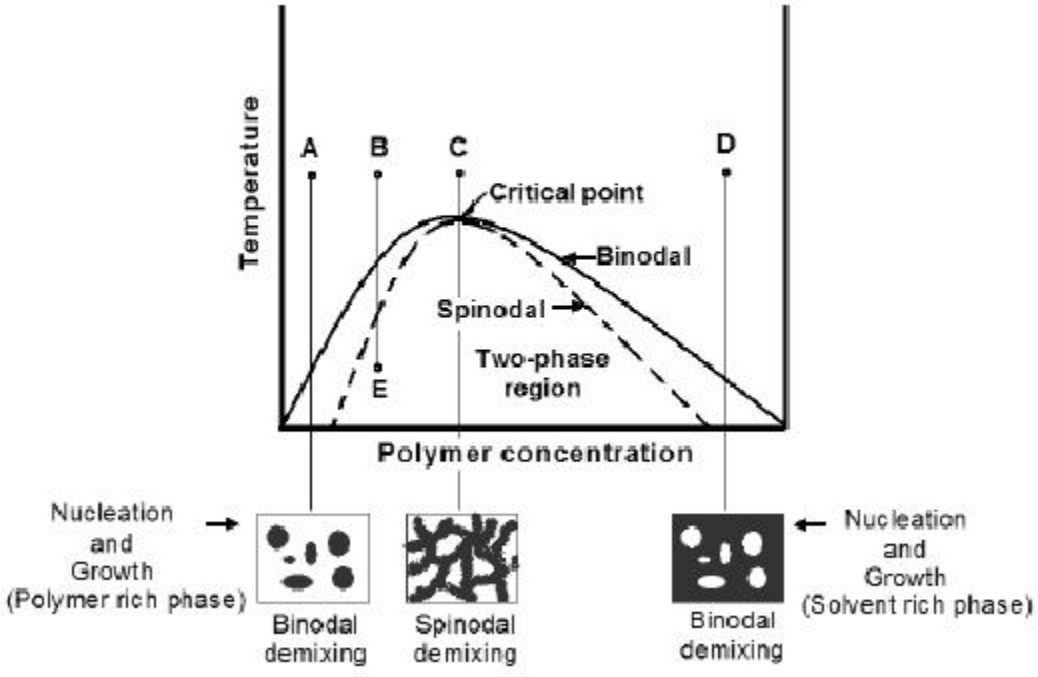


**Figure 1.15. Temperature composition plot for polymer solution with UCST.**

The temperature-composition plot for a polymer solution with an UCST as shown in Figure 1.15 can be used to understand the mechanisms that form the porous morphologies. Points A, B, C and D represent homogeneous solutions with increasing polymer concentration. The region under the binodal curve (thick curve in Figure) represents a two-phase region, which the homogeneous polymer solution phase separates into polymer rich and polymer lean phase (miscibility gap) upon decreasing the temperature. The dotted curve is the spinodal curve that demarcates the two-phase region into metastable and unstable states. The region under the spinodal curve represents the unstable state and region between spinodal and binodal curve represents the metastable state. The significance of the metastable and unstable states is that the mechanisms by which phase separation takes place are different in these regions. The initial compositions

and the temperatures through which the system passes through determine the mechanism of phase separation in these systems. For example, when the temperature of the polymer solution of composition A is reduced to induce phase separation, the system undergoes demixing in the metastable region by binodal decomposition via nucleation and growth of polymer rich phase as shown in the left hand side of Figure 1.15. Similarly, the demixing of polymer solution of composition D takes place by binodal decomposition via nucleation and growth of polymer lean phase. In contrast, the polymer solution of critical composition C when quenched passes through the critical point and phase separates purely by spinodal decomposition, which usually results in an interconnected morphology. Thus, by varying the temperature and composition of the polymer solution, demixing can be carried out via different phase separation mechanisms that form the nanoporous morphologies. Point B represents a typical polymer solution used in the synthesis of nanoporous polymers using this technique. This solution when cooled along the path BE, passes through both the metastable region where demixing takes place by binodal decomposition and then through the unstable region where demixing takes place by spinodal decomposition. Thus, the cooling rate would be an important parameter in determining the final porous morphology. If the cooling rate were high, phase separation would be predominately by spinodal decomposition. In contrast, if the cooling rate were slow enough for the formation of a nucleus, phase separation would be dominated by binodal decomposition. The other important factor is the quenching period i.e. amount of time allowed to attain equilibrium conditions. During this period, diffusion mechanisms like ripening and coalescence, which result in densification of these morphologies, become important[169].

As the mechanism of particle growth for the crystalline polymers is mainly nucleation and growth, it is possible to control the particle size, porosity etc. by controlling the crystallisation by varying parameters like polymer concentration, cooling rate and addition of nucleating agent. It is known that the coherent foams of isotactic polypropylene are not formed unless nucleating agent is added[170]. One U.S. patent discloses a method for making microporous films by incorporating a nucleating agent in a melt blend of a thermoplastic polymer and a compound miscible at the melting temperature of the polymer. Also, when the nucleating agent was used while preparing

microporous material from thermoplastics it was seen that the particle size was reduced to about 85% of the size of the particles where no nucleating agent was added. Moreover, it induced excellent stretchability, tensile strength and higher porosity in the material[171]. Another patent describes a back sheet of the sanitary products made using polypropylene with a nucleating agent. The patent uses a combination of primary and secondary nucleating agents to achieve a satisfactory overall balance of the film properties like permeability and mechanical strength. The incorporation of a nucleating agent makes the films stronger and more permeable than equivalent films without a nucleating agent[172].

## 1.8 Nucleating agents and heterogenous nucleation in polypropylene

Polypropylene, a low cost polymer, can be used in a wide variety of applications when rendered transparent with the addition of nucleating agents. The transparent PP is useful as disposable surgical products, packaging materials for food grade materials and polymer films. Heterogeneous nucleation of polypropylene has a marked effect on its transparency and tensile strength. The polymer, due to its partially amorphous nature, is not inherently transparent. The nucleating agents are therefore used to improve the clarity of the products like sheets, films, bottles, syringes etc. The nucleating agent employed serves the important function of inducing crystallisation of the polymer from the liquid state and enhances the initiation of polymer crystallisation sites so as to speed up the crystallisation of the polymer. As the nucleating agent serves to increase the rate of crystallisation of the polymer, the size of the resultant polymer particles or spherulites is reduced[172].

A large number of potential nucleating agents have been tested on polypropylene over four decades. The nucleating agents belong to various categories ranging from talc to inorganic salts of allylic and aromatic carboxylic acids and metallic benzoates[173-175]. A new class of nucleating agents based on sorbitol derivatives, which enhances the processing properties of PP greatly, was developed a few years back (Figure 1.16). The nucleating agents are dibenzylidene derivatives of sorbitol (DBS). Unlike conventional nucleators, which are dispersion type, DBS compounds are dissolution type nucleators, which must be melted and uniformly dissolved in the resin at a temperature higher than the melting point. Hamada and Ychiyami first used DBS to improve transparency in polyolefin plastics[176]. Ever since several modifications of DBS have been proposed to

improve its performance and the properties of the resultant polymers. There are two kinds of modifications employed in DBS usage. The first modification is to change the structure of DBS itself, while the second is to couple DBS with some other additive. Most of the structural changes proposed for DBS are made on either benzylidene group and ions are substituted at one or more positions in the benzene ring.

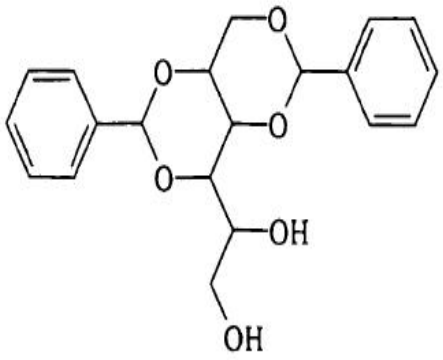


**Figure 1.16. Structure of dibenzylidene sorbitol.**

*1.8.1 Advantages of nucleated crystallisation*

Crystallisation of polymers using nucleating agents provides a number of advantages, which are discussed below.

a. Reduction in cycle time of injection molding**:** The time taken for injection molding processes are much lesser compared to non nucleated samples.

b. Increase in elasticity modulus**:** During spherulite growth a tie molecule is formed when one end of the polymer molecule is incorporated into one end of the spherulite or lamella and the other into another spherulite or lamella. Thus, a molecular bridge between the lamellae or spherulites is formed. This in turn increases the strength to separate one spherulite from other. These taught tie crystals substantially increase the small elasticity modulus of the amorphous layer. When a large number of spherulites are formed due to nucleating agents, they increase the number of tie molecules resulting in the enhancement in the elasticity modulus.

c. Haze reduction**:** Larger crystals tend to scatter the light. Light passes through the smaller and evenly sized crystals with the size of the order of wave length of light[177]. The effect of nucleation on the spherulite size is shown in Figure 1.17.

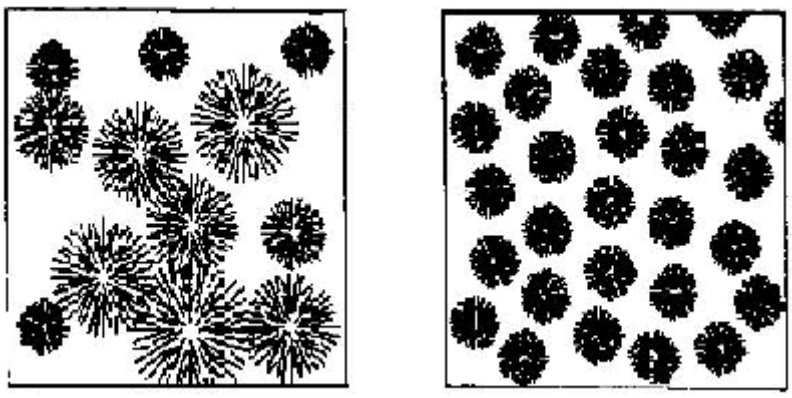

**Figure 1.17. Crystallisation without and with nucleating agent.**

The role of heterogenous nucleation of PP so as to induce porosity in the polymer has been studied in the present work. The porous properties of the resultant particles render them useful as supports for enzyme binding. The porous polypropylene has been extensively used as support for the immobilisation of lipases.

## 1.9 Lipases as biocatalysts

Lipases hold considerable promise in synthetic organic chemistry and have already found practical applications in detergents, oleochemistry, cheese production, medical therapy, and industrial synthesis of speciality chemicals. By now, lipases from over 30 biological sources have been cloned, sequenced, and expressed in host organisms. Lipases from various sources are now available in free or immobilised form or as part of a screening set (e.g. Chirazyme from Boehringer 36 Mannheim). Even cross-linked crystals of *Candida rugosa* and *Psedomonas cepacia* lipase (ChiroCLEC) are commercially available from Altus (Cambridge, MA). The tertiary structures of twelve lipases have been resolved and this now allows a more rational approach to modify lipases for specific applications.

Lipases (triglycerol hydrolases, E.C. 3.1.1.3) constitute an important class of enzymes in biocatalysis. In addition to plant and animals, in which these enzymes are widespread, many microorganisms are also capable of actively producing these enzymes in both exogenous and endogenous forms. Lipases catalyse a series of different reactions. In fact, although they were designed by nature to cleave ester bonds of triglycerols with the concomitant consumption of water molecules (hydrolysis), lipases are also able to

catalyse the reverse reaction under microaqueous conditions viz, the formation of ester bonds between alcohol and carboxylic acid moieties. These two processes can then be combined in a sequential fashion to give rise to a set of reactions generally termed as interesterifications. Lipase catalysed reactions resemble closely the pathways designed by nature for the metabolism of living beings, and so the reaction mechanism and the processes associated with them may be viewed as more environment friendly than the bulk syntheses. Furthermore, lipases are capable of producing a wide range of products with potential high purity resulting from their substrate specificity and stereospecificity [178]. Being able to couple a wide range of specificity to a high regio and enantioselectivity and specificity, they have been used extensively in the area of organic synthesis[179-181]. Their capability of working at the oil-water interface makes them unique as compared to other hydrolases, which can act only in aqueous phase.

In general, cells produce lipases to hydrolyse the extracellular fats and lipases are specially structured to act at water/organic interface. For this reason lipases appear to have optimum property among the enzymes to operate in organic solvents, wherein the interface is between the insoluble enzyme with its essential water of hydration and the organic solvent containing the acylating agent. Their broad synthetic potential is largely due to the fact that lipases, in contrast to most other enzymes, accept a wide range of substrates. They are stable in non-aqueous organic solvents and depending on the solvent system used, they can be employed for hydrolysis or esterification reactions. In addition, lipases can accommodate a wide range of substrates other than triglycerides such as aliphatic, alicyclic, bicyclic, and aromatic esters including the esters based on organometallic sandwich compounds. Lipases react with high regio and enantioselectivity and although this view is clearly oversimplified and not valid for all types of esterases and lipases, it can explain the majority of the known applications of these enzymes in organic synthesis:

(i) Simple acylation and deacylation reactions under exceptionally mild conditions;

(ii) Synthesis of amides and peptides;

(iii) Tranesterification, diastereoselective esterifications or hydrolyses of lipids;

(iv) Regioselective reactions on polyfunctional compounds (polyols, sugars);

(v) Highly enantioselective synthesis of esters, half-esters, acids, lactones, and polyesters as well as

(vi) Highly enantioselective synthesis of alocohols, diols, polyols, and amines.

In neat organic solvent, the enzymes retain the minimum amount of water, which is necessary for their catalytic activity.Ten Molecules of hydrophilic solvents can enter the inner core of the macromolecule and eventually destroy the functional structure[182]. Water-immiscible solvents, containing water below the solubility limit (ca. 0.02 to10% by weight) are suitable for dry enzymes[183]. In other cases, more polar solvents or cosolvents improve the success of transformation. The use of organic solvents is seen to enhance the enantioselectivity[184] and thermostability[185] of the enzymes, probably due to restricted conformational flexibility. Conversely, some enzymes can lose or alter their enantioselectivity in organic media[186] indicating that the conformation of the enzymes is dependent on the polarity of the medium and that individually optimised reaction conditions have to be developed for each transformation. From all the above discussion it is evident that in an adequate organic solvent, the catalytic activity can be of comparable order in aqueous medium with low water media, but overall, the rates of such (in organic media) reactions are slow.

Irrespective of the aforementioned complications, the use of organic solvents is of great importance, since this adds a new perspective to the applicability of the enzymes for organic synthesis. The advantages are obvious: (i) high solubility of most organic substrates, (ii) transformations of water-sensitive substrates in organic solvents, (iii) choice of a wide range of nucleophiles for esterifications, aminolysis, oximolysis, or thiolysis etc. (iv) suppression of product or substrate inhibition when they can be retained in organic phase, (v) greater stability of the biocatalyst, (vi) ease of operation and easy removal of the insoluble catalyst.

Lipases possess both lipolytic and esterolytic activities. The reactions are reversible and with decreased amount of water in organic solvents several inter and trans-esterifications are possible. Besides this, they are cheaply available from many sources. However, there are limitations to the lipase activity in organic medium, which is mainly due to low solubility and aggregation. This causes reduction in the lipase activity because the active sites become inaccessible for the substrates[187 188]. To increase the number of

accessible active sites and thereby the activity, enzymes are often adsorbed on solid supports[189].

### *1.9.1 Lipase immobilisation on the solid supports*

Immobilisation of the enzyme on the solid support leads to many advantages in terms of operational and storage stability, facile recovery and recycling of the enzyme as well as use in continuous operations.

Lipases can be immobilised on different supports like inert solids, ion-exchange resins, or physically entrapped/encapsulated in solids, such as cross-linked gels, microcapsules, and hollow fibres[190]. The availability of polymers with varied functionalities, versatile chemical compositions and physical properties has made them excellent candidates as supports for enzyme immobilisation. Natural polymers including polysaccharides and proteins as well as synthetic polymers, such as polystyrene and polyacrylates[191], nylon[192] have been studied to immobilise enzymes. Silica based carriers are also widely used for the immobilisation of lipases[193]. Lipases have also been immobilised on microporous and macroporous polypropylene particles (commercially available as Accurel EP and Accurel MP)[194-197].

A wide variety of immobilisation techniques have been applied to lipases, including adsorption to solid supports, covalent attachment, and entrapment in polymers. Adsorption to a solid surface is the conventional and simplest method that emphasises on non-specific interactions between the enzyme protein and the support, which is brought about by mixing the concentrated solution of enzyme with the support[198]. Major advantage here is reduction of activation steps required, cheap, and less disruption of the enzymic protein than any other chemical means of attachment. Hydrogen bonds, multiple salt linkages and Van der Waal's are the only means involved in this sort of binding.

The desired characteristics of solid supports for enzyme attachment include large surface area, good chemical, mechanical and thermal stability and insolubility. The high surface areas of porous materials provide higher protein loading capacity. With porous solids, pore structures play an important role in efficient diffusion of solutions[199]. The present study deals with immobilisation of Lipase on porous poly(ethylene-co-propylene), generated through TIPS and enantioselective esterification of Naproxen by immobilised enzyme.

**References**


1. Biot. J. B., *Mem. Cl. Sci. Math. Phys. Inst. Imp. Fr.*, 13, 1 1812.
2. Pasteur L., *Ann. Chim. Phys.*, 24, 442, 1848.
3. Dennis E. D., *Clin. Research Reg. Affairs*, 18, 181, 2001.
4. Meijer E. W., *Angew. Chem. Int. Ed.*, 40, 20, 2001
5. Aitken R. A., Parker D., Taylor R. J., Gopal J. and Kilenyi S. N. in R.A. Aitken, S.N. Kilenyi (editors): "*Asymmetric synthesis"*. London, Glasgow, New York, Tokyo, Melbourne, Madras: Blackie Academic & Professional, 1992.
6. Hauptmann S., "*Organische Chemie"*. 2nd ed. Leipzig: VEB Deutscher Verlag fürGrundstoffindustrie, 1988.
7. Fischer E., *Ber. Dstch. Chem. Ges.*, 24, 2683, 1891.
8. Bijovet J. M., Peerdeman A. P., and van Bommel A. J., *Nature*, 168, 271, 1951.
9. Jacques J., Collet A. and Wilen S. H. in "*Enantiomers, racemates and resolutions*", Wiley-Interscience publication, pp. 4, 1981.
10. Collet A., Brienne M., and Jacques J., *Bull. Soc. Chim. Fr.*, 127, 1972.
11. Eliel E., Wilen S. and Mander L., "*Stereochemistry of organic compounds"*, Ch. 7, pp 309, 2003.
12. Davankov V. A., *Pure App. Chem.*, 69, 1469, 1997.
13. Zief M. and Crane L. J. Eds, "*Chromatographic chiral separations*", pp 3, 1988.
14. Wallworth D., *Chiral chromatography*, A review of the Chromatographic Society meeting, Chiral Separation Technologies; Held in Harlow, UK, 2005.
15. Ahuja S., in "*Chiral separations by chromatography*", American Chemical Society, Washington D. C., Ch. 1, 1991.
16. Easson L. and Stedman E., *Biochem. J.*, 27, 1257, 1933.
17. Ogston, A.G., *Nature*, 163, 963, 1948.
18. Koshland D. E., Jr., *Biochemistry and molecular biology education*, 30, 27, 2002.
19. Sheldon R.A., "*Chirotechnology*", Marcel Dekker, New York, 1993.
20. Testa B., *Trends in Pharmacological Science*, 7, 60, 1986.
21. Stinson S. C., *Chem. Eng. News*, 101, 1999.

22. Gal J., *CNS Specr*.,45, 2002.

23. Nguyena L. A., Hua H. and Pham-Huyc C., *Chiral Drugs*. An Overview, pham.huy.chuong@wanadoo.fr

24. Marzo A and Heftman E., *J. Biochem. Biophys. Met*., 54, 57, 2002.

25. Jamali F., Mehvar R. and Pasutto F. M., *J. Pharma. Sci*., 78, 695, 1989.

26. Davies N. M. and Teng X. V., *Adv. Pharm*., 1, 242, 2003.

27. Landoni M. F. and Soraci A., *Current Drug Metabolism*, 2, 37, 2001.

28. Krstulovic A. M., *J. Chromatogr*., 17; 488, 53, 1989.

29. Reepmeyer J. C., *Chirality*, 8, 11, 1996.

30. Ameyibor E., *J. Liq. Chromatogr. Rel. Technol*., 20, 855, 1997.

31. Bressolle F, Audran M, Pham T. N. and Vallon J. J., *J Chromatogr. B*; 687, 303, 1996.

32. Dalgliesh, C. E., *J. Chem. Soc*., 137, 1952

33. Pirkle W. H. and Pochapsky T. C., *Chem. Rev*., 89, 347, 1989.

34. Gil-Av E., Fiebush B. and Charles-Siegler, "*Gas Chromatography*", 1966, (Ed. A. B. Littlewood), The Institute of Petroleum.

35. Sogah G. D. Y. and Cram D. J., *J. Am. Chem. Soc*., 98, 3038, 1976.

36. Harada A., Furue M. and Nozakura S. L., *J. Polym. Sci*., 16, 189, 1978.

37. Armstrong D. W., *J. Liq. Chromatogr*., 6, 895, 1980.

38. Pirkle W. P., House D.W.and Finn J. M., *J. Chromatogr*., 192, 143, 1980.

39. Salem L.; Chapuisat X.; Segal G.; Hiberty P. C.; Minot C.; Leforrestier C.and Sautet P., *J. Am. Chem. Soc*., 109, 2887, 1987.

40. Dobashi A. and Hara S. J., *J. Org. Chem*., 52, 2490, 1987.

41. Okamoto Y., Hatada K. and Kawashima M., *J. Am. Chem. Soc*., 106, 5357, 1988.

42. Class Q. B., Bassi A. and Matlin S. A., *Chirality*, 8, 131, 1996.

43. Senso A., Oliveros L. and Mingallion C., *J. Chromatogr. A*, 839, 15, 1999.

44. Okamoto Y., Hatada K., Kawashima M., *J. Am. Chem. Soc*., 106, 5357, 1984.

45. Lipkowitz. K. B., Green K., Yang J., Pearl G. and Peterson M. A., *Chirality*, 5: 51, 1993.

46. Däppen R., Arm H., and Meyer V. R., *J. Chromatogr*., 373, 1, 1986.

47. Armstrong D. W. and DeMond W., *J. Chromatogr. Sci*., 22, 411, 1984.

48. Hyun M. H. and Kim D. H., *Chirality*, 16, 294, 2004.

49. Rogozhin S. V. and Dovarkov V. A., *Chem. Commun*., 490, 1971.

51. Noctor T. A., Felix G. and Wainer I. W., *Chromatographia*, 37, 55, 1991.

52. Miwa T., Ichikawa M., Tsuno M., Htori T., Miyakava T., Kyano M. and Miyake Y., *Chem. Pharma. Bull*., 35, 682, 1987.

53. Miwa T., Ichikawa M., Tsuno M., Htori T., Miyakava T., Kyano M. and Miyake Y., *J. Chromatogr*., 227, 457, 1988.

54. Hermansson J., *J. Chromatogr*., 269, 71, 1983.

55. Ward T. J. and Farris A. B., *J. Chromatogr. A*, 906, 73, 2001.

56. Armstrong, D. W.; Rundlett K. L. and Chen J. R., *Chirality*, 6, 496, 1994.

57. Gasper M. P.; Berthod A.; Nair U. B.; Armstrong D. W., *Anal. Chem*., 68, 2501, 1996.

58. Aboul-Enin H. Y. and Ali I., *Chromatographia*, 52, 679, 2000.

59. Aboul-Enein H. Y. and Serignese V., *Chirality*, 10, 358, 1998.

60. Kleidernigg O. P., Kappe O. C., *Tetrahedron Asymm*., 8, 2057, 1997.

61. Chen S., Liu Y., Armstrong D. W., Borrell J. I., Martinez-Teipel B., Matallana J. L., *J. Liq. Chromatogr*., 18, 1495, 1995.

62. Tesarova E., Zaruba K. and Flieger M., *J. Chromatogr. A*; 844, 137, 1999.

63. Sherrington D. C. and Hodge P. Eds., "*Synthesis and separations using functional polymers*", Ch.9, pp.305, 1988.

64. Okamoto Y., Suzuki K., Ohta K., Hatada K. and Yuki H., *J. Am. Chem. Soc*., 101, 4763, 1979.

65. Okamoto Y., Suzuki K. and Yuki H., *J. Poym. Sci. Polym. Chem. Ed*., 18, 3043, 1980.

66. Blaschke G. and Donow F., *Chem. Ber*., 108, 1188, 1975.

67. Blaschke G. and Donow F., *Chem. Ber.*, 108, 2792, 1975.

68. Blaschke G., *Angew. Chem. Int. Ed*., 19, 13, 1980

69. Blaschke G., Broker W. and Fraenkel W., *Angew. Chem. Int. Ed. Engl*. 25, 830, 1986.

70. Arlt D., Bomer B., Grosser R. and Lange W., *Angew. Chem. Int. Ed. Engl.*, 30, 1662, 1991.

71. Han X., He L., Zhong Q., Beesley T. E., and Armstrong D. W., *Chromatographia*, 63, 13, 2006.

72. Nakano T., *J. Chromatogr.* A, 906, 205, 2001.

73. Wulff G., *Angew. Chem. Int. Ed. Engl.*, 34, 1812, 1995.

74. Steinke J.; Sherrington D. C. and Dunkin I. R., *Adv. Polym. Sci.*, 123, 81, 1995.

75. Wulff G. and Vesper W., *J. Chromatogr.*, 167, 171, 1978.

76. Sellegren B., Lepisto M., Mosbach K., *J. Am. Chem. Soc.*, 110, 5853, 1988.

77. Gubitz G., and Schmid M. G., *Biopharm. Drug Dispos.*, 22, 291, 2001.

78. Sellergren B., *J. Chromatogr. A*, 906, 227, 2001.

79. Fu Q., Sanbe H., Kagawa C., Kunimoto K., and Haginaka J., *Anal. Chem.*, , 75,191, 2003.

80. Panasyuk T. L.; Mirsky V. M.; Piletsky, S. A.; Wolfbeis O. S., *Anal. Chem.*, 71, 4609, 1999.

81. Piletsky S., Piletska S. V., Chen B., Karim K., Weston, D., Barrett G., Lowe, P. and Turner A.P.F., *Anal. Chem.*, 72, 4381, 2000.

82. Malitesta C., Losito I. and Zambonin P. G., *Anal. Chem.*, 71, 1366, 1999.

83. Peng H., Liang C., Zhou A., Zhang Y., Xie Q. and Yao S., *Anal. Chim. Acta*, 423, 221, 2000.

84. Dickert F. L., Tortschanoff M., Bulst W. E. and Fischerauer G., *Anal. Chem.*, 71, 4559, 1999.

85. Deore B., Chen Z. and Nagaoka T., *Anal. Chem.*, 72, 3989, 2000.

86. Pichon V., Haupt K., *J. Liq. Chromatogr. Rel. Technol.*, 29, 989, 2006.

87. Kempe M., Mosbach K., *J. Chromatogr. A*, 694, 3, 1995.

88. Grierson J. R. and Adam M. J., *J. Chromatog.*, 325, 103, 1985.

89. Charmot D., Audebert R., and Quivoron C., *J. Liq. Chromatogr.*, 8, 1753, 1985.

90. Gubitz G., *J. Liq. Chromatogr.*, 9, 519, 1986.

91. Engelhardt H., Konig T. and Kromidas S., *Chromatographia*, 21, 205, 1986.

92. Yuki Y., Saigo K., Tachibana K., and Hasegawa M., *Chem. Lett.*, 1347, 1986.

93. Snyder R. V., Angeli R. J. and Meck R. B., *J. Am. Chem. Soc*., 94(8), 1972.

94. Davankov V. A., Kurganov A. A. and Tevlin A. B., *J. Chromatogr*., 261, 223, 1983.

95. Jin R. and He B., *J. Liq. Chromatogr*., 12, 501, 1989.

96. Mahdavian A. and Khoee S., *React. Funct. Polym*., 50, 217, 2002.

97. Chen J. M., and He B., *J. App. Polym. Sci*., 61, 2029, 1996.

98. Lefebvre B., Audebert R. and Quivoron C., *Isr. J. Chem*., 15, 69, 1976/77.

99. Charmof D., Audebert R. and Quivoron C., *J. Liq. Chromatogr*., 8, 1769, 1985.

100. Snyder L. R. and Kirkland J. J., "*Introduction to Modern Liquid Chromatography*", J. Wiley & Sons, New York, 2nd edition, 1979.

101. Horváth C. (Ed.), "*High Performance Liquid Chromatography. Advances and Perspectives*", Vol. 1, Academic Press, New York, 1980.

102. Unger K.K., *J. Chromatogr. Libr*., vol. 16, Elsevier, Amsterdam, 1979.

103. Unger K.K. (Ed.), "*Packings and Stationary Phases in Chromatographic Techniques*", Marcel Dekker Inc., New York, 1990.

104. Neue U.D., "*HPLC columns: Theory, technology and practice*", Wiley-VCH, New York, 1997.

105. Nawrocki J., *J. Chromatogr. A*, 779, 29, 1997.

106. Lee. D. P., *J. Chromatogr. Sci*., 20, 203, 1982.

107. Munzer M. and Trommsdorff E. in "Polymerisation Processes", (C. E. Schildknecht and I. Skeist, ed.), High Polymers, Vol. 29, Wiley Interscience, London, p. 106, 1977.

108. Hofmann F. and Delbruck K., *Ger Pat. 150.690*, 1909.

109. Landfester K., *Macromol. Rapid. Commun*., 22*,* 896, 2001.

110. Azad A. R. M. and R. M. Fitch, in "*Polymer Colloid*"*s* II, R. M. Fitch, Ed, Plenum Press, New York, p. 951980.

111. Zerfa M. and Brooks B. W., *Chem. Eng. Sci*., 51, 3591, 1996.

112. Hashim S. and Brooks B. W., *Chem. Eng. Sci*., 57, 3703, 2002.

113. Wenning H., *Makromol. Chem*., 20, 196, 1956.

114. Wenning H., *Kunstst. Plast*., 5, 328, 1958.

115. Trommsdorff E., *Makromol. Chem.*, 13, 76, 1954.

116. Guyot A. and Bartholim. N., *Prog. Polym. Sci.*, 8, 277, 1982.

117 Flory P. J., *J. Am. Chem. Soc.*, 1941, 63, 3083.

118. Sederel W. L. and De Jong G. J., *J. Appl. Polym. Sci.*, 17, 2835, 1973.

119 Guyot A. in "*Synthesis and Separations using Functional Polymers*", (D. C. Sherrington and P. Hodge, eds.), John Wiley and Sons, Chichester, p. 1, 1988.

120. Kun K. A. and Kunin R., *J. Polym. Sci. A*, 6, 2689, 1968.

121. Jacobelli H., Bartholin M. and A. Guyot, *J. Appl. Polym. Sci.*, 23, 927, 1979.

122. Arshady R., *J. Chromatogr.*, 586, 181, 1991.

123. Majors R. E., *J. Chromtogr. Sci.*, 15, 334, 1977.

124. Dong M. W. and Gant J. R., *Liq. Chromatogr.*, 2, 294, 1986.

125. Unger K. K., Jilge G., Kinkel J. N. and Hearn M. T. W., *J. Chromatogr.*, 359, 61 1986.

126. Harkins W. D., *J. Am. Chem. Soc.*, 69, 1428, 1947.

127. Smith W. V. and Ewart R. H., *J. Chem. Phys.*, 16, 592, 1948.

128. Williams D. J. and Bodalek E. G., *J. Polym. Sci.*, A-1, 4, 3065, 1966.

129. Gardon G. L., *Emulsion Polymerization*, Ch. 6, in Polymerization Processes, Shildknecht C. E. and Skeist I., eds., John Wiley and Sons, 1977.

130. Barret K. E. J., *Dispersion polymerization in organic media*, John Wiley and Sons, NY, 1975.

131. Hansen F. K. and Uglestad J., *J. Polym. Sci. Polym. Chem. Ed.*, 16, 1953, 1978.

132. Tseng C. M., Lu Y. Y., El-Aasser M. S. and Vanderhoff J. W., *J. Polym. Sci. Polym. Chem. Ed.*, 24, 2995, 1986.

133. Zurkova E., Bouchal K., Zdenkova D., Pelzbauer Z., Svec F. and Kalal J., *J. Polym. Sci. Polym. Chem. Ed.*, 21, 2949, 1983.

134. Smith D. H., *J. Colloid Interface Sci.*, 108, 471, 1985.

135. Barby D and Haq Z., *European Patent 0,060,138*, 1982.

136. Sherrington D. C., *Makromol. Chem. Macromol. Symp.,*70/71, 303, 1993.

137. Aronson M. P. and petko M. F., *J. Colloid and Interface Sci.*, 159, 134, 1993.

138. a. Lissant K. J., "*Surfactant Science Series*", vol. 6, Emulsion and Emulsion Technology, Part 1, Marcel Dekker, Inc., 1974.

b. Nixon J. and Beerbower A., *Properties of High-Internal Phase Emulsions, Effect of Emulsifier Parameters*, American Chemical Society Meeting, Apr. 13-18, 1969, pre-print 14, 49-59, 1969.

139. Lissant K. J., *U. S. Patent 3,974*, *116*, 1976.

140. Lissant K. J., *U. S. Patent 3,617,095*, 1971.

141. Akay G and Wakeman R. J., *J. Membr. Sci.*; 88, 177, 1994.

142. Akay G, Bhumgara Z, Wakeman R. J., *Chem. Eng. Res. Des.*, 73:782, 1995

143. Wakeman R. J., Bhumgara Z. G., Akay G., *Chem. Eng. J.*, 70, 1998.

144. Akay G and Vickers J., *EP 1307402 A2*, 2003.

145. Akay G, Price V. J. and Downes S., *EP 1183328 A2*, 2002.

146. Akay G., Birch M. A. and Bokhari*, Biomaterials*; 25, 3991. 2004,

147. Mork S., Solc W.; Jitka H.; Park Chung P.; *PCT INT WO 099/09070*, Dow Chemical Co., 1999.

148. Hoisington M. A., Duke J. R. and Apen P. G., *Polymer*, 38, 3347, 1997.

149 Cameron N. R., *Polymer*, 46, 1439, 2005.

150 Li N., Benson J. R. and Kitagawa, *U. S. Patent 5,863,957*, 1999.

151 Young, A. T., *Chem. Eng. News*, 23, 1978.

152 Castro. A. J., *U. S. Patent 4, 247, 498*, 1981.

153 Tsai F. and Torkelson J. M., *Macromol.*, 23, 775, 1990.

154 Mulder M., "*Basic Principles of Membrane Technology*"; Kluwer Academic, Dordrecht, The Netherlands, 1992.

155 Lonsdale H. K., *J. Memb. Sci.*, 10, 81, 1982.

156 Pusch W. and Walch A., *Angew. Chem. Int. Ed.*, 21, 660, 1982.

157 Bush P. J., Pradhan D. and Ehrlich P., *Macromol.*, 24, 1439, 1991.

158 Pradhan D. and Ehrlich P., *J. Polym. Sci. Poly. Phys. Ed.*, 33, 1053, 1995.

159 Aubert J. H. and Clough, R. L., *Polym.*, 26, 2047, 1985.

160 Aubert J. H., *Macromol.*, 21, 3468, 1988.

161 Hiatt, W. C., Vitzthum G. H., Wagener. K. B. and Jasetialr C., "*Materials Science of Synthetic Membranes*"; Lloyd, D. R. Ed.; ACS Symp. Ser. 269; pp 228-244, 1985.

162 Dongmei L., Robert S., Alan G. and William K., *NAMS*, 2003.

163 P. Van de Witte, Dijkstra P. J., J. W. A. van den Berg and Feijen J., *J. Memb. Sci*., 117, 1, 1996.

164 Bretz K., Rasche H. and Derleth H., *U. S. Patent 6,30,0468 B1*, assigned to Solvay Deutschland GmbH, Hannover (DE) 2001.

165 Fickel W. and Ries G., *US Patent 4,454,198*, assigned to Akzo nv, Arnhem, Netherlands, 1984.

166 Ley D. A., Hiscock L. J. and Cooke M. T., *U. S. Patent 4,940,734*, assigned to American Cynamid, 1990.

167 Schaaf P., Lotz B. and Wittmann J. C., *Polymer*, 28, 193, 1987.

168 Hou W. and Lloyd T. B., *J. Appl. Polym. Sci*., 45, 1783,1992.

169 Joachim K., James L. H. and Jöns G. H., *Adv. Polym. Sci*., 147,161, 1999.

170 Whaley P. D., Kulkarni S., Ehrlich P., Stein R. S., Winter H. H., Conner W. C. and Beaucage G., *J. Polym. Sci.: Part B*, *Polym. Phys*., 36, 617, 1998.

171 Hwang K. K., *U. S. Patent 4,824,718*, assigned to Minnesota Mining and Manufacturing Company 1989.

172 Smith T. L., Masilamani D., Bui L. K., Khanna Y. P., Bray R. G., Hammond W. B., Curran S., Belles J. J. and Shari B., *Macromol*., 27, 3147, 1994.

173 Beck H. N. and Ledbetter H. D., *J. Appl. Polym. Sci*., 9, 2131, 1965.

174 Beck H. N., *J. Appl. Polym. Sci*., 11, 673, 1967.

175 Binsberg F. L. and De Lange B. G. M., *Polymer*, 11, 309, 1970.

176 Hamada K. and Ychiyama H., *U. S. Patent, 4016118*, 1977.

177 Karthigeyan N., "Nucleation and Crystallization of Polymers", a thesis submitted to the Polytechnic University, 2000.

178 Balcao V. M., Paiva A. L. and Malcata F. X., *Enz. Microb. Technol*., 18, 392, 1996.

179 Berglund P., *Biomol. Eng*., 18, 13, 2001.

180 Sharma R., Chisti Y. and Banerjee U.C., *Biotechnol. Adv*., 19, 627, 2001.

181 Denga H. and Xu Z. K., *Enz. Microb. Technol*., 35, 437, 2004.

182 Rodionova M. V., Belova A. B., Mozhaev V. V., Martinek K. and Berezin I. V., *Dokl. Akad. Nauk. USSR*, 292, 913; C. A., 106, 17, 1823, 1987.

183 Chen, C. and Sih C. J., *Angew*. *Chem*. *Int*. *Ed*. *Engl*., 28, 695, 1989.

184 Chen C., Wu S., Girdaukas G. and Sih C., *J*. *Am*. *Chem*. *Soc*., 109, 2813, 1987.

185 Zaks A. and Klibanov A. M., *Science*, 224, 1249, 1984.

186 (a) Sakurai, T.; Margolin, A. L.; Russel, A. J.; Klibanov, A. M. *J*. *Am*. *Chem*. *Soc*. 1988, 110, 72. (b) Wong, C., *Science*, 244, 1145, 1989.

187 Roberto F., Pilar A., Pilar S., Gloria F. and Guisán J. M., *Chem*. *Phys*. *Lipids,* 93, 185, 1998.

188 Koops B. C., Papadimou E., Verheij H. M., Slotboom A. J. and Egmond M. R., *Appl*. *Microbiol*. *Biotechnol*., 52, 791, 1999.

189 Balcao V.M., Vieira M.C., and Malcata F. X., *Biotechnol*. *Progr*., 12, 164, 1996.

190 Hsieh Y., Abbott A., Ellison M. S., Heidi S., *National Textile Center Annual Repor*t*,* 2002.

191 Bruno L. M., G. A. Saavedra P., de Castro H. F., de Lima-Filho J. L. and de Magalhaes Melo E. H., *World J*. *Microb*. *Biotechnol*., 20, 371, 2004.

192 Reetz M. T., Zonta A., and Simpelkamp J., *Biotechnol*. *Bioengin*., 49, 527, 1996.

193 Gulatia R., Aryab P., Malhotra B., Prasad A. K., Saxena R. Kumar K., J., Watterson A. C., and Parmar V. S., *ARKIVOC*, (iii), 159, 2003.

194 Ferrera M., Ploua F. J., Fuentesa G., Crucesa M. A., Andersen L., Kirk O., Christensen M. and Ballesteros A., *Biocatal*. *Biotrans*., 20, 63, 2002.

195 Oliveira A. C., Rosa M. F., Cabral J. M. S. and Aires-Barros M. R., *Bioproc*. *Engin*., 16, 349, 1997.

196 Salis A., Sanjust E., Solinas V. and Monduzzi M., *J*. *Mol*. *Catal*. *B: Enzym*., 24, 75, 2003.

197 Gitlesen T., Bauer M. and Adlercreutz P., *Biochim*. *Biophys*. *Acta*, 1345, 188, 1997.

198 Jonzo M. D., Hiol A., Druet D. and Comeau L. C., *J*. *Chem*. *Tech*. *Biotchnol*., 69, 463, 1997.

199. Jayasundar J. J., Baddireddi S. L., Venkateshamurthy R., Mathuranthagam J. A., Pandjassarame K. and Pennathur G., *Protein Engin*., 16, 1017, 2003.

# Chapter 2

## Aims and objectives

## 2. Aims and objectives

The usefulness of polymers in the area of chromatography is well known. Several polymer based stationary phases are available commercially. The most common are ion exchange resins available from various companies (Duolite: -Rohm and Hass, Dowex reins: Dow chemicals, etc.). These are generally based on styrene-divinyl benzene copolymers. The demand for the polymers with specific properties for various applications is ever increasing. Newer methods of synthesis are being explored to satisfy the needs. Many modifications of the conventional polymerisation methods like suspension are also developed. Inspite of this, the conventional polymerisation methods still remain useful.

The present study aimed at investigating the effectiveness of polymer supports of differing characteristics for use as chiral stationary phases. Different methods of generating spherical, porous particles useful for attachment chiral ligand/ immobilisation of enzyme were studied. The methods involved synthetic methods like suspension and concentrated emulsion polymerisation and physicochemical method like thermally induced phase separation (TIPS). Porosity generation in the above methods by changing the parameters like crosslinker, pore generating solvent in case of synthetic methods was studied. The role of nucleating agent in generation of porosity in case of TIPS was also studied.

The use of moderately polar monomers like glycidyl methacrylate, hydroxyethyl methacrylate in concentrated emulsion polymerisation is restricted because of their inability to form stable emulsions. However, the use of these monomers bearing epoxy and hydroxy groups is beneficial for further modifications. The possibility of generating porous polymers with well defined pore structures by varying parameters like crosslink density, internal phase water, initiator and suspending agent using concentrated emulsion polymerisation was investigated.

The spectacular development in the area of asymmetric synthesis has been associated in many cases with tartaric acid. The use of simple tartaric acid (TA) based chiral ligands in the reactions such as asymmetric epoxidation (Sharpless epoxidation), asymmetric allylboration, Diels-Alder, aldol and cyclopropanation reactions leading to highly enantiomerically pure products is overwhelming. The polymer bound TA has also

been used as supported catalyst for many of these reactions. TA has also been used as chiral mobile phase additive in chiral resolution by HPLC. However, there are very few reports of tartaric acid bound polymers being used as chiral stationary phases. For developing the chiral stationary phases based on tartaric acid, it is important to study the mode of attachment to the support on the stereoselective binding of the enantiomers.

The modifications of the polymers were carried out with simple, cheaply available chiral ligands such as L (+) tartaric acid and its derivatives as well as β-CD. The dependence of ligand loading onto the polymers was investigated with reference to several factors such as crosslink density, surface area, pore volume etc. Evaluation of these materials in terms of their usability as chiral supports was studied. The binding of tartaric acid and/or its derivatives to the polymers was through one of the two carboxylic acid groups. The efficacy of these polymeric chiral ligands in terms of their usability as chiral stationary phases was evaluated.

The cardiovascular, antihypertensive and antidepressants are the drugs that are the main focus in the area of chiral resolutions. Amlodipine (antihypertensive) is a drug with therapeutic activity residing in only S isomer while the other has no or very little activity. The drug has been resolved by L (+) tartaric acid. We, therefore, selected this drug for our study. The other drug which is known to form an inclusion complex with β-CD i.e. Citalopram hydrobromide has been chosen for the resolution studies. The drug is used to treat various psychological disorders like depression, anxiety disorders etc. The S isomer of this drug is therapeutically active. The drug resolution studies were carried out under batch adsorption methods.

The immobilised enzymes have been extensively used as catalysts for asymmetric synthesis. Lipases (triglycerol hydrolases, E.C. 3.1.1.3) constitute an important class of enzymes in biocatalysis. Lipases possess both lipolytic and esterolytic activities. The reactions are reversible and with decreased amount of water in organic solvents several inter and trans-esterifications are possible. Besides this, they are cheaply available from many sources. However, there are limitations to the lipase activity in organic medium, which is mainly due to low solubility and aggregation. In order to overcome these they are adsorbed on solid supports. Polypropylene has been used as support for lipase immobililsation. The enzyme binding on the support requires that the supports should

have appropriate internal and external morphologies. The morphologies of the olefinic polymers can be tailored with the help of certain additives. The nucleating agents in polypropylene serve to increase the crystallisation temperature of the polymer. This is necessary during processing of the polymer. Also, the nucleating agents impart transparency to the polymer. Thermally induced phase separations (TIPS) are often used to generate porosity in polypropylene and copolymers. The morphologies in TIPS are determined by phase separation, which occurs through nucleation and growth mechanism. The effect of nucleating agents for the generation of porosity in the polymer was studied. The porous poly(ethylene-co-propylene) so formed was used for Lipase immobilisation. The immobilised enzyme was used to study the stereospecific esterification of non-steroid anti-inflammatory drug, Naproxen.

# Chapter 3

## Synthesis and characterisation of polymers by suspension and medium/high internal phase emulsion polymerisation.

## 3. Synthesis and characterisation of polymers by suspension and medium and high internal phase emulsion polymerisation.

### 3.1 Introduction

The porous polymers have a wide range of applications as solid supports in catalysis and chromatography. Polymers that possess functional groups capable of further reactions are considered as reactive. The first reactive polymers of significance were ion-exchange resins; synthesised in 1903 by Harm and Rumpler[1]. A spectacular evolution began in 1935 with an observation that the crushed phonograph records exhibited ion exchange properties, by two English chemists, Adams and Holmes. They synthesised the resins from phenol-formaldehyde[2]. The more useful resins based on styrene-divinylbenzene were synthesised in 1950. Since then the crosslinked polymers of organic origin have been used in various applications. In 1960 Merrifield's synthesis opened up new avenues to solid phase synthesis by using solid support for peptide synthesis[3]. The concept spread rapidly to other areas of organic synthesis such as catalysis, separation science etc., thus brought a revolution in the field of crosslinked polymers. The development of numerous new polymeric reagents, catalysts, and supports, has resulted in a better awareness of the fact that the polymers could be designed to have special reactivities and this, in turn, has contributed to a new interest in reactive polymers for application in areas not directly related to synthesis, catalysis, or separation science.

Resins based on styrene-divinylbenzene gained a lot of importance due to a large scope of modifications and their applicability in number of fields. The aromatic rings can be readily modified with simple electrophillic substitution reactions such as chloromethylation, bromination, lithiation etc.[4-7].

Glycidyl methacrylate (GMA) polymers are another class of reactive resins that have received much attention. These polymers were discovered in mid-1970's by Svec et al.[8]. Due to the presence of epoxy groups a wide range of modifications are possible. A number of modifications of the crosslinked GMA polymers have been carried out. The derivatised polymers have been used in a variety of analytical applications including chromatographic separation media[9], ion exchange reins[10-11], catalyst supports[12, 13] and for enzyme immobilisation[14-16].

The objective of this study was to synthesise polymers with different properties such as pore volumes, surface areas and particle sizes. Two different polymerisation procedures were investigated in order to synthesise the polymers having desired properties viz; suspension polymerisation as well as medium internal phase emulsion (MIPE) and high internal phase emulsion (HIPE) polymerisation.

GMA co-polymers of different crosslink densities (CLD) have been synthesised by suspension polymerisation. The typical crosslink densities were in the range 25, 50, 75, 100, 150 and 200. Two different crosslinking monomers namely ethylene dimethacrylate (EGDM) and divinylbenzene (DVB) were used to synthesise the two series of polymers. The polymers were synthesised in the presence of two different pore generating solvents viz; cyclohexanol and hexanol. The effects of crosslinking monomers and porgoen on the porous properties of the polymers were studied.

The GMA-co-EGDM polymers were also synthesised using HIPE methodology. The polymerisations were carried out by changing the ratio of monomer and internal water. The internal phase volumes were changed from 33.33% to the maximum of 90.9%. It is known that the emulsions containing internal phase volumes more than 74% are called HIPEs. Emulsions containing internal phase volumes from 20 to 70% are known as medium internal phase emulsions (MIPEs)[17]. We have studied the effect of internal phase volume on the formation porous structures. The polymers of different CLDs (25, 50, 75, 100, 150, 200 and 300) were synthesised. The effect of variations in reaction parameters on the morphology, porous properties and surface functionalities was studied. Hydroxyethyl methacrylate-co-ethylene dimethacrylate (HEMA-EGDM) polymers of varying CLDs were also synthesised using the same thechnique.

### 3.2 Materials used

Glycidyl Methacrylate (GMA)**:** Empirical Formula: $C_7H_{10}O_3$; Molecular weight: 142.16; Specific Gravity: 1.042; Physical state: clear liquid; Boiling Point: 195 °C.

Hydroxyethyl methacrylate (HEMA)**:** Empirical formula: $C_6H_{10}O_3$; Molecular weight: 130.14; Specific gravity: 1.073; Physical state: clear liquid; Boiling point: 205 $^oC$.

Ethylene dimethacrylate (EGDM)**:** Empirical formula: $C_{10}H_{14}O_4$; Molecular weight: 198.22; Specific gravity: 1.051; Physical state: clear liquid; Boiling point: 260 °C.

Divinyl benzene (DVB)**:** Empirical formula: $C_{10}H_{10}$; Molecular weight: 130.19; Specific Gravity: 0.914; Boling point: 197 °C.

Cyclohexanol**:** Empirical formula: $C_6H_{12}O$; Molecular weight: 100.16; Specific gravity: 0.96; Boling point: 161 °C; Physical state: colourless liquid.

Hexanol: Empirical formula: $C_6H_{14}O$; Molecular weight: 102.18; Specific Gravity: 0.814; Boiling point: 156.6 °C**,** Physical state: colourless liquid.

Octanol**:** Empirical formula: $C_8H_{18}O$; Molecular weight: 130.23; Specific gravity: 0. 827; Boiling point: 196 °C; Physical state: colourless liquid.

n-Hexane: Empirical formula: $C_6H_{14}$; Molecular weight: 86.18; Boiling point: 69˚C; Specific gravity: 0.6548; Physical state: colourless liquid.

n-Heptane**:** Empirical formula: $C_7H_{16}$, Molecular weight: 100.21; Boiling point: 100.21; Specific gravity: 0.684; Physical state: colourless liquid.

n-Octane: Empirical formula: $C_8H_{18}$; Molecular weight: 114.23; Specific Gravity: 0.703; Boiling point: 125.52 °C; Physical state: colourless liquid.

n-Decane**:** Empirical formula: $C_{10}H_{22}$; Molecular weight: 142.29; Specific Gravity: 0.73; Boiling point: 174 °C; Physical state: colourless liquid.

Cyclohexane**:** Empirical formula: $C_6H_{12}$; Molecular weight: 84.16; Specific Gravity: 0.779; Boiling point: 80.74 °C; Physical state: colourless liquid.

Poly(vinylpyrrolidone) (PVP): Empirical formula: $(C_6H_9NO)_x$; Molecular weight: 3,60,000; Specific gravity: 1.1-1.3; Softening point: 100 °C; Physical state: Off white powder.

Azo bisisobutyronitrile (AIBN): Empirical formula: $C_8H_{12}N_4$; Molecular weight: 164.21; Specific gravity: 0.96; Melting point: 103-105°C; Physical state: white powder.

Potassium peroxydisulphate (KPS): Empirical formula: $K_2S_2O_8$; Molecular weight: 270.32; Melting point: 100°C (decomposes); Physical state: white powder.

Span 80: Empirical formula: Empirical formula: $C_{24}H_{44}O_6$; Molecular weight: 428.61; Appearance: viscous yellowish orange liquid.

Brij 52: Polyethylene glycol hexadecylether; Empirical formula: $C_{16}H_{33}(OCH_2CH_2)nOH$ n~2, Molecular weight: 330; Density: 0.978 g/mL; HLB: 5.0.

Brij 72: Polyoxyethylene(2)stearyl ether, Empirical formula: $C_{18}H_{37}(OCH_2CH_2)nOH$, n~2; Molecular weight: 359; Melting point: 44-45ºC; Density: 0.893 g/mL; HLB: 4.9.

Brij 92: Polyoxyethylene(2)oleyl ether, Empirical formula: $C_{18}H_{35}(OCH_2CH_2)nOH$, n~2; Molecular weight: 357; Density: 0.912 g/mL; HLB: 4.9.

Acetic Anhydride**:** Empirical formula: $C_4H_6O_3$; Molecular weight: 102.1; Appearance: clear liquid; Boiling point: 139.9 °C.

All the solvents used were analytical grade and were used without further purification. The solvents were dried over molecular sieves.

## 3.3 Experimental

### *3.3.1 Reaction Scheme: Synthesis of GMA- EGDM copolymer*

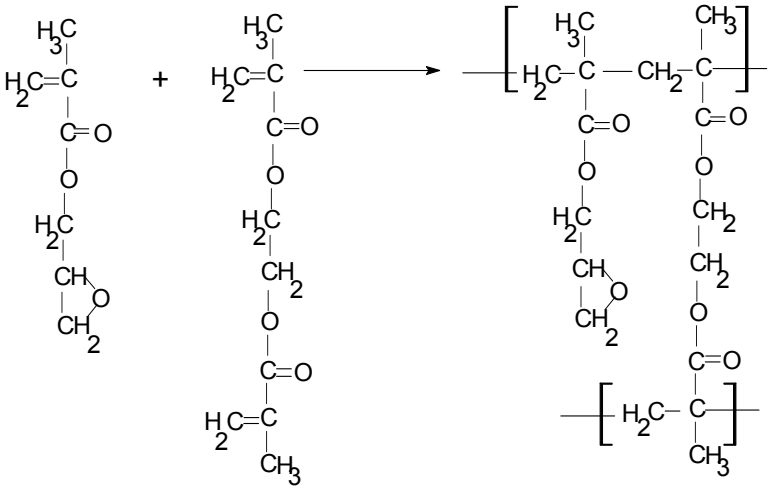

**Scheme 1.1: Synthesis of GMA-EGDM copolymers**

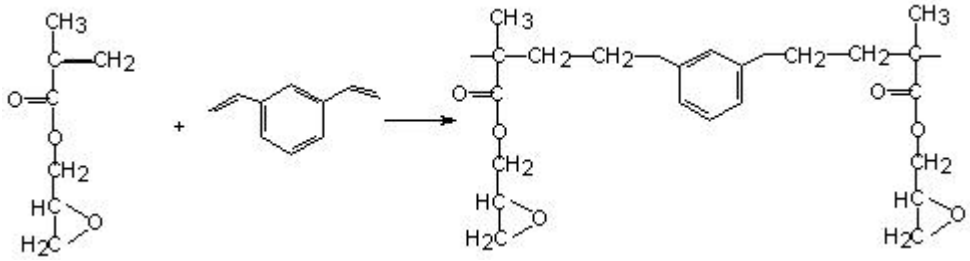

**Scheme 1.2: Synthesis of GMA-DVB copolymers**

### *3.3.2 Synthesis of GMA-EGDM and GMA-DVB copolymers by suspension polymerisation*

#### *3.3.2.1 General procedure*

The synthesis was conducted in a double walled cylindrical polymerisation reactor of 11 cm diameter and 15 cm height. The continuous phase comprised of a one-percent aqueous solution of poly(vinyl pyrrolidone). The discontinuous phase consisted

of glycidyl methacrylate, divinyl benzene/ethylene methacrylate, pore generating solvent (cyclohexanol) and initiator, azobis(isobutyronitrile) (AIBN). Stirring was started under a nitrogen overlay and the temperature was raised to 70 ºC. Polymerisation was allowed to proceed for 3 hours. The polymer beads obtained were then thoroughly washed with water and methanol and acetone. The beads were dried overnight at 50 ºC under vacuum.

A series of polymers of different crosslink densities (CLDs) were synthesised by varying the quantity of crosslinking monomer. The quantities required for different crosslink densities are tabulated in Table 3.1 and 3.2. In Table 3.1 GE7 is copolymer synthesised using cyclohexanol and GE7H is copolymer synthesised using hexanol as porogen with 25% crosslink density. Similarly, in Table 3.2 GV7 is copolymer synthesised using cyclohexanol and GV7H is copolymer synthesised using hexanol as porogen with 25% crosslink density. Similarly GE8 and GV8 correspond to 50% CLD and so on and so forth.

**Table 3.1. GMA-EGDM copolymers synthesised using cyclohexanol and hexanol as porogens by suspension polymerisation.**

| Polymer code | GMA (moles) | EGDM (moles) | CLD % | Monomer/Porogen (vol/vol) |
|---|---|---|---|---|
| GE7, GE7H | 0.0447 | 0.0111 | 25 | 1:1.61 |
| GE8, GE8H | 0.0352 | 0.0180 | 50 | 1:1.61 |
| GE9, GE9H | 0.0293 | 0.0223 | 75 | 1:1.61 |
| GE10, GE10H | 0.0249 | 0.0255 | 100 | 1:1.61 |
| GE11, GE11H | 0.0198 | 0.0292 | 150 | 1:1.61 |
| GE12, GE12H | 0.0161 | 0.0318 | 200 | 1:1.61 |

**Table 3.2. GMA-DVB copolymers synthesised using cyclohexanol and hexanol as a porogen by suspension polymerisation.**

| Polymer code | GMA (moles) | DVB (moles) | CLD % | Monomer/Porogen (vol/vol) |
|---|---|---|---|---|
| GV7, GV7H | 0.0418 | 0.0176 | 25 | 1:1.61 |
| GV8, GV8H | 0.0323 | 0.0267 | 50 | 1:1.61 |

| | | | | |
|---|---|---|---|---|
| GV9, GV9H | 0.0264 | 0.0323 | 75 | 1:1.61 |
| GV10, GV10H | 0.0220 | 0.0365 | 100 | 1:1.61 |
| GV11, GV11H | 0.0169 | 0.0414 | 150 | 1:1.61 |
| GV12, GV12H | 0.0132 | 0.0449 | 200 | 1:1.61 |

### *3.3.3 Synthesis of GMA-EGDM polymers of varying degrees of crosslinking by high internal phase emulsion polymerisation*

The required quantities of the monomer GMA and crosslinker EGDM along with the surfactant Span 80 and initiator AIBN were taken in a beaker. This constituted the oil phase. The discontinuous water phase contained water (internal water) and water-soluble initiator i.e. potassium peroxydisulphate. The discontinuous water phase was then added to the oil phase dropwise over a period of 5 minutes and blended using 8 bladed Ruston Turbine stirrer at 1400 rpm for 5 minutes. The emulsion was then dropped into the external water, containing 1% poly(vinyl pyrrolidone). The polymerisation was carried out under nitrogen at 70°C for 4.5 h. The polymeric beads were then filtered, washed with water, dried and then subjected to Soxhlet extraction with acetone for 24 h to remove the trapped surfactant, monomers etc.

The polymerisations were carried out using different quantities of discontinuous water phase, initiator and surfactant.

The quantities of the monomers for various compositions are shown in **Table 3.3.**

**Table 3.3. HIPE synthesis of GMA-EGDM copolymers by using both aqueous and oil phase initiators and PVP as suspending stabiliser.**

| Polymer code | GMA | | EGDM | | CLD | Mass | (Epoxy) |
|---|---|---|---|---|---|---|---|
| | mL | mol | mL | mol | % | g | mmol/g |
| GEH01, 11, 21 | 6.69 | 0.04904 | 2.31 | 0.01225 | 25 | 9.3988 | 5.2177 |
| GEH02, 12, 22 | 5.32 | 0.03899 | 3.68 | 0.01951 | 50 | 9.4111 | 4.1434 |
| GEH03, 13, 23 | 4.42 | 0.03240 | 4.58 | 0.02428 | 75 | 9.4192 | 3.4395 |
| GEH04, 14, 24 | 3.78 | 0.02771 | 5.22 | 0.02768 | 100 | 9.4250 | 2.9397 |
| GEH05, 15, 25 | 2.93 | 0.02148 | 6.07 | 0.03218 | 150 | 9.4326 | 2.2768 |

| | | | | | | | |
|---|---|---|---|---|---|---|---|
| GEH06, 16, 26 | 2.39 | 0.01752 | 6.61 | 0.03505 | 200 | 9.4375 | 1.8562 |
| GEH07, 17, 27 | 1.75 | 0.01283 | 7.25 | 0.03844 | 300 | 9.4433 | 1.3586 |

GEH01: GMA-EGDM copolymer, 25% CLD and with monomer: internal phase water ratio = 1:1.
GEH011: GMA-EGDM copolymer, 25% CLD and with monomer: internal phase water ratio = 1:2.
GEH21: GMA-EGDM copolymer, 25% CLD and with monomer: internal phase water ratio = 1:0.5.

**Table 3.4. Synthesis of GMA-EGDM polymer 25% CLD by HIPE, varying volumes of internal phase water.**

| Sr.No. | Polymer code | GMA | | EGDM | | Ratio of m:ipw* |
|---|---|---|---|---|---|---|
| | | mL | mol | mL | mol | |
| 1. | GEH01 | 6.69 | 0.04904 | 2.31 | 0.01255 | 1:1.0 |
| 2. | GEH11 | 6.69 | 0.04904 | 2.31 | 0.01255 | 1:2.0 |
| 3. | GEH21 | 6.69 | 0.04904 | 2.31 | 0.01255 | 1:0.5 |
| 4. | GEH31 | 6.69 | 0.04904 | 2.31 | 0.01255 | 1:2.5 |
| 5. | GEH41 | 6.69 | 0.04904 | 2.31 | 0.01255 | 1:5.0 |
| 6. | GEH51 | 6.69 | 0.04904 | 2.31 | 0.01255 | 1:10.0 |

m:iw: monomer:internal water.

**Table 3.5. HIPE synthesis of GMA-EGDM polymers by varying internal water and using porogen.**

| Sr. No | Polymer code | Ratio of m:ipw | Porogen used |
|---|---|---|---|
| 1. | GEH1a1 | 1: 2.5 | decane |
| 2. | GEH1a2 | 1: 2.5 | heptane |
| 3. | GEH1a3 | 1: 2.5 | cyclohexane |
| 4. | GEH1c1 | 1: 10.0 | decane |
| 5. | GEH1c2 | 1: 10.0 | heptane |
| 6. | GEH1c3 | 1: 10.0 | cyclohexane |

**Table 3.6. Synthesis of GEH01 with Brij surfactant**

| Sr. No. | Polymer code | Surfactant (name) | Surfactant g | GMA mL | EGDM mL | ipw mL |
|---|---|---|---|---|---|---|
| 1. | GEH01B52 | Brij 52 | 1.6 | 6.69 | 2.31 | 9 |
| 2. | GEH01B72 | Brij 72 | 1.6 | 6.69 | 2.31 | 9 |
| 3. | GEH01B92 | Brij 92 | 1.6 | 6.69 | 2.31 | 9 |

**Table 3.7. HIPE ynthesis of GMA-EGDM copolymers with organic phase initiator and calcium chloride.**

| Polymer code | GMA | | EGDM | | CLD % | Mass g | (Epoxy) mmol/g |
|---|---|---|---|---|---|---|---|
| | mL | mol | mL | mol | | | |
| GEH01O | 6.69 | 0.04904 | 2.31 | 0.01225 | 25 | 9.3988 | 5.2177 |
| GEH02O | 5.32 | 0.03899 | 3.68 | 0.01951 | 50 | 9.4111 | 4.1434 |
| GEH03O | 4.42 | 0.03240 | 4.58 | 0.02428 | 75 | 9.4192 | 3.4395 |
| GEH04O | 3.78 | 0.02771 | 5.22 | 0.02768 | 100 | 9.4250 | 2.9397 |
| GEH05O | 2.93 | 0.02148 | 6.07 | 0.03218 | 150 | 9.4326 | 2.2768 |
| GEH06O | 2.39 | 0.01752 | 6.61 | 0.03505 | 200 | 9.4375 | 1.8562 |
| GEH07O | 1.75 | 0.01283 | 7.25 | 0.03844 | 300 | 9.4433 | 1.3586 |

### *3.3.4 HIPE synthesis of HEMA-EGDM polymers with both oil and aqueous phase initiators*

The required quantities of the monomer HEMA and crosslinker EGDM along with the surfactant Span 80 and initiator AIBN were taken in a beaker. This constituted the oil phase. The discontinuous water phase / internal water contained water and water-soluble initiator i.e. potassium peroxydisulphate. The discontinuous water phase was then added to the oil phase dropwise over a period of 5 minutes and blended using 8 bladed Ruston Turbine stirrer at 1400 rpm for 5 minutes. The emulsion was then dropped into the continuous phase/external water containing 1% poly(vinyl pyrrolidone). The polymerisation was carried out under nitrogen at 70°C for 4.5 h. The polymers beads

were then filtered, washed with water, dried and then subjected to Soxhlet extraction with acetone for 24 h to remove the trapped surfactant, monomers etc.

The polymerisations were carried out using different quantities of discontinuous water phase, initiator and surfactant. The quantities of the monomers are tabulated in Table 3.8**,** using different quantities of internal water. The ratio was varied from 1:0.5, 1:1 and 1:2.

**Table 3.8. HIPE synthesis of HEMA-EGDM polymers using different volumes of discontinuous phase with both aqueous and oil phase initiator and PVP as suspending stabiliser.**

| Polymer code | HEMA | | EGDM | | CLD | Mass | (Hydroxy) |
|---|---|---|---|---|---|---|---|
| | mL | mol | mL | mol | % | g | mmol/g |
| HEH01, 11, 21 | 6.48 | 0.05343 | 2.52 | 0.01336 | 25 | 9.6016 | 5.5647 |
| HEH02, 12, 22 | 5.06 | 0.04172 | 3.94 | 0.02089 | 50 | 9.5703 | 4.3593 |
| HEH03, 13, 23 | 4.15 | 0.03422 | 4.85 | 0.02572 | 75 | 9.5516 | 3.5826 |
| HEH04, 14. 24 | 3.52 | 0.02902 | 5.48 | 0.02906 | 100 | 9.5369 | 3.0429 |
| HEH05, 15, 25 | 2.70 | 0.02226 | 6.30 | 0.03340 | 150 | 9.5175 | 2.3389 |
| HEH06, 16, 26 | 2.19 | 0.01806 | 6.81 | 0.03611 | 200 | 9.5081 | 1.8994 |
| HEH07, 17, 27 | 1.59 | 0.01311 | 7.41 | 0.03929 | 300 | 9.4942 | 1.3808 |

CLD: crosslink density

*3.3.4.1 HIPE synthesis of HEMA-EGDM copolymers using oil soluble initiator*

The procedure for making these polymers was the same as mentioned earlier. However, only oil soluble initiator i.e. AIBN was used in these systems; quantity being same as earlier. Water-soluble initiator i.e. potassium peroxydisulphate was not used.

**Table 3.9. HIPE synthesis of HEMA-EGDM polymers by using organic phase initiator (AIBN) and calcium chloride as suspending stabiliser**

| Polymer code | HEMA | | EGDM | | CLD | Mass | (Hydroxy) |
|---|---|---|---|---|---|---|---|
| | mL | mol | mL | mol | % | g | mmol/g |
| HEH01O | 6.48 | 0.05343 | 2.52 | 0.01336 | 25 | 9.6016 | 5.5647 |

| | | | | | | | |
|---|---|---|---|---|---|---|---|
| HEH02O | 5.06 | 0.04172 | 3.94 | 0.02089 | 50 | 9.5703 | 4.3593 |
| HEH03O | 4.15 | 0.03422 | 4.85 | 0.02572 | 75 | 9.5516 | 3.5826 |
| HEH04O | 3.52 | 0.02902 | 5.48 | 0.02906 | 100 | 9.5369 | 3.0429 |
| HEH05O | 2.70 | 0.02226 | 6.30 | 0.03340 | 150 | 9.5175 | 2.3389 |
| HEH06O | 2.19 | 0.01806 | 6.81 | 0.03611 | 200 | 9.5081 | 1.8994 |
| HEH07O | 1.59 | 0.01311 | 7.41 | 0.03929 | 300 | 9.4942 | 1.3808 |

**Table 3.10. HIPE synthesis of HEMA-EGDM polymers of varying crosslink densities using aqueous phase initiator ($K_2S_2O_8$) and calcium chloride as suspending stabiliser.**

| Polymer code | HEMA | | EGDM | | CLD | Mass | (hydroxy) |
|---|---|---|---|---|---|---|---|
| | mL | mol | mL | mol | % | g | mmol/g |
| HEH01A | 6.48 | 0.05343 | 2.52 | 0.01336 | 25 | 9.6016 | 5.5647 |
| HEH02A | 5.06 | 0.04172 | 3.94 | 0.02089 | 50 | 9.5703 | 4.3593 |
| HEH03A | 4.15 | 0.03422 | 4.85 | 0.02572 | 75 | 9.5516 | 3.5826 |
| HEH04A | 3.52 | 0.02902 | 5.48 | 0.02906 | 100 | 9.5369 | 3.0429 |
| HEH05A | 2.70 | 0.02226 | 6.30 | 0.03340 | 150 | 9.5175 | 2.3389 |
| HEH06A | 2.19 | 0.01806 | 6.81 | 0.03611 | 200 | 9.5081 | 1.8994 |
| HEH07A | 1.59 | 0.01311 | 7.41 | 0.03929 | 300 | 9.4942 | 1.3808 |

## 3.4 Characterisation

### *3.4.1 Porous properties of the polymers*

The porous properties of the resins are crucial for applications like chromatography since the flow is essentially governed by the pore structures.

#### *3.4.1.1 Morphology and internal structure*

The morphology and internal structure of the beads was determined by scanning electron microscopy (SEM). The dried polymer beads were mounted on stubs and sputter-coated with gold. Micrographs were taken on a JEOL JSM-5200 SEM instrument.

*3.4.1.2 Pore volume and surface area*

The pore volume and surface area were determined using mercury intrusion porosimetry and nitrogen adsorption methods. Mercury intrusion porosimetry was carried out using Autoscan 60, Quantachrome, USA, in the pressure range 0-60000 psig. BET surface areas were determined using Nova 2000e surface area analyser from Quantachrome, using nitrogen as an adsorbate. The samples were degassed for 3 h at 70º C and then ananlysed.

Although both the methods are based on surface tension, capillary forces and pressure, two different physical interactions take place. It can be shown thermodynamically that vapour condensation-evaporation and mercury intrusion-extrusion into and out of pore are similar processes operating in the two diametrically opposite extreme ends of pore size[18].

Pores are classified according to size into three categories; micropores (pore diameter smaller than 2 nm), mesopores (pore diameter 2-50 nm) and macropores (pore diameter larger than 50 nm). Pore size defines an ability of the analyte molecules to penetrate inside the particle and interact with its inner surface[19].

There are many methods for the determination of pore size and pore size distribution. Mercury intrusion porosimetry and gas adsorption are the most commonly used methods for the determination pore volume and surface areas.

*3.4.1.2.1 Mercury intrusion porosimetry (MIP)*

Pore structure analysis by mercury porosimetry is applicable when the material in question is sufficiently rigid to withstand relatively high compressive forces and does not amalgamate, i.e., react with mercury. The equipment is a high-pressure mercury-intrusion porosimeter for quantifying the opening size, size range, wall area, and volume of pores. Pore diameters between 360 and 0.003 μm can be assessed as can pore area and volume, material density, and percent porosity. Mercury porosimetry is based on the capillary law governing liquid penetration into small pores. This law, in the case of a non-wetting liquid like mercury and cylindrical pores, is expresses by the Washburn equation[20]. This P-V information serves as a unique characterisation of pore structure.

$$\mathbf{p.r = -2.\gamma.\cos\theta} \qquad 3.1$$

Where, p is pressure, r is the radius of the pore that mercury intrudes, $\gamma$ is surface tension of mercury and $\theta$ is contact angle of the mercury on the surface of the solid sample. The surface tension and contact angle of mercury are 480 $mNm^{-1}$ and $140^{o}$, respectively. The Washburn equation (3.1) can be derived from the equation of Yang and Dupre:

$$\gamma_{SV} = \gamma_{SL} + \gamma_{LV} .\cos \theta \qquad 3.2$$

Where, $\gamma_{SV}$ is the interfacial tension between solid and vapour, $\gamma_{SL}$ is interfacial tension between solid and liquid, $\gamma_{LV}$ is interfacial tension between liquid and vapour and $\theta$ is the contact angle of the liquid on pore wall. The work, W, is required to move liquid up the capillary. During capillary rise, when the solid-vapour interface disappears, solid-liquid interface appears as:

$$W = (\gamma_{SL}-\gamma_{SV}). \partial A \qquad 3.3$$

Where, $\partial$A is the area of the capillary wall covered by liquid when their level rises. According to equations 3.2 and 3.3,

$$W = - (\gamma_{LV} .\cos \theta).\partial A \qquad 3.4$$

The work required to raise a column of liquid through a height h in a capillary with radius r is identical to work required to force the liquid out of the capillary. When a volume V of liquid is forced out of the capillary with a gas at constant pressure above ambient $\partial P_{gas}$, the work is presented as:

$$W = V\partial P_{gas} \qquad 3.5$$

Equations 3.4 and 3.5 are combined to yield

$$\partial P_{gas}. V = -(\gamma. \cos \theta). \partial A \qquad 3.6$$

When the capillary is circular in cross section, parameters V and $\partial$A are given by $\pi r^2 L$ and $2\pi rL$, where L is the length of the capillary.

$$p. r = -2.\gamma. \cos \theta \qquad 3.7$$

This is known as Washburn equation, the operating equation in mercury porosimetry. The product pr is constant on keeping γ and θ constant. This implies that pressure is inversely proportional to radius. Thus, mercury will intrude progressively into narrower pores with increase in pressure. Using θ ($140^o$) and γ (0.480 N/m), the Washburn equation is p = 0.736/r. The experimental method is dependent on the wetting or contact angle between mercury and surface of the solid. This contact angle exceeds $90^o$ for non-wetting liquids but is less than $90^o$ for wetting liquids (Figure 3.1).

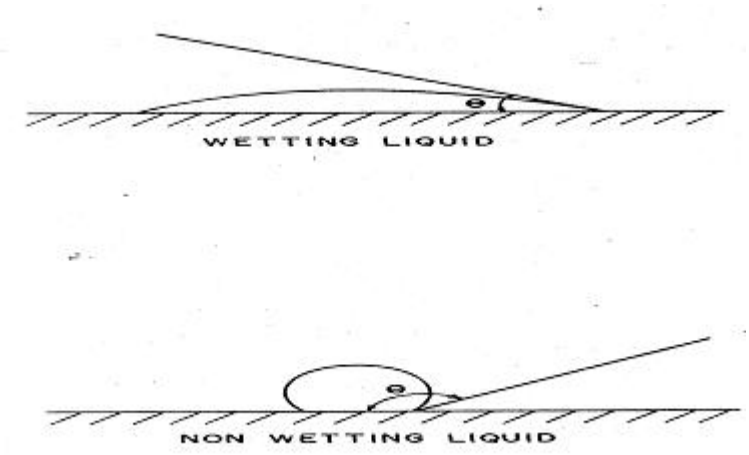


**Figure 3.1. Contact angles of wetting and non-wetting liquids.**

The experimental method is dependent on the wetting or contact angle between mercury and surface of the solid. This contact angle exceeds 90º for non-wetting liquids but is less than 90º for wetting liquids (Figure 3.1). In the experiment, gas was evacuated from the sample cell and mercury was transferred into the sample cell under vacuum. Pressure was applied to force mercury into the sample. During measurement, applied pressure p and intruded volume of mercury (V) were registered. As a result of analysis, an intrusion and extrusion curve was obtained.

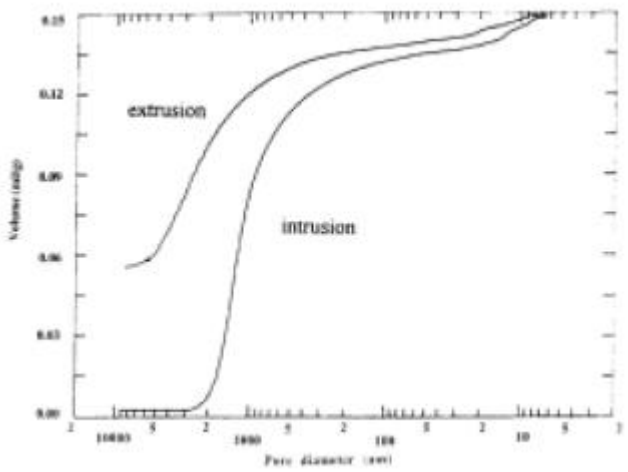


**Figure 3.2. Typical intrusion-extrusion curves obtained by mercury porosimetry.**

*3.4.1.2.2 Surface area measurement*

Gas adsorption measurements are widely used for the characterisation of a variety of porous solids (e.g. oxides, carbons, zeolites and organic polymers). Of particular importance is the application of physisorption (physical adsorption) for the determination of the surface area and pore size distribution of catalysts, industrial adsorbents, pigments, fillers and other materials. Nitrogen (at **77 ºK**) is the recommended adsorptive for determining the surface area and mesopore distribution, but it is necessary to employ a range of probe molecules to obtain a reliable assessment of the micropore size distribution. Although the role of modern techniques in characterising adsorbents and catalysis is ever increasing, classical methods based on adsorption on solids are still very popular and well utilised in surface chemistry. The classical measurements provide information about properties of a solid with respect to the adsorbing species. The classical and still most pertinent measurement in adsorption studies is the adsorption – desorption isotherm, used in the calculation of the surface area of adsorbents[21]. Of all the many gases and vapours, which are readily available and could be used as adsorptives, nitrogen has remained universally pre-eminent. With the aid of user-friendly commercial equipment and on-line data processing, it is now possible to use nitrogen adsorption at 77 ºK for both routine quality control and the investigation of new materials[22], The methods used to determine surface area, are most frequently based on the determination of the monolayer capacity of a given adsorbent by the BET method. BET theory is a well-known rule for the physical adsorption of gas molecules on a solid surface. In 1938,

Stephen Brunauer, Paul Hugh Emmet, and Edward Teller published an article about the BET theory in a journal for the first time; "BET" consists of the first initials of their family names. The concept of the theory is an extension of the Langmuir theory, which is a theory for monolayer molecular adsorption, to multilayer adsorption with the following hypotheses: (a) gas molecules physically adsorb on a solid in layers infinitely; (b) there is no interaction between each adsorption layer; and (c) the Langmuir Theory can be applied to each layer. The resulting BET equation is expressed by (3.8):

$$\frac{p}{V(p_0 - p)} = \frac{1}{V_m c} + \frac{c-1}{V_m c}\frac{p}{p_0} \qquad 3.8$$

where, V is volume adsorbed, $V_m$ is volume of monolayer, p is sample pressure, $P_0$ is saturation pressure and c is constant related to the enthalpy of adsorption (BET constant). The specific surface area ($S_{BET}$) is then calculated from $V_m$ by the equation 3.9.

$$S_{BET} = \frac{V_m \cdot n_a \cdot a_m}{m \cdot V_L} \qquad 3.9$$

Where, $n_a$ is Avogadro constant, $a_m$ is the cross sectional area occupied by each nitrogen molecule (0.162 $nm^2$), m is weight of the sample and $V_L$ is the molar volume of nitrogen gas (22414 $cm^3$). The theory is based on the assumption that the first adsorbed layer involves adsorbate/adsorbent energies, and the following layers the energies of the adsorbate/adsorbate interaction.

Adsorption studies aimed at the measurement of pore size and pore size distributions generally make use of Kelvin equation[23]. This equation relates the equilibrium vapour of a curved surface, such as that of a liquid in a capillary or pore, to the equilibrium pressure of the same liquid on a plane surface. A convenient form of Kelvin equation 3.10 is

$$\ln\frac{p}{p_0} = -\frac{2\gamma V_L}{rRT}\cos\theta \qquad 3.10$$

In the Kelvin equation, P is the equilibrium vapour pressure of a liquid in a pore of radius r, $P_0$ is the equilibrium pressure of the same liquid on a plane surface, $\gamma$ is

surface tension of the liquid, $V_L$ is molar volume of the liquid, θ is the contact angle with which the liquid meets the pore wall, R is the gas constant and T is absolute temperature. When the meniscus of condensate is concave, capillary condensation will proceed in pores of radius r as long as the adsorptive pressure is greater than pressure p.

The surface area of the polymers were measured using the single point Brauner-Emmett-Teller method by measuring the adsorption of nitrogen at liquid nitrogen temperature and at the nitrogen concentration of 30 mol% (balance helium), using a monosorb surface area analyser (Quantachrome Corp., U.S.A.), based on dynamic adsorption/desorption technique.

*3.4.1.2.3 Comparison of mercury porosimetry and nitrogen adsorption methods*

Pore structure analysis by mercury porosimetry is faster than by nitrogen adsorption. With mercury porosimetry, large pores are filled first and with increase in hydraulic pressure smaller pores get progressively filled. With nitrogen adsorption, the smallest pores are measured first at the adsorption phase and with increase in adsorbate pressure larger pores are filled[24]. The two processes occur in reverse since nitrogen and mercury are wetting and non-wetting liquids respectively on most of the surfaces. The determination range of high-pressure mercury porosimetry is wider (pore diameter 3 nm–14 μm) than that of nitrogen adsorption (0.3–300 nm), and mercury porosimetry determines larger pores that are out of the detection range of nitrogen adsorption (Figure 3.3). With nitrogen adsorption the smallest pores that are out of range of mercury porosimetry can be determined. However, results of the two methods can be compared. The comparable parameters are total pore volume, volume pore size distribution and specific surface area/total pore surface area. Although the pore size range that can be determined with adsorption is narrower than that obtained with mercury porosimetry, it is more widely used[25].

Comparisons have been made between surface areas measured by porosimtry and gas adsorption with results ranging from poor to excellent. The difference between the two methods can be used to deduce useful information not obtainable by either method. For example, when surface area calculated from adsorption data is large compared to the area measured by porosimetry, it implies that pores smaller than those penetrated by mercury at maximum pressures contribute substantial volume. Pore wall roughness is

another factor that leads to slightly larger adsorption areas than those from porosimetry. Slight surface roughness will not alter the porosimetry surface area since it is calculated from pore volume while the same roughness will be measured by gas adsorption. Ink bottle shaped pores with a narrow entrance into a wider inner body generate larger surface areas in porosimetry than those from nitrogen adsorption. Intrusion into wider inner body will not occur until sufficient pressure is applied to force mercury into the narrow entrance. It will therefore appear as if a large volume intruded into narrow pores, generating excessively high surface areas. The Figure 3.3 shows a schematic diagram of range of mercury intrusion porosimetry (Hg porosimetry) and nitrogen adsorption ($N_2$ capillary condensation).

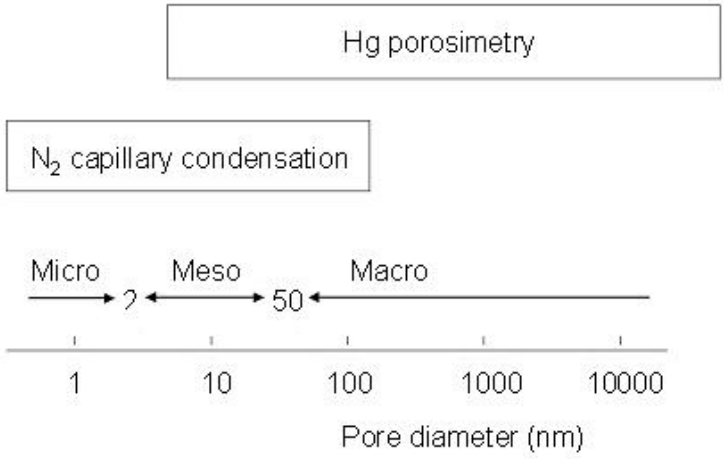


**Figure 3.3. Comparison range of pore diameters analysed by mercury intrusion porosimetry and nitrogen adsorption.**

*3.4.2 Epoxy content*

The surface epoxy groups were analysed titrimetrically using hydrochloric acid-dioxane reagent[26]. The method is based on addition of hydrogen chloride to the epoxide, which results in formation of chlorohydrin. The difference between the amount of acid added and the amount unconsumed, as determined by titration with the standard base, is a measure of epoxide content at the pore surface. The typical procedure for the titration is as follows:

To the appropriate weight of the sample, 25 mL of purified dioxane and 25 mL of 0.2N hydrochloric acid-dioxane solution were added. It was kept in dark for 15 min. To this 25 mL of neutral cresol red indicator was added and excess of acid was titrated

against 0.1N methanolic potassium hydroxide. The end point was appearance of first violet colouration.

**Calculations**

Epoxy content = (B-S) N/ 10W

Where, B = blank reading, S = main sample reading, W = weight of sample, N = normality of methanolic KOH solution.

AE = analysed epoxy groups which react with sodium hydroxide in dioxane over 6 hours at 80 ºC.

*3.4.3 Particle size analysis*

The particle size analysis was carried out using Accusizer 780/ APS with LE 2500-15 and LE 500-00.5 sensor. The Accusizer APS Automatic Particle Sizer utilises the method of single-particle optical sensing (SPOS) to quickly count and size a large number of particles one at a time, constructing a true particle size distribution (PSD). A single particle optical sensor (SPOS) measures PSD over the range of 500 nm to 500 μm. There are two physical methods that traditionally have been used to implement the SPOS technique: Light extinction (LE) and Light Scattering (LS). The LE method is based on a measurement of the decrease in the intensity of light transmitted across a flow channel carrying particles suspended in a fluid, caused by the momentary passage of an individual particle through the light beam. The LS method measures the increase in the intensity of light caused by scattering from particles, which pass through the optical sensing zone. The Accusizer combines the advantage of LE method (large size and relative insensitivity to particle composition) with the advantage of the LS method (high sensitivity- lower diameter limit).

The sample (0.05-0.10 g) was mixed with a 1% solution of surfactant Noigen 120, in water (5 mL). This mixture was sonicated for 1 min using sonicator (Ultrasonic processor, Model cv 26, resonating frequency 20KHz ± 50Hz). The suspension was then analysed in the autodilution mode.

## 3.5 Results and Discussion

*3.5.1 Particle size and its distribution (PSD)*

The suspension polymerisation generates particles with spherical morphology. The beads obtained in presence of pore generating solvent were opaque indicating the

porous nature of the polymers. The beads obtained by both the methodologies were opaque and mostly spherical. In case of emulsion templated polymerisation the beads obtained were smaller than those by suspension polymerisation.

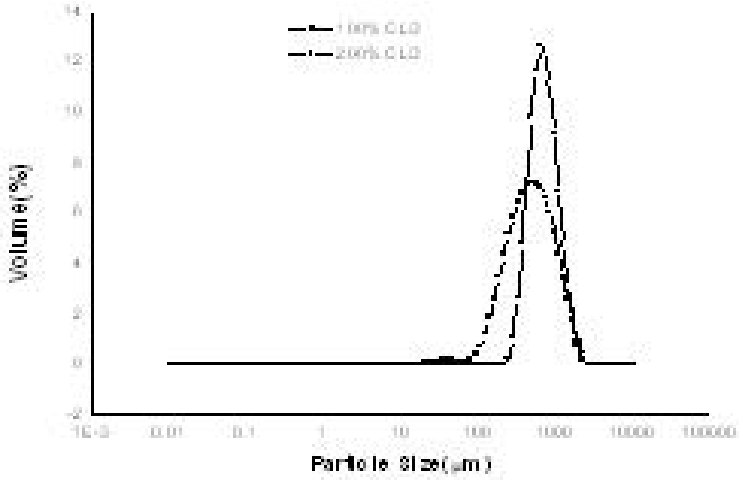


a.

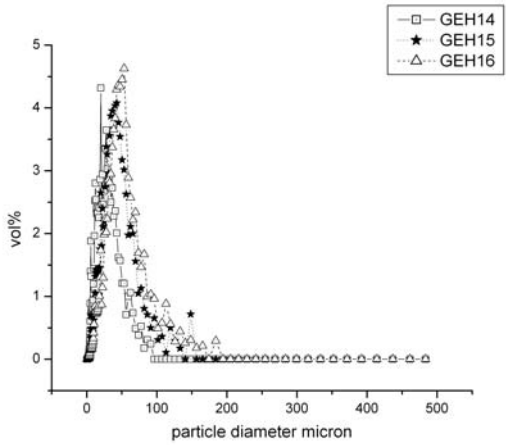


**b.**

**Figure 3.4. a. Particle size distribution of GE10 and GE12, b. particle size distribution of GEH14, GEH15 and GEH16.**

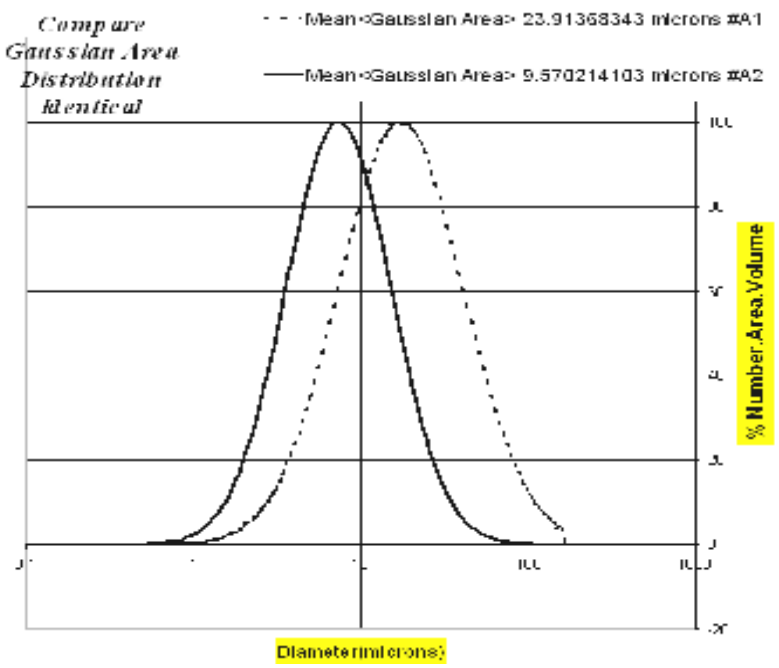


**Figure 3.5. Gaussian distribution of particle diameters with change in crosslink density (CLD) A1: -GEH16, A2: -GEH15.**

The particle size distribution of suspension and emulsion polymerised beads are shown in the Figure 3.4 a. and b. respectively**.** The beads obtained by suspension polymerisation were in the range of 100-1000 μm while those obtained by medium and high internal phase emulsion polymerisations were in the range of 0.5-200 μm. The narrow particle size distribution as compared to suspension polymerisation results because of the initial stirring speed. Unlike suspension polymerisation, the particle size in high intrernal phase emulsion polymerisation is determined by the initial rate of stirring. Here, the polymerisation proceeds in confined droplets, which are already formed at the beginning. Strirring speeds determine the particle size. It is established that an increase in agitation speed causes a reduction of droplet size formed. The droplet size formed is primarily governed by its growth time prior to detachment, which is effectively reduced at higher shear stress as a result of higher agitation speeds. This indicates that smaller droplets are produced at higher stirring rates[27]. We have synthesised beads at fairly high shear rates so the particle size is low and distribution is narrow.

In case of suspension the particle size increased with the increase in crosslinker concentration. The same trend was observed for emulsion polymerised particles with different internal phase volumes. The particle size distribution of two samples (GEH15

and GEH16) with 66.66 % internal phase was compared. The Gaussian distribution for the two samples show that the particle size distribution is broader for GEH16 as compared to GEH15 and particle size shifts towards lower particle diameter with decrease in crosslink density as shown in the Figure 3.5.

The increase in the particle size could be due to increased surface tension with increase in EGDM concentration. As recently reviewed by Arshady[28], the average size of the monomer droplets (and, hence, that of the resulting particles) are directly proportional with the diameter of vessel, the volume ratio of the droplet phase to suspension medium, the viscosity of the droplet phase, and the interfacial tension between the two immiscible phases, and inversely proportional with the diameter of stirrer, the stirring speed, the viscosity of the suspension medium, and the stabiliser concentration. The increase in the EGDM content of the polymerisation medium, in which the GMA content is constant, mainly causes an increase in the volume ratio of the droplet phase to suspension medium and the interfacial tension between the two immiscible phases, which in turn, increase the average size of the polymeric microspheres.

In case of HEMA-EGDM copolymers synthesised with organic and both phase initiators, the coagulation of the particles occurred during drying process. The fine powdery particles with irregular shapes were obtained in case of copolymers synthesised with only aqueous phase initiator and calcium chloride as the suspending agent.

### *3.5.2 Porous properties of the polymers*

#### *3.5.2.1 Morphology and internal structure*

A porous solid can be defined as any solid containing cavities, channels or interstices. Pores can be classified according to their availability to external fluid. The schematic cross section of a porous solid is shown in Figure 3.6.

The pores can be classified as closed pores and open pores. The closed pores are the pores, which are totally isolated from their neighbours as shown around **a**. The pores around **b, c, d, e** and **f** are called open pores. They have a continuous channel of communication with the external surface of the body. The pores, which are open at only one end are known as blind pores (b and f) while those open at both ends are through and through pores like around e. The pores can be categorised according to their shapes as

cylindrical (c and f), ink-bottle type (b), funnel shaped as in d and slit like pores. Many physical properties like density, thermal conductivity, mechanical strength are dependent on the pore structure of a solid. The through and through pores are especially important in case of applications like chromatography as they influence properties like fluid flow[29].

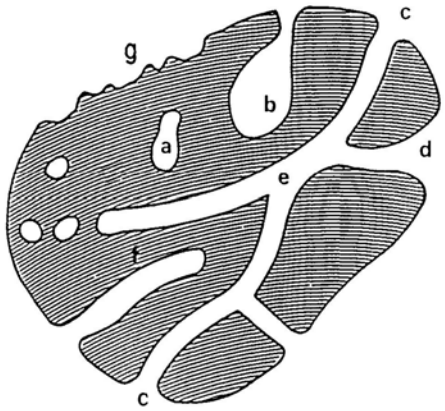


**Figure 3.6. Schematic cross section of porous solid.**

In suspension polymerisation, the morphology and properties of the copolymer beads depend on the composition of the monomeric mixture and on polymerisaton conditions. The reaction mixture for suspension copolymerisation system for the production of macroporous copolymers includes a monovinyl monomer, a divinyl monomer (crosslinker), an initiator, and the inert diluent. The decomposition of the initiator produces free radicals, which initiate the polymerisation and crosslinking reactions. After a certain reaction time, a three-dimensional network of infinitely large size may start to form. This is known as gel point and at this stage the liquid reactants change to solid like state[30]. As the polymerisation proceeds beyond the gel point the amount of soluble reaction components decrease and after complete conversion of monomers, a stage is reached where only the polymer network and diluent remain in the system. The polymers exhibit different structures and properties depending on the amounts of the crosslinker and the diluent present during the reactions as well as on the solvating power of the diluent. The bead is an aggregate of microspheres. Each microsphere consists of smaller nuclei, which are fused together as can be seen from the figure. The beads of GMA-EGDM and GMA-DVB obtained by suspension polymerisation were largely spherical and their internal structure showed typical

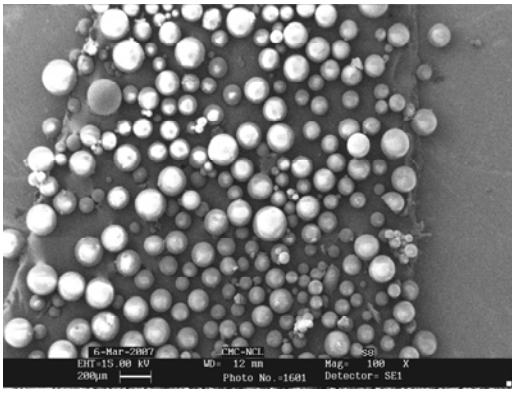


a.

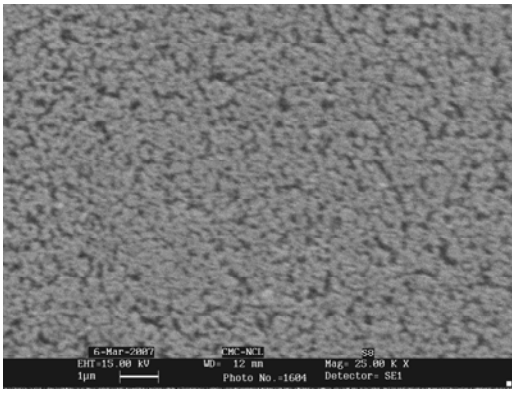


**b.**

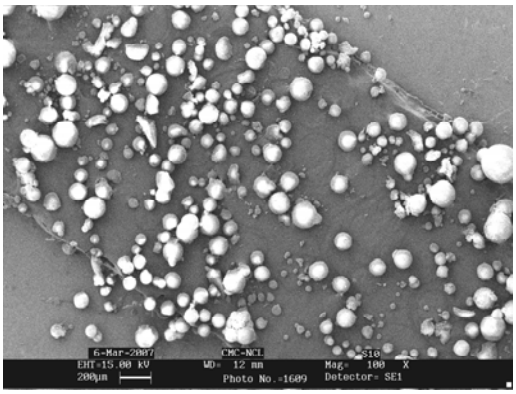


**c.**

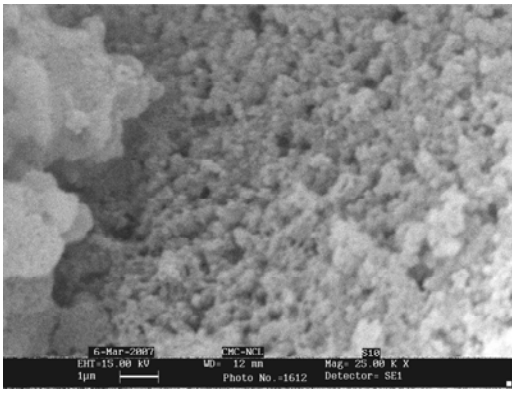


**d.**

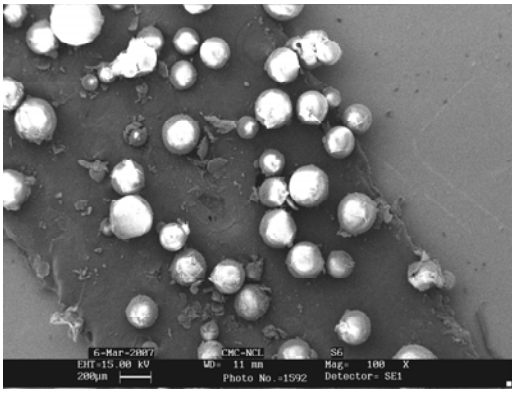


**e.**

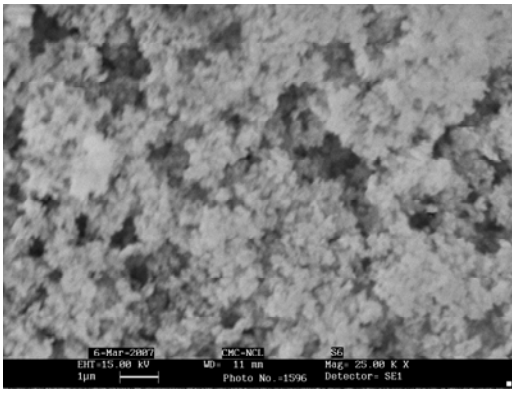


**f.**

**Figure 3.7 a. and b. Morphology and internal structure of the beads GMA-EGDM polymers synthesised using cyclohexanol as porogen at mgnification 100x and 25KX resp. c. and d. GMA-DVB beads synthesised using cyclohexanol as porogen at 100X and 25KX magnification by SP. e and f GMA-DVB beads synthesised using hexanol as porogen at 100X and 25KX respectively.**

cauliflower morphology obtained by suspension polymerisation. The scanning electron microscopic (SEM) pictures of the beads taken at various magnifications reveal the internal morphology of the beads with a significant change as the pore generating solvent is changed (Figure 3.7).

The polymers synthesised with cylohexanol as pore-generating solvent showed smaller pores while with hexanol as porogen larger pores are obtained. High surface area results from small pores present between the nuclei while intermicrosphere spacing gives rise to moderate surface areas.

The phase separation during polymerisation is largely dependent on the compatibility of the polymer network with porogen. In the case of good compatibility, the phase separation occurs at a later stage at higher conversion of monomers leading to a network of interconnecting individual microgel particles[31]. The compatibility between the polymer and the porogen increases with the solvating power of the porogen, which can be translated into solubility parameters. The solubility parameters for GMA, EGDM, DVB, cyclohexanol and hexanol are shown in Table 3.11.

**Table 3.11. Solubility parameter (δ) of GMA, EGDM and cyclohexanol**

| **Component** | **[a]δ $(cal/cm^3)^{0.5}$** |
|---|---|
| GMA | 8.05 |
| EGDM | 8.90 |
| DVB | 9.30 |
| Cyclohexanol | 11.40 |
| Hexanol | 10.76 |

**Table 3.12. Variance in (δ) with change in CLD for cyclohexanol and hexanol**

| CLD | δ′ $(cal/cm^3)^{0.5}$ GMA-EGDM | δ′ $(cal/cm^3)^{0.5}$ GMA-DVB | GE | | GV | |
|---|---|---|---|---|---|---|
| | | | $\Delta\delta_1$cy | $\Delta\delta_2$hex | $\Delta\delta_1$cy | $\Delta\delta_2$hex |
| 25 | 8.27 | 8.43 | 3.13 | 2.49 | 2.97 | 2.33 |
| 50 | 8.40 | 8.63 | 3.00 | 2.36 | 2.77 | 2.17 |

| | | | | | | |
|---|---|---|---|---|---|---|
| 75 | 8.48 | 8.75 | 2.92 | 2.28 | 2.65 | 2.01 |
| 100 | 8.54 | 8.84 | 2.86 | 2.22 | 2.56 | 1.92 |
| 150 | 8.62 | 8.95 | 2.78 | 2.14 | 2.45 | 1.61 |
| 200 | 8.67 | 9.02 | 2.73 | 2.09 | 2.38 | 1.74 |

**δ: solubility parameter; δ′: difference in solubility parameter**

It can be seen from Table 3.12 the difference in the solubility parameter (Δδ) between the copolymer and the porogen is higher for cyclohexanol than for hexanol. Thus the compatibility between the copolymer and cyclohexanol should be lower than that of hexanol. In such case larger pores due to early phase separation are expected. However, the experimental findings are showing opposite trends. The difference in porous structures cannot be explained only with δ. The precipitation rates of copolymers are also influenced by the polymerisation rate of monomer components in the compositions or by the action as a chain transfer agent to the diluent[32].

It can be seen from Tables 3.13-3.16 and Figure 3.8 that the total pore volumes of the GMA-DVB polymers with hexanol as porgen were the highest while that of the GMA-EGDM with cyclohexanol were the lowest. In case of GMA-DVB and GMA-EGDM polymers with cyclohexanol as porogen the pore volume and surface area increase simultaneously due to broad pore size distribution. As smaller pores that contribute mainly to the surface area were also generated during polymerisation, the surface area increased.

*3.5.3 Surface area and mercury porosimetry*

**Table 3.13. Poly(GMA-EGDM) synthesised with cyclohexanol as porogen**

| Properties | GE7 | GE8 | GE9 | GE10 | GE11 | GE12 |
|---|---|---|---|---|---|---|
| | 25% | 50% | 75% | 100% | 150% | 200% |
| PV(mL/g) | 0.1075 | 0.5625 | 0.5925 | 0.7250 | 0.7400 | 0.8475 |
| SA($m^2$/g) | 22.076 | 85.0631 | 105.781 | 100.691 | 110.254 | 110.578 |

**Table 3.14. Poly(GMA-EGDM) synthesised with hexanol as porogen**

| Properties | GE7H | GE8H | GE9H | GE10H | GE11H | GE12H |
|---|---|---|---|---|---|---|
| | 25% | 50% | 75% | 100% | 150% | 200% |

| | | | | | | |
|---|---|---|---|---|---|---|
| PV(mL/g) | 1.286 | 1.593 | 1.67 | 1.90 | - | - |
| SA($m^2$/g) | 6.40 | 14.57 | 78.58 | 83.97 | 85.46 | 61.21 |

**Table 3.15. Poly(GMA-DVB) synthesised with cyclohexanol as porogen**

| Properties | GV7 (25%) | GV8 (50%) | GV9 (75%) | GV10 (100%) | GV11 (150%) | GV12 (200%) |
|---|---|---|---|---|---|---|
| PV(mL/g) | 0.75 | 0.93 | 0.97 | 1.04 | 1.13 | 1.16 |
| SA($m^2$/g) | 98.10 | 115.44 | 113.20 | 112.14 | 125.43 | 124.95 |

**Table 3.16. Poly(GMA-DVB) synthesised with hexanol as porogen**

| Properties | GV7H | GV8H | GV9H | GV10H | GV11H | GV12H |
|---|---|---|---|---|---|---|
| | 25% | 50% | 75% | 100% | 150% | 200% |
| PV(mL/g) | 1.47 | 1.53 | 1.70 | 1.88 | 1.84 | 1.89 |
| SA($m^2$/g) | 24.50 | 35.40 | 46.10 | 48.00 | 50.80 | 43.90 |

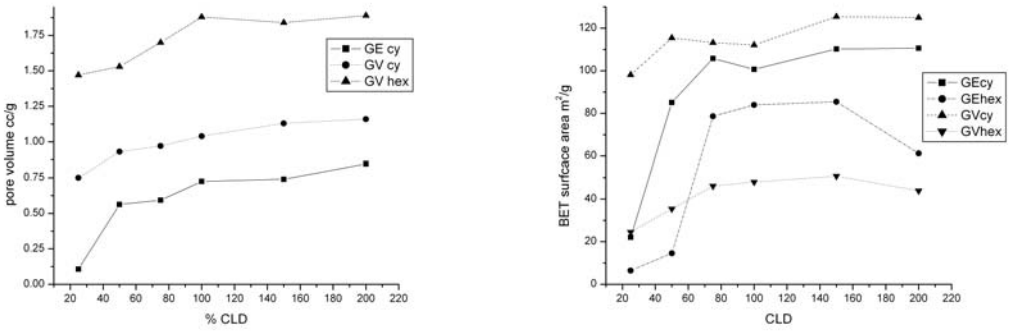


**Figure 3.8. Effect of crosslinker concentration on the surface area and pore volume for GMA-EGDM and GMA-DVB copolymers.**

As the degree of crosslinking increases the surface area also increases till crosslink density 100 and then levels off. The effect is less dramatic in case of GMA-DVB copolymers with both the porogens. However, for GMA-EGDM with both the pore generating solvents, the BET surface areas of the lower crosslink density polymers were very low and increased substantially as the CLD increased beyond 50. As the polymerisation proceeds the pendant vinyl group reacts with macroradicals to form crosslinks and multiple crosslinks. When the crosslinker concentration is increased, the

reactive pendant vinyl groups capable of further reaction increase thereby increasing the number of crosslinks. This leads to phase separation and shrinkage of particles and increase in the void space. The increase in the surface area with the crosslinker concentration can be attributable to the formation of rigid nuclei during polymerisation so that the number of smaller pores increases and their size decreases[32].

*3.5.3.1 Pore size and pore size distribution of GMA-DVB and GMA-EGDM copolymers*

The pore size and pore size distributions of the copolymers were determined using mercury intrusion porosimetry and nitrogen desorption isotherm. The nitrogen adsorption-desorption isotherms on the porous polymers give an idea about the porosity of the material.

*3.5.3.1.1 Adsorption isotherms*

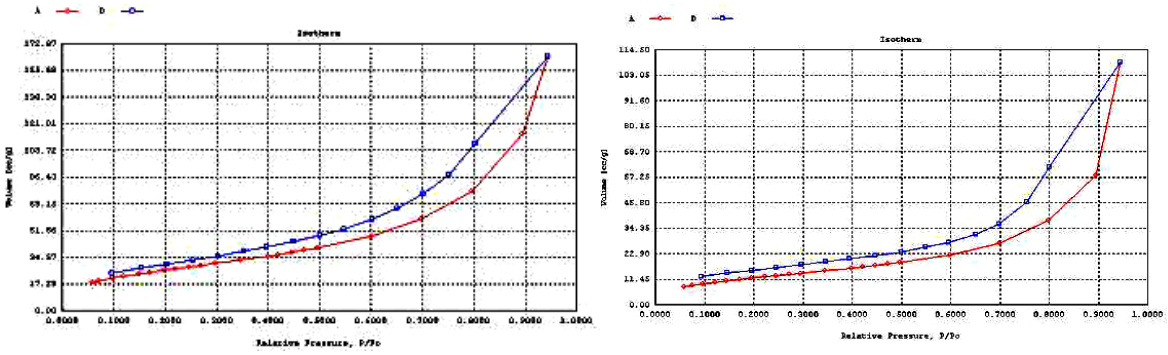


**Figure 3.9. Nitrogen adsorption isotherms obtained on a. GE10 and GV10H.**

Figure 3.9 shows typical adsorption-desorption isotherms obtained by nitrogen adsorption on the two representative samples GE10 and GV10H. The isotherms can be classified as mixed Type II-Type III isotherms according to BDDT classification[33]. There are six classes of isotherms according to this system of classification as shown in Figure 3.10.

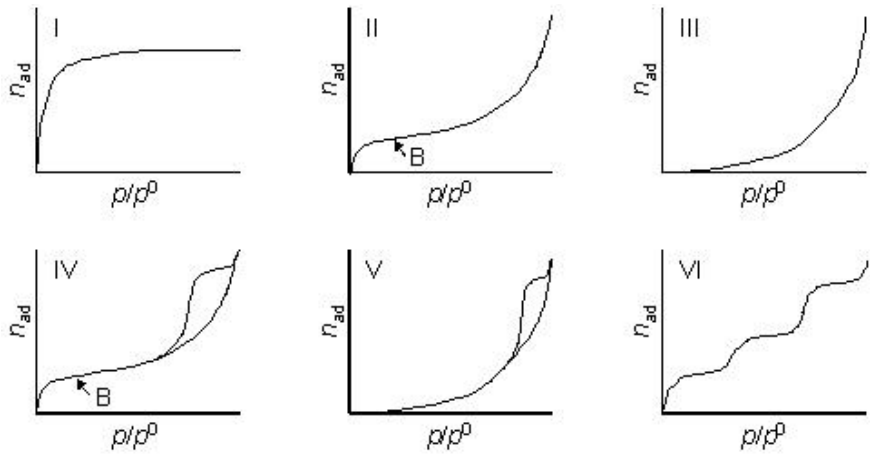


**Figure 3.10. Types of adsorption isotherms.**

Type I isotherms are given by microporous solids having relatively small external surfaces (e.g. activated carbons, molecular sieve zeolites and certain porous oxides), the limiting uptake being governed by the accessible micropore volume rather than by the internal surface area. The reversible Type II isotherm is the normal form of isotherm obtained with a non-porous or macroporous adsorbent. The Type II isotherm represents unrestricted monolayer-multilayer adsorption. Point B, the beginning of the almost linear middle section of the isotherm, is often taken to indicate the stage at which monolayer coverage is complete and multilayer adsorption about to begin. The reversible Type III isotherm is convex to the P/P° axis over its entire ranges and therefore does not exhibit a Point B. Isotherms of this type are not common, but there are a number of systems (e .g. nitrogen on polyethylene) which give isotherms with gradual curvature and an indistinct Point B .In such cases, the adsorbate-adsorbent interactions play an important role. Characteristic feature of the Type IV isotherm is its hysteresis loop, which is associated with capillary condensation taking place in mesopores, and the limiting uptake over a range of high p/p°. The initial part of the Type IV isotherm is attributed to monolayer-multilayer adsorption since it follows the same path as the corresponding part of a Type II isotherm obtained with the given adsorptive on the same surface area of the adsorbent in a non-porous form. Type IV isotherms are given by many mesoporous industrial adsorbents. The Type V isotherm is uncommon; it is related to the Type III isotherm in that the adsorbent-adsorbate interaction is weak, but is obtained with certain porous adsorbents.The Type VI isotherm, in which the sharpness of the steps depends on the system and the temperature, represents stepwise multilayer adsorption on a uniform non-

porous surface. The step-height now represents the monolayer capacity for each adsorbed layer and, in the simplest case, remains nearly constant for two or three adsorbed layers.

The isotherms also show hysteresis, the desorption lies well above adsorption. Generally, experimental isotherms measured on mesoporous solids display hysteresis loops in the mesopore region. However, hysteresis is observed only when the menisci in the adsorption and desorption paths are different in shape/diameter. Such situation is typical for open-ended cylindrical mesopores, bottle-shaped (ink bottle), or spaces between parallel sheets (slits). If cylindrical pore is closed at one end and does not contain any narrows, the adsorption isotherms will not display hysteresis loop[34]. There are four types of hysteresis loops Type H1, H2, H3 and H4. Although the effect of various factors on adsorption hysteresis is not fully understood, the shapes of hysteresis loops have often been identified with specific pore structures.

The synthesised polymers showed mixed Type II-Type III adsorption isotherm with H3 type hysteresis. The adsorption branch showed a very indistinct knee/inflection at low relative pressure below 0.3 indicating the absence of micropores. The low surface areas and high pore volumes of the polymers also suggest absence of micropores. The comparative adsorption isotherms for GMA-EGDM polymers with cyclohexanol as porogen are shown in Figure 3.9**.** As the isotherm approaches increased partial pressures, a steep rise in adsorption is realised indicating the filling of the mesopore openings and subsequently, the macropore cavities. The pore size distribution is bimodal for GMA-DVB and GMA-EGDM polymers with cyclohexanol as porogen as shown in Figure 3.11**.** The most frequently occurring pores are in the range of 50-100 and 1000-3000 $A^0$. The pore size distribution in desorption mode by nitrogen adsorption also show maxima at 100 $A^0$. The broad pore size distribution suggests presence of macropores not assessable by nitrogen adsorption. In case of GMA-DVB polymers with hexanol as porogen the pore size distribution is unimodal with pore radii located between 1000-3000 $A^0$.

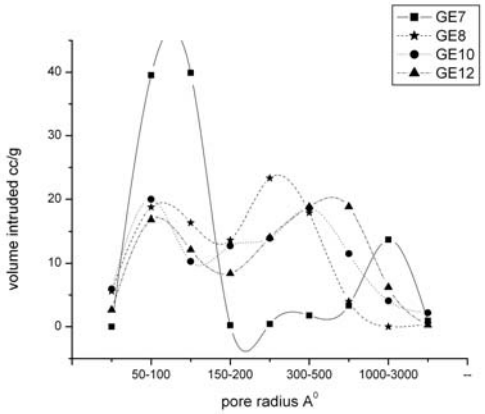


a.

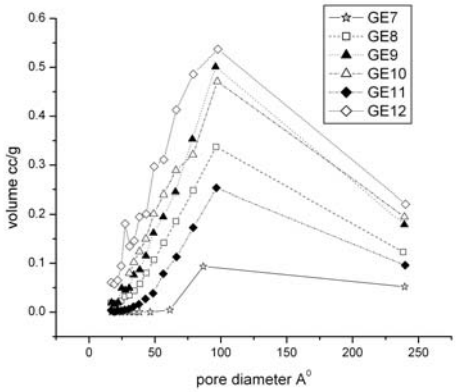


b.

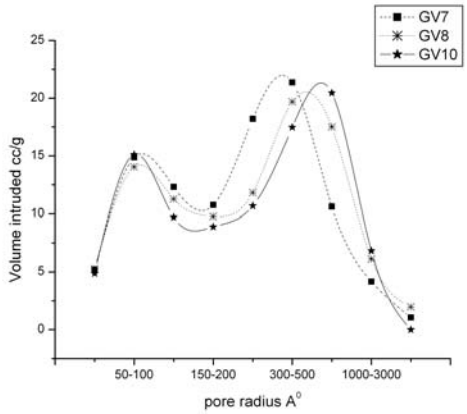


c.

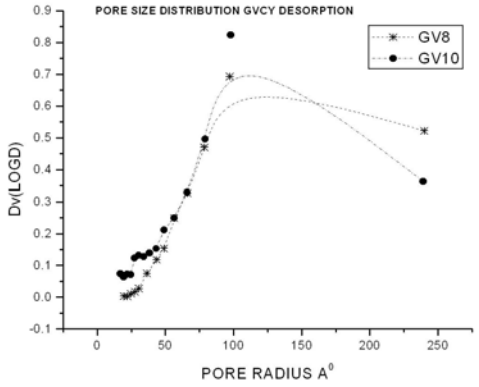


d

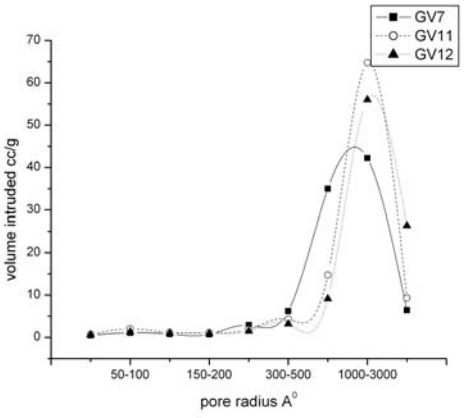


e.

**Figure 3.11. (a) and b: pore size distribution of GMA-EGDM polymers with cyclohexanol as porogen by MIP and $N_2$ adsorption, c. and d: pore size distribution of GMA-DVB polymers with cyclohexanol as porogen by MIP and $N_2$ adsorption, e: pore size distribution of GMA-DVB polymers with hexanol as porogen by MIP.**

## 3.6 Polymers synthesised using concentrated emulsions

The major application of HIPE is to produce open porous polymeric foams with well-defined morphologies. These foams generally possess extremely low densities and poor mechanical properties, which hamper their use in chromatographic applications. Li and Benson first patented a process to make spherical particle using HIPE[35]. They are characterised by large cavities of micrometer dimensions that are interconnected to adjacent cavities by smaller pores. They are further characterised by having very high total porosity, up to 90%. Polygenetics (then Biopore Corporation) obtained a license to the technology in certain fields of use, continued development of the technology and achieved major technology breakthroughs: spherical forms of the polymer called Cavilink™. Production of polymers in spherical form greatly reduces manufacturing costs and adds important properties that enable it to address many more markets than originally conceived by Unilever.

Most polyHIPE materials so far have been made with hydrophobic monomers such as styrene-divinylbenzene[36-39]. The use of more hydrophilic/more polar monomers is quite restricted for the application of emulsion polymerisation. We have chosen glycidyl methacrylate and hydroxyethyl methacrylate monomers to make the beads because they possess appropriate hydrophilicity, stability and the possibility of chemical functionalisation through epoxy and hydroxy groups. The surfactant Span 80 is most commonly used in the production of W/O emulsion. It is soluble in oil phase owing to its low hydrophile-lipophile balance (HLB). The emulsions were prepared with 17.77% (w/v) surfactant concentration relative to continuous phase.

The typical procedure for making the beads involves a. making a primary emulsion (W/O) b. suspending the formed emulsion in external water containing suspending stabiliser and polymerisation.

When the polymers were synthesised with poly(vinyl pyrrolidone) as suspending stabiliser the yields were quite low at low crosslink densities. The yields increased with increase in the crosslink density as shown in Figure 3.12. The figure shows the change in the percent yield with change in the crosslink density and internal phase water. When the ratio of monomer: discontinuous water was changed from 1:0.5 to 1:2.0 the percent yield decreased. The percent yields are tabulated in Tables 3.17-3.19.

When the polymerisations were carried out using calcium chloride as suspending stabilizer the yields were between 80-90%. The lower yield with poly(vinyl pyrrolidone) is due to loss from grafting of GMA-EGDM/ HEMA-EGDM onto poly(vinyl pyrrolidone). This is qualitatively seen by the change in the continuous phase from colourless initially to milky white at the end of polymerisation.

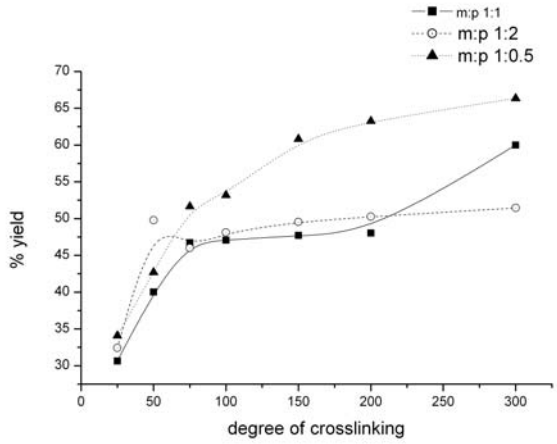


**Figure 3.12 Change in the percent yield of HIPE polymers with change in CLD and discontinuous water.**

The percent yields were calculated according to the formula shown below:

$$\% \text{ yield} = W_d / Wm \times 100 \qquad 3.11$$

Where, $W_d$ is the weight of dry polymer beads in g and $W_m$ is weight of monomers charged in the reactor. As the concentration of the crosslinker in feed increases the total number of reactive sites (vinyl groups) increase. This leads to the formation of more number of free radicals thus increasing the overall yield. As indicated earlier, when poly(vinyl pyrrolidone) was used as suspending stabiliser lower yields were obtained due to probable chain transfer to the stabiliser. Similar trend was observed for HEMA-EGDM polymers also.

**Table 3.17. Percent yield GMA-EGDM HIPE copolymers with 50% internal water**

| Polymer code | GEH01 | GEH02 | GEH03 | GEH04 | GEH05 | GEH06 | GEH07 |
|---|---|---|---|---|---|---|---|
| Yield % | 30.64 | 40.02 | 46.71 | 47.07 | 47.70 | 48.03 | 60.00 |

**Table 3.18. Percent yield GMA-EGDM HIPE copolymers with 66.6% internal water**

| Polymer code | GEH11 | GEH12 | GEH13 | GEH14 | GEH15 | GEH16 | GEH17 |
|---|---|---|---|---|---|---|---|
| Yield % | 32.41 | 49.73 | 46 | 48.13 | 49.54 | 50.26 | 51.44 |

**Table 3.19. Percent yield GMA-EGDM HIPE copolymers with 33.33% internal water**

| Polymer code | GEH21 | GEH22 | GEH23 | GEH24 | GEH25 | GEH26 | GEH27 |
|---|---|---|---|---|---|---|---|
| Yield % | 34.08 | 42.71 | 51.66 | 53.19 | 60.81 | 63.25 | 66.36 |

### *3.6.1 Morphology and internal structure of polymers synthesised using concentrated emulsion*

It was thought that only HIPEs could produce open porous highly interconnected network structures. However, recently it has been shown by Bismarc et al. that the open porous interconnected networks can also be formed from MIPE[40]. The increased volume of an organic phase in the reaction mixture gives rise to foam with increased densities, which improved the mechanical properties and reduced the chalkiness of the materials. They used 60% discontinuous phase volume. It is therefore interesting to observe the structures formed with low concentrations of discontinuous phase.

#### *3.6.1.1 Formation of emulsions*

The porous properties of the polymers synthesised by polymerising concentrated emulsions depend upon the stability of the formed emulsions which in turn is dependent on the factors like type of surfactant, its concentration, the hydrophobicity/ hydrophilicity of the monomers, temperature etc. The emulsions being thermodynamically unstable require surfactants/emulsifying agents for stabilisation. The surfactants possess polar

head groups (hydrophilic) and long fatty acid chains (lipophilic). It is because of these they can act at the interface between oil and water. They form a rigid film at the interface and prevent phase inversion. In addition to this protective barrier, emulsifiers stabilise the emulsion by reducing the interfacial tension of the system. The choice of the surfactant is dependent on the HLB (hydrophile-lipophile balance) number. The HLB number defines the polarity of nonionic surfactants in terms of an empirical quantity. The system HLB has an arbitrary scale of 1-18. HLB numbers are experimentally determined for the different emulsifiers. If an emulsifier has a low HLB number, there are a low number of hydrophilic groups on the molecule and it will have more of a lipophilic character. For example, the Spans® generally have low HLB numbers and they are oil soluble. Because of their oil soluble character, Spans® will cause the oil phase to predominate and form a W/O emulsion[41].

We have used Span 80 with HLB number 4.3 and Brij 52, 72 and 92, with HLB numbers 5.3, 4.9 and 4.9 respectively, to form the emulsions. By keeping the surfactant concentration same, the emulsions prepared with Span 80 at low internal phase water concentration (33.33%, 50%) were unstable and the stability decreased with increase in crosslinker concentration. With Brij 52 and Brij 92 reasonably stable emulsions were obtained at room temperature. The stabilisation of an emulsion with an emulsifying agent is a complex process. The polarity of the organic phase is also an important parameter for the formation of stable emulsion. The higher polarity of the organic phase requires more hydrophobic surfactant to stabilise the emulsion[42]. A surfactant dissolved in the continuous phase and adsorbed upon the interface between the two phases as an oriented interfacial film ensures the stability of the concentrated emulsion. As already stated, the stable emulsions only form when the monomer (continuous phase) is sufficiently hydrophobic. Both GMA and EGDM are not sufficiently hydrophobic to form the stable emulsions. We therefore decided to add strongly hydrophobic liquid to the oil phase in order to increase the emulsion stability. Thus, decane, heptane and cyclohexane were added to the oil phase. Thick, stable emulsions were obtained by addition of these liquids to the continuous phase.

*3.6.1.2 Formation of particles*

The morphology of the polymers obtained by polymerisation of the emulsions for 25% CLD GMA-EGDM polymers with 50%, 60% and 90% discontinuous phase volumes (MIPE and HIPE) as seen by SEM at same magnification are shown in Figure 3.13.

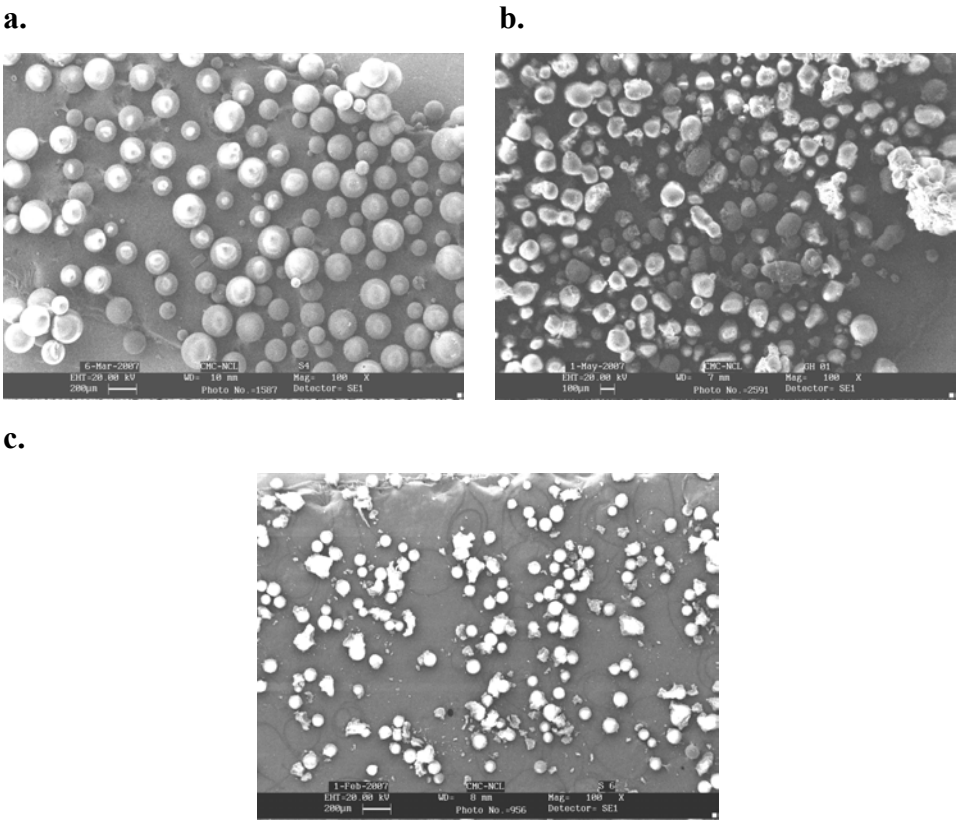


**Figure 3.13. Polymeric beads of GMA-EGDM HIPE polymer of 25% CLD with (a) 33.33% internal water (b) 66.66% internal water c. 90.90% internal water.**

With increase in the discontinuous water content the particle size reduced. Beads with irregular shapes were also obtained along with the spherical particles with increase in water content. The number of particles with irregular shapes increased as the water content was increased. There is a maximum amount of dispersed phase that can be incorporated into a concentrated emulsion. This is dependent on the interfacial free energy between the organic and water phases in the absence of surfactant. A large value of interfacial free energy implies that the organic phase is very hydrophobic and hence its interactions with water are weak. As a result the interactions between hydrocarbon chain

of surfactant and the organic molecules as well as those between the polar head groups of the surfactant and water are strong, stabilising the interface between the two phases and consequently increasing the stability of the emulsion. If the organic group interacts with the polar head groups of the surfactant, the interactions between the water and polar head groups of the surfactant become weak and the emulsion becomes unstable. The droplet coalescence as a result of destabilisation of an emulsion results in irregular shaped beads.

The Figure 3.13 shows the SEM photographs of the HEMA-EGDM particles at magnification 100 X.

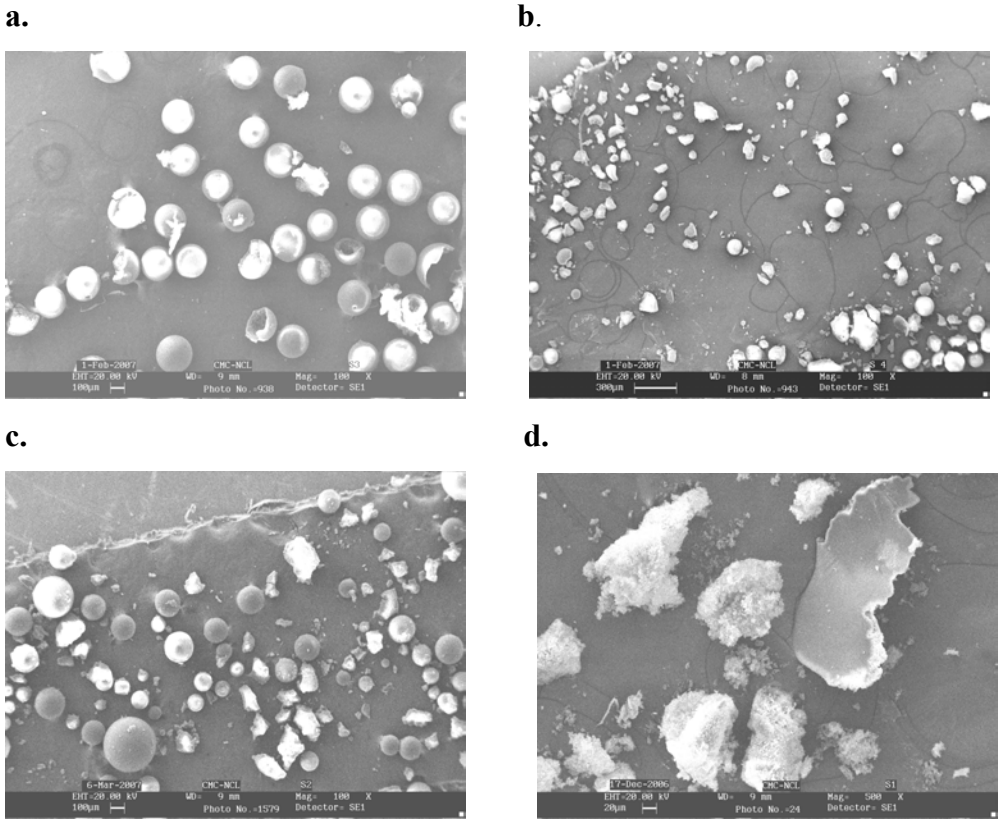


**Figure 3.14. Polymeric beads of HEMA-EGDM HIPE polymer with (a) 33.33% internal water (b) 66.66% internal water c. HEH01O d. HEH02O.**

Figure 3.14 a and b show the morphology of the beads (HEH02 and HEH12) synthesised using both phase initiator whereas the pictures c and d show the beads synthesised with organic (HEH02O) and aqueous phase (HEH02A) initiators respectively. With both phase and organic phase initiator spherical beads were obtained along with some irregular shaped particles. However, with only aqueous phase initiator the particles obtained were of distorted shapes. The coagulation of the particles takes

place during drying process. The HEMA monomer is completely soluble in water whereas EGDM is sparingly soluble in water. Thus HEMA is present mostly in the aqueous phase. Although HEMA monomer is soluble in water, the growing polymer is not. The phase separation takes place owing to this decreased solubility. The growing polymer phase separates in the aqueous phase in the form of droplets, which fuse together, and eventually becomes fixed in the form of a network[43]. The process of syneresis during phase separation results in coagulation of the particles after dying, since water along with the surfactant gets expelled out of the network. As the polyHEMA interface is extremely polar, the surfactant adsorption is only weak and so they may easily desorb if conditions such as temperature or particle concentration change. Phase separation takes place (''syneresis'', water expulsion out of the cross-linked material) during the polymerisation of HEMA in an aqueous medium. Weakly adsorbed surfactants can easily desorb under such conditions. The consequence of surfactant desorption is coagulation or coalescence of the naked polyHEMA particles[44].

Initiator type also plays an important role in determining particle size and morphology. Water-soluble initiators like potassium peroxydisulphate exist only in the water phase, but oil soluble initiators distribute between both the water and oil phases. It has been shown that the heterophase crosslinking polymerisation of HEMA in water with potassium peroxydisulphate as an initiator led to hydrogel. It was also shown that the stable HEMA latex particles could only be formed with hydrophobic initiator (AIBN) and ionic surfactant with alkyl chain length greater than ten or with surface-active initiators with alkyl chain length greater than eight[45].

It was also seen that with increase in discontinuous phase water the polymers were obtained as large precipitates. This can be attributed to droplet coalescence as the internal water diffuses out into the external phase.

The reactivity ratios of HEMA and EGDM are 0.84 (±0.20) and 6.2, respectively[46]. EGDM being much faster reacting than HEMA, homopolymerisation of both EGDM and HEMA are possible, leading to heterogeneity in the morphologies of the copolymers.

### *3.6.1.3 Internal structure of the beads*

a.

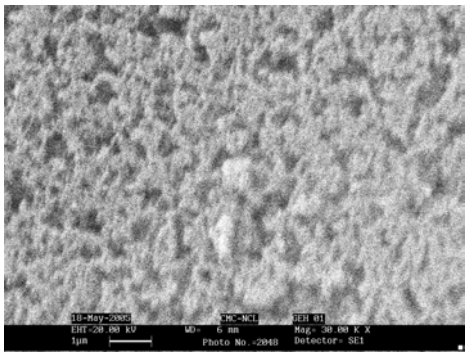


**b.**

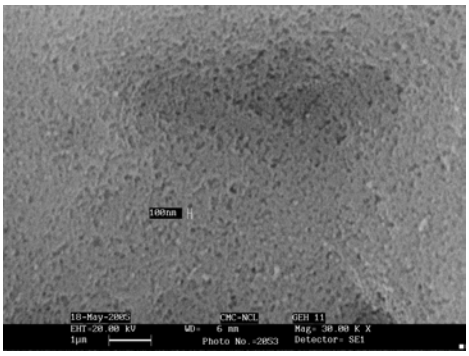


c.

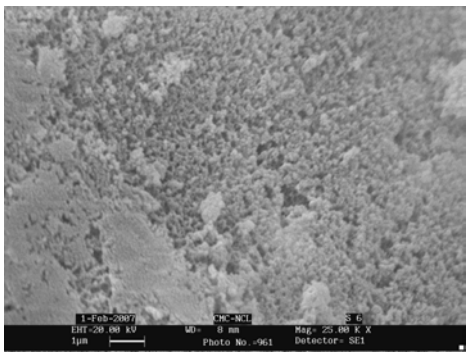


**d.**

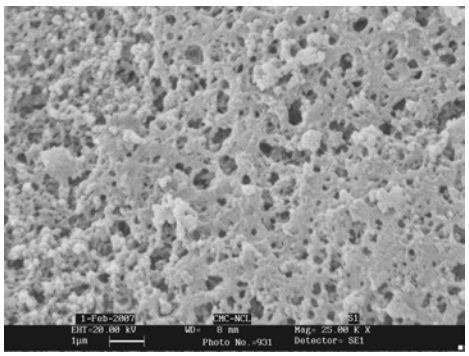


**e.**

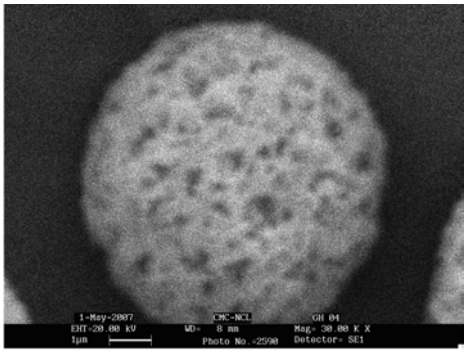


**f.**

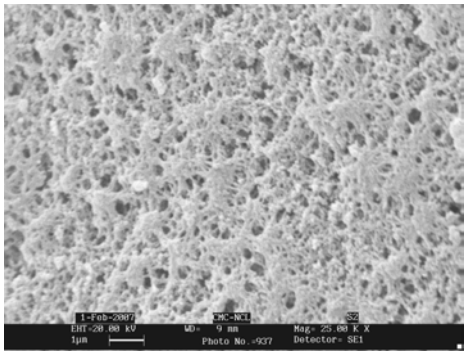

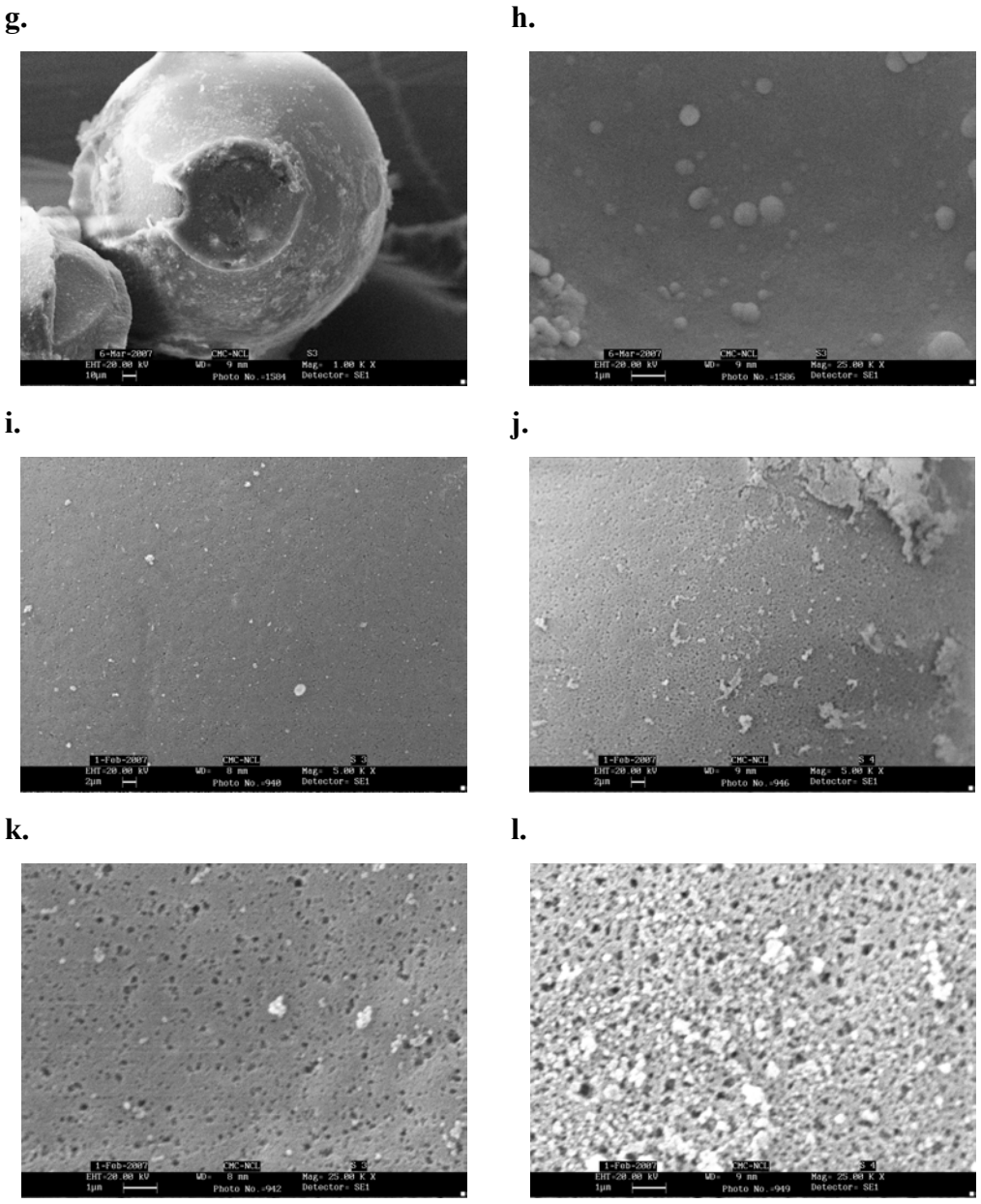


**Figure 3.15. SEM photographs of samples; (a) GEH01, (b) GEH11 and (c) GEH51 at magnification 25KX; (d) GEH02O (e) GEH04O and (f) GEHo4O at magnification 25 KX; (g). GEH01B52 at 1KX and (h). GEH01B52 at 25KX (i) HEH12 and (j) HEH02 at 5KX; (k) HEH12 and (j) HEH02 at 25KX.**

Figure 3.15 shows SEM photographs of the beads at different magnifications. The morphologies and internal structures of the polymers are distinctly different from the beads made by suspension polymerisation. The morphology of the resulting material is determined by the structure of the emulsion prior to gelation. The morphologies and the internal structure of the polymers reflect the structure of the emulsion in case when the

emulsions are stable and do not separate into individual components before gelation. During polymerisation phase separation occurs within the developing polymer structure between the internal phase droplets[47]. The properties of the emulsion like structure, stability and rheology depend on the composition, thickness and the viscoelasticity of the adsorbed stabilising layer at the oil-water interface. The stability of the emulsion with respect to creaming and coalescence depends mainly on the droplet-size distribution, the state of aggregation of droplets and the rheology of aqueous dispersion medium. The droplet size distribution is mainly dependent on the energy inputs during emulsification, as well as on nature and amount of emulsifying agent. The aggregation occurs as the adsorbing macromolecules get attached to more than one droplet at a time[48].

Figure 3.15 a, b and c shows the photomicrographs of the sample GMA-EGDM with 25% crosslink density with different concentrations of discontinuous phase. The internal structure shows the presence of pores open to the surface. The pores are non-uniform and the cell size and window size are not well defined. As already stated, these emulsions do not classify as HIPEs, since they contain low discontinuous phase volumes typically less than 74%. When a HIPE is formed the shape of discontinuous phase droplets change from spherical to polyhedral. The droplets are separated from each other by very thin continuous phase. When the polymerisation occurs, the contact areas between the droplets give rise to pore throats that leads to highly interconnected pore structure[49]. In the emulsions with higher amounts of continuous phase in the polymerisation mixture, the discontinuous phase droplets are separated from each other and there are very less or no contact areas between the two droplets. This leads to uneven porous structures in the resulting polymer.

The change in the porous structures with change in the discontinuous phase is shown in the Figure 3.15 a, b and c. It can be seen that with increase in internal water the pore size reduces. The skin formation was also observed with increase in discontinuous water. When the polymerisations were carried out with only AIBN (no potassium peroxydisulphate) and calcium chloride in the outer phase water, the porous structures resemble the structures obtained by polymerisisng HIPE as shown in the Figure 3.15 d, e and f. The bead surface shows interconnected network of pores. The presence of an electrolyte in the internal phase water is known to stabilise the emulsions against Ostwald

Ripening[50]. This suggests that the emulsions were stabilised to some extent by the presence of an electrolyte as the external phase water is emulsified into the primary emulsion thus forming a W/O/W type ternary emulsion[51].

The surface morphology of HEMA-EGDM polymers with both phase initiators is shown in the Figure 3.15 i, j (5KX), k and l (25KX**).** As the water was increased the porosity reduced. The internal phase water could diffuse to the external phase water leading to less porous material.

*3.6.1.4 Surface area, pore volume and pore size distribution*

The BET surface areas, surface areas and pore volume by mercury intrusion porosimetry of the GMA-EGDM polymers synthesised using both phase initiator and poy(vinyl pyrrolidone) as suspending stabiliser are tabulated in the Table 3.20. There is a marginal increase in the surface areas as the crosslink density is increased. The specific surface areas lie in the range of 50-100 $m^2/g$. The larger surface areas obtained by mercury intrusion porosimetry than BET indicate the presence of ink-bottle pores. There is little effect of changing the ratio of continuous phase to discontinuous phase on the surface areas as can be seen from the Table 3.22. When discontinuous water was changed from 33.33 to 90.90 % for 25 % crosslink density the surface areas showed a very marginal change. The large difference between the surface areas obtained by nitrogen adsorption and mercury intrusion porosimetry as well as low intruded pore volumes of the samples GEH06 and GEH07 indicate the presence of small pores not accessible by mercury intrusion porosimetry. This has been reflected in the pore size distribution of the two samples. The pore size distribution by mercury intrusion porosimetry shows broad distribution for the sample GEH01, with the pore sizes ranging from 50-450 $A^0$ i.e. in the mesopore range. With increase in crosslink density the pore size distribution shifts to lower pore sizes (Figure 3.17a**.**). The particle size distribution as determined from nitrogen adsorption (Figure 3.17b) shows a maxima in the region of 150 $A^0$ for the sample GEH07 while it is absent in the sample GEH01. The plot also shows the upward incline beyond 100 $A^0$, suggesting the presence of pores with diameters larger than 100 $A^0$. The total intruded pore volumes go on decreasing with the increase in crosslink density with the minimum of 0.0396 cc/g for GEH07. This shows the absence of macropores. A very large surface area by nitrogen adsorption as compared to mercury

intrusion porosimetry indicates the presence of smaller pores. The pore size distributions for the GMA-EGDM polymers with 33.33 % and 66.66 % discontinuous phase volumes are shown in Figure 3.20 and 3.21. The pore size distribution plots for GEH21, GEH24, and GEH27 polymers show broader pore size distribution for GEH21 than GEH24 and GEH27, with pores ranging from 25-2000 $A^0$. The distribution becomes narrower as the crosslink density is increased. The pore sizes for GEH24 and GEH27 lie in the range of 25-350 and 25-200 $A^0$ respectively as shown in the Figure 3.19 e and f. The same trend is observed for pore size distribution as determined by nitrogen adsorption (Figure 3.20 i). As the inner water is increased further i.e. 66.66 %, the pore size distribution becomes narrow with pore diameters ranging from 5-50$A^0$ (Figure 3.21 j and k). Thus the smallest pores are obtained with 50% inner water as compared to the polymers with lower volumes of inner water.

Table 3.21 shows the pore volume, surface area data for the GMA-EGDM polymers synthesised using AIBN as initiator and calcium chloride as suspending stabiliser. The pore volumes are in the range of 0.64-0.93 cc/g. The BET surface areas are in the range of 11-85 $m^2/g$. The surface areas increase with increase in crosslink density. The unexpected higher value of surface area for the sample GEH03O is an artifact. The surface areas by mercury intrusion porosimetry are higher than the BET surface areas. The plots of pore size distribution by mercury porosimetry for the samples GEH01O, GEH04O and GEH07O are shown in the Figure 3.18 c and d. The pore size distribution is very broad with pores in range of 2000 nm i.e. in the macropore range and also in the mesopore range. In case of GEH01O there are no pores below 500 $A^0$. This explains the low BET surface area of the sample. As the crosslink density is increased the pore size distribution becomes narrow with GEH04O showing majority of the pores in the 50-500 $A^0$ thus generating higher surface area than low crosslinked samples. The reactivity ratios of GMA and EGDM are 0.98 and 1.00. In case of GEH04O the molar composition of monomer and crosslinker is 50:50. This is expected to give regular pore network with stabilised emulsions. With 300% crosslink density however the pore size distribution again shows bimodal distribution of pores. The pore size distribution calculated from the adsorption branch of the hysteresis for the two samples GEH01O, GEH04O and GEH07O is shown in Figure 3.19. The pore size distribution also showed the presence of

smaller pores in the mesopore range. The smaller pores lie in the range of 20-50 $A^0$ and the plot showed an incline beyond 100 $A^0$ suggesting presence of larger pores.

To generate higher surface area, a solvating diluent is added to the oil phase. This will induce phase separation during later stage of polymerisation generating smaller pores and higher surface areas. The solvating ability of a solvent depends upon its solubility parameter. The solubility parameters for the hydrocarbons used in the polymerisation recipe are 7.5, 8.0 and 8.2 for heptane, decane and cyclohexane, resptectively. The solubility parameters of cyclohexane are thus close to GMA-EGDM polymers shown in Table 3.23. The surface areas obtained are not high as expected.

When Brij surfactants were used instead of span, the surface areas obtained were in the range of 65-75 $m^2/g$. The pore size distribution by mercury intrusion porosimetry shows the presence of pores in the range of 50-700 $A^0$ (Table 3.24, Figure 3.22).

The surface areas of HEMA-EGDM polymers lie in the range of 3-70 $m^2/g$ (Table 3.25). The pore size distribution as shown in Figure3.23, is broader for lower crossslink densities while it is narrower for higher crosslink densities. The distribution is bimodal with the pores in the range 50-500 $A^0$ as well as 500-3000 $A^0$ in case of polymers synthesised only with aqueous phase initiator and calcium chloride as suspending stabilizer (Figure 3.23 c). The pore volumes of HEH01A-07A are larger than the pore volumes of HEH01O-07 as shown in Table 3.26. The pore size distribution for the samples prepared with only organic phase initiator is narrower with all the pores in the range 50-1000 $A^0$ (Figure 3.23 a and b).

**Table 3.20. Surface area, pore volume data for GMA-EGDM polymers synthesised using simultaneously two initiators, AIBN and potassium peroxydisulphate.**

| Polymer code | Surface area (BET) $m^2/g$ | Surface area by (MIP) $m^2/g$ | Pore volume $cm^3/g$ |
|---|---|---|---|
| GEH-01 | 50.21 | 78.16 | 0.82 |
| GEH-02 | 51.82 | 68.64 | 0.26 |
| GEH-03 | 57.39 | 74.22 | 0.28 |
| GEH-04 | 58.91 | 48.77 | 0.20 |
| GEH-05 | 66.13 | 57.67 | 0.28 |
| GEH-06 | 99.88 | 68.34 | 0.19 |
| GEH-07 | 98.72 | 19.22 | 0.04 |
| GEH-11 | 50.81 | 79.83 | 0.42 |
| GEH-12 | 54.23 | - | - |
| GEH-13 | 59.54 | - | - |
| GEH-14 | 63.47 | 79.46 | 0.33 |
| GEH-15 | 69.05 | - | - |
| GEH-16 | 65.58 | - | - |
| GEH-17 | 66.98 | 66.73 | 0.56 |
| GEH-21 | 58.52 | 127.03 | 0.42 |
| GEH-22 | 49.79 | - | - |
| GEH-23 | 57.87 | - | - |
| GEH-24 | 69.00 | 101.68 | 0.29 |
| GEH-25 | 76.96 | - | - |
| GEH-26 | 71.49 | - | - |
| GEH-27 | 86.68 | 134.92 | 0.33 |

**Table 3.21. Surface area, pore volume data for GMA-EGDM polymers synthesised using only oil phase initiator (AIBN)**

| Polymer code | BET Surface area $m^2/g$ | Surface area by MIP $m^2/g$ | Pore volume g/cc |
|---|---|---|---|
| GEH-01O | 11.79 | 58.84 | 0.64 |
| GEH-02O | 28.99 | - | - |
| GEH-03O | 85.09 | - | - |
| GEH-04O | 46.63 | 81.43 | 0.50 |
| GEH-05O | 74. | - | - |
| GEH-06O | 57 | - | - |
| GEH-07O | 70 | 129.80 | 0.93 |

a. b.

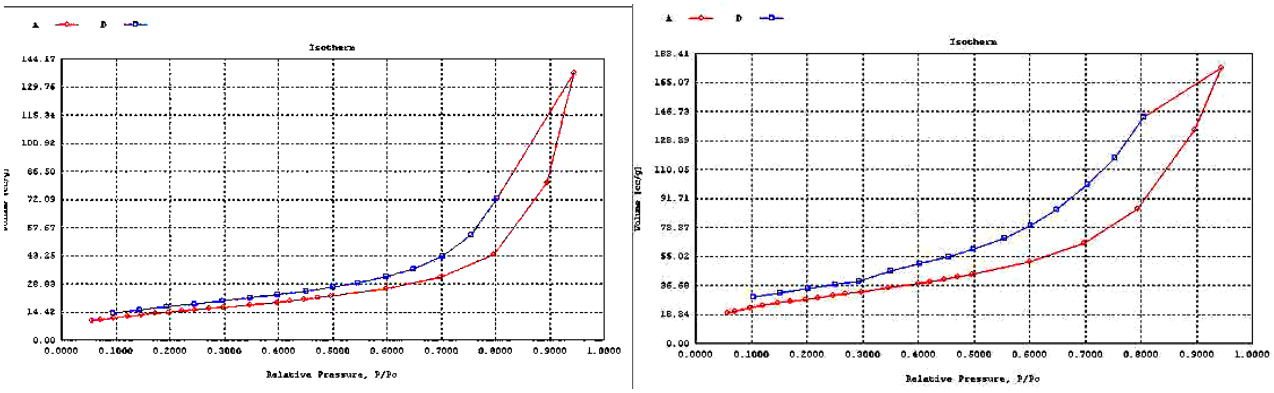


**Figure 3.16. Nitrogen adsorption-desorption isotherm of the polymers GEH01 and GEH07.**

The adsorption isotherms for the two representative samples GEH01 and GEH07 are shown in the Figure 3.16. The hysteresis loop becomes wider as the crosslink density increases from 25 to 300. The wider hysteresis loops are generally associated with low pore connectivity. This is supported by low intruded pore volume by mercury intrusion porosimetry as low pore size and low pore connectivity hinder mercury intrusion.

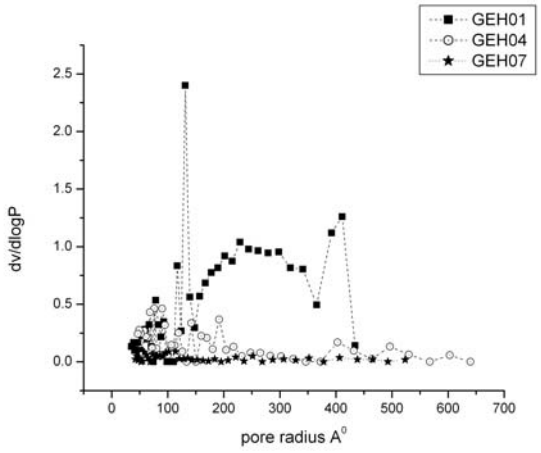


**a.**

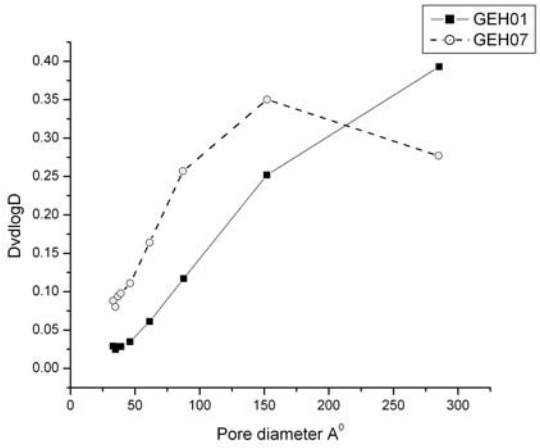


**b**.

**Figure 3.17. Pore size distribution of the samples GEH01, GEH04 and GEH07 (a) by mercury intrusion porosimetry, (b) by nitrogen adsorption.**

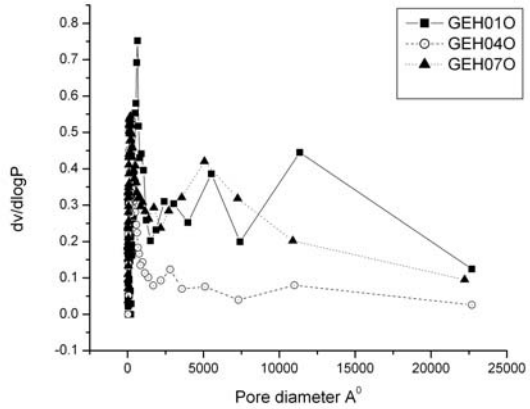


**c.**

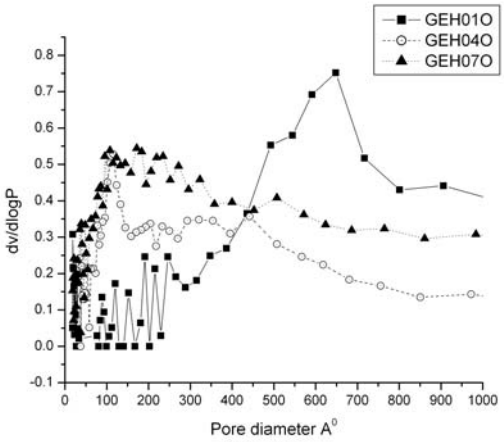


**d**.

**Figure 3.18. Pore size distribution of the samples GEH01O, GEH04O and GEH07O (c) by mercury intrusion porosimetry, (d) enlarged in the lower pore diameter region.**

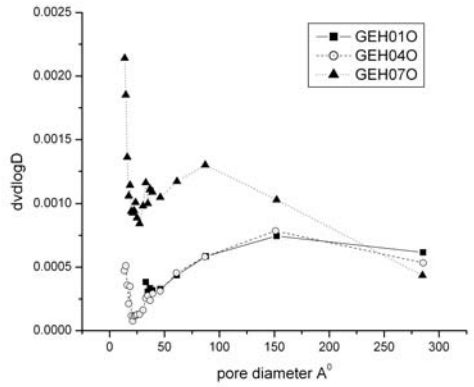


e.

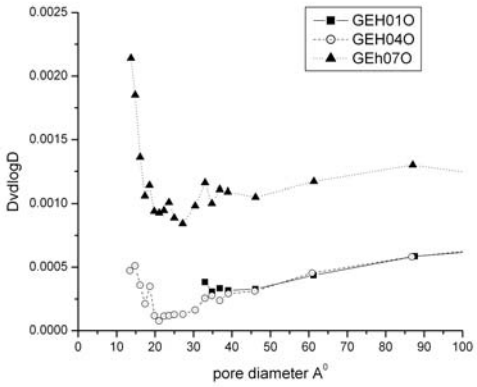


f.

**Figure 3.19. Pore size distribution of the samples GEH01O, GEH04O and GEH07O by nitrogen adsorption, b. enlarged in the lower pore diameter region**

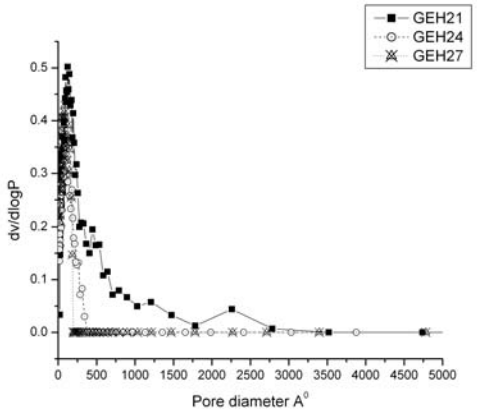


g.

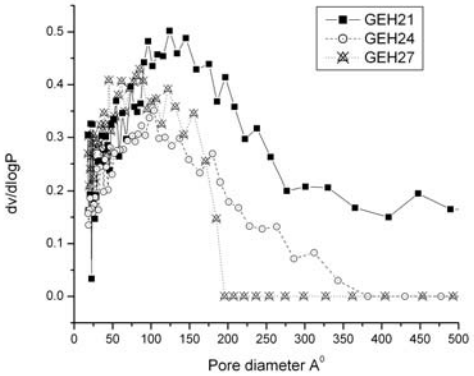


h.

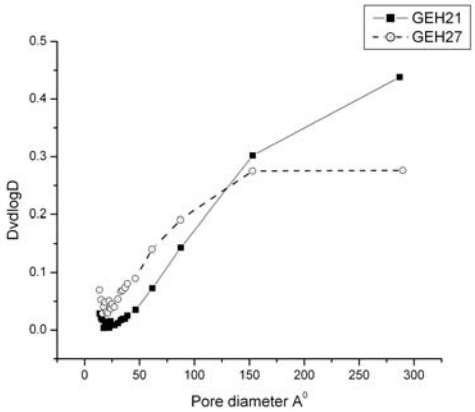


i.

**Figure 3.20. Pore size distribution of the samples GEH21, GEH24 and GEH27 by a. MIP and b. by $N_2$ adsorption.**

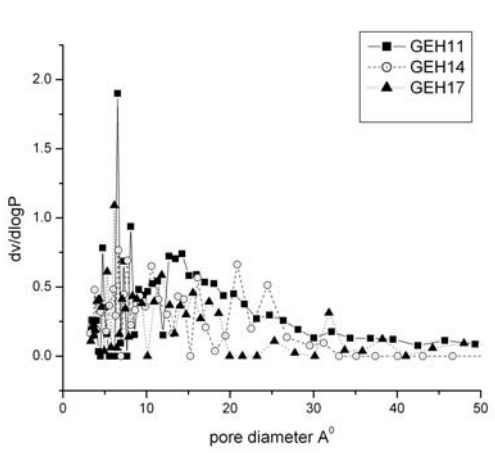


j.

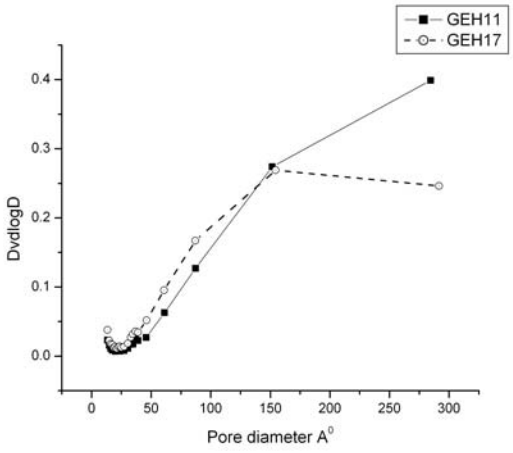


k.

**Figure 3.21. Pore size distribution of the samples GEH11, GEH14 and GEH17 by a. MIP and b. by $N_2$ adsorption.**

**Table 3.22. Effect of change in ratio of continuous to discontinuous phase on the BET surface area of 25% crosslinked GMA-EGDM polymers**

| Sr. No | Polymer code | Ratio of m:iw | Surface area $m^2/g$ |
|---|---|---|---|
| 1. | GEH21 | 1: 0.5 | 58.52 |
| 2. | GEH01 | 1: 1.0 | 50.81 |
| 3. | GEH11 | 1: 2.0 | 50.21 |
| 4. | GEH31 | 1: 2.5 | 52.1202 |
| 5. | GEH41 | 1: 5.0 | 39.6319 |
| 6. | GEH51 | 1: 10.0 | 41.5409 |

m:iw: monomer|: internal water

**Table 3.23. Effect of addition of hydrophobic liquid on the BET surface area of 25% crosslinked GMA-EGDM polymers**

| Sr. No | Polymer code | Ratio of m:iw | *Porogen used | Surface area $m^2/g$ |
|---|---|---|---|---|
| 1. | GEH1a1 | 1: 2.5 | Decane | 24.4478 |
| 2. | GEH1a2 | 1: 2.5 | heptane | 10.5791 |
| 3. | GEH1a3 | 1: 2.5 | cyclohexane | 37.3099 |
| 4. | GEH1c1 | 1: 10.0 | Decane | 9.9724 |

| | | | | |
|---|---|---|---|---|
| 5. | GEH1c2 | 1: 10.0 | heptane | 9.9261 |
| 6. | GEH1c3 | 1: 10.0 | cyclohexane | 9.2633 |

m:iw: monomer: internal water

**Table 3.24. Effect of change in the surfactant**

| Sr. No. | Polymer code | Surface area $m^2$/ g (BET) | Surface area $m^2$/g (MIP) | Pore volume $cm^3$/g |
|---|---|---|---|---|
| 1. | GEH01B52 | 69.3612 | 95.75 | 0.73 |
| 2. | GEH01B72 | 75.6535 | 59.52 | 0.45 |
| 3. | GEH02B92 | 66.3444 | 100.43 | 0.89 |

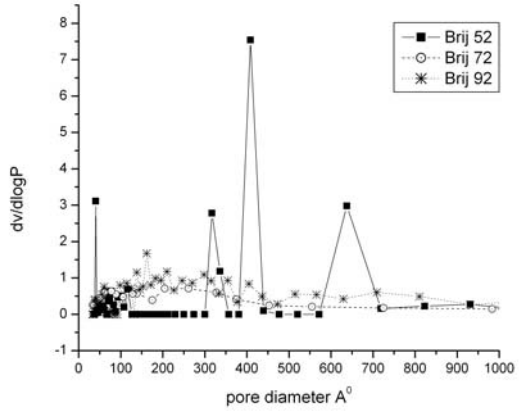


**Figure 3.22. Pore size distribution of GMA-EGDM HIPE polymers synthesised using Brij surfactants, by MIP.**

**Table 3.25. BET surface areas of the HEMA-EGDM polymers synthesised using both phase initiator and PVP as suspending stabiliser with different concentrations of discontinuous water**

| Polymer code | Surface area |
|---|---|
| HEH01 | 5.19 |
| HEH02 | 10.38 |
| HEH03 | 11. 95 |
| HEH04 | 14.16 |
| HEH05 | 27.35 |
| HEH06 | 46.02 |
| HEH07 | 41.21 |
| HEH11 | 20.42 |
| HEH12 | 35.56 |
| HEH13 | 48.90 |
| HEH14 | 59,08 |
| HEH15 | 65.87 |
| HEH16 | 66.38 |
| HEH17 | 65.13 |
| HEH21 | 12.31 |
| HEH22 | 39.97 |
| HEH23 | 36.18 |
| HEH24 | 45.32 |
| HEH25 | 62.43 |
| HEH26 | 67.13 |
| HEH27 | 69.04 |

**Table 3.26. BET surface areas of the HEMA-EGDM polymers synthesised using organic phase initiator (HEH01O-7O) as well as with aqueous phase initiator (HEH01A-7A) and calcium chloride as suspending stabiliser with different concentrations of discontinuous water**

| Polymer code | Pore volume $cm^3/g$ | Surface area $m^2/g$ |
|---|---|---|
| HEH01O | | 3.189 |
| HEH02O | 0.70 | 14.830 |
| HEH03O | | 33.944 |
| HEH04O | 0.69 | 37.560 |
| HEH05O | | 28.560 |
| HEH06O | | 46.714 |
| HEH07O | 0.48 | 58.872 |
| HEH01A | | 4.647 |
| HEH02A | 1.14 | 24.580 |
| HEH03A | | 42.395 |
| HEH04A | 1.85 | 22.488 |
| HEH05A | | 49.756 |
| HEH06A | | 50.388 |
| HEH07A | 1.57 | 60.946 |

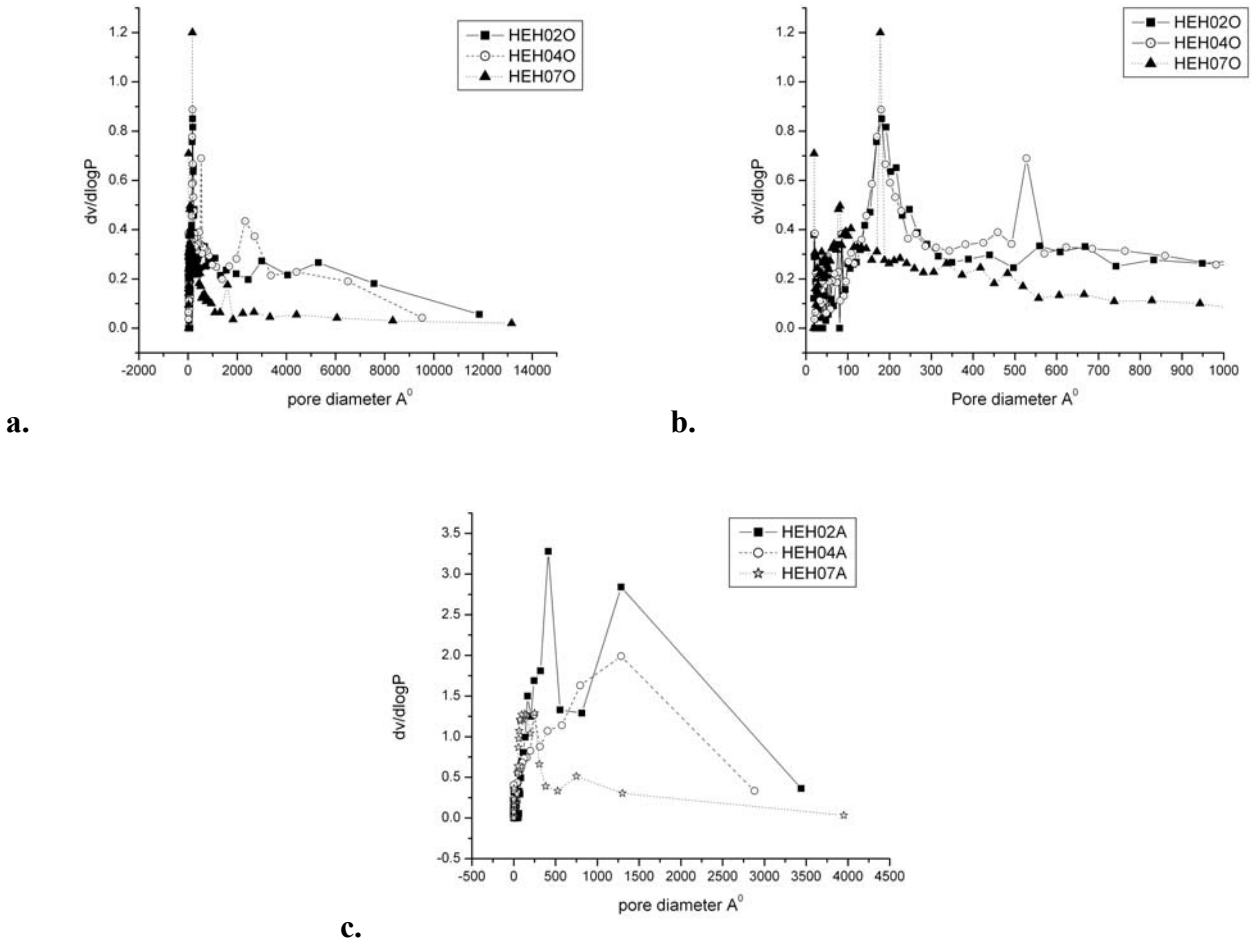


**Figure 3.23. Pore size distribution by MIP of samples; a. and b. HEH02O, HEH04O and HEH07O, c. HEH02A, HEH04A and HEH07A.**

## 3.7 Epoxy content

The epoxy content gives an estimate of the available surface epoxy groups. The surface state of the prepared copolymer beads is controlled by the surface tension between the dispersed phase and the continuous phase. The surface tension of GMA, EGDM and cyclohexanol in contact with water are approximately 6.9, 33.1 and 34.4 dyne/cm. Therefore GMA molecules will tend to migrate towards the surface of the droplets. However, in actuality, the observed epoxy content is much lesser than the theoretical value because the concentration of epoxy groups present at or near the surface, which react with hydrochloric acid, is rather low. The polymerisation condition (pH=7) did not open up epoxy groups. It is clear that a majority of the epoxy groups are buried in the bulk of the matrix and are unable to react with hydrochloric acid under analytical

conditions. Figure 3.23 represents the theoretical and analysed (surface) epoxy groups in poly(GMA-EGDM) relative to crosslink density at a monomer:porogen ratio of 1:1.61. This shows that surface tension issues are negated by other forces, which direct most epoxy groups away from the surface.

The theoretical epoxy content decreases as GMA in the copolymer decreases, from 5.22 mmol/g at 25% crosslink density to 1.88 mmol/g at 200% crosslink density. The titratable epoxy group (Figure 3.24 a.) decreases from 1.59 mmol/g at 25% crosslink density to 0.11 mmol/g at 200% crosslink density. Thus, while 30.4% epoxy groups are near the surface at 25% crosslink density, this drops to 5.9% at 200% crosslink density. With increasing crosslink density, the polymer particle size increases; the swelling and diffusion rates of reagents decrease, resulting in the much lower reactable epoxy groups. The copolymers with lower crosslink density (25%) are suitable for chromatographic columns while those with highest crosslink density are suitable for enzyme immobilisation.

The theoretical epoxy content in poly(GMA-DVB) studied here varies from 5.08 to 1.71 mmol/g (from 25 to 200% crosslink density). The experimentally observed epoxy content by titration was in the range 1.78 to 0.26 mmol/g (from 25 to 200% crosslink density). Thus, only a fraction the epoxy group in poly(GMA-DVB) beads react with hydrochloric acid, just as observed with poly(GMA-EGDM) series. A major fraction of the epoxy group in the beads is buried and is unable to react under analytical condition. However, in comparison to poly(GMA-EGDM) series, where 30.4 to 5.9% of epoxy groups were near the surface (from 25 to 200% crosslink density), in this series 35.0% to 14.9% were near the surface. Figure 3.24 b. shows the effect of crosslink density on epoxide content. Thus, substituting EGDM with a more hydrophobic comonomer (DVB) marginally reorients the epoxy group towards the surface of the pores. The other trends were along lines observed in poly(GMA-EGDM) series.

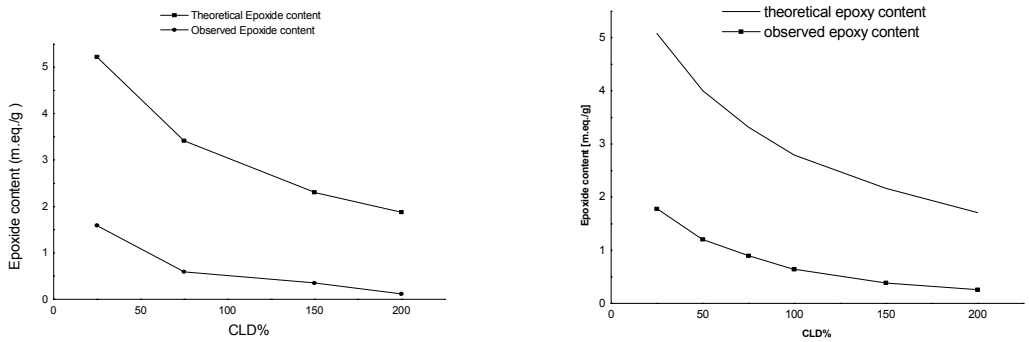


a. b.

**Figure 3.24. (a) Surface epoxy groups of the GMA-EGDM polymers synthesised by SP, (b) Surface epoxy groups of the GMA-DVB polymers synthesised by SP.**

The epoxy contents in the polymers synthesised using concentrated emulsions are shown in the Figure 3.25. The observed epoxy values for the polymers synthesised using only organic initiator are very low than the theoretical values (Figure 3.25 a). However, the polymers synthesised with both phase initiators had epoxy values close to the theoretical value for low crosslink densities (Figure 3.25 b). As the crosslink density increased beyond 75% the value deviated largely from the theoretical values. For GEH01 71% of the epoxy groups were on the surface while for GEH07 46% of the epoxy groups are present on the surface. With only AIBN as initiator the surface epoxy groups decreased from 14% (GEH01O) to 8% for the sample GEH07O.

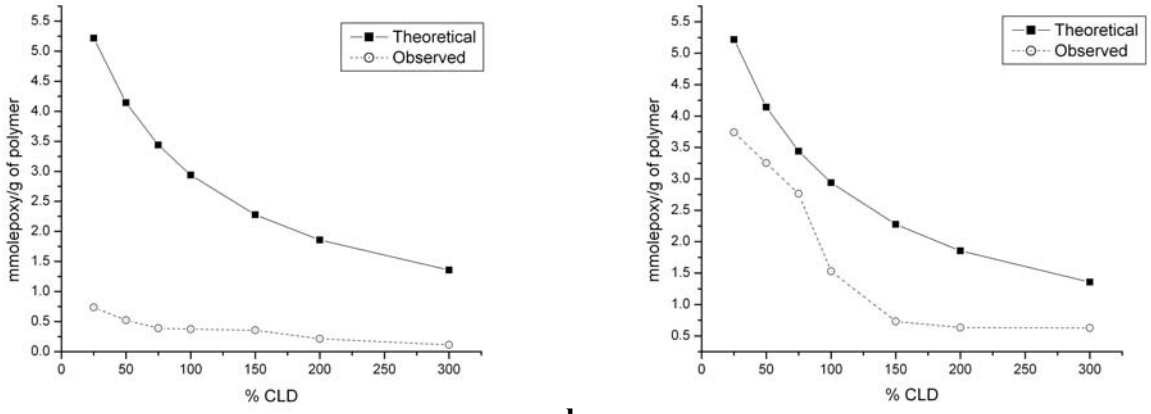


**a.** **b.**

**Figure 3.25. Surface epoxy groups of the GMA-EGDM polymers synthesised by using concentrated emulsions (a) with only oil phase initiator, (b) with both oil and aqueous phase initiators.**

**References**


1. Willis R. C., Ryan J. F. Eds., "*Chromatography: creating a central science*", ACS publication, pp 36.
2. Adams B. A. and Holmes E. L., *J. Chem. Soc. Ind.*, 54, 1T, 1935.
3. Merrifield R. B., *J. Am. Chem. Soc.*, 83, 2149, 1963.
4. Farall M. J. and Frechet J. M. J., *J. Org. Chem.*, 41, 3877, 1976.
5. Relles H. M. and Schluenz R. W., *J. Am. Chem. Soc.*, 96, 6469, 1979.
6. Braun D., *Makromol. Chem.*, 30, 85, 1959.
7. Evans D. C., George M. H. and Barrie J. A., *J. Polym. Sci. Polym. Chem. Ed.*, 12, 247, 1974.
8. Svec F., Hradil J., Coupek J. and Kalal J., *Angew. Macromol. Chem.*, 48, 135, 1975.
9. Svec F., Jelinkova M. and Votavova E., *Angew. Makromol. Chem.*, 188, 167, 1991.
10. Azanova V. V., Hradil J., Svec F., Pelzbauer Z. and Panarin E. F., *React. Polym.*, 12, 247, 1990.
11. Jelinkova M., Shataeva L. K., Tishchenko G. A. and Svec F., *React. Polym.*, 11, 253, 1989.
12. Setinek K., Blazek V., Hradil J., Svec F and Kalal J., *J. Catal.*, 80, 123, 1983.
13. Rolland A., Hérault D., Touchard F., Saluzzo C., Duval R. and Lemaire M., *Tet. Asymmetry*, 12, 811, 2001.
14. Petro M., Svec F. and Frechet J.M., *Biotechnol. Bioeng.*, 49, 355, 1996.
15. Kotha A., Raman R. C., Ponrathnam S., Kumar K. K. and Shewale J. G., *React. Funct. Polym.*, 28, 235, 1996.
16. Radivoje P., Slobodan J and Zoran V., *Biotechnol. Lett.*, 23**,** 1171, 2001.
17. Lissant K. J., *J. Colloid Int. Sci.*, 22, 462, 1966.
18. Westermarck S**.,** Academic dissertation, *Use of mercury porosimetry and nitrogen adsorption in characterisation of the pore structure of mannitol and microcrystalline cellulose powders, granules and tablets*, University of Helsinki, 2000.
19. Sing K. S. W., Everett D. H., Haul R. A. W., Moscou L., Pierotti R. A., Rouquerol J. and Siemieniewska T., *Pure and Appl. Chem.*, 57, 603-919, 1985.
20. Van Brakel J., Modry S.and Svata M., *Powder Technol.*, 29, 1-12, 1981.
21. Cortes J., *Adv. Colloid Int. Sci.*, 22, 151, 1985.
22. Sing K., *Colloids and Surfaces A: Physicochemical and Engineering Aspects*, 187–188, 3, 2001.

23. Thompson W. T., *Philos*. *Mag*., 42, 448, 1871.

24. Webb P. A. and Orr C., *Analytical methods in fine particle technology*, Micromeritics Instrument Corp., Atlanta, Georgia, p-301, 1997.

25. Allen T., "*Particle size measurement*", *5th Ed*., Chapmann and Hall, New york, USA, p. 251, 1997.

26. Kline G. M., *Analytical chemistry of polymers*, Interscience, New York, p. 123, 1959.

27. Denise S. S., Nunes F. and Coutinho M. B., *Eur*. *Polym*. *J*., 38, 1159, 2002.

28. Arshady R., *Colloid Polym*. *Sci*., 270, 717, 1992.

29. Rouquerol J., Avnir D., Fairbridge C. W., Everett D. H., Haynes J. H., Pernicone N., Ramsay J. D. F., Sing K. S. W. and Unger K. K., *Pure and Appl*. *Chem*., 66, 1739, 1994.

30. Okay O., *Prog*. *Polym*. *Sci*. 25, 711–779, 2000.

31. Qi T., Sonoda A., Makita Y., Kanoh H., Ooi K. and Hirotsu T., *J. Appl*. *Polym*. *Sci*., 83, 2374–2381 2002.

32. Kuroda H. and Osawa Z., *Eur*. *Polym*. *J*., 31, 57-62, 1995.

33. Brunauer S., Deming L. S., Deming W. S. and Teller E., *J*. *Am*. *Chem*. *Soc*., 62, 1723, 1940.

34. Marczewski A.W., *Practical guide to isotherms of adsorption on heterogeneous surfaces*, 2002.

35. Li Nai-Hong and Benson J., R., *U. S. Patent No. 5,583,162*, 1996.

36. Williams J. M., Gray A**.** J and Wilkerson M. H., *Langmuir*, 6**,** 437-444, 1990.

37. Cameron N. R., Sherrington D. C., Albiston L. and Gregory D. P., *Colloid and Polym*. *Sci*., 274, 592, 1996.

38. Cameron N. R., Sherrington D. C., Andob I. and Kurosub H., *J. Mater. Chem*., 6, 719, 1996.

39. Williams J. M.and Wrobleski D. A., *Langmuir*, 4, 656, 1988.

40. Menner A., Powell R. and Bismarck A., *Macromolecules*, 39, 2034, 2006.

41. Kuneida H. and Shinoda K., *J. Colloid and Int*. *Sci*., 107, 107, 1985.

42. Ruckenstein E. and Park J. S., *Polymer*, 33, 405, 1992.

43. Chirila T. V., Chen Y., Griffin B. J. and Constable I. J., *Polym*. *Int*., 32, 221, 1993.

44. Dusek K. and Sedlacek B., *Eur*. *Polym*. *J*., 7, 1275, 1971.

45. Tauer K, Imroz Alia A. M., Ufuk Yildiz and Sedlak M., *Polymer*, 46, 1003, 2005.

46. Ajzenberg N.and Ricard A., *J*. *Appl*. *Polym*. *Sci*., 80, 1220, 2001.

47. Sherrigton D. C., *Chem*. *Commun*., 2275, 1998.

48. Seong J. L., *Korea-Australia Rheol*. *J*., 18, 183, 2006.
49. Menner A. and Bismarck A., *Macromol*. *Symp*., 242, 19, 2006.
50 Cameron N. R., *Polymer*, 46, 1439, 2005.

# Chapter 4

## Modification of the polymers with β cyclodextrin and evaluation of the modified polymers for chiral resolution of citalopram

## 4. Modification of the polymers with β cyclodextrin and evaluation of the modified polymers for chiral resolution of citalopram.

### 4.1 Introduction

The use of cyclodextrins (CD) in the chromatographic separation and purification processes is well known and reviewed by Hinze[1]. The use of CDs as chiral mobile phase additives is restricted because of their inadequate solubilities. CDs can be incorporated into polymer matrix by two ways. One way is copolymerising the CD derivative containing polymerisable moiety with crosslinkers or vinyl monomers. The other approach is attaching the CDs to the preformed crosslinked polymers bearing appropriate functionalities either directly or through spacer arms.

Copolymers containing CD as one of the monomers were prepared and used as stationary phases. One of the first reported CD stationary phases of this type is polymeric CD-epichlorohydrin resin[2]. It has been used for the separation of various natural products like vitamins, perfumes, aromatic amino acids and diastereomers of $Co(NH_3)_4$-glucose-6-phosphate ATP. Several polyurethane resins containing β-CD crosslinked with various diisocyanates have been used with some success in LC as well as GC[3-5]. Mizobuchi et. al. synthesised polyurethane resins that contained high contents of CD (65 wt %) and were stable in organic solvents[5]. However, these polymeric gels required a long analysis time and also exhibited low mechanical stability thus hampering their use in HPLC. Attempts have therefore been made to bond CD to solid matrix.

In the field of liquid chromatography (LC), CDs as chiral selectors of stationary phases have been receiving much attention. Fujimura et al. for the first time covalently bonded *p*-tosylated CD to silica gel through a Si-NH-C bond for use in LC[6]. Subsequently, a series of β-CD bonded stationary phases with different nitrogen-containing spacers were prepared. Armstrong prepared a highly stable cyclodextrin bonded stationary phase with 6–10 atoms non-nitrogen containing spacer[7]. Lin et al. prepared a β-CD bonded stationary phase by immobilising derivatives of β-CD with the moiety containing a *s*-trizine ring onto silica gels modified different amino types of silane coupling agents[8]. Kazuo et al. obtained β-CD bonded stationary phases using 3-isocyanatopropyltriethoxysilane as coupler[9]. Grini and coworkers prepared β-CD based

stationary phases for high performance liquid chromatography by coating silica gel with β-CD polymers[10]. Attachment of CD to the silica gel has also been carried out using propylene short arm spacer[11].

Our group at NCL has successfully synthesised HEMA-EGDM polymers bearing CD, attached using isocyanates as linking agents for protein purification[12].

In the present work we have prepared cyclodextrin modified GMA-EGDM and GMA-DVB polymers by using different coupling agents. The evaluation of the polymers bearing CD moieties for chiral recognition by using batch adsorption technique is presented in this chapter.

## 4.2 Materials used

β cyclodextrin: Empirical formula: $C_{42}H_{70}O_{35}\cdot H_2O$, Molecular weight: 1135, Melting point: 298 °C, Appearance: white powder.

1,6-diisocyanatohexane (HMDI): Empirical formula: $C_8H_{12}N_2O_2$ Molecular weight: 168.2, Boiling Point: 255 °C Density: 1.047 g/cm$^3$ Appearance: colourless liquid.

Sebacoyl chloride (SC): Empirical formula: $C_{10}H_{16}Cl_2O_2$, Molecular weight: 239.14, Boiling Point: 220 °C, Density: 1.12 g /cm$^3$ Appearance: light-yellow liquid.

Glacial acetic acid: Empirical formula: $C_2H_4O_2$, Molecular weight: 60.05, Density: 1.049 g/cm$^3$, Boiling point: 118.1˚C, Appearance: colourless liquid.

Triethylamine: Empirical formula: $C_6H_{15}N$, Molecular weight: 101.1, Boiling point: 89.7 °C, Density: 0.726 g/cm$^3$, Appearance: clear liquid.

Acetic anhydride: Empirical formula $C_4H_6O_3$, Molecular weight: 102.1, Density: 1.08 g/cm$^3$, Appearance: clear liquid, Boiling point: 139.8.

Citalopram hydrobromide: Empirical formula: $C_{20}H_{22}BrFN_2O$, Molecular weight: 405.35, Melting point: 185-188°C, Appearance: White to off-white, crystalline solid.

All the solvents used were of Laboratory grade. The HPLC grade solvents, filtered through 0.45 μ filter, were used for HPLC.

## 4.3 Modifications with β-CD

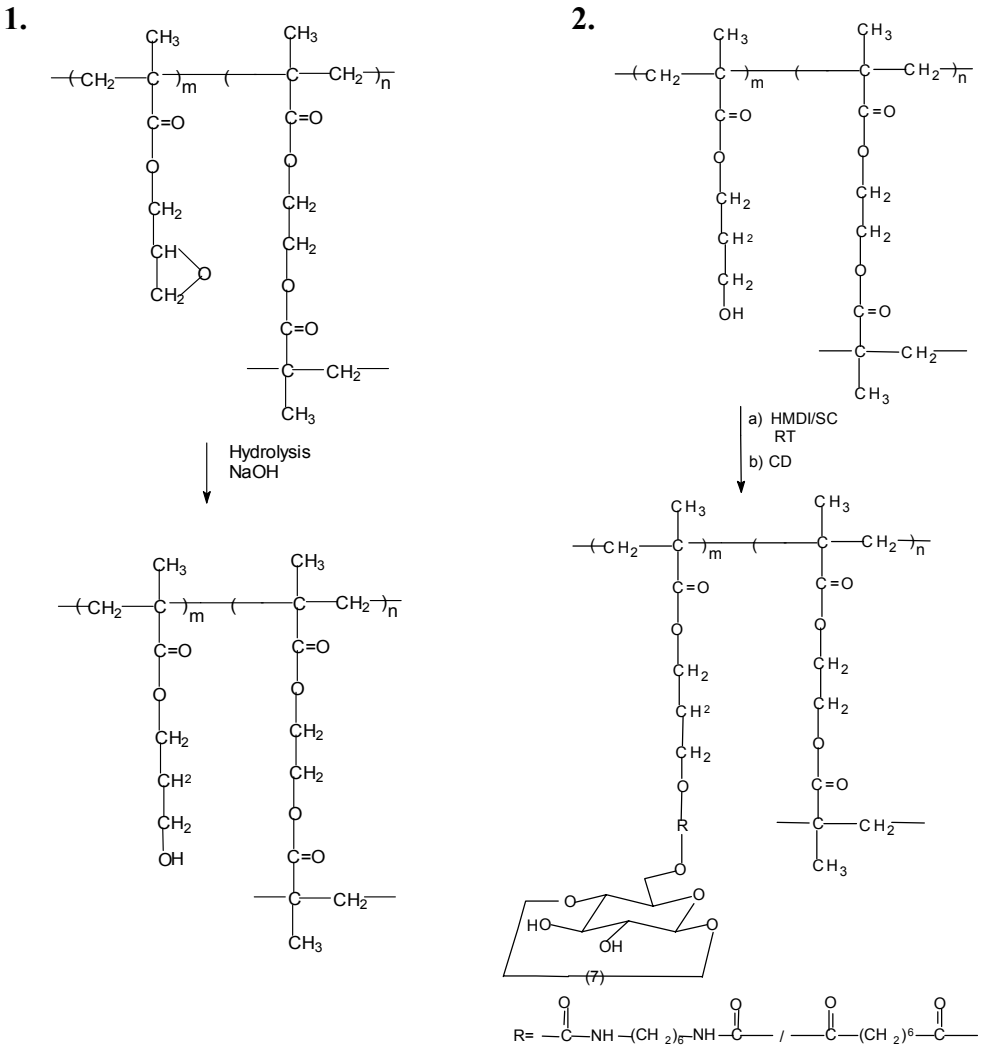


**Scheme 4.1. Modification of GMA-EGDM polymers with β-CD.**

*4.3.1 Experimental*

The GMA-DVB polymers bearing epoxy groups were subjected to hydrolysis in alkaline condition to get the hydroxyl groups. The polymers were then modified with β-CD using hexamethylene diisocyanate and sebacoyl chloride spacers.

*4.3.1.1 Hydrolysis of epoxide*

Polymer (1g) was soaked in 4 mL distilled water. To this required quantity (1:1 molar ratio based on theoretical epoxy content) of powdered sodium hydroxide was added. The polymers were left unstirred in alkaline solution for 2 days at room temperature. The beads were then filtered, neutralised with 1N hydrochloric acid and then

washed with water until the washings were neutral. The beads were finally washed with acetone and dried in vacuum oven at 50°C. The beads were analysed for the hydoxyl groups by titration according to established procedure by using acetic anhydride-pyridine reagent.

*4.3.1.2 Attachment of β-CD through spacer*

To 1 g of hydrolysed polymer beads 4 mL of dry DMF was added. Polymers were degassed in order to allow more solvent to penetrate the beads. The required quantity of hexamethylene diisocyante/sebacoyl chloride was added and kept for 24 h at room temperature. After 24 h the excess of reagent was washed off, with dry N,N dimethyl formamide and a solution of β-CD in dry N,N dimethyl formamide was then added to each of the polymers. This mixture was allowed to react for 24 h at room temperature and then poured in excess water to get rid of unreacted β-cyclodextrin as well as polymerised CD. The beads were then filtered washed with excess water and finally with acetone and then dried overnight in vacuum oven at 50 °C.

**Table 4.1. Modifications of GMA-EGDM and GMA-DVB polymers with β-CD using spacers**

| Polymer | TOH meq/g | SC mmol | SC (g) | HMDI mmol | HMDI (g) | β-CD (g) |
|---|---|---|---|---|---|---|
| GE7 | 10.442 | 10.442 | 2.48 | 10.442 | 1.75 | 1.802 |
| GE8 | 8.268 | 8.268 | 1.98 | 8.268 | 1.38 | 0.937 |
| GE9 | 6.832 | 6.832 | 1.62 | 6.832 | 1.15 | 0.674 |
| GE10 | 5.880 | 5.880 | 1.41 | 5.880 | 0.99 | 0.667 |
| GE11 | 4.606 | 4.606 | 1.10 | 4.606 | 0.68 | 0.660 |
| GE12 | 3.750 | 3.750 | 0.90 | 3.750 | 0.63 | 0.398 |
| GV9 | 6.634 | 6.634 | 1.98 | 6.634 | 1.11 | 1.015 |
| GV10 | 5.582 | 5.582 | 1.33 | 5.582 | 0.93 | 0.728 |
| GV 11 | 4.328 | 4.328 | 1.03 | 4.328 | 0.72 | 0.454 |
| GV12 | 3.418 | 3.418 | 0.82 | 3.418 | 0.58 | 0.290 |
| GV7H | 10.16 | 10.16 | 2.38 | 10.16 | 1.68 | 1.98 |
| GV8H | 6.634 | 6.634 | 1.58 | 6.634 | 1.12 | 1.017 |

| | | | | | | |
|---|---|---|---|---|---|---|
| GV10H | 5.582 | 5.582 | 1.33 | 5.582 | 0.93 | 0.728 |
| GV11H | 4.328 | 4.328 | 1.03 | 4.328 | 0.73 | 0.46 |
| GV12H | 3.418 | 3.418 | 0.82 | 3.418 | 0.58 | 0.304 |

## 4.4 Characterisation

### *4.4.1 Quantitative determination of β-CD bound to the polymer matrix*

The method is based on the fact that glucose when reacted with concentrated sulphuric acid gets oxidised to furfuraldehyde. This then reacts with phenol to form an adduct which can be analysed spectrophotometrically. β-CD, which is an oligomer of D-glucose units, breaks down to D-glucose units in presence of an acid. This can be used as a tool to estimate β-CD covalently bound to polymer[13].

For determining the unknown concentration from the absorbance values, a standard plot of various concentrations of β-CD in water against the absorbance values was plotted.

#### *4.4.1.1 Standard plot of β-CD*

The solutions of different concentrations of β-CD were made in water. 1 mL of diluted sample was placed in 20 mm test tube and 1 mL of 5% phenol solution was added and mixed in a vortex mixer. 5 ml concentrated sulphuric acid was then directly added to surface of liquid and allowed to stand for 10 minutes. The absorbance was measured at λ 490 nm. The absorbances in nm were plotted against concentration (mol/L) of CD to get a standard plot.

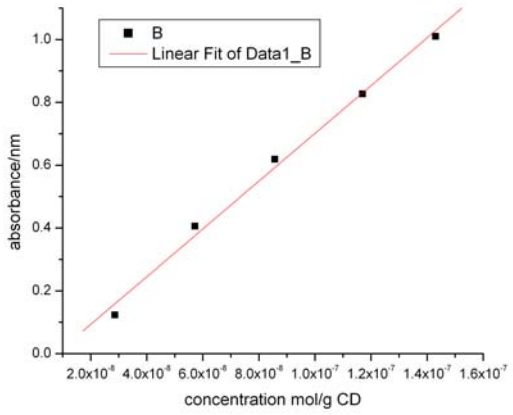


**Figure 4.1. Standard plot of β-CD.**

#### *4.4.1.2 Estimation of the CD bound on the polymer*

The method described above was repeated for the estimation of bound β-CD, except that a fixed quantity of matrix was weighed instead of a solution. The absorbance was measured at λ 490 nm. The dilutions were made wherever necessary. The concentration of β-CD was calculated from the standard plot. The polymer modified with sebacoyl chloride/ hexamethylene diisocyanate was used as reference. No colouration developed in the reference sample.

### 4.5 Inclusion complex studies with substituted phenols

β-CD is known to form inclusion complexes with a variety of aromatic compounds like nitrophenol, substituted aniline, etc. The study was undertaken to test the ability of the bonded β-CD matrix towards the sorption of aromatic compounds. The general procedure involved equilibrating the matrix containing β-CD with a solution of guest compound and analysing the supernatant spectrophotometrically. P-cresol was chosen as guest molecule. The typical procedure is given below.

The polymers GV10H (10 mg) and GV12H (10 mg) with maximum binding of β-CD were equilibrated with 5 mL solutions of p-cresol for 24 h at room temperature without stirring. The supernatant solutions were then analysed by UV. A control experiment was carried out using the same base polymer without β-CD. The concentration of the p-cresol in the supernatant was calculated from the standard plot of p-cresol in methanol.

#### *4.5.1 Inclusion complex studies with drug citalopram hydrobromide*

The polymers GV10H (0.25 g) and GV12H (0.25 g) were allowed to stand for 24 h with the solution of citalopram hydrobromide. Two sets of reactions were performed using ethanol and water as solvent for citalopram hydrobromide. The supernatants were analysed by HPLC on Chirobiotic V column. The enantiomers of citalopram hydobromide were resolved on the same column using methanol:acetic acid:triethylamine (100:0.006:0.003) as mobile phase and a standard plot was obtained.

## 4.6 Results and discussion

### *4.6.1 Attachment of β-CD to the polymer matrix*

The epoxy polymers are known to react with β-CD directly. Direct attachment of β-CD to the glycidyl methacrylate polymers has been reported. Reactive continuous rods of macroporous poly(glycidyl methacrylate-co-ethylene dimethacrylate) have been prepared by *in-situ* copolymerisation of the monomers within the confines of a 150×4.6 mm. chromatography column in the presence of porogenic diluent, and β-CD was immobilised on the continuous rods. The polymers were used for the separation of nitro phenol isomers[14]. A series of styrene/divinylbenzene copolymers, with embedded polyglycidylmethacrylate, were synthesised and β-CD was immobilised onto the crosslinked polymers[15]. The resulting β-CD polymeric adsorbent possesses specific inclusion recognition with the aromatic compounds. Plasma was used to induce graft polymerisation of GMA on PP and then CD was coupled to the graft surface[16].

Armstrong showed that when β-CD was linked to the silica matrix through short spacer with three-carbon atom chain, the coupling was difficult owing to the bulky nature of the CD molecule. However, when the length of the spacer was increased to eighteen or twenty carbon atoms there was a danger of losing the resolution[17]. Thus, it is necessary to have an appropriate spacer for coupling the CD molecule to the matrix.

Several different approaches have been adopted to couple CD to the matrix for making LC phases. The immobilisation of CD through spacers can be by two different ways: (I) a spacer arm having an alkyl chain of appropriate length is grafted onto the matrix surface and then CD is reacted with the terminal group of the spacer arm, (ii) attaching a spacer arm to the CD molecule and then reacting the end group with the matrix. It has been shown that the immobilisation process used in the preparation of CSP could affect the quality, stability and performance of the CSP[18]. While attaching a bifunctional spacer onto native CD, side reactions such as crosslinking can take place leading to an insoluble product. The reactions have to be carried out carefully under controlled conditions in order to get optimum substitution avoiding side reactions. This is quite a time consuming procedure. In order to get clean products with least contaminants, we opted for the second method to couple CD to the matrix.

The activation and coupling chemistry used here employs very facile bifunctional reagents such as diisocyanate and diacid chloride. Isocyanates are carbonyl compounds with double bonds. The urethane bond formation starts with the reaction at ambient temperature between the carbonyl carbon of the isocyanates and the alcoholic oxygen. Similarly, acid chlorides also react with alcoholic oxygen at room temperature. The polymers were reacted with β-CD after washing the polymers with sufficient dry DMF in order to remove excess of hexmethylene didisocynate/sebacoyl chloride. The isocyanates/acid chlorides being very labile for attack by moisture, the intermediates were reacted with β-CD without isolation. The attachment of β-CD molecules can take place through either primary or secondary hydroxyl groups. As the primary hydroxyl groups are more reactive than the secondary hydroxyls and are less sterically hindered, the attachment is most likely to occur through primary hydroxyls.

The milliequivalents of theoretical hydroxyl groups per gram of the polymer should be twice as that of the theoretical epoxy groups as the opening up of an epoxide generates two hydroxyl groups. The obtained values are much lesser than the theoretical values (Table 4.2). This suggests that all the epoxy groups are not accessible to the reagent. The maximum value obtained for the GE series polymers was 1.7 meq/g, i.e. 16% of the theoretical value. The values show a decrease as the crosslink density is increased, although no regular trend is obtained. Similar trends were obtained for GMA-DVB polymers with cyclohexanol as porogen and GMA-DVB polymers with hexanol as porogen.

**Table 4.2. Hydroxyl values of GMA-EGDM and GMA-DVB hydrolysed polymers**

| Polymer | *TOH ( meq/g) | Obtained (meq/g) |
|---|---|---|
| GE7 | 10.442 | 1.7 |
| GE8 | 8.268 | 1.5 |
| GE9 | 6.832 | 1.0 |
| GE10 | 5.880 | 1.1 |
| GE11 | 4.606 | 0.9 |
| GE12 | 3.750 | 0.5 |
| GV9 | 6.634 | 1.4 |
| GV10 | 5.582 | 1.3 |
| GV11 | 4.328 | 0.6 |
| GV12 | 3.418 | 0.7 |
| GV7H | 10.16 | 1.8 |
| GV9H | 6.634 | 1.0 |

| | | |
|---|---|---|
| GV10H | 5.582 | 1.2 |
| GV11H | 4.328 | 1.4 |
| GV12H | 3.418 | 1.4 |

* TOH: Theoretical hydroxyl groups

**Table 4.3. β-CD loading on GMA-EGDM polymers with cyclohexanol as porogen**

| Properties | GE7 | GE8 | GE9 | GE10 | GE11 | GE12 |
|---|---|---|---|---|---|---|
| | 25% | 50% | 75% | 100% | 150% | 200% |
| PV(mL/g) | 0.1075 | 0.5625 | 0.5925 | 0.7250 | 0.7400 | 0.8475 |
| SA($m^2$/g) | 22.076 | 85.0631 | 105.781 | 100.691 | 110.254 | 110.578 |
| CD bound mmol/g | * 0.0449 | 0.0317 | 0.0317 | 0.0291 | 0.0141 | 0.0150 |
| | ** 0.0370 | 0.0414 | 0.0837 | 0.0132 | 0.0079 | 0.0062 |

*: β-CD linked through HMDI spacer, **: β-CD linked through SC spacer

**Table 4.4. β-CD loading on GMA-DVB polymers with cyclohexanol as porogen**

| Properties | GV7 (25%) | GV8 (50%) | GV9 (75%) | GV10 (100%) | GV11 (150%) | GV12 (200%) |
|---|---|---|---|---|---|---|
| PV(mL/g) | 0.75 | 0.93 | 0.97 | 1.04 | 1.13 | 1.16 |
| SA($m^2$/g) | 98.10 | 115.44 | 113.20 | 112.14 | 125.43 | 124.95 |
| CD bound mmol/g | - | - | *0.0291 | 0.0203 | 0.0238 | 0.0141 |
| | - | - | **0.0308 | 0.0643 | 0.0969 | 0.0863 |

*: β-CD linked through HMDI spacer, **: β-CD linked through SC spacer

**Table 4.5. β-CD loading on GMA-DVB polymers with hexanol as porogen**

| Properties | GV7H | GV8H | GV9H | GV10H | GV11H | GV12H |
|---|---|---|---|---|---|---|
| PV(mL/g) | 1.47 | 1.53 | 1.70 | 1.88 | 1.84 | 1.89 |
| SA($m^2$/g) | 24.50 | 35.40 | 46.10 | 48.00 | 50.80 | 43.90 |
| CD bound mmol/g | * 0.0220 | 0.0326 | 0.0450 | 0.1700 | 0.0106 | 0.0220 |
| | ** 0.0811 | - | 0.0194 | 0.0537 | 0.1093 | 0.1744 |

*: β-CD linked through HMDI spacer, **: β-CD linked through SC spacer

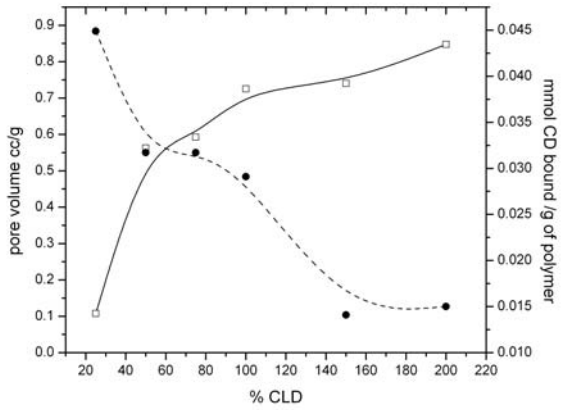


**Figure 4.2. β-CD loading on GMA –EGDM polymer with cyclohexanol as porogen and HMDI spacer, as a function of crosslink density and pore volume.**

.

*4.6.1.1 Effect of matrix properties*

The ligand loading on the porous polymers mainly depends upon the porous characteristics of the polymers as well as the available binding sites. It was observed that the maximum binding was achieved with GMA-DVB polymers with hexanol as porogen. The polymer showed the highest pore volume as compared to the GMA-EGDM and GMA-DVB polymers with cyclohexanol as porogen. The binding of β-CD to the GMA-EGDM polymers was lesser as compared to the GMA-DVB polymers. The maximum binding obtained was 0.0837 mmol/g for GE9 with SC spacer. The binding goes on decreasing as crosslink density increased, with the exception of GE9. This could be because of lesser availability of functional groups, as crosslink densities increase. This is in agreement with the obtained hydroxyl values. As the crosslik density is increased from 25-200, the surface epoxy groups go on decreasing thus reducing the surface loading of β-CD through hexamethylene spacer on GMA-EGDM polymers with cyclohexanol as porogen (Figure 4.2). In case of GMA-DVB polymer, with hexanol as porogen, maximum binding was achieved with polymer of 100% crosslink density (GV10H). The polymer showed highest pore volume, which was 1.88 mL/g. Even though the polymer of 200% crosslink density showed almost same pore volume, available functional groups were less and hence showed less binding.

*4.6.1.2 Effect of spacer group*

The binding of β-CD is higher in case of sebacoyl chloride spacer with GMA-DVB polymer and having cyclohexanol as porogen as compared to hexamethylene diisocyanate spacer (Table 4.5). The binding decreases with increase in the crosslink density. In case of hexamethylene diisocyanate, binding increases with decrease in crosslink densiy.

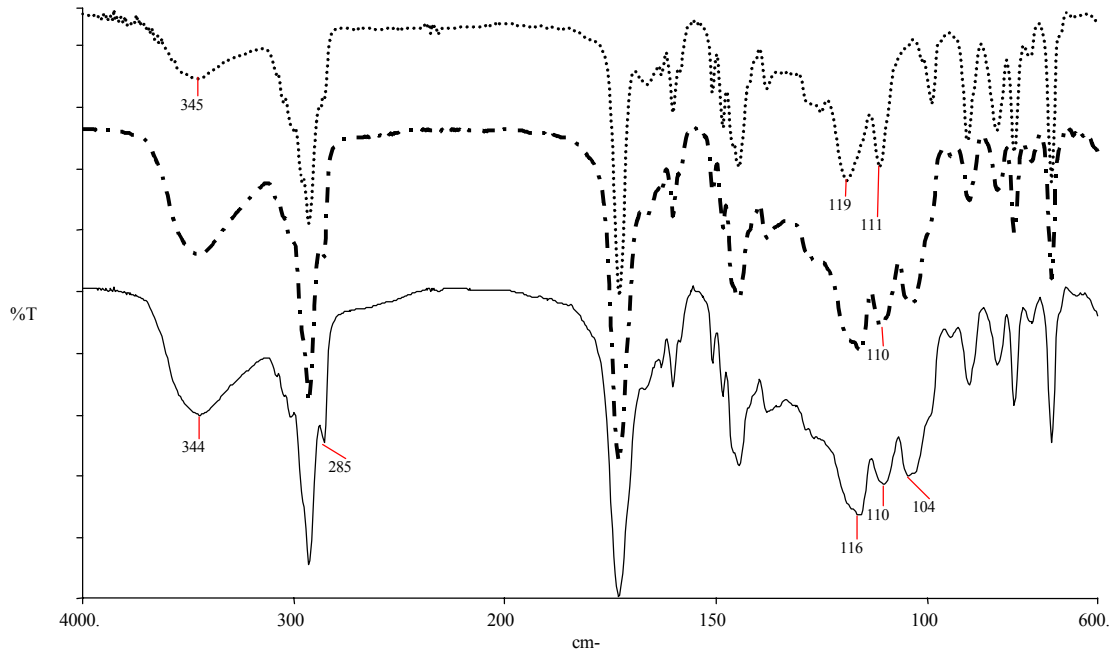


**Figre 4.3. Comparative IRs of β-CD modified polymers.**

**Table 4.6. IR absorbances of hydrolysed poly(GMA-DVB)**

| Peak position ($cm^{-1}$) | Assignment |
|---|---|
| 3532 | -OH stretching |
| 1729 | -C=O stretching |

**Table 4.7. IR absorbances of poly(GMA-DVB)-HMDI-CD**

| Peak position. ($cm^{-1}$) | Assignment |
|---|---|
| 3340 | -NH stretching |
| 3492 | -OH stretching |
| 1572 | Amide I band |
| 1625 | Amide II band |
| 1020 | Acetal linkage |

**Table 4.8. IR absorbances β-CD**

| Peak position. ($cm^{-1}$) | Assignment |
|---|---|
| 3500 | -OH stretching |
| 1020 | acetal linkage |

The peak at 3500 $cm^{-1}$, due to -OH stretching suggests the presence of -OH groups in the hydrolysed polymers. It can be clearly seen from the Tables 4.6, 4.7 and 4.8 that in the modified polymers the peaks at 3340 $cm^{-1}$, due to -NH stretching at 1572 $cm^{-1}$, amide I band and 1625 $cm^{-1}$, due to amide II band appear, suggesting amide formation as a result of reaction between OH and -NCO groups. Also, peak at 1020 $cm^{-1}$, due to glycosidic linkages of β-CD, appears in the modified polymer, suggesting presence of β-CD in the matrix[19].

*4.6.2 Standard plot of p-cresol*

A stock solution of p-cresol of 0.005 M concentrations in methanol was made. This was further diluted in order to measure the absorbance. A standard plot of concenrtration against absorbance was plotted.

**Table 4.9. Standard plot p-cresol in methanol**

| Concentration Mole/L | Absorbance Nm |
|---|---|
| $2.5x10^{-8}$ | 0.513 |
| $3.75x10^{-8}$ | 0.578 |
| $4.99x10^{-8}$ | 0.659 |
| $7.498x10^{-8}$ | 0.750 |
| $9.99x10^{-8}$ | 0.857 |

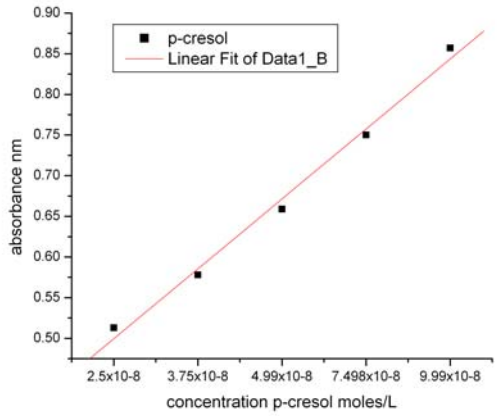


**Figure 4.3. Standard plot of p-cresol in methanol.**

**Table 4.10. Inclusion of p-cresol by GV12HSCCD**

| Initial Concentration of p-cresol mol/L | Concentration of p-cresol after equilibration mol/L | Concentration of p-cresol taken up by β-CD |
|---|---|---|
| $2.5x10^{-8}$ | $1.47x10^{-8}$ | $1.03x10^{-8}$ |
| $9.99x10^{-8}$ | $4.48x10^{-8}$ | $5.51x10^{-8}$ |

A standard plot of absorbance against molar concentration of p-cresol was plotted. The absorbance showed a increasing trend with increase in concentration (Table 4.10, Figure 4.3).

After equilibrating with β-CD bound polymer it was observed that the absorbance of the supernatant p-cresol solution goes on decreasing suggesting the complex formation. Between the two polymers studied the polymer GV12HSCCD showed the higher binding of p-cresol than the other polymer i.e. GV10HHMCD. This is probably due the longer length of the spacer, which imparts more freedom to the β-CD molecules and enahances, the comlexation.

## 4.7 Study of stereoelective inclusion of Citalopram hydrobromide

The development and introduction of selective serotonin-reuptake inhibitors (SSRIs), including fluoxetine, sertraline, paroxetine, fluvoxamine, and citalopram, represent an important advance in the pharmacotherapy of psychiatric disorders, not only depression, but also a wide range of psychiatric disorders from anxiety disorders to bulimia. The SSRIs are chemically unrelated to tricyclic, heterocyclic, and other first

generation antidepressants. They have now been increasingly used for treatment of childhood anxiety disorders. These five drugs have the predominate effect of inhibiting the neuronal reuptake of serotonin. SSRIs are the treatment of choice for many indications, including major depression, dysthymia, panic disorder, obsessive-compulsive disorder, eating disorders, and premenstrual dysphoric disorder, because of their efficacy, good side-effect profile, tolerability, and safety when overdosed, as well as with regard to patient compliance. Pharmacokinetic properties are different due to stereochemistry, metabolism, interaction/inhibition with cytochrome P450 enzymes (CYP), and participation in drug-drug interactions. Side effects of SSRIs include gastrointestinal disturbances, headache, sedation, insomnia, activation, weight gain, impaired memory, excessive perspiration, paresthesia, and sexual dysfunction[20, 21].

Citalopram is a bicyclic pthalene derivative. It is the most selective amongst the SSRIs with no, or only minimal, effect on noradrenaline and dopamine reuptake[22]. The ability of citalopram to potentiate serotonergic activity in the central nervous system via inhibition of the neuronal reuptake of 5-HT is thought to be responsible for its antidepressant action[23]. The drug inhibits the transport of neurotransmitter serotonin back into the nerve terminals and other accumulating cells. It has been shown that only one of the enantiomers, S-citalopram, stands for the reuptake inhibitor effect. S-citalopram has recently been introduced onto the market under the name of escitalopram[24].

Citalopram with the molecular formula of the racemate (RS)-1-[3-(dimethylamino)propyl]-1- (4-fluorophenyl)-1,3-dihydroisobenzofuran-5-carbonitril has one asymmetric carbon atom in the 1 position in the isobenzofuran ring, leading to a racemic formulation, of the S(+)-enantiomer (S-Cit) and the R-(-)-enantiomer (R-Cit). The hydrobromide salt is sparingly soluble in water and it is soluble and stable in ethanol for up to one year at +4˚C. The pKa for the base (molecular weight 324.39 g/mol) of citalopram is 9.5. The structure of citalopram is shown in Figure 4.4.

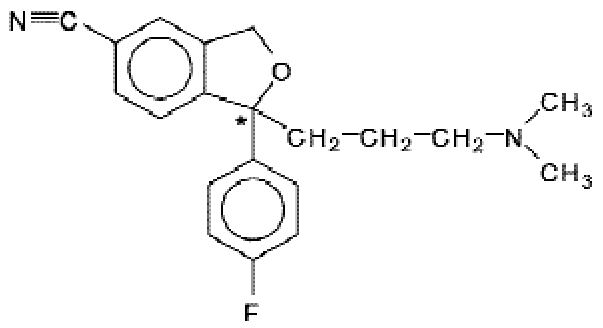

**Figure 4.4. Structure of citalopram hydrobromide.**

*4.7.1 HPLC separation of citalopram enantiomers*

Citalopram can be resolved on commercially available chiral columns such Chirobiotic V, Cyclobond, Chiracel OD[25, 26]. The HPLC separation of citalopram was carried out on Chirobiotic V column in new polar organic mode by using methanol:acetic acid: triethylamine(100:0.006:0.003) as mobile phase at the flow rate of 1 mL/minute, with UV detection wavelength (λ), 225 nm. With this mobile phase baseline separation of the enantiomers was achieved. The simultaneous separation of enatiomers of citalopram and its two N-demethylated metabolites along with the internal standard alprenolol in human plasma has been carried out using Chirobiotic V, with the mobile phase methanol:acetic acid:triethylamine 99.9:0.055:0.060. It was also shown that the R isomer elutes before the S isomer[27]. A better separation was achieved in the present study when the concentrations of acetic acid and triethylamine were lowered (Figure 4.5).

The new polar organic mode is closely related to the normal phase mode than to the reversed phase mode. Generally, it consists of an alcohol (methanol, ethanol or isopropanol) with a very small amount of acid/base added to affect the retention and selectivity. The amount of acid and base as well as the ratio of acid/base needs to be adjusted to optimise the resolution. The new polar organic mode is advantageous as it can dissolve many analyte salts that cannot be dissolved with traditional phase solvents.

Chiral analytes suitable for the new polar organic mobile phase mode should have at least two polar functional groups. These functional groups include alcohols, halogens (F, Cl, I), nitrogen (primary, secondary and tertiary amine), carbonyl, carboxyl, oxidised forms of sulphur, phosphorus, etc. At least one of the analyte's polar functional groups

must be on or near the stereogenic centre. It is also beneficial if the analyte has some steric bulk or aromatic rings close to the stereogenic centre[28].

With the above-mentioned mobile phase, the retention time obtained for the two isomers are 20.78 and 21.93 for the isomers R and S, respectively (Figure 4.5).

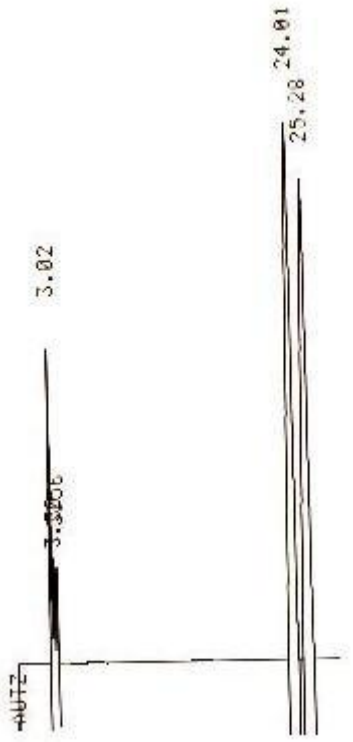


**Figure 4.5. Separation of citalopram enantiomers on Chirobiotic V.**

*4.7.1.1 Citalopram standard plot*

The dilution study was carried out in order study the effect of analyte concentration on the resolution profile of the drug. The concentration was 1.5-32 µg/mL. The plot was linear in this concentration range with linear regression coefficient R =0.99945. With this value of R the value of unknown concentration can be predicted perfectly if the area under the peak is known. This range was suitable for our analysis. We have tested the linearity of this plot with the minimum concentration of 300 ng/mL. Figure 4.6 shows the standard plot for S citalopram in the concentration range as mentioned earlier.

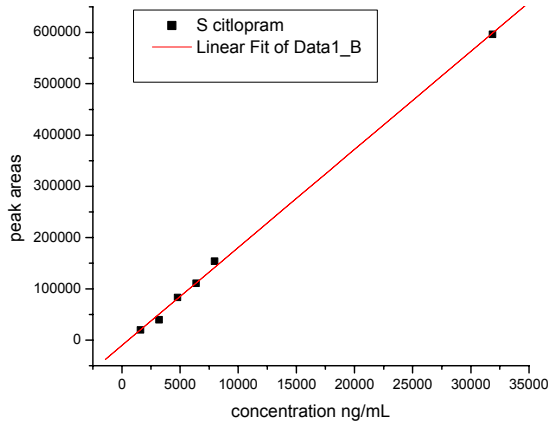


**Figure 4.6. Standard plot S citalopram hydrobromide in ethanol.**

*4.7.1.2 The capacity factor and selectivity*

The capacity factor is a measure of degree to which that component is retained on the stationary phase relative to the unretained component. Thus, capacity factor and selectivity can be determined by using the equation given in equations 4.1-4.3.

$$k'_1 = \frac{t_1 - t_0}{t_0} \qquad 4.1$$

where $k_1$' is capacity factor, $t_1$ is the retention time of less retained isomer and $t_0$ is the retention time

Similarly,

$$k'_2 = \frac{t_2 - t_0}{t_0} \qquad 4.2$$

where $k_2$' is capacity factor, $t_2$ is the retention time of less retained isomer and $t_0$ is the retention time

The selectivity α can be defined as

$$\alpha = \frac{k'_2}{k'_1} \qquad 4.3$$

This is a measure of separation between the two peaks. For optimum resolution the **α** should be between 1-5. The Table 4.11 shows the values of $k_1$', $k_2$' and α.

**Table 4.11. HPLC data for the resolution of citalopram hydrobromide**

| Retention time min | | $k_1$' | $k_2$' | α |
|---|---|---|---|---|
| R | S | | | |
| 24.01 | 25.28 | 6.95 | 7.37 | 1.06 |

*4.7.2 Citalopram inclusion study*

Recently it has been shown that the β-CD forms a 1:1 inclusion complex with citalopram in aqueous medium[29]. We were interested to study the inclusion of this drug with the cylodextrin bonded polymeric phase. For this study we have carried out batch adsorption studies of known concentration of citalopram with the polymeric sorbent. Two polymers that showed the highest binding of β-CD (GVh10HMCD and GVh12SCCD) were chosen for this study. The typical procedure involved equilibration of the drug of known concentration with the CD containing polymer at ambient temperature for 24 h. Thus, 0.25 g of the CD modified polymers were weighed into screw cap bottles. A 1mM solution of citalopram hydrobromide in ethanol and water were made. Required quantities of these solutions were then added to the polymers and equilibrated at room temperature. The molar ratio of β-CD: citalopram hydrobromide was 1:1 and 1:0.5. The analysis of the supernatant by HPLC was used to determine the stereoselective binding of the drug enantiomer. The samples were withdrawn from the supernatant solutions after 24 h. The samples were analysed after dilution with the mobile phase.

**Table 4.12. Inclusion study of Citalopram hydrobromide**

| Polymer code | β-CD mmol/g polymer | Cit HBr mmol | solvent |
|---|---|---|---|
| GV10(H)HMCD | 0.1700 | 0.1700 | EtOH |
| GV10(H)HMCD | 0.1700 | 0.0850 | $H_2O$ |
| GV12(H)SCCD | 0.1744 | 0.1744 | EtOH |
| GV12(H)SCCD | 0.1744 | 0.0872 | $H_2O$ |

The enantiomeric excess is calculated according to the formula given in equation 4.4[30].

$$ee\% = \left[\frac{(R - S)}{(R + S)}\right] \times 100 \qquad 4.4$$

where, ee%: -% enantiomeric excess

R and S : - proportions (peak areas) of R and S in the mixture

The results of the HPLC analysis are shown in the Table 4.13.

**Table 4.13. HPLC data for the inclusion study of citalopram hydrobromide**

| Polymer code | solvent | Molar ratio β-CD:Cit HBr | % Peak area rac Cit HBr 0h | | % Peak area supernatant 24h | |
|---|---|---|---|---|---|---|
| | | | R | S | R | S |
| GV10(H)HMCD | EtOH | 1:1 | 48.00 | 51.99 | 46.90 | 53.09 |
| GV10(H)HMCD | EtOH | 1:0.5 | 48.83 | 51.16 | 57.52 | 42.42 |
| GV10(H)HMCD | $H_2O$ | 1:1 | 48.00 | 51.99 | 48.33 | 51.67 |
| GV10(H)HMCD | $H_2O$ | 1:0.5 | 48.83 | 51.16 | 48.17 | 51.82 |
| GV12(H)SCCD | EtOH | 1:1 | 48.00 | 51.99 | 48.86 | 51.13 |
| GV12(H)SCCD | EtOH | 1:0.5 | 48.83 | 51.16 | 51.02 | 48.97 |
| GV12(H)SCCD | $H_2O$ | 1:1 | 48.00 | 51.99 | 53.60 | 46.39 |
| GV12(H)SCCD | $H_2O$ | 1:0.5 | 48.83 | 51.16 | 62.02 | 37.97 |

As can be seen from Table 4.13**,** GV10HHMCD showed binding of S isomer of the drug with ethanol as the solvent and 1:0.5 molar ratio of β-CD**:** citalopram hydrobromide. The increase in concentration of the R isomer and decrease in the concentration of S isomer in the supernatant shows that the S isomer is bound to the polymer. The polymer GV12HSCCD showed binding of the S-citalopram hydrobromide in all the conditions tested except with ethanol as solvent and with 1:1 molar ratio. However, the binding was low when 1:1 molar ratio was used in water as solvent. The binding was the highest in case where water was used as solvent and the molar ratio was

1:0.5. Thus, 24% of ee of R isomer was obtained in the supernatant. Conversely, we can say that 24% of the S isomer is bound to the polymer. Similarly, the enantiomeric excess for GV12HSCCD with 1:1 molar ratio in water and 1:0.5 in ethanol as solvent are 7.21 and 2.04 % respectively. The hydrophobic GMA-DVB polymers are not wetted by water while ethanol wets the polymer. This facilitates the diffusion of solvents through the pores and makes the reactive sites more accessible.

It has been shown that the racemic citalopram forms 1:1 inclusion complexes with β-CD in aqueous solution by the penetration of the aromatic ring into the β-CD cavity. The mode of penetration of F-containing ring of R and S enantiomer was identical. The chiral discrimination was appeared to be dependent on the difference in mode of entry of –CN containing rings of citalopram molecule into the β-CD cavity. The proposed mode of binding is shown in the Figure 4.7.

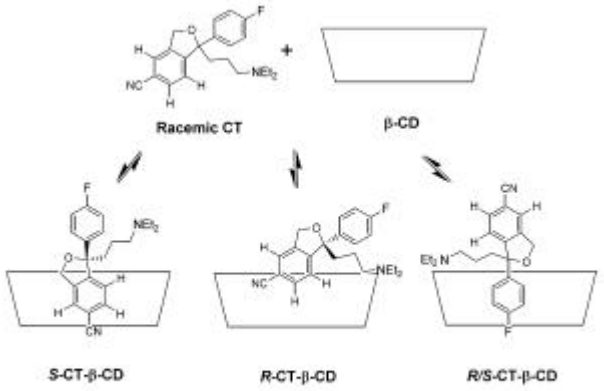


**Scheme 2.** Proposed structures for the 1 : 1 complexes formed between (*R*,*S*)-citalopram and *β*-CD.

**Figure 4.7. Mode of inclusion of citalopram isomers into the CD cavity.**

The inclusion results show a better trend in case of the polymers modified with sebacoyl chloride spacer. This could be because the length of the sebacoyl chloride spacer is more than the hexamethylene spacer. Thus, the β-CD molecules will have restricted space for orientation so that the inclusion will take place easily. In case of SC spacer the steric interactions are minimised as the β-CD molecules are spaced more distantly as compared to hexamethylene spacer. Also, it is now well established that the nitrogen containing spacers interact with the analyte molecules affecting the retention and elution selectivities[11].

**References**


1. Hinze W. L., *Sep. and Pur. Methods*, 10, 159-237, 1981.
2. Tingyue.G, Gow-Jen T. S. and George T., *J. Incl. Phenom. and Macro. Chem.*, 58, 375-379, 2006.
3. Case L. C. and Case L. K., *U. S. Patent 3,502,601*, 1970.
4. Hayakawa T., Yamamda T., Hidaka S., Yamagishi M. Takeda K. and Toda F., *Polym. Prep. Am. Chem. Soc., Div. Polym. Chem.*, 20, 530, 1979.
5. Mizobuchi Y., Tanaka M. and Shono T., *J. Chromtogr.*, 208, 35, 1981.
6. Fujimura K., Ueda T and Ando T., *Anal. Chem.*, 55, 446, 1983.
7. Hinze W. L., Riehl T. E., Armstrong D. W. DeMond W., Alak A. and Ward T., *Anal. Chem.*, 57, 237, 1985.
8. Lin C. E., Chen C. H., Lin C. H., Yang M. H. and Jiang J. C., *J. Chromatogr. Sci.*, 27, 665, 1989.
9. Kazauo N., Hiroya F., Hiroshi K., Hiroo W. and Keisuke M., *J. Chromatogr. A,* 694, 111, 1995.
10. Grini G., Lekchiri Y. and Morcellet M., *Chromatographia*, 40, 296, 1995.
11. Liu M., Da S., Feng Y. and Li L., *Anal. Chim. Acta*, 533, 89, 2005.
12. Nayak D. P., Kotha A. M., Patkar A. Y., Yemul O. P., Ponrathnam S. and Rajan C. R., *Indian Patent Appl. No. 1034/DEL/2000*, 2001.
13. Dubois M., Gilles K. A. and Hamilton J. K., *Anal. Chem.*, 28, 350, 1956.
14. Haiyan L., Shenghui L. and Gengliang Y., *Chem. J. Int.*, 8, 55, 2006.
15. Zhao X. and He B., *React. Polym.*, 24, 9-16, 1994.
16. Hirotsu T., *Thin Solid Films*, 506, 173, 2006.
17. Kim M., Way J. D. and Baldwin M., *Kor. J. Chem. Eng.*, 21, 465, 2004.
18. Muderawan W. I and., Ong T., *J. Sep. Sci.*, 29, 1849, 2006.
19. Lui Y., Fan X. and Gao L., *Macromol. Biosci.*, 3, 715, 2003.
20. Carlsson B., *From achiral to chiral analysis of citalopram*, Dissertation Linköping, Sweden, 2003.
21. Masand, P. S., and Gupta, S., *Harv. Rev. Psychiatry*, *7*, 69, 1999.
22. Sanchez C. and Hyttel J., *Cell Mol. Neurobiol.*, 19, 467, 1999.
23. Joubert A. F., Sanchez C., and Larsen F., *Hum. Psychopharmacol. 15*, 439, 2000.
24. Montgomery S. A., Loft H., Sanchez C., Reines E. H., and Papp M., *Pharmacol Toxicol* 88, 282-286, 2001.
25. Zeng Z., Jamour, M. and Klotz U., *Therap. Drug Mon.*, 22, 219, 2000.

26. Carlsson B and Norlancler B., *Chromatographia***,** 53, 266, 2001.

27**.** Kosel M., Eap C. B., Amey M.and Baumann P., *J. Chromatgr. B,* 719, 234-238, 1998.

28. Chirobiotic™ Handbook, A guide to using macrocyclic glycopeptide bonded phases for chiral LC separations Astec, Advanced Separation technologies Inc.

29. Ali S. M., Maheshwari A. and Fozdar B. I., *Magn. Reson. Chem.*; 45, 253–256, 2007.

30. Lomberg L. G. and Wan H., *Electrophoresis*, 21, 1940-1962, 2000.

# Chapter 5

## Modifications with tartaric acid / derivatised tartaric acid and evaluation for chiral resolution of amlodipine

## 5. Modifications with tartaric acid / derivatised tartaric acid and evaluation for chiral resolution of amlodipine

### 5.1 Introduction

Optical resolutions via diastereoisomeric salt formation are usually based on the separation of diastereoisomers by fractional crystallisation[1]. The process is very laborious since several recrystallisations are required to obtain a pure diastereomer. Optical resolutions with several recrystallisation steps cannot be scaled up economically into industrial scale, since they require large amounts of solvents, high volume vessels, and much time. Faster and cheaper methods of resolution are being explored. The chromatographic methods are amongst them[2].

The cheapest and most commonly used chiral resolving agent is L (+) tartaric acid (TA). L (+) tartaric acid has been used to resolve many racemic amines. It can be used in their native and derivatised forms[3]. The use of L (+) tartaric acid and its derivatives such as dibenzoyl and ditolyl tartaric acids as resolving agents have been extensively studied and is well documented[4]. Reports on tartaric acid being used in chromatography as mobile phase additive are also available [5].

Tartaric acid /derivatised tartaric acid bound polymers have been used in variety of applications such as supported catalysis. Tartrate-functionalised polystyrene copolymers were prepared with divinylbenzene, tetraethyleneglycol diacrylate, and diallyl tartrate as the crosslinking agents. These insoluble materials possess the unique advantages of heterogeneous reagents. These resins were used to support the asymmetric epoxidation of allylic alcohols along with titanium tetraisopropoxide and *tert*-butyl hydroperoxide with reasonably good yields and a high enantiomeric excess[6]. Also linear poly(tartarate)esters have been synthesised and bound to crosslinked styrene-divinyl benzene polymers. These supported ligands were used for the epoxidation trans hex-2-en-1-ol with titanium tetraisopropoxide and tert-butyl hydroperoxide [7]. Soluble polymer supported linear poly(tartrate)esters were also used for Sharpless epoxidation of alkenes with very good enantiomeric excess [8].

Chiral stationary phases based on derivatised tartaric acid have been successfully used for the resolution of many racemates. A chiral stationary phase for capillary GC based on (R, R)-N, N' dialkyltartramide bound to polysiloxane has been synthesised. The

chiral selector was attached to the polysiloxane backbone via 11 methylene units. Capillary gas chromatography using this chiral stationary phase was found to be capable of recognising the molecular chirality of several volatile enantiomers containing 1,2-diols, substituted amines, ketones and carboxylic acids. The mode of complexation was shown to be dual hydrogen binding between (R, R)-tartramide moiety and solute enantiomers to be resolved[9]. Allenmark and coworkers synthesised network polymeric chiral selectors by catalysed copolymerisation of chiral monomers with diallyl groups with multifunctional hydrosilane molecules. Derivatives of *N*, *N*′-diallyl-L-tartradiamide (DATD) and derivatives of *trans*-9, 10-dihydro-9, 10-ethanoanthracene- (11*S*, 12S)-11,12-dicarboxylic acid have been used as monomers [10-12].

In the present work we have synthesised GMA-EGDM and HEMA-EGDM copolymers bearing native as well as derivatised tartaric acid as pendant chiral ligands. The polymers were screened for stereoselective adsorption of antihypertensive drug amlodipine. Also, linear poly(GMA) was synthesised and reacted with L (+) tartaric acid. The resulting crosslinked material was also used for the drug binding studies.

## 5.2 Materials

L (+) Tartaric acid (L (+) TA): Empirical formula: $C_4H_6O_6$, Molecular weight: 150.087, Melting point: 168-170°C, Appearance: white powder.

L (+) Diacetyl tartaric anhydride (L (+) DATAn)**:** Empirical formula: $C_8H_8O_7$, Molecular weight: 216.14, melting point: 134 °C, Appearance: white, crystalline.

L (+) Dibenzoyl tartariv anhydride (L (+) DBTAn)**:** Empirical formula**:** $C_{18}H_{14}O_8$, Molecular weight: 358.30**,** Melting point**:** 194 °C

L (+) Dibenzoyl tartaric acid (L (+) DBTAc)**:** Empirical formula: $C_{18}H_{14}O_8$, Molecular weight: Melting point: 90 °C, Apperance: white powder.

L (+) Ditoluyl tartaric acid (L (+) DTTAc): Empirical formula: $C_{20}H_{18}O_8$, Molecular weight: 386.35, Melting point: 169-171 °C, Appearance: white solid

Amlodipine free bas: Empirical formula: $C_{20}H_{25}ClN_2O_5$, Molecular weight: 408.89, Melting point: 178-179°C, Appearance: white solid. Amlodipine was obtained from Glochem Industries Ltd, Hyderabad, India.

## 5.3 Methods

The support activation by chiral ligands involved the synthesis of tartaric acid derivatives and binding them to the support. Thus, L (+) diacetyl tartaric anhydride, L (+) dibenzoyl tartaric anhydride, and L (+)dibenzoyl tartaric acid were synthesised in the laboratory. The procedures are described below.

### *5.3.1 Synthesis of L (+) DATAn*

Acetic anhydride (250 mL, 2.6 mol) was placed in a one litre three-necked flask equipped with a magnetic stirrer. Sulphuric acid (1 mL) was added, followed by 65.8 g (0.447 mol) of L (+) tartaric acid. Some heat was evolved and after a short time crystals began to form. The reaction mixture was heated to 90˚C for 30 minutes, after cooling overnight, the crystalline product was collected on a Buchner funnel, washed with 25 mL portions of anhydrous toluene and placed in a vacuum desiccator. The purity of the product was checked by melting point. The optical rotation was checked using Jasco polarimeter DIP 181 with chloroform as solvent [13].

### *5.3.2 Synthesis of L (+) dibenzoyl tartaric anhydride (DBTAn)*

Tartaric acid (15 g, 0.1 mol) and benzoyl chloride (45 g, 0.32 mol) were heated in an Erlenmeyer flask slowly up to 150˚C for three hours. The reaction mixture became homogenous after half an hour. The mixture then again solidified after cooling to room temperature. To the mixture was then added anhydrous toluene to remove unreacted benzoyl chloride. The washings were repeated 2-3 times. The product was filtered on Buchner funnel and dried in vacuum oven overnight. The product purity was checked by melting point [14].

### *5.3.3 Synthesis of dibenzoyl tartaric acid (DBTAc) from DBTAn*

10 g of the DBTAn was taken in a round bottom flask. To this 45 mL water was added and the reaction mixture was heated to boil for one and half hours. The product was settled at the bottom of the round bottom flask as heavy oil. The oil was solidified after cooling the contents of the flask to room temperature overnight. The product was dried and melting point was determined [13].

## 5.4 Reaction scheme

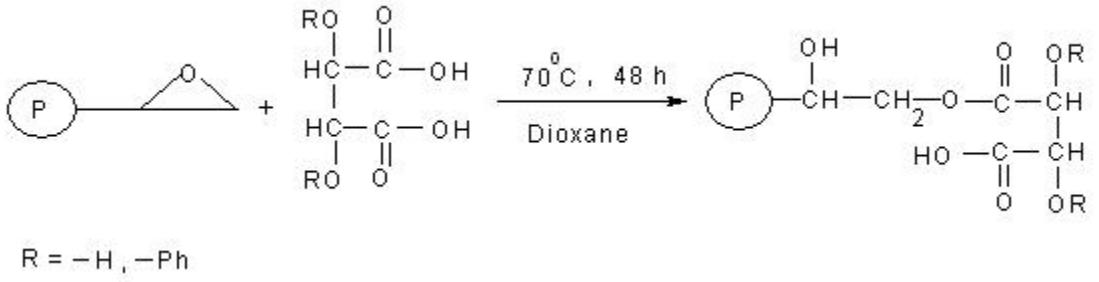


**Scheme 5.1: Modification of GMA-EGDM copolymers with L (+) tartaric acid**

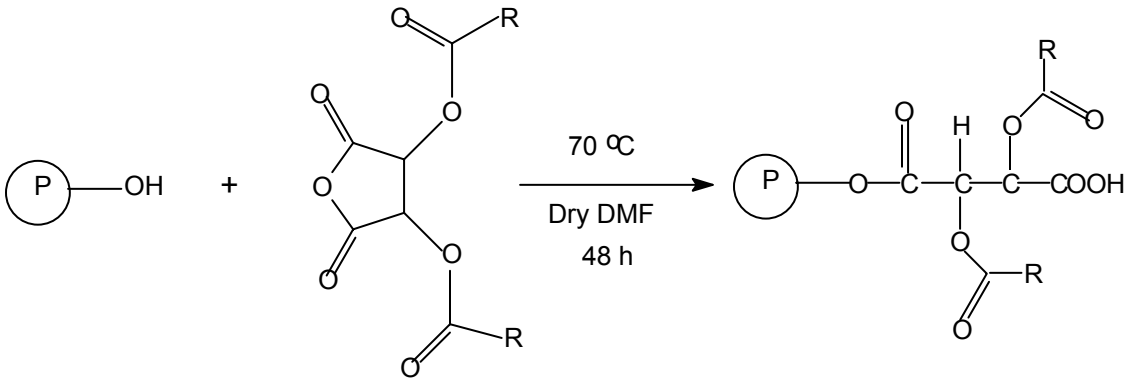


**Scheme 5.2: Modification of HEMA-EGDM copolymers with L (+) tartaric acid derivatives**

## 5.5 Functionalisation of GMA–EGDM copolymers

### *5.5.1 Procedure*

To 1 g of polymer beads was added 4 mL of 1,4-dioxane and degassed under vacuum to allow free penetration of the solvent inside the beads. The polymers were allowed to swell overnight in the solvent before the reaction. Then the required quantity of the ligand dissolved in minimum quantity of solvent was added to the beads and the beads were equilibrated for 48 h at 70˚C. The quantities are tabulated in Table 5.1. After 48 h the supernatant from the reaction mixture was decanted and the beads were washed with the solvent 2-3 times and filtered. The dry beads were then soxhlet extracted for 24

h using acetone to remove all the unreacted chiral ligand and dried in vacuum oven. The dried beads were analysed for the bound ligand titrimetrically.

*5.5.1.1 Determination of free carboxyl groups*

The dried polymer beads (0.1 g) were soaked in standard 0.1N sodium hydroxide (25 mL) for 3 h. An aliquot from the supernatant (10 mL) was removed and titrated against standard 0.1N hydrochloric acid. The acid capacity of the beads was determined by taking unmodified polymer as reference.

Modifications of HEMA-EGDM copolymers with L (+) diacetyl tartaric anhydride, L (+) dibenzoyl tartaric anhydride were also carried out under the same conditions with dry dimethyl formamide as solvent instead of dioxane. The reactions were carried out under nitrogen atmosphere and calcium chloride as drying agent. The data is given in Table 5.3.

**Table 5.1. Modifications of GE HIPE polymers with L (+) TA**

| Sr. No. | Poly. code | CLD % | Epoxy mmol/g | TA (react) g |
|---|---|---|---|---|
| 1. | GEH01-LT | 25 | 5.2177 | 0.7831 |
| 2. | GEH02-LT | 50 | 4.1434 | 0.6219 |
| 3. | GEH03-LT | 75 | 3.4395 | 0.5162 |
| 4. | GEH04-LT | 100 | 2.9397 | 0.4412 |
| 5. | GEH05-LT | 150 | 2.2768 | 0.3417 |
| 6. | GEH06-LT | 200 | 1.8562 | 0.2786 |
| 7. | GEH07-LT | 300 | 1.3586 | 0.2039 |
| 8. | GEH01-LT | 25 | 5.2177 | 0.7831 |
| 9. | GEH02-LT | 50 | 4.1434 | 0.6219 |
| 10. | GEH03-LT | 75 | 3.4395 | 0.5162 |
| 11. | GEH04-LT | 100 | 2.9397 | 0.4412 |
| 12. | GEH05-LT | 150 | 2.2768 | 0.3417 |

| | | | | |
|---|---|---|---|---|
| 13. | GEH06-LT | 200 | 1.8562 | 0.2786 |
| 14. | GEH07-LT | 300 | 1.3586 | 0.2039 |

*5.5.2 Synthesis of linear poly(glycidyl methacrylate)*

The linear poly(glycidyl methacrylate) was synthesised using precipitative polymerisation. The synthesis was carried out in a jacketed, double walled, glass reactor. Pet ether was used as non-solvent. GMA monomer (17.70 g) along with the initiator AIBN (0.71 g) was added to petroleum ether under stirring at 250 rpm. The reaction was continued for 3 h at 65 ºC under nitrogen. The precipitated polymer particles were collected on a Buchner funnel and were dried in the vacuum oven[15].

*5.5.2.1 Modifications of the linear poly(glycidyl methacrylate)( PGMA) with L (+) tartaric acid*

Modifications of linear poly(glycidyl methacrylate) polymers with L (+) tartaric acid were carried out in 1,4-dioxane. The required quantity of PGMA was dissolved in 1,4-dioxane in a plastic container. L (+) tartaric acid was then added to the mixture and the polymers were heated at 70ºC in a shaking water bath for 48h. The quantities are shown in Table 5.2. Three sets of reactions were carried out with 1:2, 1:4 and 1:6 molar ratio of epoxy: tartaric acid and at different dilutions. With highest concentration of tartaric acid the polymers precipitated after 30 min-1 h. After 48 h, the precipitated polymers were removed and the supernatants were made acidic using 1 N hydrochloric acid and then neutralised with 1 N sodium hydroxide. The supernatants were then concentrated and the polymers precipitated using acetone. The precipitated polymers were washed several times with water and then dried in oven. The solubilities of the resulting polymers were checked in various solvents. The polymers were characterised by IR spectroscopy.

**Table 5.2. Modifications of linear poly(glycidyl methacrylate)**

| Sr. No. I$^{st}$ set | PGMA(g) | Dioxane(ml) | L(+) TA (g) | Code |
|---|---|---|---|---|
| 1. | 1.421 | 25 | 3 | PGMA3a1 |
| 2. | 1.421 | 50 | 3 | PGMA3a2 |
| 3. | 1.421 | 100 | 3 | PGMA3a3 |
| **II$^{nd}$ set** | **PGMA(g)** | **Dioxane(ml)** | **L(+) TA (g)** | **Code** |
| 1. | 1.421 | 25 | 6 | PGMA3b1 |
| 2. | 1.421 | 50 | 6 | PGMA3b2 |
| 3. | 1.421 | 100 | 6 | PGMA3b3 |
| **III$^{rd}$ set** | **PGMA(g)** | **Dioxane(ml)** | **L(+) TA (g)** | **Code** |
| 1. | 1.421 | 25 | 9 | PGMA3c1 |
| 2. | 1.421 | 50 | 9 | PGMA3c2 |
| 3. | 1.421 | 100 | 9 | PGMA3c3 |

**Table 5.3. Modifications of HEMA-EGDM HIPE polymers with L (+) DATAn**

| Sr.No. | Poly. code | CLD % | Hydroxy mmol/g | DATAn (r) g |
|---|---|---|---|---|
| 1. | HEH01-LAT | 25 | 5.5650 | 1.2028 |
| 2. | HEH02-LAT | 50 | 4.3621 | 0.9428 |
| 3. | HEH03-LAT | 75 | 3.5867 | 0.7752 |
| 4. | HEH04-LAT | 100 | 3.0454 | 0.6582 |
| 5. | HEH05-LAT | 150 | 2.3393 | 0.5056 |
| 6. | HEH06-LAT | 200 | 1.8990 | 0.4104 |
| 7. | HEH07-LAT | 300 | 1.3797 | 0.2982 |
| 8. | HEH11-LAT | 25 | 5.5650 | 1.2028 |

| | | | | |
|---|---|---|---|---|
| 9. | HEH12-LAT | 50 | 4.3621 | 0.9428 |
| 10. | HEH13-LAT | 75 | 3.5867 | 0.7752 |
| 11. | HEH14-LAT | 100 | 3.0454 | 0.6582 |
| 12. | HEH15-LAT | 150 | 2.3393 | 0.5056 |
| 13. | HEH16-LAT | 200 | 1.8990 | 0.4104 |
| 14. | HEH17-LAT | 300 | 1.3797 | 0.2982 |

**Table 5.4. Modifications of HEMA-EGDM HIPE polymers with L (+) DBTAn**

| Sr. No. | Poly. code | CLD % | Hydroxy mmol/g | DBTAn (r) g |
|---|---|---|---|---|
| 1. | HEH01-LBT | 25 | 5.5647 | 1.8935 |
| 2. | HEH02-LBT | 50 | 4.3593 | 1.4833 |
| 3. | HEH03-LBT | 75 | 3.5826 | 1.2191 |
| 4. | HEH04-LBT | 100 | 3.0429 | 1.0354 |
| 5. | HEH05-LBT | 150 | 2.3389 | 0.7959 |
| 6. | HEH06-LBT | 200 | 1.8994 | 0.6463 |
| 7. | HEH07-LBT | 300 | 1.3808 | 0.4698 |
| 8. | HEH11-LBT | 25 | 5.5647 | 1.8935 |
| 9. | HEH12-LBT | 50 | 4.3593 | 1.4833 |
| 10. | HEH13-LBT | 75 | 3.5826 | 1.2191 |
| 11. | HEH14-LBT | 100 | 3.0429 | 1.0354 |
| 12. | HEH15-LBT | 150 | 2.3389 | 0.7959 |
| 13. | HEH16-LBT | 200 | 1.8994 | 0.6463 |
| 14. | HEH17-LBT | 300 | 1.3808 | 0.4698 |

*5.5.2.2 IR analysis*

The modified polymers were analysed for the presence of carboxylic acid groups by IR spectroscopy using Perkin Elmer Spectrum GX model. The samples were dried at 60˚ C in vacuo before analysis and then made into pellets with dried potassium bromide.

*5.5.2.3 Resolution of amlodipine enantiomers*

HPLC separation of amlodipine enantiomers was carried out using Chirobiotic V column using methanol:acetic acid:triethylamine (100:0.02:0.01, v/v/v) as mobile phase[16]. A standard plot was obtained by varying the concetration of racemic amlodipine (100-1000 µg/mL). In order to know the order of elution R and S amlodipine enantiomers, they were obtained in pure form by resolution with L (+) tartaric acid.

*5.5.2.4 Resolution of amlodipine enantiomers using L (+) tartaric acid*

To a stirred solution of 1.14 g (R, S)-amlodipine in 5.60 mL dimethyl sulphoxide was added a solution of 21 g L (+) tartaric acid (0.5 mole equivalents) in 5.60 mL dimethyl sulphoxide. Precipitation began within 5 minutes, and the resulting slurry was stirred overnight at room temperature. The solid was collected by filtration, washing with dimethyl sulphoxide followed by acetone. It was then dried at 50 ºC in vacuo overnight to give R (+) amlodipine-hemi-L-tartrate-mono-DMSO-solvate. The product was then refluxed with methanol to get the monohydrate. Amlodipine free-base was obtained by hydrolysing the salt using 2N sodium hydroxide and then extracting with ethyl acetate[17]. The organic layer was dried over sodium sulphate and evaporated to get the pure R (+) amlopdipine. S (-) amlodipine was obtained from the supernatant. The S (-) salt thus obtained was hydrolysed using sodium hydroxide to get free S(-) amlodipine. The purity of the resulting product was checked by HPLC on Chirobiotic V column.

*5.5.2.5 Resolution of amlodipine enantiomers using polymeric tartaric acid*

The polymer with maximum loading of tartaric acid (GEH01) was taken in a conical flask (0.25 g). It was soaked in dimethyl sulphoxide (0.5 mL) and then saturated solutions of amlodipine in DMSO were added according to molar ratio of polymer bound tartaric acid: amlodipine being 1:1, 1:0.5, 1:0.4 and 1:0.25 (Table 5.5). The samples were withdrawn from the reaction mixture using capillaries at 2, 8, 16 and 24 h. All the reactions were carried out at room temperature and the samples were kept in dark in order protect from light. The samples were analysed by HPLC on Chirobiotic V column.

**Table 5.5. Resolution of amlodipine using polymer bound TA**

| Sr. No. | mmol TA/g polymer | Mmol amplodipine | Ratio of TA: Amlodipine |
|---|---|---|---|
| 1. | 0.163 | 0.163 | 1:1.0 |
| 2. | 0.163 | 0.0817 | 1:0.5 |
| 3. | 0.163 | 0.0654 | 1:0.4 |
| 4. | 0.163 | 0.0408 | 1:0.25 |

A similar set of reactions was carried out using the poly(glycidyl methacrylate) polymer modified with tartaric acid with 1:2 molar ratio (PGMA3b2). The procedure was same as earlier. The reactions were carried out on 0.1 g of the polymer instead of 0.25 g. The data is given in Table 5.6.

**Table 5.6. Resolution of amlodipine enantiomers using PGMA3b2 polymers**

| Sr. No. | mmol TA/g polymer | mmol amplodipine | Ratio of TA: Amlodipine |
|---|---|---|---|
| 1. | 5.16 | 5.16 | 1:1.0 |
| 2. | 5.16 | 2.58 | 1:0.5 |
| 3. | 5.16 | 2.06 | 1:0.4 |
| 4. | 5.16 | 1.29 | 1:0.25 |

## 5.6 Results and discussion

### *5.6.1 Synthesis of chiral ligands*

The chiral ligands were synthsised according to the reported procedures. The optical purity was determined using Jasco polarimeter. The melting points and the optical rotations are given in the Table 5.5.

**Table 5.7. Physical properties of the chiral ligands**

| Sr. No. | Chiral ligand | Observed m.p | Literature m.p. | Observed specific rotation | Literature value of specific rotation |
|---|---|---|---|---|---|
| 1. | DATAn | 132˚C | 134˚C | +67.57 (acetone) | +62.00 (acetone) |
| 2. | DBTAn | 192˚C | 192-195˚C | +190.00 ($CHCl_3$) | +196.0 ($CHCl_3$) |
| 3. | DBTAc | 87˚C | 88-89˚C | +109.00 (ETOH) | +109-112 ((c=1.5, EtOH)) |

The synthesised anhydride chiral ligands were stored in desiccators in order to prevent hydrolysis by moisture. The ligands were tested for racemisation during 48 h at

70 ºC (under the reaction conditions). It was observed that no racemisation took place under the specified conditions.

*5.6.2 Attachment of chiral ligands to the supports*

The reaction of glycidyl group with –COOH is very facile and is generally self catalysed[18]. A strong acid hydrolyses the epoxide to a diol while with milder acids like carboxylic acids the reactions occur as shown below.

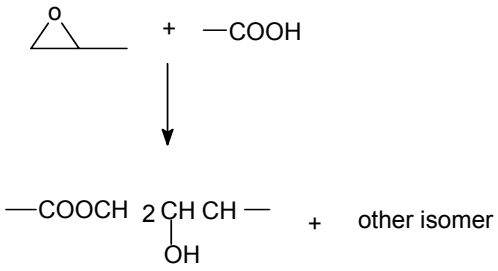


The reaction is a typical nucleophilic substitution reaction where, the attack on the epoxide ring takes place on the less hindered carbon atom. Since we have used a dicarboxylic acid the following reaction is expected

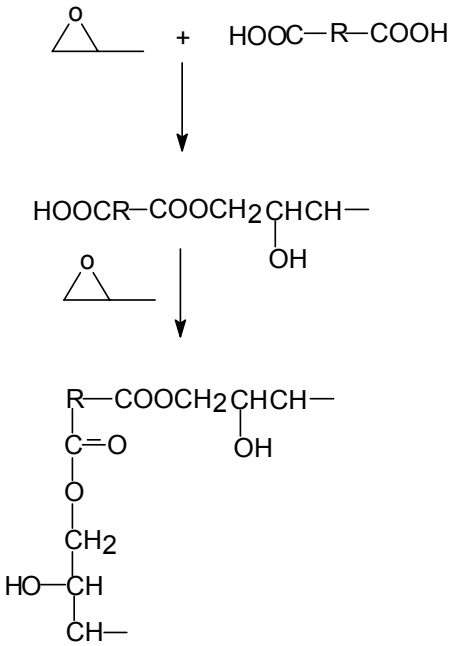


Thus, a crosslinked product is expected. In case of linear poly(glycidyl methacrylate) the reaction yielded crosslinked product. Poly(glycidyl methacrylate) was initially soluble in dioxane, dimethyl sulphoxide, dimethyl formamide, acetone and was

insoluble in methanol, ethanol and water. The product after reaction with L (+) TA was insoluble in all the above solvents. The products swelled in methanol, dioxane and water.

The IR of PGMA showed peaks at 850 and 910 $cm^{-1}$ due to epoxide ring (Figure 5.1 a, b and c)[19]. The disappearance of this peak and appearance of the peak at 3500 $cm^{-1}$ due to hydroxyl group confirms the incorporation of tartaric acid into the polymer. There is also broadening of peak due to carbonyl group at 1720 $cm^{-1}$ in the modified poly(glycidyl methacrylate).

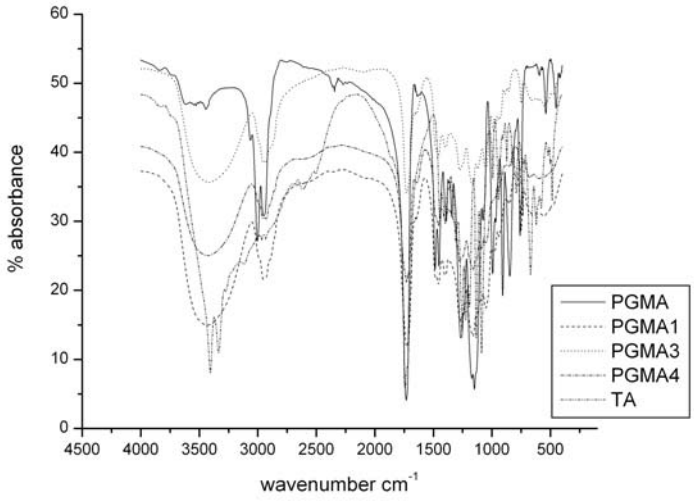


**a.**

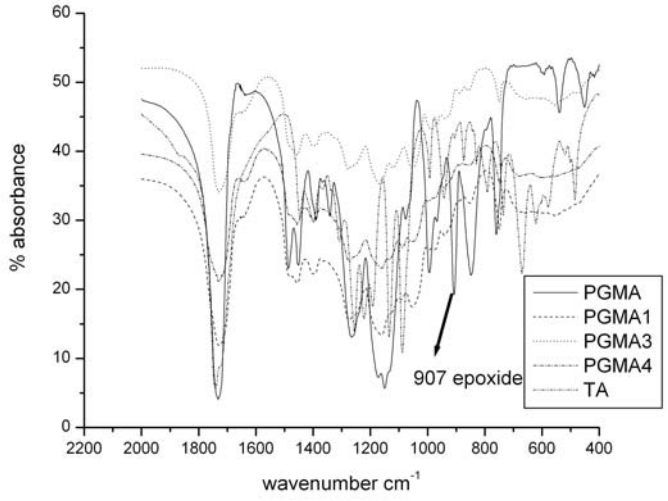


**b**.

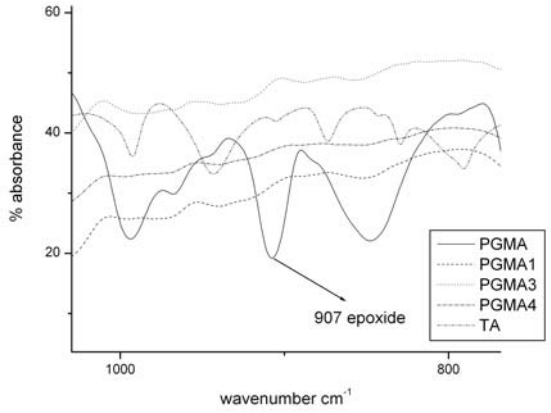


**c.**

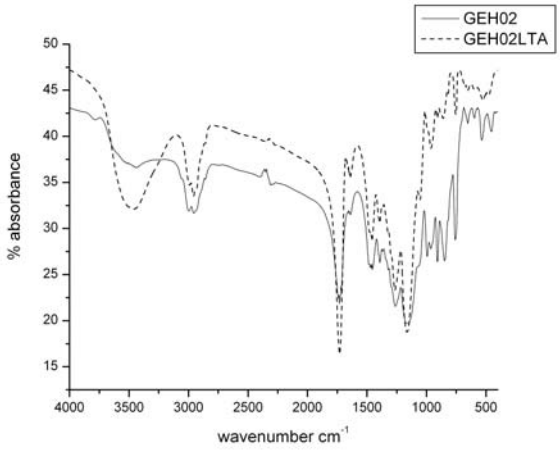


**d**.

**Figure 5.1. IR spectra of linear poly(glycidyl methcrylate) with L (+) tartaric acid (a.), enlarged (b.) and (c.), GEH01 modified with L (+) TA (d.)**

In case of crosslinked GMA-EGDM polymers the possibility of crosslinking through carboxylic acid groups is remote as the reactants are already heterophase. Also, since the polymers are crosslinked the network chain expansion is very much restricted resulting in less swellability. Thus, the reactive epoxide groups are held apart from each other hence reducing the probability of crosslinking through carboxylic acid group. Figure 5.2 shows the IRs of crosslinked GMA-EGDM polymers before and after reaction

with tartaric acid. The peak due to hydroxyl group appeared at 3500cm$^{-1}$ and the peak due to epoxide at 907cm$^{-1}$ disappeared.

The anhydride ligands were reacted directly with the hydroxy polymers in dry dimethyl formamide. It is a solvent for poly(HEMA) and the crosslinked HEMA-EGDM polymers swelled in this solvent. This allows free penetration of solvent as well as the reactants in the pores. The IR spectra of HEMA-EGDM copolymers before and after reaction with DATA are shown in Figure 5.2**.** The increase in the intensity of the peak at 3500 cm$^{-1}$ due to hydroxyl group and increase in the intensity of the peak at 1720 cm$^{-1}$ confirmed the attachment of the ligand to the matrix.

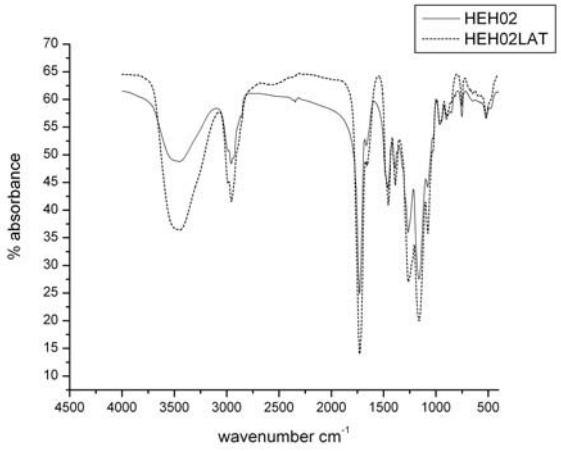


**Figure 5.2. IR spectrum of HEH02 modified with L (+) DATAn.**

**Table 5.8. Modification of GMA-EGDM (series 1) with L (+) Tartaric acid [(2R, 3R)-(+)-tartaric acid]**

| Sr. No. | Poly. code | Epoxy mmol/g | TA (bound) mg/g | PV mL/g | SA m2/g |
|---|---|---|---|---|---|
| 1. | GEH01-LT | 5.2177 | 120 | 0.8241 | 50.21 |
| 2. | GEH02-LT | 4.1434 | 45 | 0.2604 | 51.82 |
| 3. | GEH03-LT | 3.4395 | 60 | 0.2773 | 57.39 |
| 4. | GEH04-LT | 2.9397 | 30 | 0.1995 | 58.91 |
| 5. | GEH05-LT | 2.2768 | 30 | 0.1957 | 66.13 |
| 6. | GEH06-LT | 1.8562 | 30 | 0.2836 | 99.88 |

| | | | | | |
|---|---|---|---|---|---|
| 7. | GEH07-LT | 1.3586 | 60 | 0.0396 | 98.72 |
| 8. | GEH11-LT | 5.2177 | 105 | 0.4200 | 50.81 |
| 9. | GEH12-LT | 4.1434 | 90 | | 54.23 |
| 10. | GEH13-LT | 3.4395 | 75 | | 59.54 |
| 11. | GEH14-LT | 2.9397 | 45 | 0.3300 | 63.47 |
| 12. | GEH15-LT | 2.2768 | 30 | | 69.05 |
| 13. | GEH16-LT | 1.8562 | 90 | | 65.58 |
| 14. | GEH17-LT | 1.3586 | 75 | 0.5600 | 66.98 |

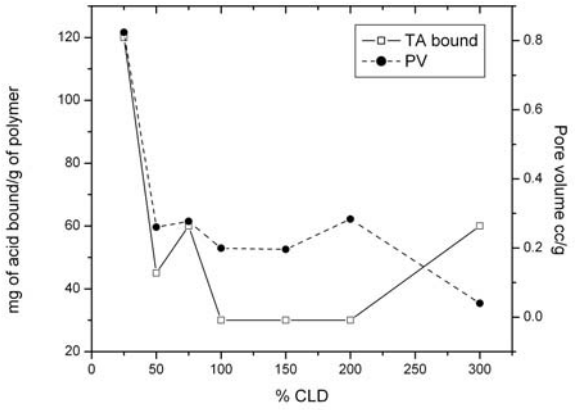


**Figure 5.3. Tartaric acid bound to GMA-EGDM polymers synthesised with 50% inner water as a function of CLD.**

**Table 5.9. Modification of HEMA-EGDM (series 1) with [(2R,3R)-(+)-Diacetyl tartaric anhydride]**

| Sr. No. | Poly. code | Hydroxy mmol/g | DATA bound mg/g | SA $m^2/g$ |
|---|---|---|---|---|
| 1. | HEH01-LAT | 5.5650 | 86 | 5.19 |
| 2. | HEH02-LAT | 4.3621 | 130 | 10.38 |
| 3. | HEH03-LAT | 3.5867 | 65 | 11. 95 |
| 4. | HEH04-LAT | 3.0454 | 65 | 14.16 |

| | | | | |
|---|---|---|---|---|
| 5. | HEH05-LAT | 2.3393 | 86 | 27.35 |
| 6. | HEH06-LAT | 1.8990 | 86 | 46.02 |
| 7. | HEH07-LAT | 1.3797 | 65 | 41.21 |
| 8. | HEH11-LAT | 5.5650 | 151 | 20.42 |
| 9. | HEH12-LAT | 4.3621 | 194 | 35.56 |
| 10. | HEH13-LAT | 3.5867 | 151 | 48.90 |
| 11. | HEH14-LAT | 3.0454 | 151 | 59,08 |
| 12. | HEH15-LAT | 2.3393 | 108 | 65.87 |
| 13. | HEH16-LAT | 1.8990 | 86 | 66.38 |
| 14. | HEH17-LAT | 1.3797 | 108 | 65.13 |

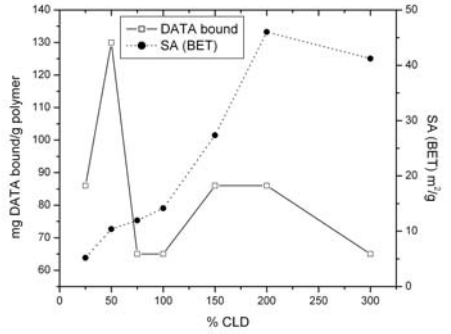


a.

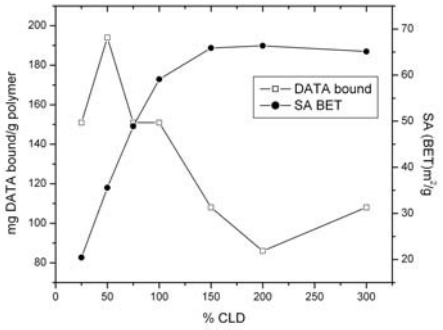


b.

**Figure 5.4. DATAc bound to HEMA-EGDM polymers synthesised with 50% inner water (a.) and 66.6% inner water (b.) as a function of CLD.**

**Table 5.10. Modification of HEMA-EGDM with L-diacetyl tartaric anhydride [(2R,3R)-(+)-diacetyl tartaric anhydride]**

| Sr. No. | Poly. code | Hydroxy mmol/g | DBTA (b) mg/g | SA $m^2/g$ |
|---|---|---|---|---|
| 1. | HEH01-LBT | 5.5647 | 662 | 5.19 |
| 2. | HEH02-LBT | 4.3593 | 309 | 10.38 |
| 3. | HEH03-LBT | 3.5826 | 265 | 11. 95 |

| | | | | |
|---|---|---|---|---|
| 4. | HEH04-LBT | 3.0429 | 221 | 14.16 |
| 5. | HEH05-LBT | 2.3389 | 265 | 27.35 |
| 6. | HEH06-LBT | 1.8994 | 221 | 46.02 |
| 7. | HEH07-LBT | 1.3808 | 221 | 41.21 |
| 8. | HEH11-LBT | 5.5647 | 486 | 20.42 |
| 9. | HEH12-LBT | 4.3593 | 662 | 35.56 |
| 10. | HEH13-LBT | 3.5826 | 441 | 48.90 |
| 11. | HEH14-LBT | 3.0429 | 441 | 59.08 |
| 12. | HEH15-LBT | 2.3389 | 265 | 65.87 |
| 13. | HEH16-LBT | 1.8994 | 177 | 66.38 |
| 14. | HEH17-LBT | 1.3808 | 177 | 65.13 |

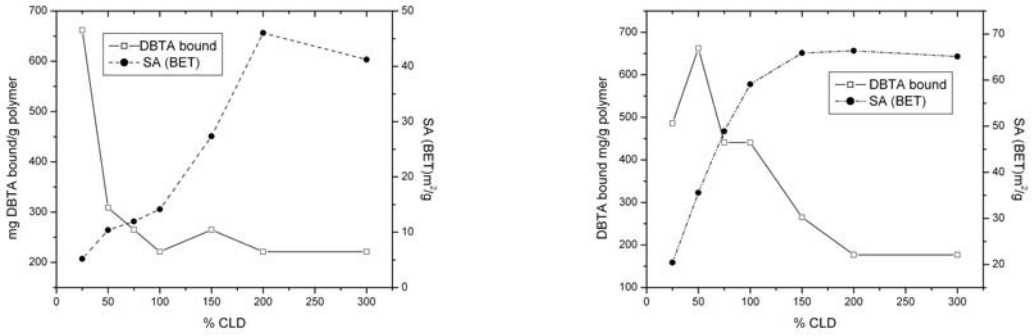


**Figure 5.5. DBTAc bound to HEMA-EGDM polymers synthesised with 50% inner water (a.) and 66.6% inner water (b.) as a function of CLD.**

The attachment of L (+) tartaric acid to GMA-EGDM copolymers decreased with the increase in % crosslink density (Table 5.8). Figure 5.3 shows the dependence of ligand binding and SA (BET) on the % crosslink density. Although the SA increased with increase in crosslink density the ligand binding decreased with maximum binding (120 mg/g, 0.79 mmol/g) obtained in case of GEH01. In case of HEMA-EGDM polymers (Tables 5.9 and 5.10) the maximum binding obtained with DATA as chiral ligand was 194 mg/g (0.89 mmol/g) while, with DBTA the maximum binding was 662 mg/g (1.85

mmol/g). The binding followed the same trend as GMA-EGDM copolymers except that the loading was highest in case of 50% crosslink density, as shown in Figures 5.4 and 5.5. In general the binding was dependent on the available surface functionalities. The polymer GEH01 that showed maximum binding of the ligand was derivatised with DBTAc as well as DTTAc under the same conditions as tartaric acid.

## 5.7 Resolution studies

### *5.7.1 Chiral resolution of amlodipine base*

Amlodipine (3-ethyl, 5-methyl 2-[(2-aminoethoxymethyl]-4-(0-chlorophenyl)-1, 4-dihydro-6-methyl-3, 5-pyridinedicarboxylate) is a member of a group of drugs known as 1,4-dihydropyridines (1,4-DHPs). These are a class of nitrogen containing heterocycles having six membered rings. The pharmacological properties of 1, 4-DHPs have been studied for several decades. The dihydropyridine structure is involved in biological redox processes[20]. These are long acting calcium channel blockers and useful for the treatment of cardiovascular disorders. The most common side effects are caused by excessive vasodialation.

Bayer introduced nifedipine in 1975[21]. Many other drugs like nicardipine, nivaldipine, felodipine, amlodipine, nitrendipine etc. have been marketed later. Racemic amlodipine besylate (benzene sulphonate) is used for the treatment of hypertension and angina. The S(-) isomer is having calcium channel blocker activity while the R(+) isomer has little or no calcium channel blocking activity. Earlier attempts to resolve amlodipine include resolution of amlodipine azide ester with optically active 2-methoxy-2-phenyl ethanol, resolution of amlodipine base with camphanic acid and L(+) or D(-) tartaric acid[22, 23].

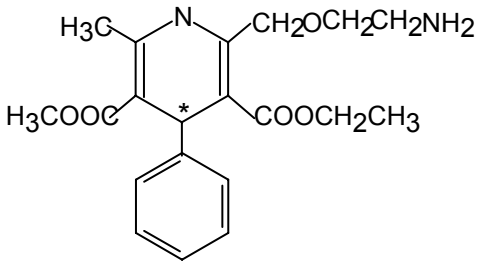

**Figure 5.6. Structure of amlodipine**

*5.7.2 HPLC separation of amlodipine isomers on chirobiotic V*

The initial trial to resolve amlodipine on Chirobiotic column were carried out with the reported mobile phase i.e. 100:0.5:0.1 methanol: acetic acid: triethylamine. This however, did not give expected resolution. When the concentration of both acetic acid and triethylamine were reduced better resolution was obtained. Very marginal change in the concentration of acid and base can affect the resolution. When the concentrations of acid and base were reduced to 0.02 and 0.01 respectively a baseline separation of the two isomers was achieved as in Figure 5.7**.**

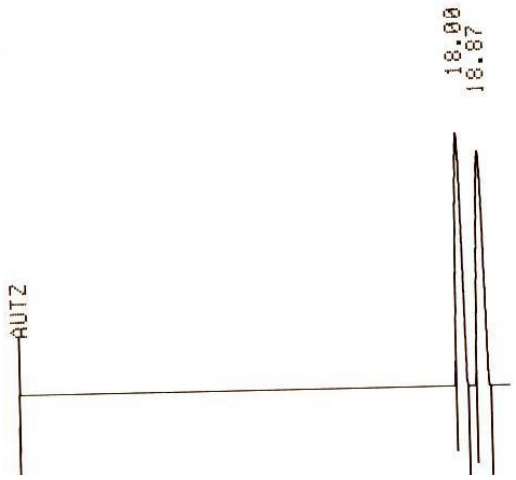


**Figure 5.7. Resolution of amlodipine enantiomers on chirobiotic V column using mobile phase methanol:acetic acid:triethylamine, 100:0.02:0.01.**

The capacity factor and selectivity are shown in the Table 5.11.

**Table 5.11. HPLC data for the resolution of amlodipine enantiomers**

| Sr. No. | Retention time min | | $k_1$' | $k_2$' | α |
|---|---|---|---|---|---|
| | R | S | | | |
| 1. | 18.00 | 18.87 | 4.14 | 4.39 | 1.06 |

**$k_1$', $k_2$': capacity factors, α: selectivity**

*5.7.2.1 Amlodipine standard plot*

The dilution study was carried out in order study the effect of analyte concentration on the resolution profile of the drug. The concentration was 100-1000 µg/mL. The plot was linear in this concentration range with linear regression coefficient R =0.99957. With this value of R the value of unknown concentration can be predicted

perfectly if the area under the peak is known. This range was suitable for our analysis. Figure 5.8 shows the standard plot for R amlodipine in the concentration range as mentioned earlier.

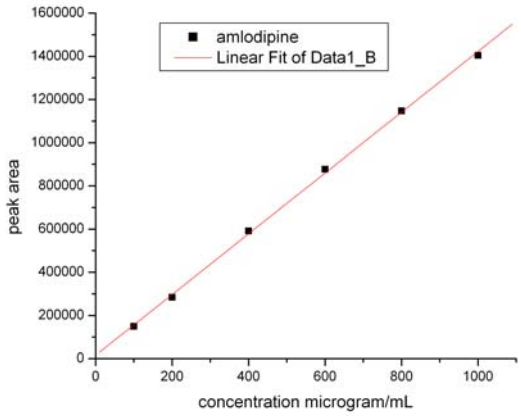


**Figure 5.8. Standard plot for R- amlodipine**

*5.7.2.2 Resolution of amlodipine using L (+) tartaric acid*

L(+) tartaric acid forms a diastereisomeric salt with amlodipine enantiomers. Depending on the difference in solubilities of these salts one of them, having lower solubility than the other gets precipitated and the other remains in the solution. It is known that L (+) tartaric acid forms a salt with R (+) amlodipine i.e. R (+) amlodipine hemi L (+) tartrate which gets precipitated while the other salt i.e. S (-)amlodipine hemi L (+) tartrate remains in the solution which was obtained in pure form by keeping the supernatant overnight. When individual standards were analysed by HPLC on Chirobiotic V column it was seen that the S (-) isomer elutes before R (+) isomer.

*5.7.2.3 Resolution studies using crosslinked GMA- EGDM polymer bound tartaric acid*

The resolutions were carried out in batch adsorption mode. The batch adsorption method for the evaluation of solid chiral selectors as potential chiral stationary phases involves the enantioselective partition of a racemate between the support bearing chiral moieties and the solvent, which, is generally achiral. The peak areas obtained from HPLC analysis of the supernatant are used to determine the ratio of enantiomers.

The polymers (0.25 g) were soaked in minimum quantity of DMSO (500 μL) in order to just immerse the beads completely. The polymers were left in the solvent for 30

min. in order to allow free diffusion of solvents inside the pores. Saturated solutions of (R, S) amlodipine were then added to these polymers and the polymers were left in the dark, as amlodipine solutions are sensitive to light. The samples were withdrawn from the reaction mixtures by using capillaries and analysed by HPLC on Chirobiotic V column. The % areas are given in the Table 5.12

The percent peak areas show a gradual increase in the area of S isomer and a decrease in the area of R isomer as can be seen from Table 5.12 and Figure 5.9. This suggests that the R isomer of amlodipine is adsorbed by the support bearing tartaric acid ligands. It was also seen that with 1:1 molar ratio of tartaric acid: amlodipine, the resolution is slower than that with 1:0.4 molar ratio. Thus, the enantiomeric excess obtained in case of 1:0.4 molar ratio after 24 h was 8% while for 1:1 molar ratio it was 4%. The adsorption of R isomer increases with time with maximum at 48 h and then starts to decline.

**Table 5.12. Change in the percent area of amlodipine at different time intervals**

| Ratio GEH01LT:Amlo | Relative percent of the two enantiomers | | | | | | | | | | | |
|---|---|---|---|---|---|---|---|---|---|---|---|---|
| | 2h | | 8h | | 16h | | 24h | | 48h | | 72h | |
| | S | R | S | R | S | R | S | R | S | R | S | R |
| 1:1.00 | 43.36 | 56.64 | 44.53 | 55.46 | 45.76 | 54.23 | 47.48 | 52.52 | | | | |
| 1:0.50 | 45.82 | 54.18 | 46.01 | 53.98 | 48.14 | 51.86 | 51.67 | 48.33 | | | | |
| 1:0.40 | 44.85 | 55.14 | 49.14 | 50.86 | 51.77 | 48.23 | 51.60 | 48.39 | 54.48 | 45.51 | 52.85 | 47.15 |
| 1:0.25 | 46.80 | 53.19 | 46.80 | 53.20 | 45.39 | 54.60 | 48.15 | 51.85 | | | | |

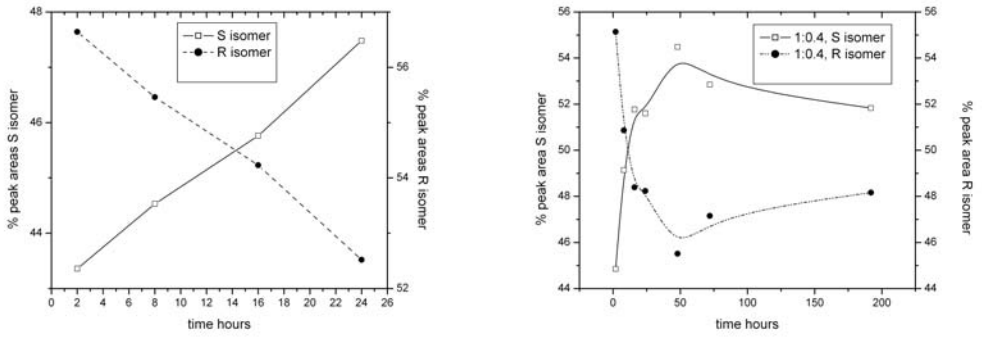


**Figure 5.9. Resolution of (R, S) amlodipine with GEH01LT at different time intervals**

Surprisingly, when GEH01DTTA, GEH01DBTA were used for the resolution studies, no noticeable change was observed in the percent peak areas of the supernatants. This is probably due to the bulky substituenets producing steric hindrance for the favorable orientation of the chiral ligands. When linear poly(glycidyl methacrylate) crosslinked with tartaric acid was used, no resolution was noticed. This is probably because of unavailability of both the carboxylic acid groups.

**References**


1. Newman P., "*Optical resolution procedures for chemical compounds*", vols. 1–3, New York, Optical Resolution Information Center, ManhattanCollege; 1978–84.
2. Kozma D. and Fogassy R., *Chirality*, 13, 428-430, 2001.
3. Kozma D., Madarasz Z., Acs M. and Fogassy E., *Tetrahedron Asym*. 5, 193, 1994.
4. Gawronski J. and Gawronska K., *Tartaric and malic acids in synthesis*, Wiley-Interscience publication, 1999.
5. Branka L., Dusanka R., Zorica V. and Danica A., *J. Plan*. *Chromatogr*. *TLC*, 18, 294-299, 2005.
6. Suresh P. S., Srinivasan M. and Pillai V. N. R**.,** *J*. *Polym*. *Sci: Part A*, *Polym*. *Chem*., 38, 161, 2000.
7. Canali L., Karjalainen J. K., Sherrington D. C. and Hormi O., *Chem*. *Commun*., 124, 1997.
8. Guo H., Shi X., Qiao Z., Hou S. and Wang M., *Chem*. *Comm*., 118, 2002.
9. Dobashi Y., Nakamura K., Saeki T., Matsuo M., Hara S. and Dobashi A., *J*. *Org*. *Chem*., 56, 3299-3305, 1991.
10. Allenmark S. G, Andersson S., Möller P. and Sanchez D., *Chirality*, 7, 248, 1995.
11. Thunberg L., Allenmark S., Friberg A., Ek F.and Frejd T., *Chirality*, 16, 614–624, 2004.
12. Thunberg L., Allenmark S., *J*. *Chromatogr*. *A*, 1026, 65, 2004.
13. Shriner R. L. and Furrow C. L., *Org*. *Synth*., *Coll*. *Vol*. *IV*, 242, 1963.
14. Lucas H. J. and Baumgarten W., *J*. *Am*. *Chem. Soc*., 63, 1653, 1941.
15. Hoshino M. and Arishima K., *J. Appl. Polym*. *Sci*., 57, 921, 1995.
16. Boatto G., Nieddu M., Faedda M. V. and Caprariis P., *Chirality*, 15, 494, 2003.
17. Joshi R. R., Joshi R. A., Karade N. B. and Gurjar M. K., *U*. *S*. *Patent 6,846,932*, assigned to Council of Scientific and Industrial Research, India, 2005.
18. Shechter L. and Wynstra J., *Ind*. *Eng*. *Chem*., 48, 86, 1956.
19. Fukuda T., Kohara N., Onoci Y. and Inacaki H., *J*. *Appl*. *Polym*. *Sci*., 45, 2201, 1991.
20. Sobolev A., Franssen M. C. R., Duburs G. and Groot A., *Biocat*. *Bioinform*., 22, 231, 2004.
21. Bosser F. and Vater W., *Naturwissenschaften*, 58, 578, 1971

22. Arrowsmith J. E., Campbell S. F., Cross P. E., Stabs J. K., Burges R. A., *J. Med. Chem*., 29, 1696, 1986.

23. Goldman S., Stoltefuss J. and Born L., *J. Med. Chem*., 35, 3341, 1992.

# Chapter 6

## Porous poly(ethylene-co-propylene) for lipase immobilisation

## 6. Porous polyethylene-co-propylene for lipase immobilisation

### 6.1 Introduction

As we have already seen, the synthetic procedures of making spherical porous polymer beads are emulsion and suspension polymerisation. There are several other physicochemical techniques for making microporous polymer beads, which include atomising polymer solution in heated stream of gas and at the same time evaporating the solvent, incorporation of microporous solid particles which are subsequently leached out, use of thermally induced phase separation processes, etc[1].

Formation of membranes by TIPS has been mostly studied on polypropylene. The porous polypropylene has been extensively used as support for the immobilisation of lipases. Lipases (triglycerol hydrolases, E.C. 3.1.1.3) constitute an important class of enzymes in biocatalysis. Lipases possess both lipolytic and esterolytic activities. The reactions are reversible and with decreased amount of water in organic solvents several inter and trans-esterifications are possible. Besides this, they are cheaply available from many sources. However, there are limitations to the lipase activity in organic medium, which is mainly due to low solubility and aggregation. This causes reduction in the lipase activity because the active sites become inaccessible for the substrates[2, 3]. To increase the number of accessible active sites and thereby the activity, enzymes are often adsorbed on solid supports [4].

Immobilisation of the enzyme on the solid support leads to many advantages in terms of operational and storage stability, facile recovery and recycling of the enzyme as well as use in continuous operations. The most extensively used support for lipase immobilisation is polypropylene owing to its high hydrophobicity. The immobilisation involves diffusion of enzyme into the pores, co-operative hydrophic interaction and binding reaction of free enzymes with the methyl group at the pore surface. The pore structure, pore volume, orientation of methyl group and surface area therefore play important roles in enzyme binding.

We report the effect of heterogeneous nucleation on the morphology of particles of poly(ethylene-co-propylene). We have synthesised different sorbitol based nucleating agents using Amberlyst 15. The bisbenzylidene sorbitols thus synthesised were used as nucleating agents to generate pores in polyethylene-co-propylene particles. The particles

were used as supports for immobilisation of *Candida rugosa* lipase (CRL) to study the enantioselective esterification of naproxen.

## 6.2 Materials

Sorbitol**:** Empirical formula: $C_6H_{14}O_6$, Molecular weight: 182.17, Melting point: 95ºC, Appearance: white granules.

Benzaldehyde**:** Empirical formula: $C_7H_6O$, Molecular weight: 106.13, Benzaldehyde was disitlled under vacuum before reaction.

4-Chloro benzaldehyde: Empirical formula: $C_7H_5OCl$, 140.57, Melting point: 45-50ºC, Appearance: - white solid

3,4-Dimethylbenzaldehyde**:** Empirical formula: $C_9H_{10}O$, Molecular weight: 134.18, boiling point: 226ºC, Appearance: pale yellow liquid

Poly(ethylene-co-propylene)**:** The polymer was virgin poly(ethylene-co-propylene) without any additives, with 2-3% ethylene content. The nucleating agents 1,3:2,4- bis(4-chloro benzylidene) sorbitol (4-CDBS) and 1,3:2,4- bis(3,4-dimethyl benzylidene) sorbitol (3,4-DMDBS) were synthesized by us. All the solvents used were of laboratory grade and were used without further purification.

Lipase (*Candida rugosa*) was obtained from Europa.

pNPP (*para* Nitro Phenyl Palmitate) substrate was from Sigma Aldrich.

Folin Ciocalteau reagent was from SD Fine Chemicals.

(R,S) 2-(6-methoxynaphthalen-2-yl) propanoic acid (naproxen) was obtained from

(R,S) naproxen methyl ester by hydrolysis. Hexane, isopropanol and methanol, of HPLC grade, were used without further purification for HPLC analysis.

S (+) Naproxen was obtained from Dr. Reddy's Laboratory, Hyderabad, India.

## 6.3 Methods

### *6.3.1 Synthesis of 1,3:2,4 bis(4-chloro benzylidene) sorbitol*

Sorbitol (10 g, 0.0549 mol) was dissolved in water (4.28 g) to make a 70% solution. To this solution 4-chloro benzaldehyde (15.43 g, 0.1098 mol) was added along with 50 mL of cyclohexane and Amberlyst 15 (0.2 mol%, 0.07 g). The water present in the reaction mixture was removed azeotropically at 70°C for 5 h. The reaction mixture solidified in the flask during this time, which was removed by dissolving in hot acetone. The solution was then filtered to remove the catalyst. The benzylidene derivative was

obtained by evaporating acetone. Similarly, 1,3:2,4 bis(3,4-dimethyl benzylidene) sorbitol was synthesized using 3, 4-dimethyl benzaldehyde[5].

**Table 6.1 Synthesis of nucleating agents.**

| **Aldehyde** | **Nucleatig agent code** | **Sorbitol (mole)** | **Aldehye (mole)** | **Amberlyst** | |
|---|---|---|---|---|---|
| | | | | **Mmol** | **g** |
| unsubstituted | DBS | 0.05489 | 0.1098 | 4.7362 | 1 |
| 4-Chloro | 4-CDBS | 0.05489 | 0.1098 | 4.7362 | 1 |
| 3,4-Dimethyl | 3,4DMDS | 0.05489 | 0.1098 | 4.7362 | 1 |

*6.3.2 Non-nucleated poly(ethylene-co-propylene)*

The poly(ethylene-co-propylene) (1 g) was dissolved in p-xylene (10 mL) by heating at 140°C under stirring for 3 h. The homogenous solution thus obtained was then quenched at 70°C for 2 h without stirring. The solid thus obtained was then washed with isopropanol, filtered and dried overnight in the vacuum oven at 50°C.

**Table 6.2. Synthesis of polymeric particles with different concentrations of nucleating agents.**

| Polymer | Nucleating agents used | Nucleating agent, Wt% |
|---|---|---|
| PP-VR | - | - |
| PP-1DM | 3,4DMMDBS | 0.25 |
| PP-2DM | 3,4DMMDBS | 1.00 |
| PP-3DM | 3,4DMMDBS | 5.00 |
| PP-1 CD | 4-CDBS | 0.25 |
| PP-2CD | 4-CDBS | 1.00 |
| PP-3CD | 4-CDBS | 5.00 |
| PP-1DBS | DBS | 0.25 |
| PP-2DBS | DBS | 1.00 |
| PP-3DBS | DBS | 5.00 |

Note: PP-VR non-nucleated PP
PP-1DM, PP-2DM and PP-3DM: - Poly(ethylene-co-propylene) with 0.25, 1 and 5% 3,4DMDBS as NA.
PP-1CD, PP-2CD and PP-3CD: - Poly(ethylene-co-propylene) with 0.25, 1 and 5% 4-CDBS as NA.
PP-1DBS, PP-2DBS and PP-3DBS: - Poly(ethylene-co-propylene) with 0.25, 1 and 5% 4-CDBS as NA.

*6.3.2.1 Nucleated poly(ethylene-co-propylene)*

The above procedure was repeated with the addition of DBS, 4-CDBS and 3,4-DMDBS, in different concentrations, during dissolution to obtain nucleated poly(ethylene-co-propylene). The data is listed in Table 6.2**.**

*6.3.3 Characterisation*

The particles formed were characterised by SEM for morphology and internal structure. The particles were mounted on stubs and sputter coated with gold. The photographs were taken on a JEOL JSM-5200 SEM instrument. The particle size distribution was determined using Accusizer APS. The samples (0.05-0.10 g) were dispersed in water containing surfactant (Noigen 120) and sonicated before analysing. DSC (Metler-4000, thermal analyzer coupled to DSC-30S cell) was carried out to

investigate the effect of nucleating agent on the crystallisation temperature of the polymer. The heating and cooling rates were 10 ºC/min. The pore volumes were determined using mercury intrusion porosimetry (Autoscan 33, Quantachrome, USA) in the pressure range 0-60000 psig. Surface area was determined by nitrogen adsorption method (Nova2000e). The samples were degassed for 3h at 50 ºC before analysis. The nucleated samples were also characterised by IR.

*6.3.4 Immobilisation*

*6.3.4.1 Preparation of enzyme solution*

The enzyme (0.20 g) was added to 12.5 mL of 0.5M sodium phosphate buffer of pH 7. The suspension was stirred magnetically at a slow speed for 45 minutes. The solution was then centrifuged at 10,000 rpm for 10 minutes.

*6.3.4.2 Pretreatment of polymers*

The polymers (0.25 g) were pretreated with 5 mL of ethanol for an hour. The polymers were then given two washes with distilled water for 30 min each.

*6.3.4.3 Immobilisation*

The enzyme solution (4 mg/mL) was added to the pretreated polymers. The mixture was kept in shaker water bath at 37°C for 18 h at 160 rpm. The mixture was then filtered and the polymers were washed with 10 mL 0.5 M sodium phosphate buffer for 30 minutes at 37°C and 140 rpm. The immobilised enzymes (IME) were then filtered and dried in vacuum. The enzyme activity in the supernatant was estimated by using pNPP as substrate[6] and the protein content were determined by Lowry's method[7].

*6.3.4.3.1 p-NPP assay method*

Substrate was prepared fresh by dissolving *p*-NPP (30 mg), 2-propanol (10 mL) and Triton X-100 (0.1 mL) in 100 mL of phosphate buffer (0.05 M, pH 7.0). Reaction mixture consisted of 0.1 mL diluted lipase, 0.9 mL of *p*-NPP substrate solution and 1 mL of phosphate buffer (0.05M, pH 7.0). It was incubated in a water bath at 37 C for 30 min followed by addition of 2 mL 2-propanol. Absorbance was determined at 410 nm (Shimadzu UV absorption spectrophotometer-160). The unit of enzyme activity unit was defined as the amount of enzyme required for hydrolysing 1nM *p*-NPP per minute under the described conditions.

*6.3.5 Esterification reaction conditions*

Commercial lipase (105 mg) was added to dry hexane (15 mL) containing racemic naproxen (0.2 mM) and n-butanol (5 mM). The solvent and alcohol were dried using activated 4 Aº molecular sieves. The reaction mixture was kept in a shaker water bath at 37°C, at 120 rpm. The samples were analysed by HPLC on Chirobiotic V.

*6.3.5.1 Esterification reaction using immobilised enzyme*

Immobilised enzymes were dried in vacuum before subjecting to esterification. The reaction was continued for 48 h and the samples were analysed. The dried immobilised enzyme (0.25 g) was added to dried hexane (15 mL) and dried n-butanol (0.45 mL). The reaction mixture was kept in shaker water bath at 37ºC at 120 rpm for 18 h. The reaction mixture was then filtered and the filtrate was analysed by HPLC. The immobilised enzyme was then washed for 30 minutes with a mixture of dry hexane (15 mL) and n-butanol (0.45 mL). The washed immobilised enzyme was further used for second cycle.

**6.4 HPLC Analysis**

The percent conversion of (R, S) 2-(6-methoxynaphthalen-2-yl) propanoic acid (naproxen) to S (+) 2-(6-methoxynaphthalen-2-yl) propanoic acid butyl ester was analysed at 254 nm on Chirobiotic V column using n-hexane: isopropanol (80:20 v/v) as the mobile phase.

**6.5 Results and Discussion**

*6.5.1 Synthesis of nucleating agents*

The bisbenzylidene sorbitol is generally synthesised by reacting an aqueous solution of sorbitol with benzaldehyde using a suitable organic solvent in the presence of a dehydrating catalyst. The water formed during the reaction is removed by azeotropic distillation. When two moles of benzaldehyde are used per mole of sorbitol a disubstituted product is obtained along with a trace amount of monobenzylidene sorbitol as impurity. This procedure has been modified several times to overcome some of the limitations such as gelling of the reaction mixture, prevention of the formation of side products such as mono and tribenzylidene sorbitol as well as to improve the yield [8-11]. Several substituted benzaldehydes have been evaluated for special applications such as packaging of food grade materials, optical materials etc[12, 13]. The catalyst has to be

neutralised and removed from the product after the reaction is completed. We have evaluated the suitability of a commercially available cation exchange resin Amberlyst 15 as catalyst for this reaction. The catalyst can be simply filtered off after the reaction and hence also, the catalyst is eco-friendly. The melting points of the crude products are 213 ºC and 227 ºC for 3,4-DMDBS and 4-CDBS.

**Table 6.3. Properties of nucleating agents.**

| Substituent on benzaldehyde | Nucleating agents code | % yield | m.p |
|---|---|---|---|
| unsubstituted | DBS | 55% | 180 |
| 4-Chloro | 4-CDBS | 48% | 213 |
| 3,4-Dimethyl | 3,4DMDBS | 30% | 227 |

*6.5.1.1 Infrared analysis of bisqbenzylidene sorbitol*

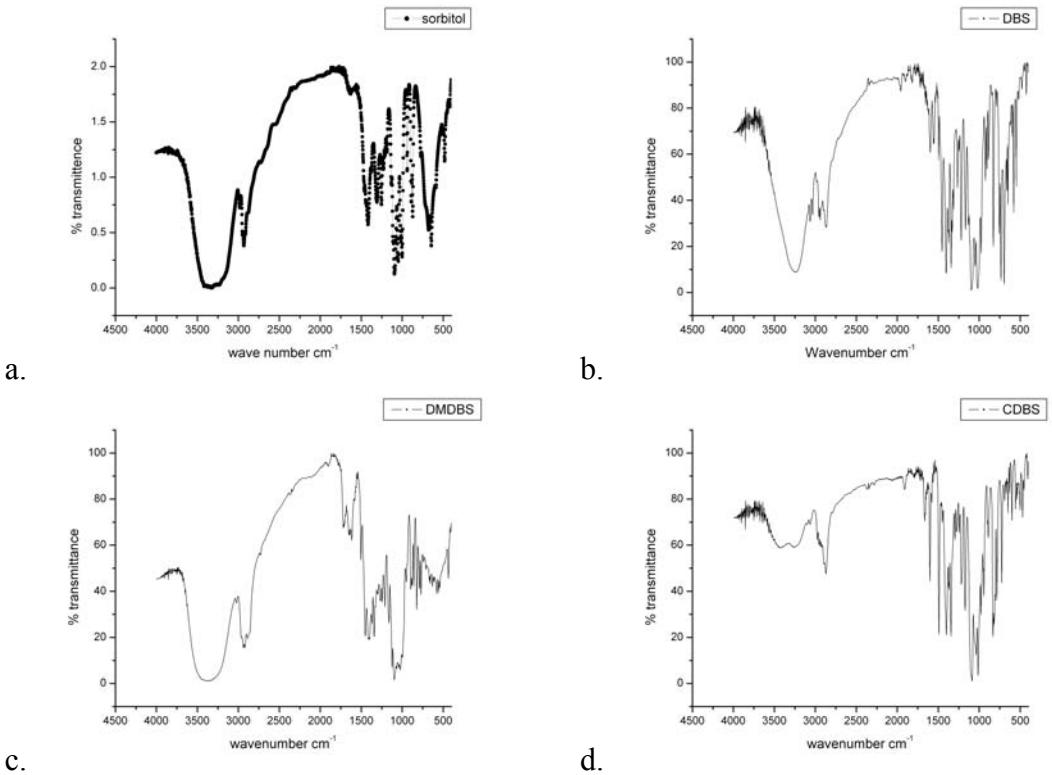


a. b. c. d.

**Figure 6.1. IR spectra of (a.) sorbitol (b.) DBS (c.) DMDBS and (d.) CDBS.**

The IRs show peaks due to aromatic rings in the region 1500-1600 $cm^{-1}$, which are absent in sorbitol.

*6.5.2 Differential Scanning Calorimetry (DSC)*

The nucleated samples were analysed by DSC to study the effect of nucleating agent on the crystallisation temperature of poly(ethylene-co propylene). The Table 6.4 shows the data obtained by DSC analysis.

**Table 6.4. Crystallisation temperatures of nucleated polymers as determined by DSC.**

| Polymer code | Nucleating agent | Crystallisation temperature |
|---|---|---|
| PP-VR | - | 93.3 |
| PP-2DM | 3,4 DMDBS | 107.9 |
| PP-2CD | 4-CDBS | 110.5 |

The nucleators raise the crystallisation temperature. They provide a surface, which reduces the free energy barrier to primary nucleation. The substituents on the aromatic ring influence the nucleating properties by altering the interfacial energies depending upon the polarities[14, 15].

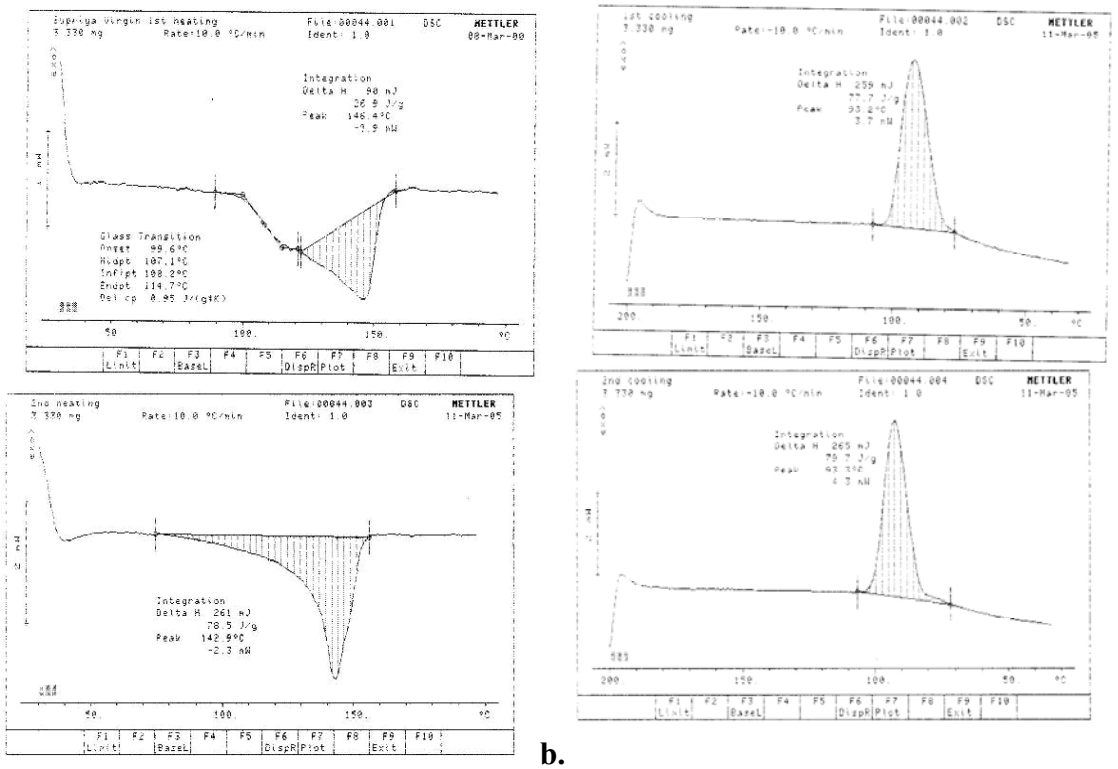


**a.** **b.**

**Figure 6.2. DSC thermograms of poly(ethylene-co-propylene) (a.)during heating (b.) during cooling.**

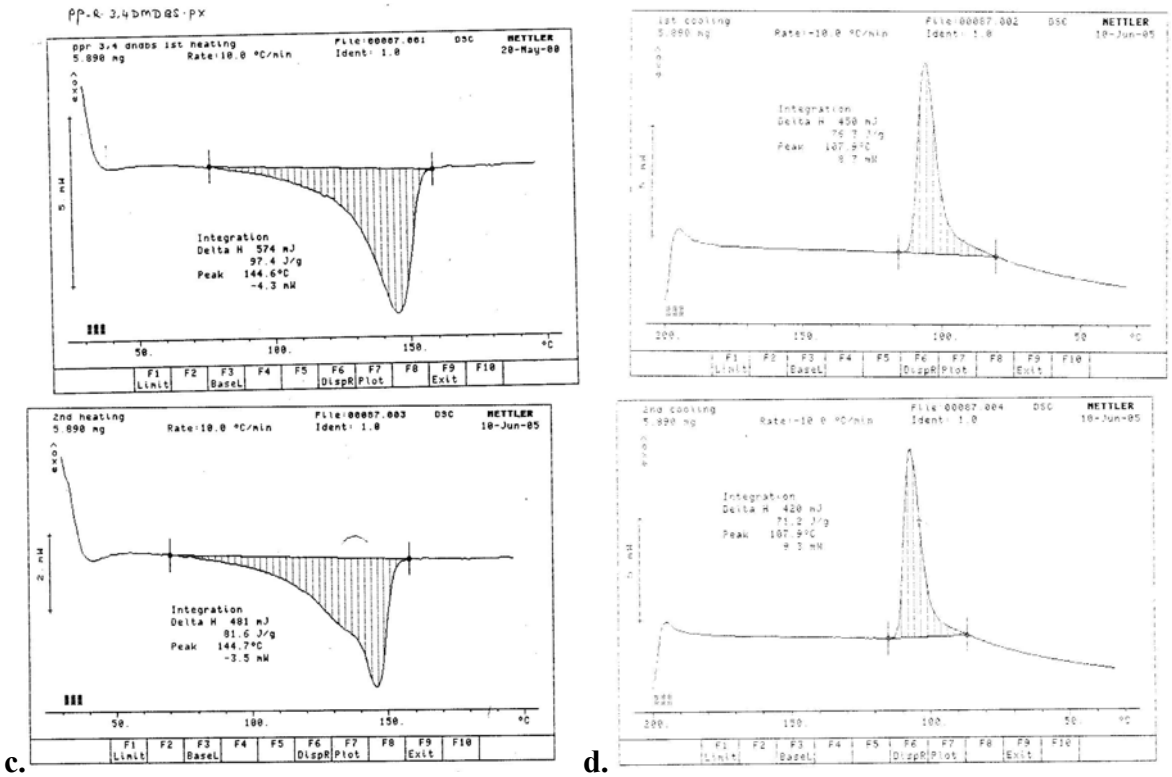


c. d.

**Figure 6.3. DSC thermograms of PP-2DM (c.) during heating (d.) during cooling.**

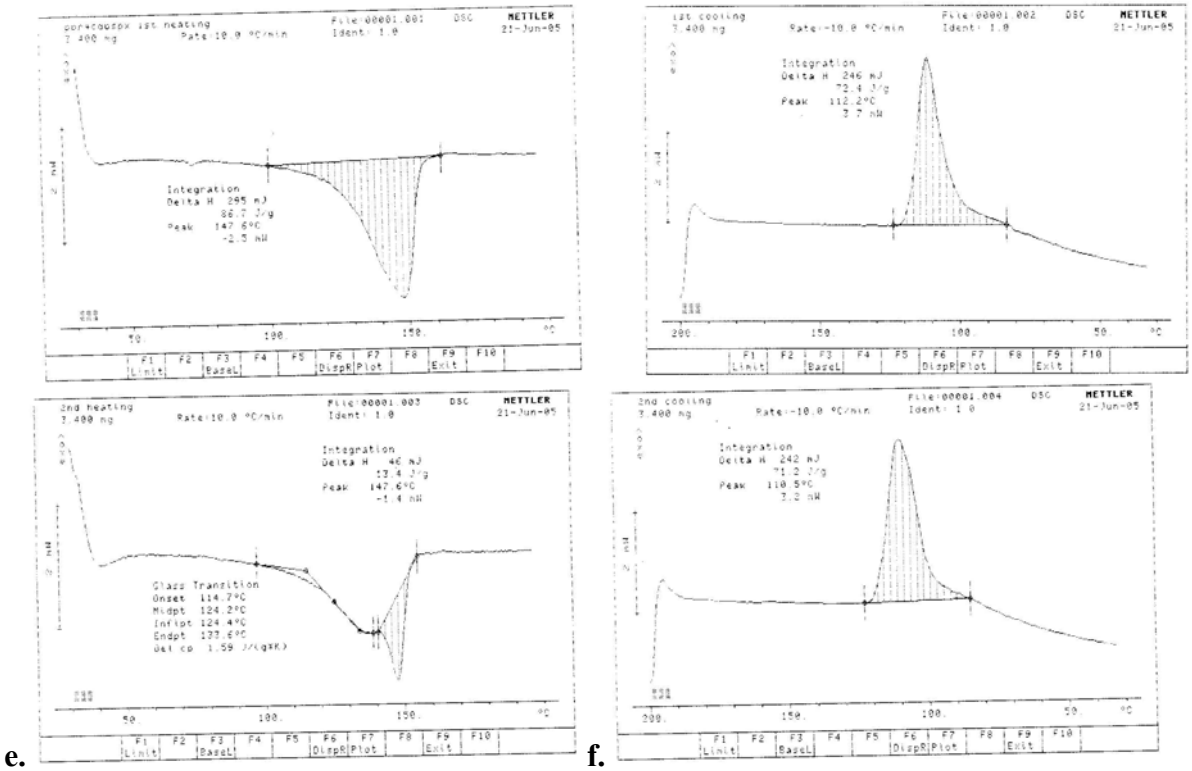


e. f.

**Figure 6.4. DSC thermograms of PP-2CD (c.) during heating (d.) during cooling.**

*6.5.3 Formation of porous particles*

*6.5.3.1 Particle size distribution*

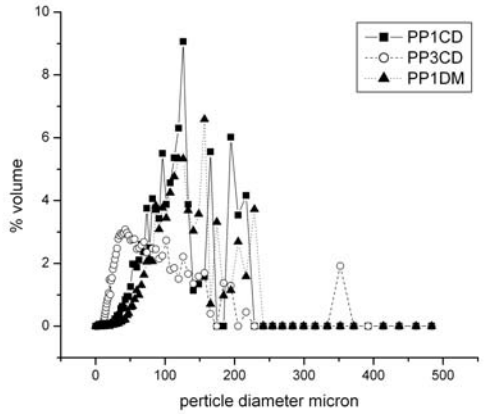


**Figure 6.5. Particle size distribution of PP-1CD, PP-3CD and PP-1DM.**

Figure 6.4 shows the particle size distribution for 3 samples PP1-CD, PP-1DM and PP-3CD. The particles were in the range 0-250 micron. The particle size distribution broadens with increasing concentration of nucleating agent. This could be due to increased number of nuclei with increase in concentration of nucleating agent. The large numbers of spherulites grow until they impinge upon each other, forming a large globule.

a. 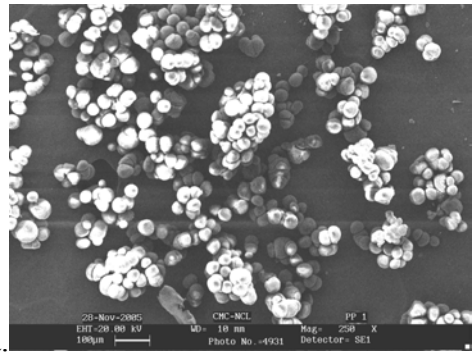

b. 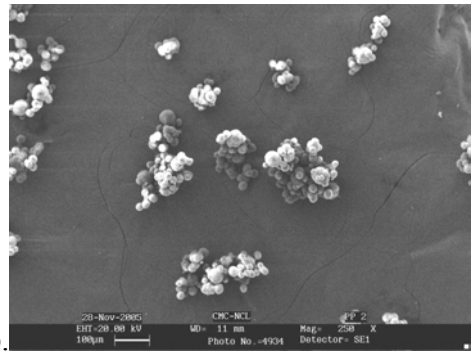

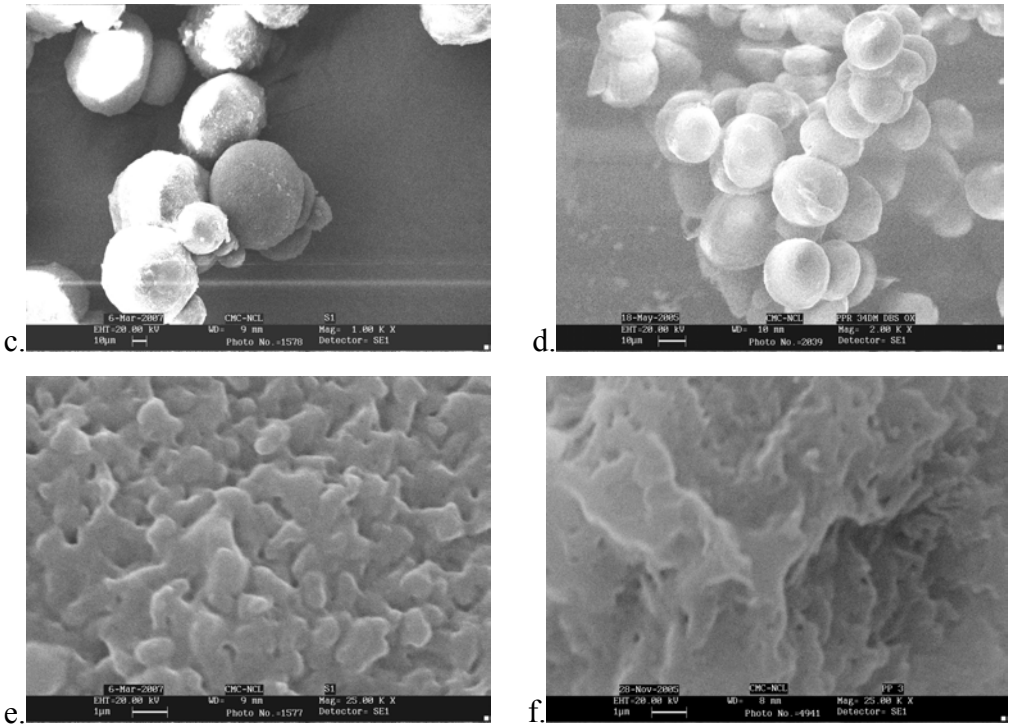


**Figure 6.6. SEM photograghs of samples PP-2DM (a, c and e at 100x, 1000x and 25KX) and PP-2CD (b, d and f, at 100x, 1000x and 25KX).**

The SEM images (Figure 6.5) of the polymers show that the particles formed are spherical, but with a rough surface. The surface morphology also reveals the lamellar growth. In the TIPS process, the polymer is dissolved in the diluent at high temperature and then cooled to induce phase separation[16]. The TIPS takes place either through solid-liquid phase separation where the polymer crystallises out of solution or through liquid-liquid phase separation where in the polymer rich continuous phase and polymer poor droplet phases are formed up on cooling. Microporous membranes are formed when the polymer rich phase constitutes the continuous phase, above the critical composition of the polymer. When the polymer concentration is lower than that at the critical point, the polymer rich phase becomes a dispersed phase after phase separation and the polymer lean phase becomes the matrix phase thereby forming the particles. The phase separation proceeds through spinodal decomposition or nucleation and growth mechanism. The formation of particles with characteristic morphologies is dependent on factors such as concentration of polymer, quenching temperature, etc[17].

Semidilute solutions of polyethylene upon cooling are known to generate crystalline structures[18]. The morphologies reflect the interplay of a liquid-liquid phase

separation process and the nucleation of the polymer crystals. Homogenous nucleation yields smooth particles while heterogeneous nucleation produces particles with rough surfaces. The polypropylene particle formation has been studied and shown to be by nucleation and growth mechanism[19]. The particle size was dependent on the factors such as the quenching temperature, polymer concentration etc. There is a report on formation of monodisperse nylon particles due to phase separation carried out using 1 weight % solution in a θ solvent above the θ temperature and cooling it rapidly[20]. The resulting morphologies differed with the type of nylon used. The uniformity of the resultant particles was attributed to the large number of growing nuclei that form during cooling, inhibiting the further growth of the new particles.

During the quench, the polymer solution phase-separates, giving rise to a large number of concentrated domains. The heterogeneities in the solution such as nucleating agent act as seeds for polymer crystallisation and initiate lamellar growth. The growth is directed outward giving rise to surface roughness. The smaller, smooth particles appear to result from the crystallisation of heterogeneity-free droplets of concentrated polymer solution produced in the phase separation process.

In the TIPS process the formation of globules is governed by the liquid-liquid phase separation where the solution separates into polymer rich and polymer poor phases followed by nucleation and growth. Generally, this mechanism predominates in crystalline polymers. The porosity in this process arises as a result of the diluent trapped in inter and intra lamellar spaces during crystallization. Up on removal of the diluent, the void spaces become pores.

It is seen from the pore volume data estimated by mercury porosimetry in Table 6.5 that the nucleated polyethylene-co-propylene samples prepared in this study possess higher pore volume than the non-nucleated samples. The presence of nucleating agent probably increases the number of nuclei thus reducing the size of the spherulite and causing an increase in pore volume. It is seen from Figure 6.6 that the pore volumes of these samples increases with the addition of nucleating agent.

**Table 6.5. Pore volumes of nucleated samples.**

| Polymer code | Pore volume $g/cm^3$ |
|---|---|
| PP-VR | 0.219 |
| PP-1DM | 0.470 |
| PP-2DM | 0.670 |
| PP-3DM | 1.365 |
| PP-1 CD | 0.080 |
| PP-2CD | 0.482 |
| PP-3CD | 0.491 |

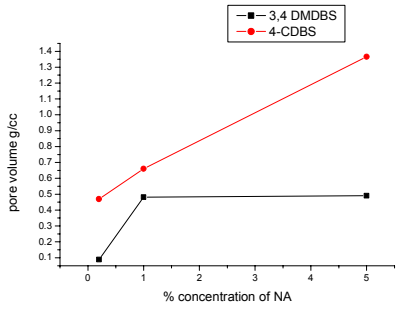


**Figure 6.7. Change in the pore volume of nucleated samples with the change in concentration of NA.**

The pore volume distribution, also determined by mercury intrusion porosimetry (MIP), is shown in Figure 6.9. In polymers PP-2DM and PP-3DM the pores are uniformly distributed from 5 to 25 nm. The surface area in these two polymers is high as compared to PP-1DM. Surface areas, as determined by MIP for PP-2DM and PP-4DM, are 59.09 and 50.00 $m^2/g$. In PP-2CD and PP-4CD wide distribution of pores, from 5 to 400 nm, is seen and the surface areas 15.10 and 27.69 $m^2/g$, respectively. Smaller pore diameters evolve in higher surface areas. The pore diameter, however, should preferably not be smaller than 10 nm, as the large lipase molecules will not be able to enter such small pores[21, 22].

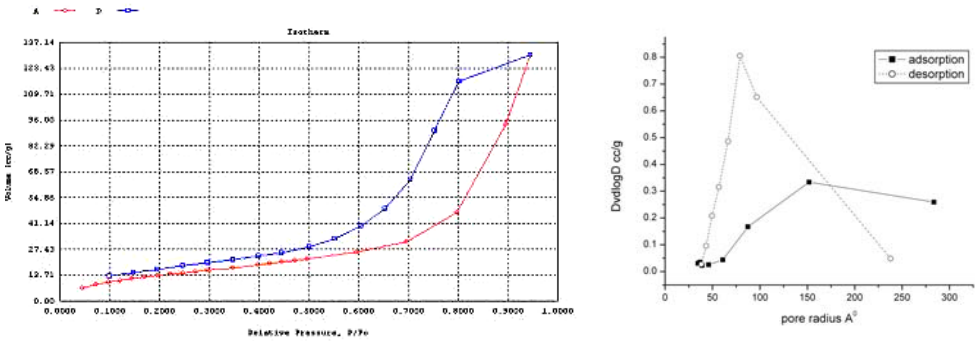


**Figure 6.8. Nitrogen adsorption isotherm for the sample PP-2DM and pore size distribution.**

Figure 6.7 shows nitrogen adsorption isotherm of the sample PP-2DM. The plot can be classified as mixed Type II- Type III according to BDDT classification [23]. The very large hysteresis loop indicates presence of bottle neck or slit like pores. The pore size distribution determined on desorption branch of hysteresis shows that the pores are distributed in the range of 50-250 $A^0$ i.e. (5-25 nm), which is in good agreement with mercury intrusion porosimetry.

## 6.6 Immobilisation and biotransformation

Immobilised lipase from *Candida rugosa* has successfully been used in a variety of applications such as interesterification, ester synthesis and transesterification reactions[24]. Lipases have also been useful as industrial catalyst for the resolution of racemic acids and alcohols and in a variety of fields such as household detergents, oils, fats, dairy, organic media, leather and paper industries[25]. Lipases are used as chiral catalysts in organic synthesis. Some examples about stereoselective esterification or hydrolysis of several drug racemates for its resolution using lipases have been published[26].

2-Aryl propionic acids, such as naproxen and ibuprofen, are examples of chemical compounds with their activity restricted to only one of the isomers. These compounds are among the most commonly used analgesics in the treatment of acute and chronic pain and inflammation. The anti-inflammatory and analgesic effects of the profens are attributed almost exclusively to the *S*-enantiomer. Most frequently reported adverse effects are gastric erosion and renal dysfunction.

Lipases have been successfully used in resolution of profens in the past few years [27]. The profens were firstly converted to esters chemically and then enantioselectively

hydrolysed to the active S-acid by biocatalysis, or alternatively the active S-form was converted to S-ester in organic media by lipase-catalysed esterification and followed by chemical hydrolysis of the S-ester to the S-acid. Both approaches involve two steps.

Novozym 435, an immobilised lipase from *Candida antarctica,* can resolve racemic ketoprofen, and the reaction rate of unwanted R-isomer of ketoprofen is faster than that of the active S-isomer, thereby making a one step process possible[28]. A facile enzymatic esterification process for the direct synthesis (S)-naproxen [and (S)-ibuprofen] 2-*N*-morpholinoethyl ester prodrug from racemic (S)-naproxen [and (S)-ibuprofen] has been developed using lipases as the biocatalyst in organic solvent[29, 30]. Enzymatic enantioselective hydrolysis of naproxen esters by lipases has been studied, in which high enantioselectivity for the *(S)* enantiomer was obtained by using *Candida cylindracea* lipase [31]. Enzymatic enantioselective esterification of racemic 2-(6-methoxy-2-naphthyl) propionic acid by *Candida cylindracea* lipase in the non-conventional medium, including organic solvents and supercritical carbon dioxide, has been thoroughly investigated [32], [33]. Attempts have also been made to develop an optimal resolution condition by investigating how solvents, co-substrate, reaction temperature, and even the pressure of supercritical fluid, affect the enantioselectivity and reaction rate[32]. The lipase from *Candida rugosa* was immobilized on three commercially available macroporous adsorptive resins for kinetic resolution of ibuprofen. The enantioselectivity of the immobilised lipase was 2.2 times as much as that of the native lipase for the kinetic resolution of ibuprofen with 1-propanol in isooctane at 30ºC[34].

The available surface area, both internal (pore size) and external (bead size or tube diameter), determines the enzyme binding capacity. The activity of the immobilised enzyme will also depend up on the bulk mass transfer and local diffusion properties of the system[35]. The wetting of the polymer with a solvent allows the passage of the solvent through the pores, clearing the pore network.

### *6.6.1 Immobilisation with and without pre treatment*

#### *6.6.1.1 Effect of wetting and contact time on immobilisation*

The results of the effect of wetting, non-wetting and contact time are listed in Tables 6.6 and 6.7.

**Table 6.6. Effect of pre-treatment of poly(ethylene-co-propylene) on protein binding.**

| Polymer | Protein content (μg/mL) | Supernatant Protein (μg/mL) | |
|---|---|---|---|
| | | 4 h | 18 h |
| PP-2DM | 631 | 282 | 155 |
| PP-4DM | 631 | 288 | 193 |

**Table 6.7. Effect of non pre-treatment of poly(ethylene-propylene) on protein binding.**

| Polymer | Protein content (μg/mL) | Supernatant Protein (μg/mL) | |
|---|---|---|---|
| | | 4 h | 18 h |
| PP-2DM | 631 | 484 | 356 |
| PP-4DM | 631 | 526 | 329 |

The lower density polymers do not disperse uniformly in the enzyme solution. Hence, effect of pretreatment is an important aspect to be studied. The polymer was pretreated with 5 mL of ethanol for an hour before subjecting to immobilisation. After pre-treating, the polymers were subjected to immobilisation for two differing times, 4 and 18 h. The effect of wetting as well as contact time of enzyme with support was determined after analysing the supernatant for protein content. From the table it is clear that pre-treatment of support enhances the protein binding. Pre-treatment of support lead to opening of pores, which facilitates the enzyme diffusion. Pretreatment and increase in contact time increases the amount of protein binding.

*6.6.2 Effect of pore volume and surface area on esterification of R S naproxen to S (+) butyl ester*

It is seen from Table 6.8 and Figure 6.8 that the esterification of R, S naproxen for enzyme bound on PP-2DM was the highest as compared to the other polymers i.e. PP-3DM, PP-2CD, PP-3CD although the pore volumes of these polymers were higher as compared to the pore volume of PP-2DM. This can be due to the narrow pore size distribution of the polymer PP-2DM, as seen from Figure 6.9. The other polymers have a wider pore size distribution.

In most models of enzyme immobilisation the solid support is assumed to contain pores with uniform sizes. In reality the porous solids contain wider pore size distribution. The predicted amount of enzyme could be appreciably different from that for support with uniform pore size [36]. With increase in contacting time and enzyme concentration, the depth of penetration of enzyme into porous particles increases. In contrast to shell type enzyme distribution (enzyme bound only at or near the surface of the porous particle) observed for supports with uniform distribution of pores, the enzyme distribution in the support with non-uniform pores displays a flatter enzyme activity profile extending into the central core of the porous support[37, 38]. The larger pores allow free passage of the enzyme molecule into the particle and leads to uniform distribution of enzyme inside the particle. This however leads to lesser availability of active sites leading to lower biotransformation. There was 2-4% loss of activity when the immobilised enzyme was used for the second cycle of biotransformation.

**Table 6.8. Effect of pore volume on esterfication of R, S naproxen to S(+) butyl ester.**

| Sr. No. | Polymer code | Pore volume $cm^3/g$ | % biotransformation I $^{st}$ cycle | % biotransformation II $^{nd}$cycle |
|---|---|---|---|---|
| 1 | PP-VR | 0.2187 | 4.80 | 2.10 |
| 2 | PP-2DM | 0.4820 | 11.0 | 9.00 |
| 3 | PP-4DM | 0.4910 | 9.94 | 6.50 |
| 4 | PP-2CD | 0.6692 | 8.69 | 5.45 |
| 5 | PP-4CD | 1.3650 | 6.55 | 3.89 |

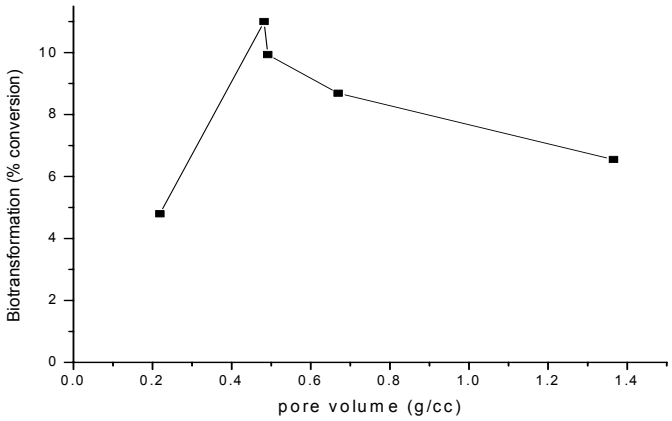


**Figure 6.9. Effect of pore volume on biotransformation.**

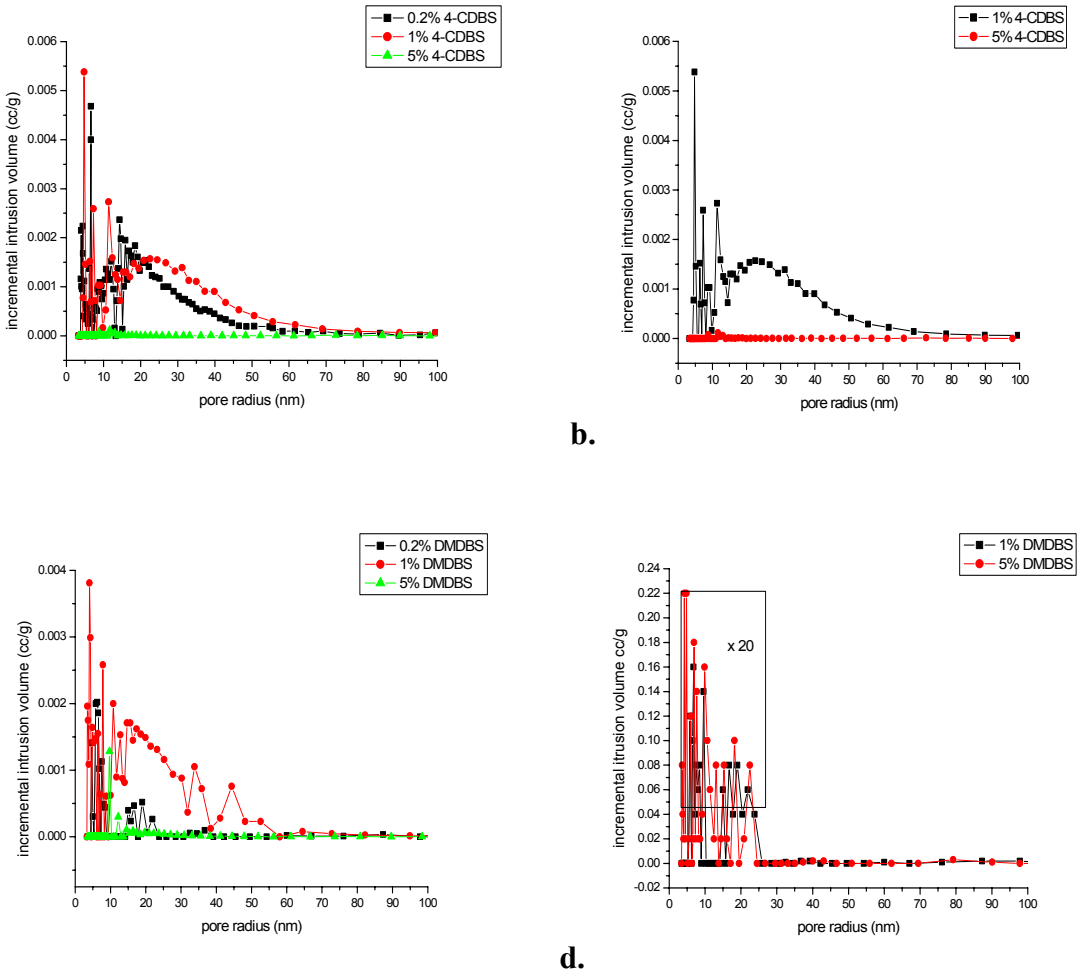


**Figure 6.10 Pore size distribution of the samples with different percentages of nucleating agent, (a) and (b) with 4-CDBS; (c) and (d) with 3, 4-DMDBS.**

### *6.6.3 HPLC analysis*

In this work, a method using one-time injection to determine conversion of the stereoselective esterification of racemic naproxen with n-butanol catalysed by immobilized lipase was developed with a commercially available chiral HPLC column Chirobiotic V (Astec). Naproxen can be resolved on Chirobiotic V column using mobile phase THF:0.1% triethylammonium acetate (TEAA), pH 7 (10:90) with the flow rate 1.0mL/minute[39]. This mobile phase was however was not compatible with our reaction medium, since the reactions were carried out in non-aqueous conditions. We therefore opted for the normal phase conditions to achieve the separation of naproxen and naproxen butyl ester. The mobile phase used was n-hexane: isopropyl alcohol: methanol (100:4:4, v/v).

Initially, (R, S) naproxen was analysed with the mobile phase 20% tetrahydrofuran in triethyl ammonium acetate buffer of pH 7. A very good baseline separation with retention times of 9.93 and 10.89 with $\alpha$ =1.14 was obtained. When the reaction mixture was analysed with this mobile phase the resolution was totally lost. This could be due to immiscibility of the solvents used in the reaction with that of mobile phase. When a small quantity of methanol was added to the reaction mixture to dissolve it in the buffered mobile phase a very poor resolution was obtained. In order to achieve simultaneous separation of naproxen and naproxen butyl ester we tried out normal phase HPLC conditions.

The standard S (+) naproxen butyl ester was synthesised in order to see the elution order. With the above-mentioned mobile phase, partial resolution of the naproxen enantiomers as well as good separation of butyl ester was achieved. The retention times for naproxen enantiomers were 16.09 and 16.48 with $\alpha$ = 0.7, which indicates poor resolution. The resolution of R, S naproxen ester was achieved with $\alpha$ = 2.00. When the reaction mixture was injected, there was an increase in the percent peak area of S (+) naproxen butyl ester (retention time matching with the standard S (+) butyl ester). Thus, indicating the stereospecificity of the bound enzyme towards S isomer of naproxen.

**References**


1. Viklund C., Svec F. and Jean M. J. F., *Chem*. *Mater*., 8, 744, 1996.
2. Roberto F., Pilar A., Pilar S., Gloria F. and Guisán J. M., *Chem*. *Phys*. *Lipids*, 93, 185, 1998.
3. Koops B. C., Papadimou E., Verheij H. M., Slotboom A. J. and Egmond M. R., *Appl*. *Microbiol*. *Biotechnol*. 52, 791, 1999.
4. Balcao V.M., Vieira M.C., and Malcata F. X., *Biotechnol*. *Progr*., 12, 164, 1996.
5. Smith T., Masilamany D., Bui L. K., Brambilla R., Khanna Y. P. and Gabriel K. A., *J*. *Appl*. *Polym*. *Sci*., 52, 591, 1994.
6. Winkler U.K. and Stuckmann M., *J*. *Bacteriol*., 138, 663, 1979.
7. Lowry O.H., Roseburgh N., Farrand A.L. Randall R., *J*. *Biol*. *Chem*. 193, 265, 1951.
8 Mahaffey R.L., *U. S. Patent 4, 371, 645*, assigned to Milliken Research Corporation 1983.
9. Machell G., *U. S. Patent 4, 562, 265*, assigned to Milliken Research Corporation 1985.
10. Scrievens W. A. and Salley J. M., *U. S. Patent 5,731,474*, assigned to Milliken Research Corporation,1998.
11 Jones J. R. and Mehl N. A., *U. S. Patent 6,495,620*, assigned to Milliken and Company, 2002.
12. Dotson D. L., Burkhart B. M., Anderson J. D., Jones J. R. and Sheppard S. R., *U. S. Patent 6,555, 696*, assigned to Milliken and Company, 2003.
13. Marcel M. and Mulder J. Eds., "*Basic principles of membrane technology*", Kluwer Academic Publishers, pp 109, 1996.
14. Beck H. N. and Ledbetter H. D., *J*. *Appl*. *Polym*. *Sci*., 9, 2131, 1965.
15. Kawai Y., Sasagawa K., Malki M., Ueila H. and Maiyamoto M., *U. S. Patent, 4314049*, 1982**.**
16. Van de Witte P., Dijkstra P. J., Van der Berg J. W. A. and Feijen J., *J*. *Memb*. *Sci*., 117, 1, 1996.
17. D. Lee, F. J. Hua, G. E. Kim, *Polym*. *Mater*. *Sci*. *Eng*., 85, 399, 2001.
18. Schaaf P., Lotz B. and Wittmann J. C., *Polymer*, 28, 193, 1987.
19. Matsuyama H., Termoto M., Kuwana M. and Kitamura Y., *Polymer*, 41, 8673, 2000.
20. Hou W. and Lloyd T. B., *J*. *Appl*. *Polym*. *Sci*., 45, 1783, 1992.
21. Whaley P. D., Kulkarni S., Ehrlich P., Stein R. S., Winter H. H., Conner W. C. and Beaucage G., *J*. *Polym*. *Sci*.*: Part B*, *Polym*. *Phys*., 36, 617, 1998.

22. Pedersen S. and Eigtved P., *WO9015868,* assigned to Novonordisk AS (DK), 1990.

23. Brunauer S., Deming L. S., Deming W. S. and Teller E., *J. Am. Chem. Soc*., 62, 1723, 1940.

24. Avila R., Ruiz R., Amarao-Gonzalez D., Diaz O., Gonzalez J. A. and Nunez A., *J. Latin American Applied Research*, 35, 307-311, 2005.

25. Ahuja S. Eds., "*Chiral separations by chromatography*", Oxford University Press.

26. Hari Krishna S. and Karanth N. G., *Catal*. *Re*v., 44**,** 499, 2002.

27. Duan G., Ching C. B., Lim E. and Ang C. H., *Biotechnol*. *Lett*., 19, 1051, 1997.

28. Chang C. S. and Tsai S. W., *Enzyme Microb*. *Technol*., 20, 635, 1997.

30. Tsai S. W., Lin J. J., Chang C. S. and Chen J. P., *Biotechnol*. *Prog*., 13, 82, 1997.

31. Tsai S., Lu C. and Chang C., *Biotechnol*. *Bioeng*., 51**,** 148, 1997.

32. Tsai S. and Wei H., *Biotechnol*. *Bioeng*., 43, 64, 1994.

33. Tsai S. and Wei H., *Enzyme Microb*. *Technol*., 16, 328, 1994.

34. Jau-Yann W., Shi-Wenn L., *Enzyme and Microb*. *Technol*., 26, 124, 2000.

35. Yu H. W., Wu J. C. and Ching C. B. *Biotechnol*. *Lett*., 26, 629, 2004.

36. Worsfold P. J. *Pure Appl***.** *Chem*., 67, 597, 1995.

37. Hossain M. M. and Do D. D, *Biotechnol*. *Bioeng*., 27, 842, 1985.

38. Borchet A. and Bucholz K**.,** *Biotechnol. Bioeng*., 26, 727, 1984.

39. Chirobiotic™ Handbook, A guide to using macrocyclic glycopeptide bonded phases for chiral LC separations Astec, Advanced Separation technologies Inc.

# Chapter 7

## Conclusions and future work

# 7. Conclusions and future work

## 7.1 Conclusions

The two different methodologies (suspension and concentrated emulsion) employed for the synthesis of spherical, porous polymers to be used as supports in chromatographic applications, resulted in the formation of polymers with different properties. Larger particles (100-1000 μm) are obtained in case of suspension polymerisation while the particles with 0.5-200 μm diameters are obtained in concentrated emulsion polymerisation.

The synthesis of GMA-EGDM and GMA-DVB polymers by suspension polymerisation using cyclohexanol and hexanol as pore generating solvents yielded polymers with different morphologies and porous properties. Use of hexanol as pore generating medium resulted in higher pore volumes and low surface areas indicating the presence of only macropores (pores in the range of 1000-3000 $A^0$). Suspension polymerisation of GMA-DVB and GMA-EGDM with cyclohexanol as porogen resulted in bimodal distribution of pores and higher surface areas suggesting the presence of both mesopores and macropores. Although the solvating ability of cyclohexanol is lower than that of hexanol, smaller pores are obtained with cyclohexanol, which is contradictory to the solvating ability of the solvents. Influence of other factors like polymerisation rates of monomer components as well as chain transfer to the diluent is probably more prevalent as compared to solubility parameter. Increase in the amount of crosslinker resulted in increase in surface areas and pore volume with a simultaneous decrease in the surface epoxy groups.

Polymerisations carried out using concentrated emulsions of GMA-EGDM and HEMA-EGDM, with both aqueous and oil phase initiators and poly(vinyl pyrrolidone) resulted in spherical, porous polymers. The pore size distribution in case of GMA-EGDM and HEMA-EGDM polymers synthesised using only organic phase initiator and calcium chloride as protective colloid is wider (25-2500 nm, typical of HIPE) as compared to the polymers synthesised with both phase initiators and poly(vinyl pyrrolidone) as suspending agent. This could be probably due to stabilisation of primary emulsion by calcium chloride present in the outer phase getting emulsified into the emulsion and forming a ternary emulsion. In both methods of polymerisation only macro and

mesopores were formed. Increase in internal water, addition of diluents to the oil phase and using Brij surfactants resulted in marginal change in surface areas and porosities of the polymers.

The surface epoxy groups decreased as the crosslink density increased. With both phase initiators and poly(vinyl pyrrolidone) as suspending stabiliser, the available surface epoxy groups were the highest while they were the lowest for polymers synthesised with organic phase initiator.

Polymerisation of HEMA-EGDM using both phase initiators and poly(vinyl pyrrolidone) as suspending stabiliser yielded large, agglomerated polymers. The particles were obtained with surface porosities and low to medium surface areas. The particles obtained with only oil phase initiator and calcium chloride as suspending stabiliser resulted in spherical, porous particles with surface areas 3-70$m^2$/g. The pore sizes were in the range of 50-1000 $A^0$. With aqueous phase initiator, bimodal distribution of pores in the range 50-3000 $A^0$ was obtained.

Although the loading of β-CD molecules on the polymers (GMA-EGDM and GMA-DVB) was found to be dependent on the available surface functional groups, it is not the only detrimental factor. The pore volume, surface areas also play an important role in ligand loading. The binding of β-CD through hexamethylene diisocyanate and sebacoyl chloride spacer was the highest in case of GMA-DVB polymers synthesised using hexanol as porogen. The highest loading (0.1744 mmol/g) was achieved for GV12H with sebacoyl chloride spacer. With hexamethylene spacer the highest loading was 0.1700 mmol/g, for the polymer GV10H. The two polymers had almost the same pore volumes.

The study of stereospecific inclusion of citalopram enantiomers by GV10HHMCD and GV12HSCCD showed that β-CD modified polymers selectively bind S isomer of citalopram and binding is better in case of GV10H with sebacoyl spacer. This is attributable to the minimised steric interactions due to increased length of spacer. The binding was also found to be dependent on the solvent.

L (+) tartaric acid was successfully bound to the GMA-EGDM HIPE polymers. The amount of ligand loaded onto the polymers was found to be dependent on the amount of crosslinker in the polymerisation mixture and was independent of the internal phase

volume. Thus, the highest loading was obtained with 25% crosslinked GMA-EGDM polymer. The modifications of HEMA-EGDM polymers made by HIPE methodology with diacetyl and dibenzoyl tartaric anhydrides also showed a similar trend.

Linear polyglycidyl methacryalate when modified with L (+) tartaric acid gave crosslinked products with swellability in different solvents like methanol, water and dioxane. The study of antihypertensive drug amlodipine binding to the L (+) tartaric acid revealed that binding of S isomer of amlodipine took place, as seen from the analysis by HPLC.These modified polymers could be considered as potential candidates for use in chiral HPLC columns.

The heterogeneous nucleation of the poly(ethylene-co-propylene) resulted in higher pore volumes than the non-nucleated poly(ethylene-co-propylene). The lipase binding on nucleated polypropylene depended on the pore size distribution of the polymer. The heterogeneously nucleated polymers with 1% and 5% 3,4 DMDBS as the nucleating agent showed uniform distribution of pores ranging from 10-25 nm. The uniform pore size distribution results in higher enzyme binding. The enzyme binding also depends on the pre-treatment and time of contact of polymer and the enzyme solution. The higher enzyme binding results in higher biotransformation, which is evident from HPLC results.

**7.2 Future work**

The polymer synthesis methodologies resulted in polymers with maximum surface areas lying in the range of 100-150 $m^2/g$. For applications like chromatographic stationary phases require still higher surface areas (~ 300 $m^2/g$). In order to achieve higher surface areas, well-defined porosities as well as narrow pore size distribution, solvating diluents can be used in the polymerisation mixture. In HIPE polymerisation of polar monomers like GMA and HEMA with Span 80 as surfactant, more hydrophobic crosslinker like divinyl benzene could be used as it can help stabilising the emulsion by reducing the interfacial energy. The use of calcium chloride in the internal phase water also can be studied with organic phase initiator.

The derivatisation of attached β-CD molecules in order to achieve higher selectivity for other structurally similar drugs also can be explored. Binding of tartaric acid and its derivatives through spacers to the polymers and their use in chiral resolutions

is also an interesting area to be explored. The metal complexes of bound tartaric acid and their derivatives could be investigated for the resolution of amino acids etc.

Modifications of monomers like GMA and HEMA with tartaric acid based ligands and their subsequent polymerisation also can lead to polymers with wide applicability.